Assessment of CV-1 as a Production Cell Line for Large Scale Manufacturing of a Lister Strain Oncolytic Vaccinia Virus

Shuchang Liu

A thesis submitted to the University College London in partial fulfilment of the degree of Doctor of Philosophy

Department of Biochemical Engineering
University College London
Torrington Place, London
WC1E 6BT

DECLARATION

I, Shuchang Liu, confirm that the work presented in this thesis is my own. Where information has been derived from other sources, I confirm that this has been indicated in the thesis.

Abstract

Oncolytic Vaccinia virus (OVV) has emerged as a promising therapeutic agent for cancer treatment. However, the development of an effective manufacturing process for OVV has yet to be fulfilled. This thesis explored and evaluated the potential of using CV-1, a continuous cell line derived from monkey kidney with an indefinite lifespan, to develop a scalable production process for an oncolytic vaccinia virus.

CV-1 cells have been widely used for vaccinia virus production in research labs. The cell line was originally maintained in serum-containing medium (SCM) statically. In this study, the cell line was adapted to grow in two serum-free media, VP-SFM and OptiPRO, with OptiPRO proving to be the most suitable. The adapted cell line, CV-1-OPT, exhibited the shortest doubling time, highest plating efficiency, a recovery ratio comparable to that of SCM, and a saturation density 85% of that observed in SCM. CV-1-OPT also demonstrated effective proliferation on microcarriers, with cell densities reaching similar levels in batch cultures regardless of initial seeding densities, and elevating up to 1.87×10^6 cells/ml when intermittent feeding strategies were employed.

The production of an oncolytic vaccinia virus, VVL-15 RFP, was studied using the previously developed microcarrier-based CV-1-OPT suspension culture system. The cells were infected during their mid-late to late exponential phase when the density was between 9.27×10^5 to 1.52×10^6 cells/mL, with a multiplicity of infection (MOI) ranging from 0.1 to 1. The maximal specific viral productivity achieved was 71.9 pfu/cell. Infection at a low cell density with a high MOI led to a reduction in production time.

The study results demonstrate the successful adaptation of CV-1 cells to OptiPRO SFM, their efficient proliferation on Cytodex-1 microcarrier and capability in supporting VVL-15 RFP expansion. These promising findings suggest that CV-1 cells could potentially serve as a feasible option for large-scale production of oncolytic VV.

Impact Statement

The impact of this work will be seen on multiple fronts:

The study of CV-1 growth properties facilitates further understanding of the cell line. The exploration of VVL-15 oncolytic Vaccinia virus production process serve the purpose of creating a better understanding of the interactions among virus, cell substrate and culture conditions, identifying yield limiting stages and laying a foundation for the rational design and optimization of the OVV manufacturing process. It also sheds some light on the replication dynamics and release kinetics of Vaccinia virus under different production formats, and offers insights into manufacturing of oncolytic virus of similar kind.

The continued development of the production process may lead to further research opportunities in areas such as kinetic modelling of Vaccinia virus replication in host cells, nutritional needs and metabolism change in Vaccinia virus-infected host cells, as well as development of methods for efficiently harvesting virus-infected cells on microcarriers etc. It can also be useful when establishing relevant manufacture guidelines or standards for oncolytic virus.

The finished process design may be adapted and/or used as a technological platform for the manufacture of various oncolytic Vaccinia viral products, therefore reducing process development associated time and cost, and opening up the employment, business and investment opportunities in UK's pharmaceutical sector.

UCL Research Paper Declaration Form

referencing the doctoral candidate's own published work(s)

1. **For a research manuscript that has already been published** (if not yet published, please skip to section 2)

   a) **What is the title of the manuscript?**
   Establishing elements of a synthetic biology platform for Vaccinia virus production: BioBrick™ design, serum-free virus production and microcarrier-based cultivation of CV-1 cells

   b) **Please include a link to or doi for the work**
   doi: 10.1016/j.heliyon.2017.e00238. eCollection 2017 Feb

   c) **Where was the work published?**
   Heliyon

   d) **Who published the work?** (e.g. OUP)
   Elsevier

   e) **When was the work published?**
   February 2017

   f) **List the manuscript's authors in the order they appear on the publication**
   Shuchang Liu, Ludmila Ruban, Yaohe Wang, Yuhong Zhou, Darren N. Nesbeth

   g) **Was the work peer reviewed?**
   Yes

   h) **Have you retained the copyright?**
   Yes

   i) **Was an earlier form of the manuscript uploaded to a preprint server?** (e.g. medRxiv). If 'Yes', please give a link or doi)
   Yes. Https://doi.org/10.1101/042275

   If 'No', please seek permission from the relevant publisher and check the box next to the below statement:

   ☐

   *I acknowledge permission of the publisher named under **1d** to include in this thesis portions of the publication named as included in **1c**.*

2. **For a research manuscript prepared for publication but that has not yet been published** (if already published, please skip to section 3)

   a) **What is the current title of the manuscript?**
   N/A

b) **Has the manuscript been uploaded to a preprint server?** (e.g. medRxiv; if 'Yes', please give a link or doi)
N/A

c) **Where is the work intended to be published?** (e.g. journal names)
N/A

d) **List the manuscript's authors in the intended authorship order**
N/A

e) **Stage of publication** (e.g. in submission)
N/A

3. **For multi-authored work, please give a statement of contribution covering all authors** (if single-author, please skip to section 4)

Shuchang Liu: Conceived and designed the experiments; performed the experiment; analysed and interpreted the data; contributed reagents, materials, analysis tools or data.

Ludmila Ruban: Contributed reagents, materials, analysis tools or data.

Yaohe Wang: Conceived and designed the experiments; contributed reagents, materials, analysis tools or data.

Yuhong Zhou: Conceived and designed the experiments; contributed reagents, materials, analysis tools or data.

Darren N. Nesbeth: Conceived and designed the experiments; contributed reagents, materials, analysis tools or data.

The authors declare no conflict of interest.

4. **In which chapter(s) of your thesis can this material be found?**

3

5. **e-Signatures confirming that the information above is accurate** (this form should be co-signed by the supervisor/ senior author unless this is not appropriate, e.g. if the paper was a single-author work)

Candidate (e-Signature)

Date:
21-May-2024

Supervisor (e-Signature)

Date
22-May-2024

Acknowledgements

I wish to express my thanks to my first and second supervisors, Dr Yuhong Zhou and Dr Darren N. Nesbeth.

I would like to express my deep appreciation to the Department of Biochemical Engineering for the support extended to me.

I am immensely grateful to my advisor, Professor Yaohe Wang, and his team from Barts Cancer Institute, Queen Mary University of London, for their generosity in providing research materials and offering invaluable guidance and support.

I extend my thanks to the Centre for Cancer Biomarkers and Bio-therapeutics, Barts Cancer Institute, Queen Mary University of London, for their support in providing access to laboratory facilities and space for my research.

Special appreciation goes to Ms. Ruban, whose expertise in lab techniques and willingness to offer her time and guidance have been instrumental in my research journey.

I am deeply grateful to Dr Tarrant for his encouragement and guidance, which have played an important role in my personal and academic growth.

My heartfelt thanks go to Professor Peter Dunnill and Mrs. Dunnill for their generous financial support, which has been indispensable in enabling me to pursue my academic endeavours.

I want to express my gratitude to my friends Miao, Yichen, Ning, Ya, and Zara for their kindness and friendship throughout this journey.

Last but not least, I extend my heartfelt gratitude to my family for their unwavering support, boundless love, patience, and encouragement throughout my journey in pursuing a PhD and navigating life's challenges. Their presence has been an invaluable blessing in my life.

Table of Contents

Table of Figures

List of Tables

Abbreviation

ALT	Alanine Transaminase
ADCF	Animal-derived Component Free
APC	Antigen-Presenting Cells
AST	Aspartate Aminotransferase
ATCC	American Type Culture Collection
ATG	Antithymocyte Globulin
ATP	Adenosine Triphosphate
BiTE	Bispecific T-cell Engager
BSA	Bovine Serum Albumin
BSE	Bovine Spongiform Encephalopathy
CDM	Chemically Defined Media
CDV	Cidofovir
CEA	Carcinoembryonic Antigen
CEF	Chicken Embryonic Fibroblasts
CEV	Cell-associated Enveloped Virus
CPA	Cyclophosphamide
CPE	Cytopathic Effect
CRT	Calreticulin
CV-1-OPT	CV-1 cells adpated to growth in OptiPROTM serum free medium
DAMPs	Damage-Associated Molecular Patterns
DC	Dendritic Cell
DEAE	N,N-diethylaminoethyl
DIP	Defective Interfering Particles
DMEM	Dulbecco's Modified Eagle Medium

DMSO	Dimethyl Sulfoxide (DMSO)
DNA	Deoxyribonucleic Acid
DO	Dissolved Oxygen
DOE	Design of Experiments
ECACC	European Collection of Authenticated Cell Cultures
ECL	Enhanced Chemiluminescence
ECS	Extra-Capillary Space
EDTA	Ethylenediaminetetraacetic Acid
EEV	Extracellular Enveloped Virus
EGFR	Epidermal Growth Factor Receptor
eIF2	Eukaryotic Initiation Factor 2
EMA	European Medicines Agency
EMEM	Eagle's Minimum Essential Medium
FBS	Foetal Bovine Serum
FCS	Foetal Calf Serum
FDA	U.S. Food and Drug Administration
GMP	Good Manufacturing Practice
HCP	Host Cell Proteins
HEK293	Human Embryonic Kidney 293 cells
HEPES	N'-2-Hydroxyethylpiperazine-N'-2 ethanesulphonic Acid
HIF	Hypoxia-Inducible Factor
HMGB1	High Mobility Group Box protein 1
hNIS	human sodium iodide symporter (hNIS)
HNSCC	HNSCC (head and neck squamous cell carcinoma)
ICD	immunogenic cell death (ICD)
ICI	Immune checkpoint inhibitors (ICI)

ICS	intra-capillary space (ICS)
IFN	Interferon
IMV	Intracellular Mature Virus
ITES	Insulin, Transferrin, Ethanolamine, Selenium
ITS	Insulin, Transferrin, Selenium
JNK	c-Jun N-terminal kinase
kbp	Kilo Base Pairs
kDa	Kilo Dalton
MAPK	Mitogen-Activated Protein Kinase
MDCK	Madin-Darby Canine Kidney
MOC	Mini-Organ Cultures
MOI	Multiplicity of Infection
MVA	Modified Vaccinia Ankara
NYCBOH	New York City Board of Health
OV	Oncolytic viruses
pAKT	phosphorylated Akt
PBS	Phosphate-Buffered Saline
PBST	Phosphate Buffered Saline with Tween® 20
PD-1	Programmed Cell Death Protein 1
PD-L1	Programmed Cell Death Protein Ligand 1
PFM	Protein-Free Media
PFU	Plaque-Forming Unit
PHDs	Prolyl Hydroxylases
PVDF	Immobilon-P Polyvinylidene Fluoride
RFP	Red Florescent Protein
RNR	Ribonucleotide Reductase

RPM	Revolutions per Minute
SCM	Serum-Containing Medium
SD	Standard Deviation
SFM	Serum Free Medium
TAA	Tumour-Associated Antigen
tAKT	Total Akt
TCA	Tricarboxylic Acid
TCID50	Median Tissue Culture Infectious Dose
TK	Thymidine Kinase
TME	Tumour Microenvironment
TNF	Tumour Necrosis Factor
TOH	Time of Harvest
TOI	Time of Infection
VEGF	Vascular Endothelial Growth Factor
VGF	Vaccinia Growth Factor
VIG	Vaccinia Immune Globulin
VSV	Vesicular Stomatitis Virus
VV	Vaccinia Virus
VVL	Lister strain Vaccinia Virus
WHO	World Health Organization
WR	Western Reverse
WRDD	Western Reserve strain Double viral gene Deleted

Chapter 1. Introduction

1.1 Vaccinia virus and oncolytic virotherapy

1.1.1 Major roles of Vaccinia virus in medical history

The precise origin of vaccinia virus (VV) remains unclear. Although VV is well known for its role as a vaccine during the World Health Organization (WHO) smallpox eradication programme in the late 1970s, it is the cowpox virus that was first employed as a vaccine for smallpox back to more than 200 years ago. Since then, this vaccination material had been passaged through a series of individuals. In the 1930s, it was realized that the strain being used at that time was not, or was no longer the same as cowpox virus. The new strain was named Vaccinia Virus (Shen & Nemunaitis 2004).

The elimination of smallpox did not end the research interest in VV. The search for a safe and effective smallpox vaccine continued, perceiving the potential threat of using smallpox as a biological weapon. Since then, various strategies have been adopted to develop a series of novel attenuated variants of VV with enhanced safety profiles. These include adopting sterile cell culture and viral production techniques, serial passages in a different species other than human and genetic manipulation of the VV genome (Jacobs et al. 2009; Verardi et al. 2012).

The use of VV as a vaccine vector against animal and human infectious diseases dates back to early 1980s (Moss 2013). One of the successful implementations involves the genetically engineered VV expressing rabies glycoprotein (G), which played an important role in combatting rabies in wildlife across Europe and North America (Verardi et al. 2012).

A number of VV-based human vaccines targeting different infectious agents, such as HIV, hepatitis, influenza and malaria have been reported to be undergoing preclinical or clinical trials (Sanchez-Sampedro et al., 2015). Popular emerging candidate VV strains on which the recombinant vaccines have been based include MVA (Modified Vaccinia Ankara) and NYVAC (New York City Board of Health). The former has been attenuated by classical serial passage method and the latter has its nonessential virulence and host range genes deleted (Ober et al. 2002). The strains are considered safer for clinical use compared with their replication-competent counterparts and can

be administered multiple times even in recipients with pre-existing immunity (Verardi et al. 2012).

With the identification of tumour-associated antigens (TAA), immunotherapies using VV engineered to express TAAs as well as immune enhancing genes to induce potent immune responses in the patient have emerged as a new form of cancer treatment. In a broad sense, this type of treatment does not necessarily require tissue-specific targeting and viral propagation (Guo et al. 2005). One example is the recombinant CEA-MUC-1-TRICOM Vaccinia-based vaccine, which contains the transgenes encoding for triad of co-stimulatory molecules (B7.1, intercellular adhesion molecule 1 and lymphocyte function-associated antigen 3) along with carcinoembryonic antigen (CEA) and mucin-1 (Muc-1) for Muc-1 and CEA-expressing cancer. When used with the recombinant CEA-MUC-1-TRICOM fowlpox-based vaccine in the form of prime-boost, the vaccine has demonstrated preliminary evidence of clinical response in patients with different types of cancer (Mohebtash et al, 2012; Gulley et al. 2008; Kaufman et al. 2007).

On the other hand, the idea of exploiting the natural oncolytic capacity of replication competent VV to destroy tumours has gradually realized with the aid of the recent development in recombinant DNA technology and ever-growing knowledge in tumour cell biology and virology (Yaghchi et al. 2016). This will be examined in depth in the following sections.

1.1.2 Oncolytic virus

Oncolytic viruses (OVs) comprise replication-competent viral strains either naturally tumour tropic, or genetically modified for tumour tropism, capable of infecting and killing cancer cells without harming normal tissue.

The use of viruses to treat tumours can be traced back to more than a century ago. Among the first case reports, N. G. De Pace described the substantial regression of cervical cancer in his patient who received the Pasteur-Roux live attenuated rabies vaccine (Sinkovics and Horvath, 2008). However, most often the viruses were not considered effective as therapeutic reagents in cancer treatment because of their failure to meet the clinical expectations and address safety concerns, which can be attributed to the scarcity of methods to control virulence and create viruses with greater tumour specificity (Kelly & Russell, 2007). In the 1990s, the development of reverse genetics

and genetic engineering paved the way for capitalising on the oncolytic potential of viruses. Today, IMLYGIC™ (T-VEC/Talimogene Laherparepvec), an engineered immune-stimulatory herpes simplex virus (HSV), is the first oncolytic viral therapy approved by the U.S. Food and Drug Administration (FDA) and European Medicines Agency (EMA) for use in patients with advanced or unresectable melanoma, setting off new wave of interest in oncolytic virotherapy (Amgen®, 2015; Amgen®, 2015).

Generally speaking, the tumour tropism of OVs is a result of the viral infection and proliferation capitalizing on the virus-specific receptors overexpressed on tumour cells, the aberrant signalling pathway in tumour cells (Kaufman et al., 2015) and the hypoxic, high metabolic tumour microenvironment (Guo, 2011).

Besides being able to selectively and continuously replicate in tumour, OVs typically possess the following features: the ability to infect dividing as well as non-dividing cells, interaction with uninfected surrounding cells forming syncytia, high replication rate and stability *in vivo*, lack of the ability to integrate into host cell chromosomes, lack of severe side effects, and the capability of being genetically engineered (Verheije and Rottier, 2012).

In addition to mediating direct lysis of infected cells (oncolysis), which releases infectious viral progeny that infect and lyse neighbouring tumour cells, OVs also destroy tumour via induction of systemic tumour-specific immune response (Kaufman et al., 2015). Oncolysis triggers immunogenic cell death characterized by the release of TAAs, cellular damage-associated molecular patterns (DAMPs) and pathogen-associated molecular patterns (PAMPs) (Guo et al., 2014). The viral infection in the tumour together with the exposure of these immunomodulatory molecules lead to the attraction of various immune cells to the tumour microenvironment (TME) followed by the priming of a host innate and adaptive antitumour immune response (Workenhe and Mossman, 2014). Some OVs, such as VV and vesicular stomatitis virus (VSV), can also hinder tumour progression via disrupting tumour vasculature therefore impeding tumour blood supply (Breitbach et al., 2011).

OVs can be generally classified into DNA and RNA viruses depending on the type of nucleic acid carried. **Table 1.1** lists the viral species used in the construction of OVs in oncology clinical trials.

Table 1.1 Viral species used in the construction of OVs in oncology clinical trials.

OV Genome	DNA	RNA
Virus Species	Adenovirus, vaccinia virus, parvovirus, herpes simplex virus (Ungerechts et al., 2016; Miest & Cattaneo, 2014)	Coxsackievirus (Bradley et al., 2011), Newcastle disease virus (Lam et al., 2011), Seneca Valley virus (Reddy et al., 2007), measles virus, vesicular stomatitis virus, poliovirus, murine leukaemia virus, reovirus (Tanner & Roberto, 2014; Perez et al., 2012)

1.1.3 Features of Vaccinia virus as an alternative cancer therapy

Vaccinia Virus belongs to the genus *Orthopoxvirus* from the *Poxvirus* family. It is an enveloped brick-shaped double-stranded lytic DNA virus with dimensions of 250 by 350 nm (Carter et al., 2003). There are many inherent biological properties of VV that contribute to its usefulness and effectiveness as oncolytic viral-therapeutics.

(1) The entire life cycle of VV takes place in the cytoplasm.

The virus depends mostly on its own encoded proteins for genome replication and transcription and never enters the host cell nucleus (Guse et al., 2011). This eliminates the safety concern that the VV DNA would integrate into the host chromosome.

(2) The life cycle of VV is fast and efficient.

The VV early mRNA is detectable within 20 minutes post-infection. Since the initiation of transcription is independent of host cells enzymes, the transcription of VV DNA into early mRNAs starts immediately upon infection. A complete early transcription system has been incorporated into the core of an infectious VV (Moss, 2001).

Within 2 hours of infection, DNA replication occurs and the VV almost completely inhibits the synthesis of host cell protein by shutting down the host mRNA synthesis and speeding up the degradation of cellular mRNA (Chou et al., 2012, Thorne et al.,

2005). This strategy effectively counteracts the antiviral response induced by host cells and allows efficient subversion of host functions for viral protein synthesis and replication.

As soon as 6 hours post-infection, the first progeny VVs are released to infect new host cells. The rapid spread of VV is of great importance to virotherapy as oncolytic viruses are expected to quickly sweep through tumour cells. In contrast, the spread of adenovirus that has also been studied extensively as an oncolytic virus is relatively slow. Its progeny are not released until the lysis of the host cells 48-72 hours post-infection (Thorne et al., 2005; Shen & Nemunaitis 2004).

Within 12 hours of infection, about 10,000 copies of the viral genome can be generated from each cell, of which half are incorporated into infectious particles (Shen & Nemunaitis 2004).

(3) Different infectious forms of VV enable efficient virus dissemination.

During the life cycle, VV has two morphologically distinct infectious forms that play different roles in spreading the virus (Mathew et al., 1998).

As outlined in **Figure 1.1**, the replication of VV commences with attachment and entry of virions into susceptible cells. The infecting virions then start their gene expression, followed by uncoating and DNA replication before the formation of intracecllular mature virions (IMV) which constitutes the most abundant form of VV (Moss, 2001).

IMV is sensitive to complement and antibody neutralization, thus is more likely to be destroyed when spreading between cells within a host. However, the virus is physically robust: it can survive desiccation and ambient temperature outside the host cells and can resist physical forces generated during process recovery and purification. So this form of VV is well suited for mediating virus transport from host to host (Smith et al., 2003; Vanderplasschen et al., 1998). At this stage, most virions have completed their morphogenesis, and IMV are discharged from cells upon cell lysis (Roberts & Smith, 2008).

The remaining IMV leave to get wrapped by a double membrane. The virions are then transported to the surface of the infected cells, where the outermost membrane of each virion fuses with the plasma membrane of the host cell (Moss, 2001). These infectious

virions will either remain adherent to the cell surface or detach from cells. The former form is termed cell-associated enveloped virus (CEV) and the latter form is called 24 extracellular enveloped virus (EEV). CEV induces the formation of actin tails that propel the virions from their host cells into the neighbouring cells.

CEV/EEV, constituting less than 1% of progeny (Ferguson et al., 2020), possess an additional membrane compared to IMV virions. This outer membrane incorporates complement control proteins derived from both virus and the host cells, which protects the EEV against recognition and elimination by complement. In comparison with the IMV, EEV is also relatively resistant to antibody neutralization (Smith et al., 2002). These features allow the virions to disseminate to distant organs in a host without being eradicated easily by the immune system. It is of particular importance in oncolytic treatment as it offers the opportunity to treat both primary and metastatic tumour sites in a host at the same time (Smith et al., 2003). However, the outer membrane of EEV is very fragile and can be ruptured easily, turning the particle back to its unwrapped infectious form (IMV). EEV is not ideal for host-to-host infection (Vanderplasschen et al., 1998) and the GMP (Good Manufacturing Practice) -standard VV used in clinical settings is typically in the IMV form (Ferguson et al., 2020).

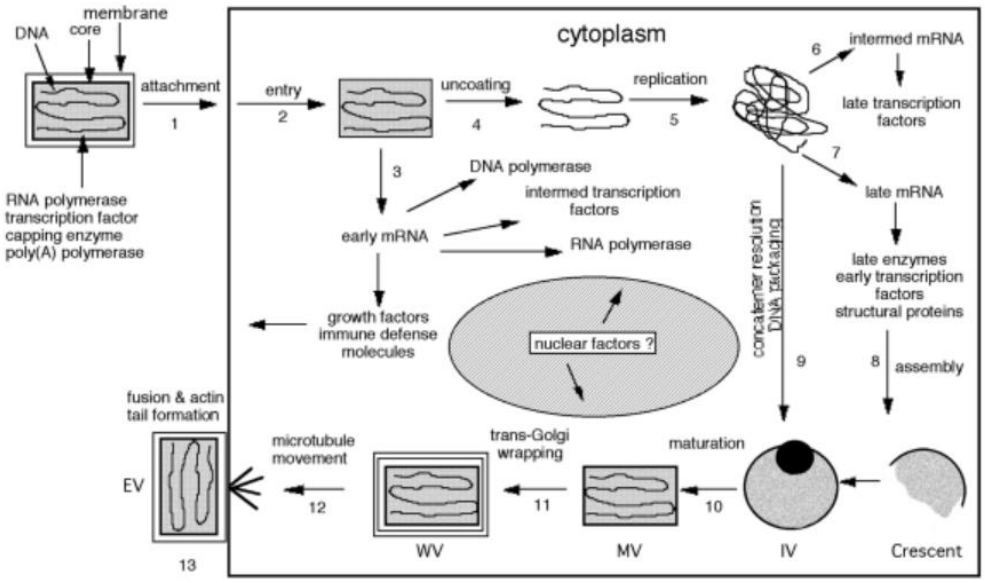

Figure 1.1: Diagram of the Vaccinia virus replication cycle. The VV replication cycle begins with a virion attaching to a cell (1) and releasing its core into the cytoplasm (2). Early mRNA is synthesized by core and translated into various proteins (3). After uncoating (4), DNA replication takes place (5), followed by the transcription and translation of intermediate and late genes (6-8). Structural proteins and other components are assembled into immature virions (9). These immature virions mature into infectious intracellular mature virions (IMVs) (10). IMVs are wrapped, transported to the cell periphery (11), gain actin tails, and are released as extracellular enveloped virions (EEVs) (12-13). *Note*. From "Poxviridae: the viruses and their replication," by Moss, B., in D. M. Knipe, P. M. Howley, D. E. Griffin, & B. N. Fields (Eds.), *Fields Virology* (5th ed., p.2914), 2007, Lippincott Williams & Wilkins, a Wolters Kluwer business. Copyright 2007 by Wolters Kluwer Heath, Lippincott Williams & Wilkins. Reprinted with permission.

(4) VV exhibits broad natural tropism for tumour tissue.

VV has a broad host range, but no one specific receptor has been identified as responsible for VV binding and entry to host cells. This affords the opportunity for oncolytic VV to treat tumours that arise from various tissues (Moss, 2001).

The natural tumour tropism of VV can be attributed to hallmark change(s) over the course of tumour progression during which the activities of certain metabolic and signal transduction pathways are altered in favour of the survival and growth of cancer cells. Many pathways important for maintaining cellular homeostasis in normal cells also play effective roles in viral clearance. Thus, the deregulation of these pathways provides a supportive environment for viral replication (Ilkow et al., 2014).

For example, the multiplication of VV requires the activation of MAPK/ERK pathway that is tightly regulated under normal conditions to avoid uncontrolled proliferation and unscheduled cell death (Andrade et al., 2004). Although VV itself can active the pathway by binding the self-encoded extracellular secretory Vaccinia Growth Factor (VGF) to cell growth factor receptors (such as Epidermal Growth Factor Receptor (EGFR), the MAPK/ERK pathway in a wide range of human cancer cells has been constitutively activated (Roberts & Der 2007; Ilkow et al., 2014). This pre-existing condition in cancer cells creates a very encouraging environment for VV replication. Other hallmark changes that may contribute to the natural tumour tropism of VV are listed in **Table 1.2**.

In comparison to normal vessels, the leakiness of blood vessels in tumours significantly increases. This structural abnormality may also be accountable for the VV tumour tropism as it allows extravasation of large VV particles from circulation and entry into tumour tissues (Goel et al., 2011; Shen & Nemunaitis 2004). Moreover, the upregulated expression of VEGF during tumour angiogenesis has been found to enhance VV internalization and promote VV infection with tumour tissue, which may again play a role in tumour tropism (Hiley et al., 2013).

Table 1.2 Summary of hallmark changes in cancer cells that contribute to the VV tumour tropism.

Proteins involved in cell growth	Function in normal cells	Dysfunction/ dysregulation in tumour cells	Effect on VV oncotropism	References
Interferon (IFN)	IFN plays important roles in mediating cellular antiviral response, inhibiting cell growth, inducing apoptosis, and modulating immune response.	It was estimated that 65-70% of tumour cell lines showed IFN defects.	Defects in IFN signalling in tumour cells weaken cellular antiviral responses to different degrees.	Stark et al., 1998; Ilkow et al., 2014.
Ribonucleotide Reductase (RNR)	RNR catalyses the conversion of ribonucleotides to 2′-deoxyribonucleotides, preparing the precursors for DNA synthesis.	Large enhancement of RNR is observed in malignant cells. RNR activity is highly correlated with tumour growth rate.	Increased nucleotide pools in tumour cells provide sufficient building blocks of DNA to allow viral replication.	Kolberg et al., 2004; Ilkow et al., 2014; Elford et al., 1970.
Thymidine Kinase (TK)	TK catalyses the phosphorylation reaction of thymidine, one of the key steps in DNA synthesis.	Increased TK levels have been associated with prognostic indicators for various types of cancers.	Increased nucleotide pools in tumour cells provide sufficient building blocks of DNA to allow viral replication.	Ilkow et al., 2014; O'Neill et al., 2001.

Table 1.2 (*Continued*)

Proteins involved in cell growth	Function in normal cells	Dysfunction/ dysregulation in tumour cells	Effect on VV oncotropism	References
Eukaryotic Initiation Factor 2 (eIF2)	eIF2 is involved in the initiation of protein synthesis. Phosphorylation of eIF2 leads to the arrest of host cell protein synthesis and initiation of antiviral responses.	Dysregulated phosphorylation of eIF2 has been observed during tumourigenesis in certain types of cancer.	Elevated efficiency of protein translation promotes the production of viral polypeptides and compromises cellular antiviral responses.	Lobo et al., 2000; Ilkow et al., 2014. Perkins & Barber 2004.
Vascular Endothelial Growth Factor (VEGF)	VEGF is a major regulator of angiogenesis and vascular permeability. It also stimulates cell migration and proliferation and protects cells from apoptosis.	Overexpression of VEGF is associated with tumour progression and metastasis.	Increased VEGF levels result in enhanced VV uptake through activation of the PI3K AKT signalling pathway.	Hiley et al., 2013; Neufeld et al., 1999.

(5) VV genome has a large capacity for foreign DNA sequence.

The tumour-selective, replication-competent feature of oncolytic virus is often observed clinically as not potent enough to impart significant antitumour effects. One of the strategies widely adopted to address this weakness is to arm the oncolytic viruses with therapeutic genes, which equips the viruses with enhanced cytotoxicity via multiple mechanisms (Terry and Kuhn, 2002). VV can carry over 25 kilo-base pairs (kbp) of exogenous genes, which is large compared with the capacity of other commonly used viral vectors such as adenovirus (8kbp), Adeno-associated viral vectors (5kbp), Retroviral vectors (8kbp) and Lentivirus (9kbp) (Smith & Moss 1983; Vannucci et al., 2013).

(6) VV can replicate efficiently in hypoxic conditions.

Hypoxia, characterized by deprivation of sufficient oxygen supply in normal tissues, is a common feature found in solid tumours.

Hypoxia-inducible factor (HIF) is a transcription factor that facilitates cellular adaptation to hypoxia by mediating cell response to hypoxia. Under normoxia, HIF-1α is hydroxylated on the two proline residues by oxygen-dependent prolyl hydroxylases (PHDs), before being ubiquitinated by the von Hippel-Lindau-containing (VHL-containing) E3 ubiquitin ligase complex. The process leads to the degradation of HIF-1α. Under hypoxia, PHDs are inactive, stabilizing HIF-1α and allowing a build-up in the nucleus to induce transcription of genes involved in adaptation of hypoxia (Ziello et al., 2007; Koh & Powis, 2012).

Mazzon et al. (2013) observed that VV induces a hypoxic cellular response under normoxic conditions to promote infectivity. Mediated by the direct and specific binding of PHD2 and the viral protein C16, VV infection rapidly inhibits the hydroxylation of HIF, allowing HIF-1α to translocate into nucleus and subsequently up-regulate HIF-responsive genes. As hypoxia is a common feature of solid tumours, the ability of VV to benefit from hypoxia for infection and replication could potentially advantage the virus in targeted tumour destruction.

Therefore, unlike oncolytic adenovirus, of which the potency is attenuated under hypoxic conditions due to the compromised viral lytic potential or/and yield of infectious virus particles, Lister strain VV demonstrated comparable efficacy in infection, replication, viral protein and transgene expression in a panel of pancreatic cancer cell lines under hypoxic and normoxic conditions (Shen & Hermiston, 2005; Shen & Hermiston, 2006; Hiley et al, 2010). Moreover,

of the four pancreatic cancer cell lines used for cytotoxicity evaluation, the virus demonstrated increased cytotoxicity in CFPac1 and MiaPaca2 under hypoxic conditions whilst equally effective cell lysis was shown in the other two cell lines regardless of the oxygen concentration supplied.

(7) Antiviral agents against VV are available.

Should adverse events or in the rare cases of localized or systemic infection of VV occur, medications are available for effective treatment.

Human plasma containing high titres of anti-vaccinia antibodies were collected from healthy donors who had previously been inoculated against smallpox, and were used for the manufacture of intravenous Vaccinia Immune Globulin (VIG). Two intravenous VIG products (VIGIV Cangene and VIGIV Dynport) have been licensed by the Food and Drug Administration for the treatment of patients with complications due to Vaccinia vaccination (Wittek, 2006).

There are a number of compounds that have demonstrated great therapeutic potentials for protection against VV infection in animal models. ST-246 is a low-molecular-weight compound that blocks the cytopathic effect of orthopoxivurs and inhibits the formation of extracellular VV (Grosenbach et al., 2011; Yang et al., 2005). 4'-thioIDU (idoxuridine) and cidofovir (CDV) are nucleoside analogues that inhibit VV DNA synthesis (Kern et al., 2009; Saeb-Parsy, 1999). CMX001 is an orally-administered prodrug formulation of CDV and is converted intracellularly to CDV. Compared with CDV, CMX001 has shown greater *in vitro* potency, a higher genetic barrier to resistance and substantially less nephrotoxicity (Lanier et al., 2010).

1.1.4 Safety of the VV

VV has shown an excellent safety profile since its widespread use as a smallpox vaccine. Mild reactions to VVs included injection site reactions (pain, soreness and redness), constitutional symptoms (e.g. fever, malaise, and fatigue) and regional lymphadenopathy (Belongia and Naleway, 2003). Strain-dependent serious adverse events included encephalitis (2-1200/10^6 vaccinations), encephalopathy (3-50/10^6 vaccinations), eczema vaccinatum (8-80/10^6 vaccinations), progressive vaccinia (1/10^6 vaccinations), and generalized vaccinia (1-70/10^6

vaccinations) (Poland et al., 2005). During a national surveillance conducted in the United States in 1968, a total incidence of 572 major complications in 14,168,000 smallpox vaccinations was reported and the overall death rate was $1/10^6$ naive vaccinations (Lane et al., 1969).

Promising preliminary safety of Oncolytic VV in early clinical trials has been established (Guse et al., 2010). In fact, JX-594, a recombinant Wyeth strain oncolytic VV, has been demonstrated to be 'generally well tolerated' in clinical studies on various types of tumours via different administration routes (Merrick, Ilett and Melcher, 2009; Breitbach et al., 2011; Park et al., 2008). Transient flu-like symptoms are most common among the treatment related adverse events reported. Occasional severe side effects (above grade 3) within the dosage ranges investigated have been observed, such as pain in a rib, elevation of aspartate aminotransferase (AST) or alanine transaminase (ALT) to AST ratio (Heo et al., 2013; Breitbach et al., 2011; Park et al., 2015; Jaime et al., 2012; Lauer et al., 2013; Mell et al., 2015; Krug et al., 2015; Zeh et al., 2015; Park et al., 2008). A firm conclusion regarding the safety of oncolytic VVs cannot be reached based on the studies of only a few hundred patients in total at the current stage, as rare adverse events would be expected to be detectable only in a larger cohort with wider use of the therapies.

1.1.5 Oncolytic Lister strain Vaccinia virus as therapeutic cancer vaccines

Although clinical experience with Lister strain VV (VVL) had been extensive, Lister strain was not initially considered an optimal candidate for the design of oncolytic VV. Instead, the NYCBOH-derived Western Reverse (WR) strain was selected as the most effective oncolytic VV strain. The conclusion was drawn based on its replication competency in two human tumour cell lines, A2780 and HCT 116, in a comparative study that involved 10 VV strains including VVL. Without compromising its oncolytic potency, the WR strain was then engineered by deleting both thymidine kinase (TK) and vaccinia growth factor (VGF) genes (WRDD) to enhance its tumour selectivity (Thorne et al., 2007).

Recently, the antitumour potencies of WRDD strain and VVL strain with TK gene deletion (VVL15) were further evaluated using a broader range of *in vitro* and *in vivo* cancer models (Hughes et al., 2015). Of the 12 additional human tumour cell lines tested *in vitro*, VVL15 demonstrated superior cytotoxicity over WRDD in 11 cell lines and equivalent cytotoxicity to

WRDD in one cell line. In a number of immunocompetent mouse cancer models, VVL15 also showed greater antitumour potency and tumour-selective replication than WRDD.

An 8% difference between genome sequences of Lister strain and other VV strains was observed (Garcel et al., 2007), which may cause the phenotypic and functional variations between strains (Ahmed et al., 2015). For example, compared with WR strain, VVL encodes at least three extra cytokine binding proteins that include two tumour necrosis factor (TNF) binding proteins and one interleukin (IL)-18 binding protein. Upon infection, these binding proteins block the ability of TNFs and IL-18 to interact with their corresponding cellular receptors, thereby attenuating host antiviral defences (Reading et al., 2002; Smith et al., 2000). However, VVL is deleted for at least one cytokine (IFN) binding protein gene, B18R, that is present in the WR genome (Alcami´ et al., 2000). Comparison between Lister and WR strains also demonstrates difference in genomic sequences that encode anti-apoptotic protein serpin SPI2 (WR195) (Ahmed et al., 2015). In addition, Lister strain codes for L156, an immunomodulatory protein that demonstrated *in vivo* pro-inflammatory properties. The gene that manufactures L156, namely A39R, has a frameshift mutation in the WR strain, presumably resulting in the production of a non-funtional truncated version of the protein (Zhang et al., 2009, Gardner et al., 2001). Much remains to be clarified about the impacts of these VV strain-based genetic differences on the induction of anticancer immune responses, host toxicity, and anticancer efficacy.

1.1.6 Mechanisms of oncolytic VVL antitumour efficacy

Oncolytic Lister strain VV, like other oncolytic viruses, mediates tumour cell death via direct and indirect mechanisms that involve direct oncolysis, vascular effects and innate and adaptive immunity.

(1) Direct viral oncolysis

Oncolytic VV can direcly infect, propagate in and lyse tumour cells, leaving the healthy cells unharmed. The released progeny virions can in turn spread to surrounding tumour cells and cause further direct destruction (Al Yaghchi et al., 2015).

Chen et al. (2011) observed a critical role of viral-mediated direct tumour cell killing in VVL oncolytic virotherapy. The increased replication efficiency of a series of recombinant VVL in tumour cell cultures was indicative of enhanced antitumour efficacy in the corresponding tumour xenografts.

(2) Local vascular destruction

Breitbach et al. (2013) observed the infection and disruption of tumour-associated vasculature in humans by JX-549, an oncolytic VV engineered from the Wyeth vaccine strain. The authors suggested that VV infection of tumour-associated endothelial cells is ascribed to the dysregulation of EGFR/Ras signalling pathways and elevated levels of VEGF within tumour vasculature. The infection is believed to give rise to formation of clots and mechanical blockage of vessels, causing damage and collapse of tumour vasculature. The authors also proposed that the infection-induced changes in endothelial cell cytoskeleton may too contribute to the disruption of tumour vasculature. Ahmed et al. (2014) have observed the infection and destruction of tumour-associated vascular endothelial cells by a Lister strain VV with TK deletion (VVL15).

(3) Amplification of host anticancer immune responses

Both adaptive and innate immune systems play important roles in oncolytic VV therapy.

The antiviral immune response elicited by oncolytic VV infection can be redirected to tumour. A prior viral infection of a host can enhance the infiltration of CD4+ and $CD8^+$ T-lymphocytes into tumour borne by the host upon subsequent challenge with the same virus. Mice that had been immunized with a derivative of the VV WR strain (vSP) were inoculated with colorectal adenocarcinoma CT26 cells to establish subcutaneous tumours. Intratumoural injection of vSP redirected the immune response against vSP to tumours, which led to the reduction in tumour volume and increase in infiltration of lymphocytes in tumour sides compared to naïve hosts (Hu et al., 2007). A similar phenomenon with VVL15 was also observed (Ahmed et al., 2014).

Via direct oncolysis, oncolytic VV can trigger immunogenic cell death (ICD) characterized by the release and/or exposure of damage-associated molecular patterns (DAMPs), such as adenosine triphosphate (ATP), calreticulin (CRT), and high mobility group box 1 (HMGB1), to the immune system. These danger signals (DAMPs) are able to activate and mature antigen-presenting cells (APCs) via interacting with receptors and ligands on immature dendritic cells

(DCs) and subsequently facilitating the process of phagocytosis. The activated DCs can in turn elicit anti-tumour T cell response and stimulate long-lived tumour immunity (Inoue & Tani, 2014; Bartlett et al., 2013).

The innate immune system also contributes to the antitumour efficacy of oncolytic VV. Cell line-specific tumour regression mediated via GLV-1h68, a recombinant VVL, was observed in xenografts deprived of adaptive immune function. Expression profiling demonstrated a positive association between the tumour rejection and upregulation of immune genes consistent with innate defence activation (Worschech et al., 2009).

1.1.7 'Armed' oncolytic VVL

Integration of relevant therapeutic transgenes into VVL backbone has been demonstrated to reinforce all the mechanisms above and improve the overall anti-tumour effect of therapy.

p53 is a gene that functions as a powerful tumour suppressor. Its mutations are present in more than half of cancers (Freed-Pastor & Prives, 2012). When armed with p53, VVL can express and restore this dysfunctional gene in cancer cells, which consequently promotes the direct virus-mediated cytotoxicity. Fodor et al. (2005) observed an apoptotic morphology among a majority of murine bladder cancer cells infected with replication competent VVL containing a human p53 gene (rVV-p53). The infection induced far greater cell death than the control virus *in vitro*. Instillation of rVV-p53 into a syngeneic orthotropic murine tumour model reduced tumour incidence and increased survival compared with control.

Endostatin and angiostatin are two potent endogenous angiogenesis inhibitors. The injection of VVL engineered to encode an endostatin–angiostatin fusion transgene gave rise to lower tumour micro-vessel density, improved survival and decreased virus-induced side effects in a human HNSCC (head and neck squamous cell carcinoma) xenograft model compared with the control virus (Tysome et al., 2011).

Interleukin IL-2 and IL-12 are immunomodulatory cytokines with potent ability to induce anti-tumour activity. Recombinant VVLs expressing IL2, IL12 or both induced a high level of cytokine expression and significant inhibition of tumour growth compared with their unarmed control counterpart following low-dose intratumoural administration in a C6 glioma xenograft model (Chen et al., 2001).

Bispecific T-cell engager (BiTE) molecules are engineered bispecific antibodies that tether T lymphocytes to tumour cells via simultaneously binding specific surface antigens on tumour cells and T cells (Chen et al., 2016). This leads to direct cytotoxicity activity toward cancer cells regardless of their oncolytic VV infection status. *In vitro* experimentation has demonstrated that an oncolytic VV armed with BiTE (EphA2-TEA-VV) was capable of inducing bystander killing of non-infected A549 cancer cell line at relatively high MOIs. Augmented antitumour effects have also been observed in the A549 xenograft tumour model that received the BiTE-armed oncolytic VV compared with the unarmed control (Yu et al., 2014).

The list above is not exhaustive. Numerous transgenes expressing immunomodulatory cytokines and molecules, prodrug-converting enzymes, antiangiogenic agents and other factors capable of improving viral spread and penetration within tumour have been investigated and evaluated on their abilities to improve the antitumour efficacy of VVs (Kim & Thorne, 2009).

1.1.8 Combination therapy for cancer with oncolytic VVL

Oncolytic virotherapy can be much more efficacious when combined with other modalities of cancer treatments as it is non-cross resistant with most other forms of cancer therapy.

(1) Combination of oncolytic VVL with chemotherapy.

Synergistic antitumour efficacy has been reported between oncolytic VVL and chemotherapy. For example, cyclophosphamide (CPA) is a chemotherapy drug commonly used for the treatment of lymphomas, leukaemia, myeloma, lung cancer and breast cancer. It is known to cause crosslinking of DNA and ultimately induce apoptosis. It has been used jointly with GLV-1h68 in a lung adenocarcinoma xenograft model and demonstrated in vitro synergy. The enhanced tumour growth inhibition achieved by the combination therapy is believed due to the tumour-killing effect of GLV-1h68 and the additional therapeutic effect that CPA exerts on normal endothelial cells of tumour vasculature (Hofmann, Weibel and Szalay, 2014).

VVL can also enhance the local delivery of chemotherapies. A prodrug is an inert chemotherapeutic compound that requires enzymatic activation *in vivo* to achieve full activity. Prodrug convertases are responsible for the conversion of a relatively safe prodrug into a highly toxic metabolite (Miest & Cattaneo, 2014). By harnessing its tumour-tropic properties, VVL

carrying transgenes that express the prodrug convertases can restrict the expression of the fully activated, highly potent cytotoxic agents to within the tumour microenvironment, thereby reducing the systemic toxicity.

GLV-1h68 contains a transgene that encodes β-galactosidase. (1S)-seco-CBI-DMAI-b-D-galactoside 1 is a prodrug that was developed based on the highly potent natural antibiotic duocarmycin SA and can be activated by β-galactosidase. Tumour size in GI-101A breast cancer xenografts treated with the prodrug and GLV-1h68 reduced significantly in comparison with the non-prodrug-treated GLV-1h68-injected control (Seubert et al., 2011).

(2) Combination of oncolytic VVL with radiation therapy.

Synergistic antitumour efficacy has been reported between oncolytic VVL and radiation therapy. Kyula et al. (2014) revealed that GLV-1h68 in conjunction with radiotherapy significantly delayed tumour growth and increased survival in a ^{V600E}BRAF mutant melanoma xenograft model compared to either treatment alone. GLV-1h68 infection was found to induce phosphorylation of MAPK in a number of melanoma cell types and active one or more MAPK signalling pathway(s) including JNK (c-Jun N-terminal kinase) pathway, which results in elevated TNF-α secretion. TNF-α had been shown to function as a survival signal in BRAF mutant melanoma cells. Radiation therapy can cause attenuation of GLV-1h68-induced JNK phosphorylation and inhibition of JNK pathway in the BRAF mutant cells, therefore reducing TNF-α secretion and facilitating BRAF mutant cell death.

VVL can also enhance the local delivery of radiation therapy. For example, human sodium iodide symporter (hNIS) is a naturally occurring protein that occurs predominantly in the human thyroid. It enables cells to concentrate iodide or similar isotopes intracellularly (Miest & Cattaneo, 2014). When incorporated into the genome of VVL, a transgene expressing hNIS can be localized to the tumour microenvironment, thus inducing radiation poisoning that specifically targets tumours.

GLV-1h153 is a recombinant VVL that expresses hNIS. The combination of GLV-1h153 with radioactive iodine (^{131}I) therapy has demonstrated effective stabilisation of tumour growth and significant improvement of survival in PC3 prostate cancer xenografts compared with either therapy alone (Mansfield et al., 2016).

1.2 CV-1 Cell Line in viral vaccine production

1.2.1 History and cultivation of CV-1 cell line

Like other viruses, VV is an obligate parasite that requires a host for nutritional needs and replication. Choice of cell lines will not only affect the productivity, safety and efficacy of a viral product, but also the performance of manufacturing process. Therefore, selection of an optimal host cell line and the media that supports healthy cell growth and efficient oncolytic VV production is of vital importance.

The CV-1 cell line (ATCC-CCL-70) was first established in 1964 with a tissue section cut from the kidney of a 141-days-old normal male African green monkey (*Cercopithecus aethiops*) by Jensen et al. (1964) who described the cell type as epithelial. However, other resources, including American Type Culture Collection (ATCC) and the European Collection of Authenticated Cell Cultures (ECACC), refer to CV-1 as a fibroblast cell line ("CV-1 CCL-70™", n.d.; "ECACC General Cell Collection: CV-1", n.d.).

The discrepancies between literature sources in the description of the cell type can be a result of different culture conditions. At low confluence, the cells are well spread and more stretched, displaying bipolar or multipolar shapes (**Figure 1.2a**, **1.2b**), which is more fibroblast-like. However, once the cells reach near-confluence, they appear much more regular and polygonal, demonstrating an epithelial-like morphology (**Figure 1.2c**). As both bipolar and elongated cell shapes can be observed in our confluent CV-1 culture (**Figure 1.2d**), we consider CV-1 as fibroblast in this thesis.

As an adherent cell line, CV-1 needs to attach to a suitable substrate. Expansion of CV-1 has been reported mostly in traditional culture plates, roller bottles or multi-tray systems under static conditions, and in a few cases on microcarriers in suspension (**Table 1.3**). Growth media are usually Eagle's Medium-based and supplemented with 5% to 10% (v/v) of serum with one exception in SFM supplemented with milk (**Table 1.3**). The splitting ratio is recommended as 1:2 – 1:6 depending on the confluence of the culture prior to passage (Jensen et al., 1964; "CV-1 CCL-70™", n.d.; "ECACC General Cell Collection: CV-1", n.d.; Contreras et al., 1985). The cell line exhibits a population doubling time of 18-22 hours when grown in Eagle's medium with 5-10% serum (D'Alisa & Gershey 1980; Hagedorn et al., 1985).

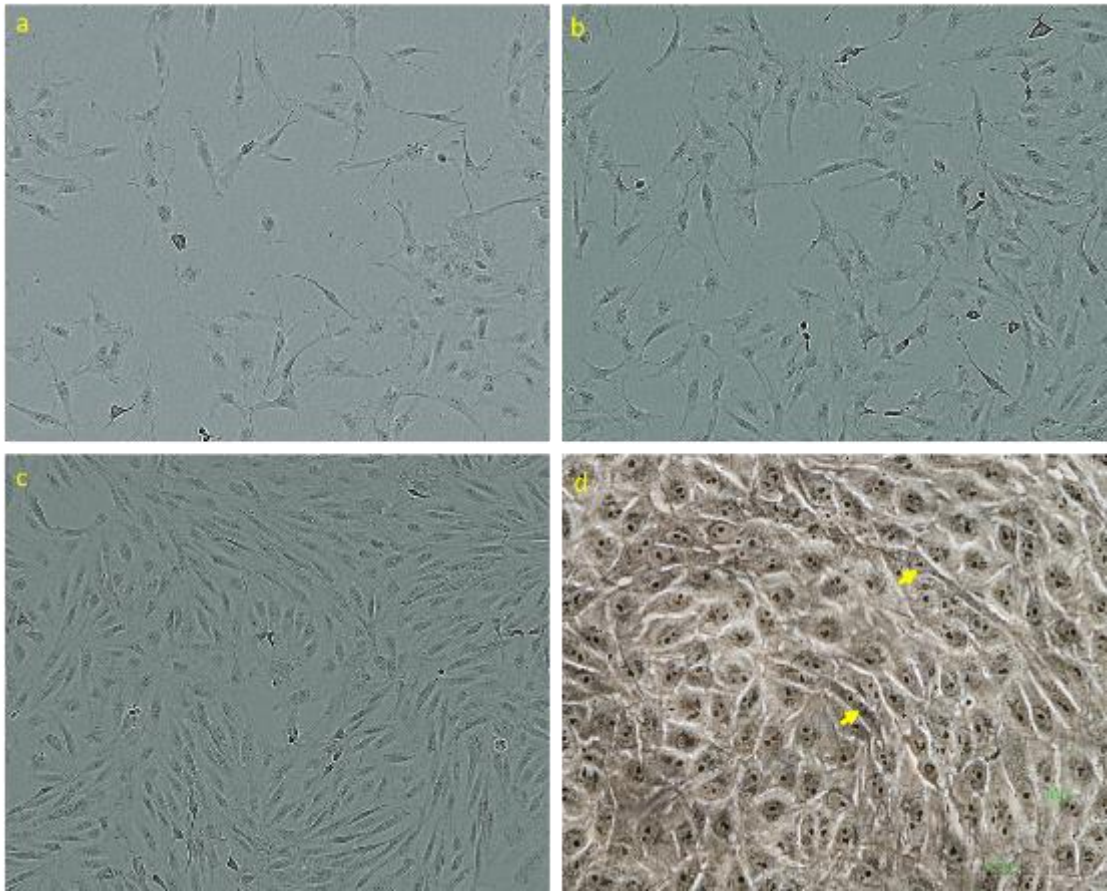

Figure 1.2: Morphology of CV-1 cell line. (a) (b) (c): Images for CV-1 cells grown in DMEM + 2mM Glutamine + 10% FBS 24, 48 and 96 hours post seeding respectively ("CV-1 CCL-70™", n.d.); (d) Image for CV-1 cells grown in our lab in DMEM + 10% FBS at 100% confluence at 20× magnifications. Yellow arrows indicate more typical spindle-shaped fibroblast cells.

Table 1.3 Summary of culture conditions of CV-1 cell line.

Cell Growth Medium	Type of Culture	Culture Vessel	Reference
DMEM + 10% FBS + HEPES/ antibiotic-antimycotic solution	Static	Tissue culture plates, flasks; roller bottles	Ehrig et al., 2013; Mered et al., 1980
	Microcarrier	DEAE-Sephadex beads at low anion exchange capacity in spinner flasks with a working volume of 100 ml	Mered et al., 1980
DMEM + 5% FCS + antibiotic solution	Static	Tissue culture flasks	Ahmed, 2015
DMEM + 10% FCS	Static	Roller bottles; cell factory	Giard et al., 1977; Hiley, 2011
	Microcarrier	DEAE-Sephadex-like beads at low anion exchange capacity in spinner flasks with a working volume of 100 ml	Giard et al., 1977
DMEM + 2% bovine colostrum (SFM)	Static	Tissue culture plates coated with/ without fibronectin	Sue Steimer et al., 1981
DMEM + 10% bovine milk obtained 80 days after the onset of lactation (SFM)	Static	Fibronectin-coated tissue culture plates	
EMEM +10% FBS	Static	Roller bottles	Gershey and D 'Alisa, 1980

1.2.2 Transformation and tumourigenicity testing of CV-1 cell line

Some safety and quality concerns for cell-derived biological products have arisen due to the existence of extraneous contaminants or from the properties of the cell line adopted to produce the product. Therefore, cells must be scrutinized appropriately so as not to cause adverse events in patients. On this front, the guidance documents issued by the international regulatory authorities (European Medicines Agency, World Health Organisation and the Food and Drug Administration) require comprehensive characterization and testing of the cell line to confirm its identity, purity, and suitability for manufacturing use (EMA, 1998; WHO Expert Committee on Biological Standardization, 2013; U.S. FDA, 2010). There are additional concerns for continuous cell lines as acquisition of their indefinite *in vitro* life span could involve oncogenic and viral components. When using these cell lines for production, attentions should be given to the efficient removal of residual cells, host-cell DNA, adventitious and endogenous agents, and detailed analysis of the cell line's tumourigenicity is required.

Petricciani et al. (1987) and Contreras et al. (1985) have tested CV-1 cells at low passage levels for the ability to form tumours in antithymocyte globulin (ATG)-treated new born rats and nude mice. Results from both papers suggested that CV-1 cells were non-tumourigenic. However, similar to Vero cells, CV-1 cells at high passage numbers (146 to 257 times) formed invasive adenocarcinomas at the inoculation site of the rat model. Increased tumourigenicity of CV-1 cells was observed with increasing cell passage (Furesz et al., 1989). Results obtained from the *in vitro* tumourigenicity assays using chick embryo skin, muscle organ cultures or soft agarose, confirmed the results from rodent testing: CV-1 cells at low passage levels exhibited limited mitotic activity, non-invasiveness and no induction of transformed colonies (Petricciani et al., 1987; Contreras et al., 1985); yet, increased cell passage led to higher cell colony formation (Furesz et al., 1989) as shown in **Table 1.4**.

Table 1.5 lists the additional characterization and qualification tests that CV-1 may need to undertake before being used for vaccine manufacturing.

Table 1.4 Summary of results of tumourigenicity tests for CV-1 cell line.

Study Type	Test System	Passage Number	Result	Reference
In Vitro	soft agarose colony formation assay	33,38,46	No formation of any colonies	Contreras et al., 1985; Petricciani et al., 1987
		146 to 257	Increased tumourigenicity with increasing cell passage	Furesz et al., 1989
	Mini-Organ Cultures (MOC) assay	33,38,46	No invasion of the human muscle cells	Contreras et al., 1985; Petricciani et al., 1987
	Chick embryo skin assay	33	Low mitotic activity	Contreras et al., 1985
In Vivo	Athymic nude mice	38, 46	No tumour nodule detected	Petricciani et al., 1987
		36	All mice produced small nodules at day 7 post-inoculation. All nodules regressed but some were still detectable at 21 days. Neither local invasion nor metastasis was detected.	Contreras et al., 1985
	Antithymocyte globulin (ATG) treated new born Wistar rats	37	Small nodules were produced in all rats at day 6 post-inoculation and fully regressed by day 21. Neither local invasion nor metastasis was detected.	Contreras et al., 1985
		146 to 257	Increased tumourigenicity with increasing cell passage	Furesz et al., 1989

Table 1.5 The characterization and qualification tests that may be required of CV-1 prior to its use for vaccine manufacturing (adapted from U.S. FDA, 2010).

Test type and detection subject			Aim of the test
Adventitious agents	*In vitro* tests for viruses	Cell culture safety tests	To assess cell line for contamination with human or simian viruses, such as adenoviruses, influenza viruses, poxviruses, herpes B virus etc.
		Transmission Electron Microscopy	To ensure the absence of viral particles in a cell line
		Biochemical tests and infectivity tests for retroviruses	To ensure the absence of infectious retrovirus in a cell line
		PCR or other specific *in vitro* tests	To assess cell line for contamination with viruses that cannot be easily grown in culture, such as HIV, hepatitis B virus, hepatitis C virus etc.
	In vitro tests for non-viral agents	Mycoplasma	To ensure the absence of mycoplasma contamination
		Bacterial and fungal sterility	To ensure the absence of bacteria and fungi
		Mycobacteria testing	To ensure the absence of mycobacteria
Cell properties	Further tumourigenicity tests		To assess tumour-forming potential of a cell line after inoculation into animals
	Oncogenicity tests		To detect the presence of oncogenic substances
	Identity testing of cell line		To ensure that the cell identity is as stated
	Genetic stability testing		To verify that the cell line is genetically stable from the establishment of the Master Cell Bank all the way through to/ beyond the end of production.

Continuous cell lines, although tumourigenic at certain passage levels, are generally considered as acceptable as host cell lines in bio-manufacturing provided that the products have been highly purified during the manufacturing process (WHO Expert Committee on Biological Standardization, 2013). The passage level of the cells in production should be restricted and the cell characterization should be performed at or beyond the maximum-utilized passage number. In fact, several tumourigenic cell lines, such as Vero and Madin-Darby canine kidney (MDCK) cells, are currently being used in the manufacture of human viral vaccines, upon the extensive characterization of their tumourigenic and oncogenic potential and careful risk-benefit evaluation. The Vero cell line has been licenced for the production of rotavirus (RotaTeq® and Rotarix®), Japanese encephalitis (JE-VAX), smallpox (ACAM2000) and influenza vaccines (Preflucel® and Celvapan®) (Barrett et al., 2009; Milián & Kamen, 2015) and the MDCK cell line has been licenced for the production of influenza vaccine (Flucelvax®) (Milián & Kamen, 2015).

1.2.3 CV-1 cell line as a vaccine production host

To our knowledge, manufacturing of CV-1 cell-derived vaccines has been confined to lab scale. In 1981, CV-1 cells were used to produce poliovirus type 1, 2 and 3 in both static and microcarrier cultures. The viral volumetric (pfu /ml) and specific (pfu /cell) productivities in microcarrier spinner flasks were not significantly different from those in conventional T-flasks and roller bottles (Mered et al., 1981). CV-1 cells have also served as a laboratory cell line for propagation of different strains of VV, including Lister strain VV (Ehrig et al., 2013; Hiley et al., 2013; Yu et al., 2014; Ahmed et al., 2015). The production capacity was expanded in a scale-out manner by the addition of parallel culture flasks. The Yaba-like disease (YLD) virus, which is also from the Poxvirus family but belongs to the yatapoxvirus genus, act as a substitute for VV in cancer gene therapy. Hu et al. (2001) reported the production of high-titre (10^{10} pfu /ml) YLD virus in CV-1 cells in T-150 flasks.

1.3 Anchorage-dependent cell based viral vaccine manufacturing

1.3.1 Development of serum-free media for viral vaccine production

1.3.1.1 Development of serum-free media

During the early years of *in vitro* cultivation of mammalian cells, biological fluids, such as lymph, serum, plasma clot and other blood or tissue extracts, were used as culture media of which the components were not specifically defined (Rodriguez-Hernandez et al., 2014). Meanwhile, the successful cultivation of animal cells in these natural media has given the scientists strong impetus to specify the growth-promoting substances within the natural materials and to substitute them with defined components.

One noteworthy pioneer in the development of synthetic media was Harry Eagle. In 1955, he reported a basal nutrient formulation (BME) that featured a balanced salt solution, sugars, 13 essential amino acids and eight necessary vitamins (Eagle, 1955). In 1959, Eagle modified BME by increasing the concentration of amino acids (Eagle, 1959). The revised formulation has been known as minimal essential medium (MEM). Both BME and MEM have found wide applications in the culture of cell lines and laid the foundations for most nutrient media prepared today (Gruber and Jayme, 1994), including DMEM used in this thesis. However, the media still needs supplementation with plasma, serum, or tissue extracts to adequately support cell growth.

From this point onwards, two different parallel development strategies for synthetic media were undertaken. One strategy focused primarily on the optimization of nutrient concentrations for maximizing proliferation. The other strategy put effort into the elimination of serum (Jayme, Watanabe, & Shimada, 1997).

Adopting animal serum in the manufacturing process presents drawbacks mainly due to the potential presence of microbial contaminants (viruses, bacteria, and fungi) or the bovine spongiform encephalopathy (BSE) agent. Also, the high protein content introduced by serum brings about challenges of removing the proteins during downstream processing (Burgener and Butler, 2006). The geographical and seasonal differences in serum composition and the variations among batches can result in inconsistencies in growth-promoting properties and final product quality (Dimasi, 2011). Finally yet importantly, serum of excellent quality is an expensive supplement with limited availability.

The initial step in the development of serum-free media involves the substitution of serum with protein hydrolysates of bovine source such as Primatone^{TM} RL or bactopeptone and with the addition of a number of animal-derived proteins (Siemensma et al., 2010). The combination of insulin, transferrin and selenium (ITS) has proved to be an effective serum substitute required by many cells (Barnes & Sato, 1980). Moreover, Hiroki Murakami et al. (1982) discovered that ethanolamine is necessary for the serum-free cultivation of hybridomas and other rapidly growing cell types. The mixture of these four substances (insulin, transferrin, selenium, ethanolamine) (ITES) has become commercially available and been employed as a supplement to basal media to enable the growth and expansion of various cell types under serum-free conditions.

Even though such SFM are more defined than SCM, the risk of bringing harmful contaminants such as viruses and prions to the final therapeutic product by using animal-derived components still exists, suggesting that only a complete substitution of components of animal origin with non-animal derived materials is conductive to a relatively safe SFM (Merten 2002; Galbraith 2002). In addition, the European Medicines Agency (2011) explicitly expresses the preference for the use of non-animal alternatives where available and requires justification of the use of materials of animal origin. Driven by the regulatory concerns, increased efforts have been directed towards formulating serum free and animal-derived component free (ADCF) media. Animal-derived substances are replaced by various substitutes, such as plant-based hydrolysates including those derived from wheat, soy and cottonseed, bioactive synthetic chemicals and recombinant versions of the proteins produced in microorganisms such as insulin and various growth and attachment factors. **Table 1.6** summarizes the animal-derived components commonly used in cell culture and/or viral production medium and their non-animal replacements.

Typically, protein-free media (PFM) is not only serum-free but also free of polypeptides elements usually detected by standard protein assays. This may further reduce the potential risks of introducing adventitious contaminants, such as those associated with fermentation of raw materials for the manufacture of recombinant proteins. The absence of proteins in media may also alleviate the number and complexity of purification steps required to separate and remove contaminants from the desired product, thus minimizing product loss and improving efficiency in downstream processing (Jayme & Smith, 2000). PFM may still contain undefined constituents such as peptide fractions from protein hydrolysates produced from plants or animals (if not ADCF) using acids or enzymes.

In contrast to the types of media mentioned above, chemically defined media (CDM) requires that all constituents and their concentrations be known. They are usually (but not always) protein-free and composed exclusively of low-molar-mass additives. Supplements such as hormones and growth factors obtained from synthetic, recombinant, plant or animal sources can only be considered appropriate in CDM if they are highly purified (Van Der Valk et al., 2010). Therefore, there is a slight or even negligible potential for introducing adventitious agents. Furthermore, these media offer stability and reproducibility for cell culture. **Table 1.7** summarizes the major distinctions among the different types of synthetic media.

In general terms, exclusion of serum in media adversely affects the universality of the culture environment (Jayme & Smith, 2000). The variability of growth requirements between cell lines narrows the range of cell types that a single SFM can be applied to. To obtain optimum growth and yield performances in a given SFM, additional nutritional adjustment may be required based on the specific needs of a particular cell line.

On the other hand, elimination of serum has led to enhanced biological performances compared with their serum supplemented counterpart (Burgener & Butler, 2006). This is related to the removal of serum-associated inhibitors, neutralizing antibodies and protease in the media (Jayme & Smith, 2000).

Table 1.6 Common animal-derived medium constituents and their non-animal alternatives (adapted from Jayme & Smith, 2000).

Constituent	Functions	Animal Origin	Non-animal Replacement
Insulin	A protein hormone that promotes cell proliferation and helps cells uptake and utilize glucose, amino acids and lipids.	Bovine or porcine pancreas	Zinc; bovine or human recombinant
Transferrin	A universal iron carrier protein that facilitate transportation of iron into cells.	Bovine, porcine or human plasma fraction	Iron-complexes (Inorganic iron salt + chelator)
Attachment and growth factors	Polypeptides that promote attachment, spreading and growth of cells (on culture vessels)	Murine or bovine organ digests	Recombinant factors; collagen precursors
Fragments of serum protein (e.g., albumin, fetuin)	To serve as carriers for various low molecular weight substances; may promote cell adhesion, spreading and growth (Bjorkerud & Bjorkerud, 1994; Taub, 1990).	Bovine or other animal serum	Synthetic; lipid transporting alternatives; plant-derived hydrolysates
Amino acids (e.g., hydroxyproline, tyrosine, cysteine)	Monomers to proteins; make up all proteinaceous material of the cell; used for cell growth and maintenance (Salazar, Keusgen, & Von Hagen, 2016).	Human hair, avian feathers, bovine collagen, bovine or porcine bone gelatin	Synthetic, recombinant or plant-derived amino acids
Protein hydrolysates	A source of free amino acids, small peptides, lipids, inorganic salts, carbohydrates, and vitamins	Bovine milk, peptones	Plant-derived hydrolysates
Lipids / sterols	To serve as structural constituents of cell membranes, in energy storage and signal transduction.	lanoline, piscine lipids, egg oil, bovine tallow, porcine liver	Plant-derived sterols; synthetic and plant-derived fatty acids
Detergents (e.g., Tween 80)	To enhance the solubilisation of the lipophilic substances in the media.	Bovine tallow	Plant-derived fatty acids

Table 1.7 Comparison of compositions of different types of synthetic media.

Synthetic Media	Type	Serum	Protein	Animal Source	All Components Identifiable
Serum containing media		+	+	+	-
Serum free media	SFM	-	+	+	-
	ADCF	-	+	-	-
	PFM	-	-	-/ +	-
	CDM	-	-/ +*	-/ +*	+

(+) =present in medium; (-) =absent from medium; (*) = highly purified

1.3.1.2 Serum-free viral vaccine production

Table 1.8 summarizes serum-free production of human viral vaccines in the most common host cell lines. Compared with continuous cell lines, the development of complete serum-free processes based on primary or diploid cell lines has not been easy as a result of the complex nutritional requirements of these cells.

Since the 1970's, continuous cell lines have been gradually accepted for safe and effective viral vaccine manufacturing. Characterized and validated spontaneous immortalized cell lines (such as VERO, MDCK and EB66) and engineered immortalized cell lines (such as HEK293, PER.C6 and AGE1.CR.pIX) have been established for this purpose. An increased number of serum-free processes for manufacturing clinical trial or commercial-scale human viral vaccines has emerged:

Optaflu®/ Flucelvax®, a regulatory authorities-approved trivalent inactivated subunit influenza, is propagated in MDCK cells in a serum-free and protein-free medium (Hu et al., 2011). The FDA licensed smallpox vaccine ACAM 2000® has been produced using Vero cells under serum-free conditions in 1200L commercial-scale bioreactors (Monath et al., 2004). The Vero cell line has also been employed to manufacture 17 different seasonal and pandemic (-like) influenza vaccine strains in a serum protein free medium under GMP conditions (Kistner, 2013). Propagation of clinical grade oncolytic measles viruses (MV-CEA and MV-NIS) in Vero cells has been carried out in medium without serum at 25-50L scale using cell factories (Ungerechts et al., 2016).

Regarding feasibility studies, a variety of viruses have been propagated at laboratory scale entirely free of serum using continuous cell lines in a range of production formats (**Table 1.8**).

Peak volumetric (virus quantities/ ml) were compared between viruses produced in serum-free and serum-containing media (**Table 1.9**). In more than 70% of the cases, comparable or higher peak volumetric productivities were obtained under serum-free conditions compared with their counterparts in serum-containing media, suggesting the usefulness of SFM in supporting cell growth and/or virus proliferation.

Table 1.8 Cell growth and viral vaccine production in SFM.

	Cell Line	Origin	Viruses (Vaccines)	SFM	Production process	Reference
Primary Cell	CEF	Chicken embryo fibroblast	Poxvirus (myxoma virus strain Lausanne, VV Copenhagen, canarypox, Modified Vaccinia Ankara (MVA)	VP-SFM	Plate cultures; 850 cm^2 roller bottles; lab scale fixed bed bioreactor with carriers	Gilbert et al., 2005; Knowles et al., 2013
Diploid Cell Line	MRC5	Human embryonic lung	Measles, Varicella-zoster, Dengue viruses, NYCBH strain VV	IPT-AF, DMEM/ Ham's F-12 (2:1, v/v)	Microcarriers + spinner flasks/ lab scale bioreactors; plate cultures	Rourou et al., 2014; Chun et al., 2005; Liu et al., 2008
Continuous Cell Lines	MDCK	Canine kidney	Influenza A (H1N1, H5N1), influenza B virus, live attenuated influenza vaccines (LAIV), live cold-adapted (CA) attenuated influenza vaccine (A H3N2, A H1N1 and B)	MDCK-SFM1, MDCK-SFM2, Ex-cell MDCK, Plus-MDCK, MediV100 SFM, SMIF8, EpiSerf, Ex-CellMDCK, Axcevir-MDCK, SFM4BHK21, UltraMDCK	Microcarriers + Erlenmeyer flasks/ spinner flasks/ lab scale stirred/ wave bioreactors; suspension adapted MDCK cells + shaker flasks/ lab scale stirred / wave bioreactor; 850 cm^2 roller bottles; plate cultures	Huang et al., 2015; Hu et al., 2011; Aggarwal et al., 2011; Genzel et al., 2006; Van Wielink et al., 2010; Ghendon et al., 2005; Tree et al., 2001; Genzel et al., 2006; Genzel et al., 2009.
	Vero	African green monkey kidney	Japanese encephalitis virus, poliovirus Sabin 1, poliovirus 1, 2 and 3, dengue viruses, rabies, NYCBH strain VV, vesicular stomatitis virus, herpes simplex virus, 17DD yellow fever virus, enterovirus 71, paramyxovirus, lytic virus, reovirus, measles, Influenza virus seasonal (H1N1, H3N2, B) and pandemic (-like) (H5N1, H1N1, and H9N2), MEDI-534 chimeric human parainfluenza virus type 3/respiratory syncytial virus	VP-SFM, MDSS2, IPF-AF, M-VSFM, Williams' Medium E, EX-CELL Vero, OptiPRO	Plate cultures; cell factory; microcarriers + spinner flasks/ lab and industrial scale stirred bioreactors/ lab, pilot and industrial scale fixed bed bioreactor with carriers	Butler et al., 2000; Yuk et al., 2006; Knowles et al., 2013; Toriniwa and Komiya, 2007; Merten et al., 1997; Rourou et al., 2014; Rourou et al., 2007; Liu et al., 2008; Monath et al., 2004; Paillet et al., 2009; Forno, 2013; Souza et al., 2009; Chen et al., 2011; Mattos et al., 2015; Wu et al., 2004; Ungerechts et al., 2016; Kistner, 2013; Langfield et al., 2011
	HEK293	Human embryonic kidney	Influenza A (H1N1), adenovirus, adeno-associated virus	CD293, 293-4-06, 50% CD 293 + 50% SFM4HEK-293, 10% CDM4HEK293 + 85% F17 + ~ 5% Optimem, Optipro or F17, HyQSFM4Transfx293	Plate cultures; microcarriers + lab scale stirred bioreactors; suspension adapted HEK293 cells + Erlenmeyer flasks/ lab scale and pilot scale stirred bioreactors/ 4.3-20L WAVE bioreactors	Tsao et al., 2001; Shen et al., 2015; Grieger et al., 2016; Iyer et al., 1999; Petiot et al., 2011

Table 1.8 (*Continued*)

	Cell Line	Origin	Viruses (Vaccines)	SFM	Production process	Reference
Continuous Cell Lines	PER.C6	Human embryonic retina	Influenza A and B strains, poliovirus serotype 1, 2 and 3, recombinant Adenovirus	Excell 525, Permexcis, Permab	850 cm^2 roller bottles; lab scale bioreactors	Pau et al., 2001; Sanders et al., 2013; Xie et al., 2002
	AGE1.CR, AGE1.CR.pIX	Duck retina	Influenza A (H1N1, H3N2) , influenza B Virus, MVA, canarypox, fowlpox virus, cold-adapted influenza A (H1N1), cold-adapted B influenza virus	adenovirus expression medium (AEM), HyQ®SFM4MegaVir, CD-U2, CD-VP	T-flask; 1L wave bioreactor; 1-50L bioreactors	Lohr et al., 2012; Lohr et al., 2009; Jordan et al., 2011

Table 1.9 Comparison of peak volumetric and specific virus productivity in serum-containing and serum-free media.

Cell Line	Virus	Medium		Process	Volumetric virus productivity		Level increase in volumetric virus productivity	Reference
		SCM	SFM		SCM	SFM		
CEF	Canarypox	DMEM+2% or 10% FBS	VP-SFM	850 cm^2 roller bottle	1.30×10^9 pfu/ml	3.01×10^8 pfu/ml	-76.9%	Gilbert et al., 2005
				T-25 flasks	1.14×10^7 pfu/ml	1.26×10^7 pfu/ml	+10.5%	
	MVA				2.27×10^8 pfu/ml	3.28×10^9 pfu/ml	+13.4 folds	
	VV Copenhagen				1.21×10^7 pfu/ml	3.58×10^7 pfu/ml	+1.96 folds	
	Myxoma strain Lausanne				9.46×10^6 pfu/ml	2.34×10^6 pfu/ml	-75.3%	
MRC5	Measles	MEM +10% FCS	IPT-AF	Cytodex 1, 250 ml spinner flask and 2L bioreactor	10^7 TCID50/mL	$10^{4.62}$ TCID50/mL	-2.22%	Rourou et al., 2014
	Varicella-zoster	Cell growth: DMEM + 5% FBS; Virus Infection: DMEM + 2% FBS	DMEM/ Ham's F-12 (2:1, v/v) + supplements	T-25 flasks	cell-free virus: 8.2×10^4 pfu/T-25	cell-free virus: 8.2×10^4 pfu/T-25	0.00%	Chun et al., 2005
					cell-associated virus: 7.3×10^5 pfu/T-25	cell-associated virus: 7.6×10^5 pfu/T-25	+4.11%	
	Dengue virus Den-1 Hawaii	DMEM + 10% FBS	M-VSFM	Cytodex 1, 100 ml spinner flasks	$(1.7\pm0.1)\times10^6$ pfu/ml	$(4.0\pm0.1)\times10^6$ pfu/ml	+1.35 folds	Liu et al., 2008
	Dengue virus Den-2 NGC				$(1.2\pm0.0)\times10^7$ pfu/ml	$(2.2\pm0.0)\times10^7$ pfu/ml	+83.3%	
	Dengue virus Den-3 H-87				$(1.3\pm0.1)\times10^4$ pfu/ml	$(3.0\pm0.1)\times10^4$ pfu/ml	+1.31 folds	
	Dengue virus Den-4 H-241				$(2.0\pm0.2)\times10^3$ pfu/ml	$(2.9\pm0.2)\times10^3$ pfu/ml	45.0%	
HEK293	Adenovirus Ad-dl312	DMEM+ 10% FBS	SFM (Life Technologies)	SCM: Cytodex 3, 2L or 4L bioreactors	$0.675\text{-}1.45\times10^{10}$ TCID50/mL	$0.325\text{-}1.45\times10^{10}$ TCID50/mL	-51.9%	Iyer et al., 1999
				SFM: suspension adapted HEK293, 2L bioreactor				

Table 1.9 (*Continued*)

Cell Line	Virus	Medium		Process	Volumetric virus productivity		Increase in volumetric virus productivity observed in SFM as compared to SCM	Reference
		SCM	SFM		SCM	SFM		
MDCK	Influenza H1N1	DMEM+ 10% FBS	MDCK-SFM1	Cytodex 3, 3L bioreactors	$(5.72\pm0.84)\times10^9$ virions/ml	$(3.13\pm0.95)\times10^9$ virions/ ml	-45.3%	Huang et al., 2015
	Live attenuated influenza H3N2 CA reassortant	Eagle MEM + 5% foetal serum	Axcevir-MDCK	Cytodex 1, 1 L spinner flask	$10^{8.5}$ EID50/ ml	$10^{9.0\text{-}9.5}$ EID50/ ml	+2.16 to +9.00 folds	Ghendon et al., 2005
	Live attenuated influenza B CA reassortant							
Vero	Poliovirus Sabin 1	DMEM+ 2% FCS	MDSS2	Static dish culture	$10^{6.75}$ TCID50/50µl	$10^{6.67}$ TCID50/50µl	+4.71%	Merten et al., 1997
	Rabies	MEM+ 10% FCS	IPF-AF	Cytodex 1, 2L bioreactor, recirculation	Comparable to that obtained in SFM	3.5×10^7 FFU/ml	Comparable	Rourou et al., 2014
	enterovirus 71	M199 + 10% FBS	M-VSFM	Cytodex-1, 2 L bioreactor	Extracellular: 8.9×10^7 TCID50/ml	Extracellular: 5.8×10^7 TCID50/ml	-34.8%	Wu et al., 2004
					Intracellular: 3.2×10^6 TCID50/ml	Intracellular: 9.0×10^6 TCID50/ml	+1.81 folds	
	Dengue virus Den-1 Hawaii	DMEM + 10% FBS		Cytodex 1, 100 ml spinner flasks	$(6.0\pm0.1)\times10^5$ pfu/ml	$(7.7\pm0.1)\times10^5$ pfu/ml	+28.33%	Liu et al., 2008
	Dengue virus Den-2 NGC				$(6.8\pm0.3)\times10^5$ pfu/ml	$(2.0\pm0.1)\times10^6$ pfu/ml	+1.94 folds	
	Dengue virus Den-3 H-87				$(4.5\pm0.7)\times10^3$ pfu/ml	$(1.3\pm0.3)\times10^4$ pfu/ml	+1.89 folds	
	Dengue virus Den-4 H-241				$(2.5\pm0.7)\times10^2$ pfu/ml	$(9.0\pm2.8)\times10^2$ pfu/ml	+2.60 folds	
	Vesicular stomatitis virus	Home-made SFM +2% FCS	Home-made SFM	Suspension adapted Vero, spinner flasks	1.7×10^8 TCID50/ml	4.6×10^5 TCID50/ml	-99.7%	Paillet et al., 2009
	17DD yellow fever virus	DMEM + 5% FBS	VP-SFM	Cytodex-1, 100ml spinner flasks	2.4×10^6 pfu/ml	5.5×10^7 pfu/ml	+22 folds	Souza et al., 2009

1.3.2 Adherent cell culture systems at intermediate to large scale for the production of viral vaccines

Anchorage-dependent cells have been traditionally utilized in many cell-culture-based human viral vaccine propagation systems (Genzel, 2015). Over the past decades, different cell culture systems for efficient viral production have been developed.

1.3.2.1 Adaptation to suspension culture

For an anchorage-dependent cell line that can be adapted to suspension growth without weakening its susceptibility to viral infection, it would be more desirable to use its suspension-adapted cell lineage for viral vaccine manufacturing (Warnock and Al-Rubeai, 2006). Novatis Vaccines GmbH has succesfully adapted the originally adherent MDCK cell line to grow freely suspended (Gregersen, 2008). The resulting cell line was named MDCK 33016 and has been used to manufacture the influenza vaccine Optaflu®/ Flucelvax®.

Scale-up of suspension cells primarily involves a rise in culture volume and is straightforward as it no longer requires the provision of cell attachment surface, thus avoiding steps of detachment and reattachment between successive cell cultivation (Van Wielink et al., 2010). Realization of process up-scaling can be relatively quick as soon as the basic culture parameters are comprehended. Besides, suspension culture systems are generally economic with regard to space, offering a reletively homogeneous culture environemnt, and allowing for precise, non-interuptive and even real-time monitoring and/or control of the physico-chemical (such as pH, temperature, dissolved oxygen) and physiological environment (such as glucose, lactate and ammonia).

1.3.2.2 Planar technologies

In 1933, George Gey from Johns Hopkins University proposed the concept of culturing cells in a rotating system (Gey, 1933), which inspired the invention of roller bottle. In 1978, a license for the manufacture of the RA27/3 strain of live attenuated rubella virus vaccine was granted to Merck Sharp & Dohme in the United States. The vaccine was manufactured in human diploid fibroblasts (WI-38) in roller bottle culture (Elliot, 1990). Besides the provision of increased surface area compared with traditional static culture flasks, roller bottles enhance nutritional homogeneity and gas exchange as a result of the gentle agitation and thinner medium coverage of cylindrical sidewall.

In 1978, scientists at Rentschler Biotechnologie GmbH joined T-flasks together to scale up the production of interferon beta with human fibroblasts. This served as the prototype of multi-tray bioreactor. In comparison with roller bottles (**Figure 1.3a**), multi-tray systems (**Figure 1.3b**) feature higher cell-to-volume ratios, less incubator space, reduced amount of manual handling, lower requirement on operator skills and improved process control. Some systems such as CellCube® and Xpansion® can be connected with additional apparatus for pH and dissolved oxygen (DO) regulation, gas mixing, medium conditioning and circulation (Blasey, Isch and Bernard, 1995; Legmann, 2016).

These two common types of parallelized static monolayer culture devices share some common disadvantages: they are labour intensive, have a relatively large footprint, high risk of contamination, limited choices for inoculation and harvesting methods and restricted monitoring and control of process parameters. Additionally, these devices are not truly scalable. Their scale-up is more of a scale-out, which is realized by adding extra culture units to increase the surface area.

Despite the drawbacks, roller bottles and multi-tray cultivation systems are still used in industrial production. This can be attributed to their relatively low cost, easy and well-established and well-characterized handling procedures. The invention of their fully automated counterparts (**Figure 1.3c** & **d**) further strengthens the systems' commercial implementation as it enables the handling of large quantities of culture units with significantly reduced manual work, likeliness of contamination and potential for human operational errors. The fully automated system CellMate™ has been applied to handle roller bottles that grow MRC-5 or Vero cell line for the production of Varivax® (a live Varicella Virus vaccine) or influenza vaccines Celvapan® and Vepacel® (Tap Biosystems, n.d.).

Figure 1.3: Static culture devices for adherent cell viral vaccine production. (a) Roller bottles with standard or expanded surfaces and a number of different surface areas; pictured are Corning® Roller Bottles (Corning, n.d.). (b) Multi-tray system consisting of a series of stacked trays; pictured are Corning® CellSTACK® cell culture chambers (Corning, n.d.). (c) Automated roller bottle processing; pictured is Cellmate automated cell culture system from TAP Biosystems (TAP Biosystems, n.d.). (d) Automated multi-tray units processing; pictured is Nunc™ automatic cell factory manipulator (Thermo Scientific, n.d.).

1.3.2.3 Microcarriers

For the adherent cell lines which have experienced difficulties in their suspension adaptation or of which the viral production performance is impaired post-adaptation, culturing them on microcarriers can be an alternative. Generally speaking, a microcarrier is a micron-sized spherical-shaped matrix that supports the attachment and expansion of adherent cells in suspension culture (**Figure 1.4**). The use of microcarriers allows the creation of a quasi-suspension environment: on one hand, similar to static culture, cells grow adherently on the outer surface (plus inner surface in the case of macrocarriers) of the matrix; on the other hand, like suspension culture, microcarriers with cells attached are kept in suspension throughout

most of the duration of the culture process. As a result, microcarrier systems provide not only the cultivation surface essential for adherent cells but also a higher surface area-to-volume ratio compared with the planar technologies. Furthermore, the procedure for isolating microcarriers from the culture medium is inherently uncomplicated, typically achieved through the settling of beads. This simplicity offers flexibility for adjusting the volume during fermentation, enabling operations such as medium replacement and nutrient supply.

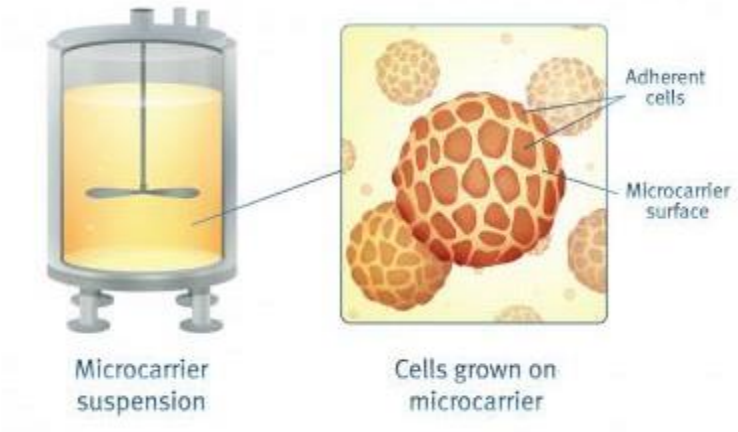

Figure 1.4: Diagrammatic drawing of attached cells on microcarriers in suspension culture (ChemoMetec, n.d.)**.**

There are three common forms of microcarriers used in the production of virus-based therapeutic products: charged carriers, coated carriers, and macroporous carriers (macrocarriers).

Charge density on the culture surface appears to be critical for cell adhesion and spreading (Maroudas, 1975). Examples of commercially available microcarriers bearing charges on their surface are Cytpdex-1™ (GE Healthcare), Plastic Plus and Hillex® (SoloHill Eng). Diploid and continuous cell lines, such as MDCK, Vero and MRC-5, have been successfully propagated on these microcarriers to produce viruses including influenza, rabies, dengue, enterovirus 71 and measles (Genzel et al., 2004; Liu et al., 2011; Paul Life Sciences, 2016; Rourou et al., 2014).

Interactions of cells and extracellular matrix proteins (ECM) such as collagen, laminin and fibronectins can direct cell adhesion and proliferation (Yue, 2014). Consequently, efficient cell attachment is anticipated with the use of microcarriers coated with ECM. For instance, collagen-coated microcarriers have been applied in the cultivation of difficult-to-grow cell lines, such as human osteoblasts, chondrocytes, and human mesenchymal stem cells (Overstreet et al., 2003; Rafiq et al., 2016). The microcarriers have also been reported to support the

production of influenza and rabies viral vaccines in MDCK and Vero cell lines respectively (Milián & Kamen, 2015; Frazzati-Gallina et al., 2001). Yet, concerns about the safety of final drug products manufactured based on ECM-coated microcarrier have been raised since a large number of these surface coatings are protein-based or/and animal-derived.

Macrocarriers are macroporous microcarriers (**Figure 1.5**) that provide large internal surface area for cell attachment and thereby protect cells from shear stress. Studies have demonstrated their use in propagating rabies virus and reovirus in Vero cells (Yokomizo et al., 2004; Butler, Burgener and Coombs, 2000). Nevertheless, the macroporous structures can cause reduced accessibility of entrapped cells to viral infection and increased technical difficulties in harvesting the virus-containing cells (Berry et al., 1999).

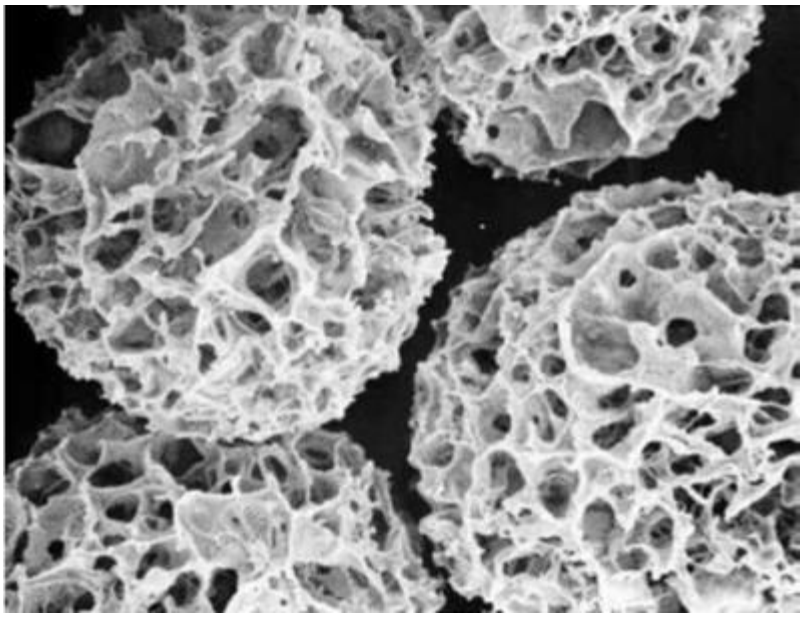

Figure 1.5: Scanning elactron microscope (SEM) pictures of empty Cytopore macroporous microcarrier (GE Helathcare Life Sciences, 2005)**.**

Employment of microcarriers is one of the prominent options for cultivating anchorage-dependent cells at industrial scale (Montagnon et al., 1984; Milián & Kamen, 2015; Monath et al., 2004). The advantages of using microcarrier in cell production also apply to viral production. Therefore, cultivation of viral vaccines using microcarrier based mammalian cell culture process is finding increasing industrial applications, such as the production of smallpox vaccine, influenza vaccines and Polio vaccines (Monath et al., 2004, The Dish, 2015, Milián & Kamen, 2015). The production scale of microcarrier culture can go up to 6000L, which has been demonstrated by the manufacturing of the influenza H5N1 vaccine from Vero cells for Phase III clinical trials (Baxter) (Bielitzki et al., 2007).

Scale-up of microcarrier process involves some intermediate steps. Prior to bioreactor culture, cells are first transferred from static culture system to shake flasks or spinner flasks that resemble a simplified lab-scale version of the bioreactors (**Figure 1.6**). One major technical challenge associated with large-scale manufacturing is the demand for relatively high cell inoculum density (Esmeralda Gallo–Ramírez et al., 2015). This becomes even more obvious when culturing cells in SFM due to the comparatively low efficiency of cell attachment on microcarriers in the absence of serum. One potential solution is the use of bead-to-bead cell transfer method. By diluting the existing culture with fresh microcarriers and fresh medium, some of the cells grown on old confluent beads start to migrate to and proliferate on the bare ones. The method has been utilized for the cultivation of cell lines such as Vero and MDCK (Wang & Ouyang, 1999; Liu et al., 2010).

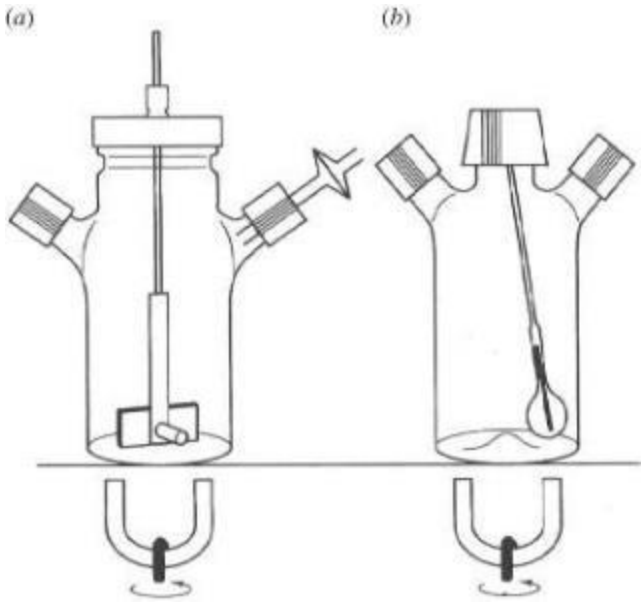

Figure 1.6: Diagrammatic drawing of two different types of spinner flasks: (1) spinner with a magnetic bar stirrer and (b) spinner with a ball-shapped eccentrically rotating agitator. *Note*. From "Advances in cell culture: anchorage dependence," by O. W. Merten, 2015, *Philosophical transactions of the Royal Society of London. Series B, Biological sciences, 370*(1661), 20140040. (https://doi.org/10.1098/rstb.2014.0040). Reprinted with permission.

1.3.2.4 Packed-bed systems

Similar to microcarrier systems, packed-bed systems provide cells with attachment matrices in suspension. Supporting matrices mainly include highly porous beads and strips made of mesh-like polyester materials (Warnock, Bratch and Al-Rubeai, 2005). Cells are entrapped in the

matrices that shelter them from shear forces. Unlike microcarriers suspended freely in the reactors, the matrix (bed) is immobile and supplied constantly with nutrients and oxygen (**Figure 1.7**). However, such sheltering and immobility could lead to reduced cell accessibility, particularly with respect to the direct quantification of viable cell numbers.

Packed-bed systems offer a large growth surface area while retaining a very small footprint. A large scale packed-bed bioreactor for viral production can afford a surface area of 500 m^2 in only 25L of fixed-bed (Knowles et al., 2013). This is equivalent to 1038 ten-layer CellSTACKs, 3771 roller bottles at 1750 cm^2 each, or a 500L working volume stirred bioreactor with 3g/L Cytodex-1 microcarriers in respect of similar surface area. The primary limitation in scale-up lies in mass transfer due to the formation of oxygen, nutrient and waste gradients along the axial length of the bioreactor (Warnock, Bratch and Al-Rubeai, 2005).

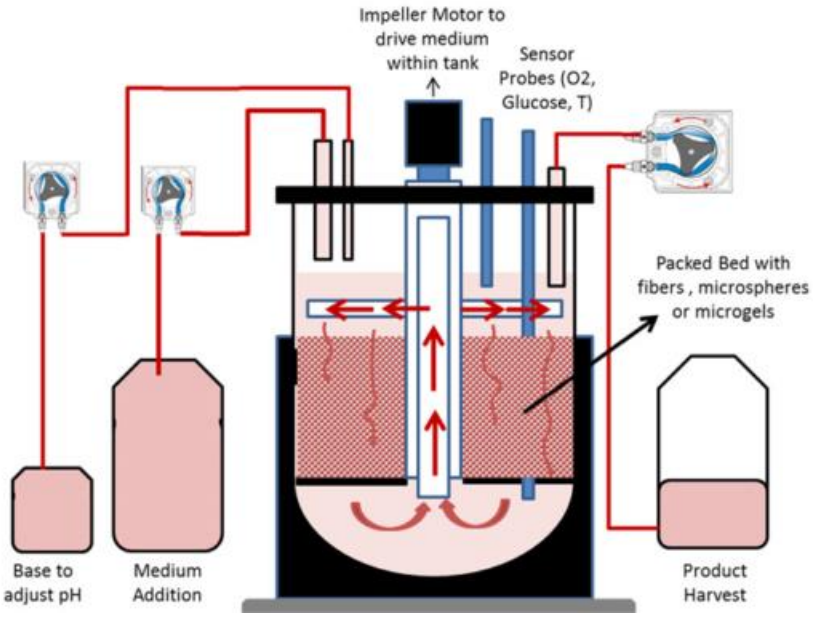

Figure 1.7: Diagrammatic drawing of cell expansion in a packed-bed bioreactor. *Note*. From "Large scale industrialized cell expansion: producing the critical raw material for biofabrication processes," by A. Kumar & B. Starly, 2015, *Biofabrication, 7*(1661), 044103. (https://doi.org/10.1088/1758-5090/7/4/044103). Reprinted with permission.

1.3.2.5 Hollow fibre bioreactor systems

A hollow fibre bioreactor is composed of a cylindrical-shaped cartridge that encases multiple tube-shaped, semi-permeable capillary fibre membranes (**Figure 1.8**). It is a compact system that offers a surface to volume ratio as high as 200 cm^2 per mL (Legazpi et al., 2016). A large

hollow fibre cartridge module can provide a surface area of 2.1 m^2 in a total volume as little as 180 ml (Sheu et al., 2015). This is equivalent to a 1.6 L working volume stirred bioreactor with 3g/L Cytodex-1 microcarriers in respect of similar surface area.

Typically, cells are inoculated in the extra-capillary space (ECS) of the cartridge and subsequently grow on the outer surface of the capillaries. Medium flows through the intra-capillary space (ICS) of hollow fibres. The porous fibre membranes allow very fast exchange of small molecules such as nutrients and waste by-products across the pores. This enables culture of cells at very high densities which as a result can lead to augmented cell-based production and productivity of biopharmaceutical products. Studies have reported the expansion of host cell lines to densities in the order of 10^7 cells/mL to 10^8 cells/mL in viral vaccine production (Tapia et al., 2016; Gardner et al., 2001).

Hollow fibre bioreactor systems have been used for large-laboratory/small volume production scale of adenovirus in suspension 293 cells (Tapia et al., 2014), lentiviral vector in adherent HEK 293T cells (Sheu et al., 2015) and influenza A virus in both adherent and suspension MDCK cell lines (Tapia et al., 2014).

Scaling-up of hollow fibre bioreactor systems has been difficult. A Non-uniform culture environment with large diffusional gradients along the fibre axis can result in nutrient deficiency at the distal end of the fibre and therefore heterogeneous distribution of cells within the cartridge. This situation will get more severe as the length of the hollow fibre unit increases (Tharakan & Chau, 1986). In addition, hollow fibre bioreactor systems are less suitable for in-situ monitoring and could impose excessive process complexity in harvesting infected adherent cells at large scale.

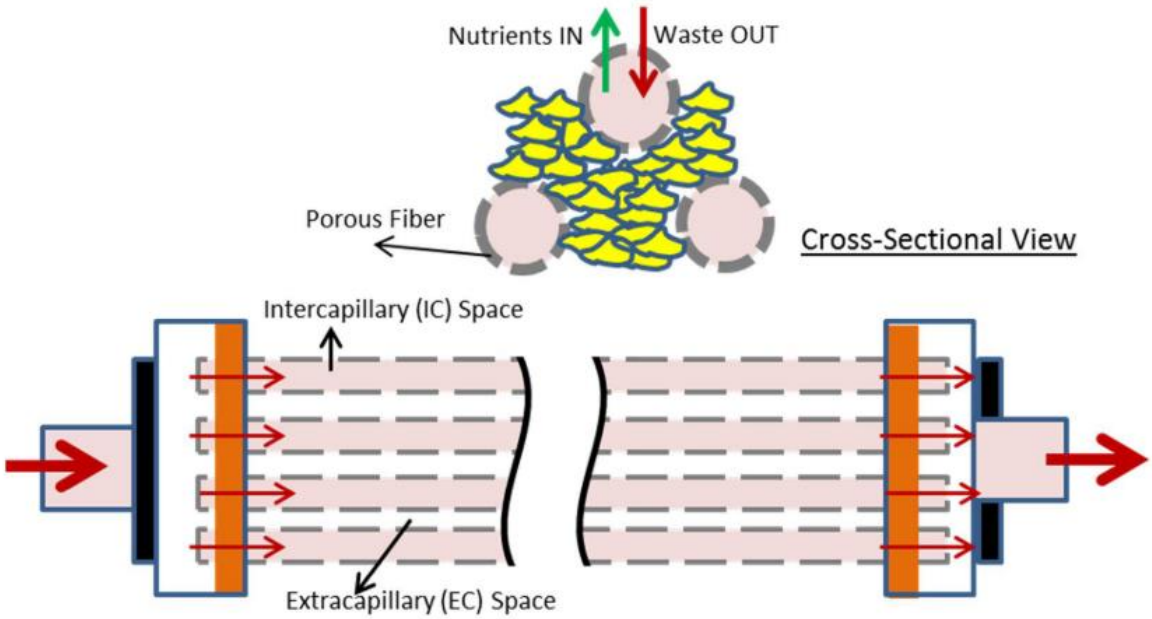

Figure 1.8: Diagrammatic drawing of a hollow fibre bioreactor. *Note*. From "Large scale industrialized cell expansion: producing the critical raw material for biofabrication processes," by A. Kumar & B. Starly, 2015, *Biofabrication*, *7*(1661), 044103. (https://doi.org/10.1088/ /1758-5090/7/4/044103). Reprinted with permission.

1.3.2.6 Disposable bioreactor systems

Different types of reusable and novel disposable bioreactors are available to accommodate the production formats mentioned in previous sections (**Figure 1.9**). Compared with the traditional cylinder-shaped vessels, single-use technology offers more flexibility in bioreactor designs (Whitford and Fairbank, 2011) and has been well known for their low capital investment, reduced possibility of cross-contamination, decreased requirements for equipment setup, cleaning and validation, short turnaround time and increased capacity (Warnock and Al-Rubeai, 2006).

Single-use vessel technology has been incorporated into the production processes of adherent cell-based viral vaccine. Manufacture of both smallpox vaccines Imvanex (Bavarian Nordic) in CEF cells and ACAM2000 in Vero cells involves the adoption of disposable reaction vessels (CHMP, 2013; Smart, 2013). The capacity of single-use bioreactors is currently available at production volumes up to 6000L (ABEC's CSR^{TM} bioreactor). The ceiling on size is no longer down to constraints on the construction of disposable bioreactors but centres around market demand (Shukla and Gottschalk, 2013).

From a regulatory perspective, the primary challenge of adopting disposable bioreactors is the inadequate validation process for determination of extractables and leachables in single-use materials, which could potentially contribute impurities to products (Arnaud, 2015; Shukla and Gottschalk, 2013).

Figure 1.9: Disposable culture devices for adherent cell viral vaccine production. (a) A single-use Cellbag^{TM} bioreactor on a special rocking platform; pictured is GE WAVE Bioreactor^{TM} 20/50system with WAVEPOD II integrated controller (GE Helathcare, 2011). (b) a stirred tank bioreactor lined with an integral single-use bag; pictured is a Flexsafe STR® bag in the bioreactor BIOSTAT STR® 2000 (Sartorius, n.d.). (c) a disposable fixed-bed bioreactor; picutured is the single-use iCELLis 500 bioreactor (Knowles et al., 2013). (d) a disposable hollow fibre bioreactor cartridge; pictured is a FiberCell® Systems cartridge with tubing (FiberCell Systems, n.d.).

1.3.3 Production of Clinical Grade Oncolytic VV

Not much information on the manufacturing processes for the clinical grade oncolytic VVs has been reported in the public domain. The oncolytic virus JX-594 was produced in Hela cells (Caroline et al., 2013) and vvDD were expanded in Vero cells (Zeh et al., 2015). The producer cells were grown in Dulbecco's Modified Eagle's medium (DMEM) supplemented with 10% foetal bovine serum (FBS) in adherent culture vessels including cell factories and RC-40 roller bottle packs. The quantity of virus recovered from 40L scale fermentation in 40 extended surface roller bottles was 5×10^{12} pfu (Ungerechts et al., 2016).

When utilizing tumourigenic or tumour-derived cell lines such as HeLa for the production of biological products, there are notable regulatory concerns related to the potential induction of tumour allografts and the transmission of viruses, oncogenic agents, and cell components, which could lead to the development of tumours in the recipients of the treatment (Aubrit et al., 2015). These risks are heightened for live viral vaccines, where virus inactivation and removal steps need to be minimized, as in the case of oncolytic viral vaccines. Consequently, clearance strategies and thorough characterization of such cell lines are necessary to demonstrate the absence of adventitious agents throughout production, which can lead to increased manufacturing costs. Furthermore, as discussed in section 1.3.1.1, the use of animal serum in bio-manufacturing processes also raises safety concerns for various reasons.

The utilization of serum-free mediums in vaccine production has become a growing trend. The expansion of VV in serum free culture medium can be dated back to 1960s when a comparison was made between VV replication in mouse-lung cells in medium with and without the presence of horse serum (Pumper et al., 1960). As mentioned in section 1.3.1.2, the FDA-approved live attenuated smallpox vaccine ACAM 2000 is manufactured by infecting Vero cells under serum-free conditions (Monath et al., 2004).

However, dose requirement of VV for oncolytic efficacy can be much higher than that for prophylactic efficacy. In comparison with an ACAM2000 dose containing $2.5\text{-}12.5\text{x}10^5$ plaque forming units (pfu) (Petersen et al., 2015), a significantly larger dose ($1\text{x}10^8\text{-}1\text{x}10^9$ pfu) of oncolytic VV need to be administered intravenously to patients for the purpose of effective delivery to tumours (Heo et al., 2013). This demand for satisfactory yields of oncolytic VV becomes an important factor in limiting the current best production condition of oncolytic VV to serum-containing medium (SCM) in adherent tumour cell cultures (Ungerechts et al., 2016).

Therefore, further studies on the process development still need to be carried out to optimize the production of oncolytic VV. Ideally, a serum-free suspension culture system with the goal of minimizing risks and real potential to scale-up for production of high-titre virus is on demand.

1.4 Aim and Objectives

The overall aim of this thesis is to assess if CV-1 cell line has the potential for the large-scale production of an engineered oncolytic Vaccinia virus. The approach taken will demonstrate the characteristics of CV-1 cell line and its utility for oncolytic VV production in a serum free scalable system. Within the context of this work, a Lister Strain genetically modified VV, VVL-15 RFP, will be the test strain used.

The objectives of the study are summarised below:

(1) The initial objective is to adapt CV-1 to two types of serum free media. A production cell line for VVL-15 RFP is to be selected among the cell lines either adapted to SFM or growth in SCM. The selection of the production cell line will be based on cell proliferation ability, plating efficiency, recovery ratio after cryopreservation, and their viral productivities. This work is described in Chapter 3.

(2) In Chapter 4, the production cell line will be tested for its ability to survive under suspension cultivation conditions, which is considered as the first step towards scale-up. The cell line will be subjected to either suspension adaptation or microcarrier culture. Both processes will be evaluated regarding the cell proliferation ability. For microcarrier culture, impact of factors on growth will be examined, which include addition of shear protectant, cell inoculum density and feeding strategy. The evaluation will take account of quantitative analysis of cell attachment, growth, and metabolites. Optimal growth conditions will be determined and subsequently be used to produce VVL-15 RFP.

(3) Next, the impact of factors on VVL-15 RFP production will be investigated and the utility of this microcarrier cultivation process for the viral production will be demonstrated and compared with that of static cultivation process. The investigation will include quantitative analysis of viral productivities and/or CV-1-OPT cell growth at different Vascular Epidermal Growth Factor (VEGF) concentrations, Multiplicity of Infection (MOI) or Time of Infection (TOI) levels. This work is presented in Chapter 5.

(4) Finally, in Chapter 6, recommendation will be made for future research and developments.

Chapter 2. Material and Methods

2.1 Cell lines and maintenance

All cells were maintained at 37 °C, 5% CO_2 and were regularly assayed for mycoplasma contamination.

The cell lines used in the study are listed in **Table 2.1**.

Cell Line	Organ of Origin	Host	Immortalisation	Culture Medium
CV-1	kidney	green monkey	No	DMEM+5% FBS
				OptiPRO+ 4mM GlutaMAX
				VP-SFM+ 4mM GlutaMAX

CV-1 cell passage P3 was a kind gift of Professor Yaohe Wang at Queen Mary University of London and originally obtained from the American Type Culture Collection (VA, USA). Culture Media used were the High Glucose Dulbecco's Modified Eagle's Medium (DMEM) supplemented with 5% Foetal Bovine Serum (FBS) (PAA Lobotomies, Pasching, Austria); OptiPRO and VP-SFM, both supplemented with 4mM GlutaMAX (Life Technologies, New York, USA).

2.1.1 Maintenance of CV-1 cell line in static culture

CV-1 cells cultured in DMEM with 5% FBS were seeded at 10^4 cells/cm^2 and passaged every four days. Trypsin EDTA (1x) 0.05% / 0.02% in DPBS (PAA Lobotomies, Pasching, Austria) was used for cell detachment.

CV-1 cells adapted to OptiPRO and VP-SFM were passaged every 4 days at densities of 10^4 cells/cm^2 and 2×10^4 cells/cm^2 respectively. Cells growth in both media were dissociated by TrypLE Select (Life Technologies, New York, USA).

2.2 Cell banking

CV-1 growth in 10% FBS DMEM at passage number 6 were frozen in 90% (v/v) FBS and10% (v/v) Dimethyl Sulfoxide (DMSO) (Sigma-Aldrich, Ayrshire, UK). Cells adapted to OptiPRO and VP-SFM at passage number 18 were cryopreserved in a mixture of 10% (v/v) DMSO, 45% (v/v) fresh culture medium, 45% (v/v) conditioned medium harvested from day 2,3 and 4 cultures, and 0.1% (v/v) 2% (w/v) methylcellulose (Sigma-Aldrich, St Louis, MO). Cells were frozen at $3\text{-}5\times10^6$ cells/ml and each 1 ml aliquot was dispensed into a 1.2 ml cyrovial (Thermo Scientific, UK). The cryovials were kept in Mr. Frosty freezing containers (Thermo Scientific, UK) overnight before being transferred to a liquid nitrogen tank.

2.3 Vaccinia virus VVL15-RFP lab scale production

2.3.1 Vaccinia virus VVL-15 RFP

VVL-15 RFP was a kind gift of Professor Yaohe Wang. It is an engineered Lister strain VV. The gene that encodes Thymidine Kinase (TK) in VVL-15 RFP was replaced by a gene expressing Red Florescent Protein (RFP). The TK deletion in the Lister Strain VV further enhances the tumour selectivity of VVL-15 RFP.

2.3.2 Lab scale production of Vaccinia virus VVL-15 RFP

CV-1 cells grown to 90% confluence in a T-175 tissue culture flask were infected with purified VVL-15 RFP at Multiplicity of Infection (MOI) 0.1. Cells were scrape harvested 48-72 hours post infection upon identification of cytopathic effect (CPE) by eyes. The broth was treated over three cycles of freezing in liquid nitrogen and thawing in a 37ºC water bath and used as primary expansion to infect 36 T-175 flasks of CV-1 cells at 90% confluence. 48-72 hours later, the infected cells were harvested by scarping and centrifuged at 3,500 rpm for 15 minutes at 4ºC until all the cells were collected into one single pellet. The pellet was washed with Phosphate Buffered Saline (PBS), resuspended in 12 ml of 10mM Tris-HCl pH 9.0 and went through two freeze-thaw cycles prior to being stored at -80ºC until further purification.

2.3.3 Purification of VVL-15 RFP

Upon thawing, the lysate suspension was homogenised with 60 strokes of a 40ml glass-glass Dounce homogenizer (Fischer Scientific, Loughborough, UK), then ultra-sonicated for 30

seconds. The homogenate was centrifuged at 3,500 rpm for 5 minutes at 4ºC, and the viral supernatant was collected and diluted to 30ml with 10mM Tris-HCl pH 9.0. Each 7.5ml of diluted supernatant was laid gently on top of 17ml of 36% sucrose (w/v) 10mM Tris-HCl pH 9.0 in one 36ml SW17 Beckman ultracentrifuge tube (Beckman Coulter, Bucks, UK). Each pair of tubes was carefully balanced by weighing them. The tubes were then ultra-centrifuged at 13,500 rpm for 80 minutes at 4ºC. After carefully aspirating off all the supernatant, the pellet in each tube was resuspended in 4ml of 1mM Tris-HCl pH 9.0.

A discontinuous sucrose density gradient was prepared by slowly pipetting 4ml 40% sucrose (w/v) 10mM Tris-HCl directly into the bottom of a SW17 Beckman ultracentrifuge tube, layering 4ml 35% sucrose on the top of it, followed by 4ml 30% sucrose and then 4ml 25% concentration. 2ml viral resuspension was gently layered on the top of the density gradient. After careful balancing by weight, the tubes were ultra-centrifuged using swinging-bucket rotors at 13,500 rpm for 60 minutes at 4ºC. Each supernatant was removed, and each purified pellet was resuspended in 2ml resuspension buffer which contained 90% (v/v) PBS, 10% (v/v) glycerol, and 138mM NaCl at pH 7.4. The purified viral solution in the tubes was collected into one Falcon tube, divided into aliquots and stored at -80 ºC. The virus titre was determined by TCID50 plaque assay.

2.4 Adaptation of CV-1 cells to serum free media

One vial of CV-1 cells cryopreserved in 90% (v/v) FBS and 10% DMSO was revived in 10% FBS DMEM and passaged 3 times prior to sequential adaptation to VP-SFM or OptiPRO SFM. To derive the serum free CV-1 cell lines, cells were first sub-cultured into T-25 flasks with 10 ml of medium per flask consisting of 25% (v/v) of the SFM and 75% (v/v) of the original medium. The ratio of SFM to original medium was increased stepwise until the cells were placed in 100% SFM (**Table 2.2**). Cells were passaged three additional times in corresponding SFM prior to cryopreserving aliquots in liquid nitrogen. VP-SFM and OptiPRO-adapted CV-1 cells at passages 23 to 40 were used for experiments.

Table 2.2 Stepwise conversion to serum-free growth of CV-1 cells.

Passage Number	Ratio of OptiPRO/ VP-SFM to 10% FBS DMEM	Serum Concentration (%)
7-9	0:100	10
10	25:75	7.5
11	50:50	5
12	75:25	2.5
13	90:10	1
14	90:10	1
15-18	100:0	0

2.5 Cell analytical methods

2.5.1 Average growth rate

Cells at the end of each passage during SFM adaptation were counted using trypan blue on a haemocytometer and the average cell growth rate (day^{-1}) was calculated as shown in Equation 2.1,

$$\text{Average growth rate} = \frac{ln(C_H) - \ln(C_S)}{D} \qquad 2.1$$

Where, C_s is the initial seeding density (cells / cm^2) of a passage; C_H is viable cell density (cells / cm^2) at the end of the passage; and D is culture duration (days).

2.5.2 Specific growth rate and doubling time calculation

Cells cultured statically were seeded at 2,000 cells / cm^2 in 7.5 ml of corresponding medium in T-25 flasks and incubated at 37 °C, 5% CO_2. Cells were harvested every 24 hours and counted using trypan blue. Triplicate flasks of each condition were sacrificed at each sampling time point. Triplicate samples of cells grown in microcarrier culture in each spinner flask were counted every 24 hours. Specific growth rate, μ (h^{-1}) was calculated as shown in Equation 2.2,

$$\mu = \frac{1}{t} \times \ln \frac{X}{X_0} \qquad 2.2$$

Where, x_0 is the starting total cell number per flask; t is the culture duration (hours); x is the total cell number per flask after t hours.

During the exponential phase of cell growth, a plot of ln(x) versus t gives a straight line of which the slope is the maximum specific growth rate μ_{max}.

Cell doubling time (hours) was calculated as shown in Equation 2.3.

$$\text{Cell doubling time} = \frac{\ln 2}{\mu_{max}} \qquad 2.3$$

2.5.3 Lag time and saturation density calculation

Lag time was obtained from the cell growth profile. It was calculated as the time at the intercept of the seeding concentration (blue dash line) with the line extrapolated from the exponential phase (red dash-dotted line) (**Figure 2.1**).

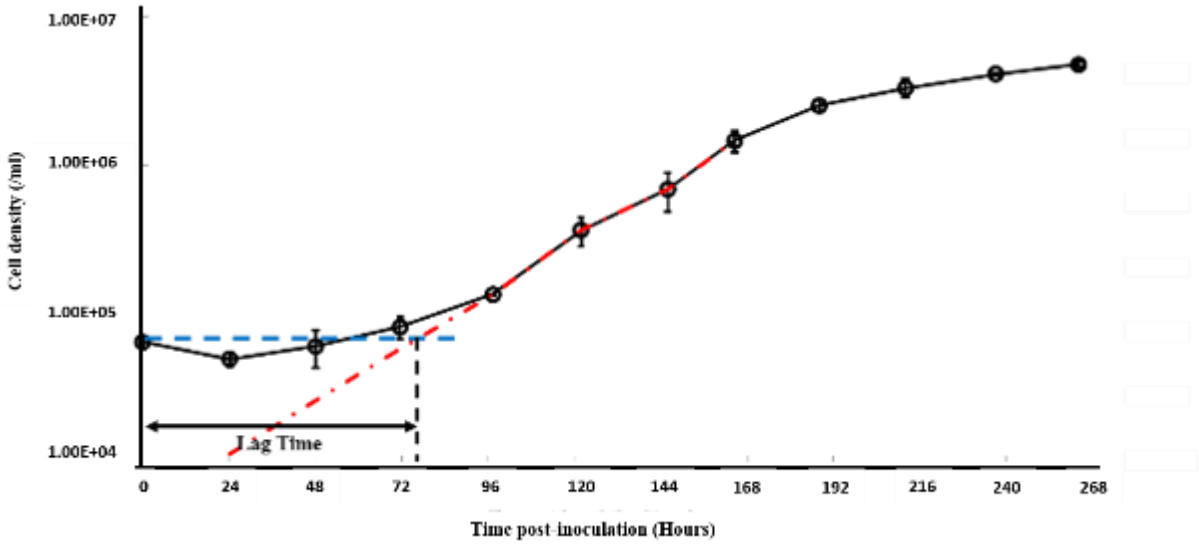

Figure 2.1: Cell growth profile. Semilog plot of the cell density against time post-inoculation.

2.5.4 Plating efficiency calculation

Dissociated cells were pipetted into single cell suspension and seeded in T-25 flasks at densities of 2, 10 and 20 cells / cm^2 and incubated at 37 °C, 5% CO_2. Total volume of medium in each flask was 7.5 ml. After 11, 15 and 21 days of cultivations, formation of individual cell colonies in OptiPRO, 5% FBS DMEM and VP-SFM were visible to the naked eyes respectively. Colonies were washed once with 2 ml PBS then fixed in 2 ml of 10% (v/v) formalin (Sigma-Aldrich) in PBS for 10 minutes at room temperature. After removal of the formalin solution, colonies were stained with 2 ml of 0.1% (w/v) crystal violet (Sigma-Aldrich, China) in 20% (v/v) ethanol for 10 minutes. Residual dye was removed by washing with water. Stained

colonies were counted manually. Plating efficiency (%) was calculated as shown in Equation 2.4,

$$\text{Plating efficiency} = \frac{\text{Number of colonies formed}}{\text{Number of cells seeded}} \times 100\% \qquad 2.4$$

2.5.5 Cell recovery ratio calculation

Cells had been cryopreserved in liquid nitrogen for over 10 months prior to revival. Cells were thawed in a 37°C waterbath and were transferred into pre-warmed corresponding medium once defrost. Each mixture was centrifuged for 3 minutes at 1,300 rpm and supernatant was removed. Cells were then resuspended in 0.5ml medium and counted using trypan blue prior to being seeded into a T-25 flask in 7.5 ml of medium and incubated at 37 °C, 5% CO_2. After 24 hours, culture medium containing unattached cells was collected and centrifuged at 1300 rpm for 3 minutes. Each cell pellet obtained was resuspended in 50 µl fresh medium and cell number was counted. Cell recovery ratio was calculated as shown in Equation 2.5,

$$\text{Cell recoery ratio (\%)} = 100\% - \frac{N_F}{N_T} \times 100\% \qquad 2.5$$

Where, N_T is the total number of cells initially seeded; N_F is the total number of unattached cells in the medium 24 hours post seeding.

2.6 Microcarrier cell culture

2.6.1 Siliconisation of glassware

To minimize the adherence of microcarriers and cells to glass, the inner wall of glassware that would come in contact with the Cytodex-1 microcarriers (GE Healthcare, Sweden) was siliconized, which included impellers, the interior surface of Techne 250mL spinner flasks (125 ml working volume) (Bibby Scientific Ltd, Staffordshire, UK) and glass bottles. All glassware was cleaned using a laboratory glassware washer and air dried prior to siliconisation. After addition of a small volume of Sigmacote (Sigma-Aldrich, St. Louis, MO), the flask / bottle was swirled until the entire surface was covered. Any excess Sigmacote was then removed. Each impeller was siliconized by immersing its bulb-shaped rod in a 50ml Falcon tube containing 35ml of Sigmacote for 10 seconds. All siliconized glassware was allowed to dry in a fume hood

overnight before being thoroughly washed with Milli-Q water for 3 times and air-dried. Each impeller was assembled into a flask and tested on a Techne MCS-104S biological stirrer (Bibby Scientific Ltd, Staffordshire, UK) to ensure its smooth rotation. The completely assembled spinner flasks were autoclaved on a cycle of 20 minutes at 121°C. All glassware was re-siliconized every two uses.

2.6.2 Cytodex-1 microcarrier preparation

Microcarriers were prepared according to the manufacturer's instructions. An appropriate mass of dry Cytodex-1 microcarriers were added to a siliconized glass bottle and swollen in Ca^{2+} and Mg^{2+} free PBS, pH 7.4 (Life Technologies, Paisley, UK) at 100 ml /g Cytodex-1 overnight. After hydration, the microcarriers were allowed to settle and the supernatant was removed and replaced with fresh Ca^{2+} and Mg^{2+} free PBS, pH 7.4 to a final concentration of 50 ml /g Cytodex-1. The microcarriers were autoclaved at 121°C for 20 minutes.

One day before use, the sterilized microcarriers were allowed to settle, 70% (v/v) supernatant was discarded and replaced with the same volume of fresh OptiPRO. The liquids were mixed up by shaking the bottle. The whole process was repeated. After removal of 70% (v/v) supernatant for the second time, microcarriers were pre-conditioned with OptiPRO to a final concentration of 100 ml /g Cytodex-1 overnight in a fridge at 4°C.

2.6.3 Cell inoculation and microcarrier culture

The concentration of microcarriers was 3g/L through all experiments. The total culture volume in a spinner flask was 100 ml unless otherwise specified. The microcarrier-containing bottle was mixed thoroughly by swirling and 30 ml of homogenous mixture was quickly withdrawn and transferred to each flask. The flasks were incubated at 37 °C, 5% CO_2 before inoculation with cells. OptiPRO adapted CV-1 cells growing in T-225 flasks for 4 days were harvested and dissociated into suspension of single cells using TrypLE Select, followed by centrifugation at 1300 rpm for 5 minutes. Cells were resuspended in OptiPRO pre-warmed at 37 °C and cell concentration was determined by crystal violet method. Each flask was seeded with desired number of cells, followed by addition of pre-warmed OptiPRO to make a total volume of 100ml.

A total culture volume of 120 ml was prepared by adding 36 ml of well-mixed microcarrier suspension and 84 ml of OptiPRO-adapted CV-1 cell broth in fresh warm OptiPRO to the same spinner flask.

Cultures were placed on the stirrer in a 37°C 5% CO_2 incubator, exposed to intermittent agitation at 30 rpm for 30 seconds every 30 minutes for the first 48 hours. Continuous agitation was used from day 3 onwards, at 30rpm from 48 to 72 hours and 35 rpm from 72 hours towards the end of the culture.

2.6.4 Removal of analytical samples and medium exchange

The entire spinner flask apparatus was placed in biological safety cabinet and the stirrer was set to agitate the vessel at 60 rpm. When conducting only cell count, 1.4 ml of culture mixture was removed through one of the side arm ports of a spinner flask and transferred to a sterilized 2-ml micro-centrifuge tube. Triplicate samples were taken from each flask at each time point.

For experiments with the need for medium exchange, each day after sampling microcarriers were allowed to settle and culture supernatant was exchanged with pre-warmed fresh OptiPRO at a 70% volume of total remaining culture broth in each flask. The daily medium exchange volumes for a cultivation period of 10 days are shown in **Table 2.3**.

After sampling or medium exchange, the entire spinner flask apparatus was transferred back to the incubator and the agitation speed was readjusted according to the experimental requirements.

Each sample was mixed gently by pipetting up and down 3 times before 0.2 ml of the suspension was transferred to a sterile 1.2ml micro-centrifuge tube for cell counting using crystal violet method. The remaining sample was further mixed by carefully pipetting up and down 3 times and another 0.2 ml of the suspension was transferred to a well of a 24-well plate for crystal violet staining. The left-over sample was subjected to metabolites analysis using BioProfile FLEX Analyzer.

Table 2.3 Daily supernatant exchange volumes for a cultivation period of 10 days.

Time Post Cell Inoculation (Hours)	Volume of Remaining Broth after Daily Sampling (ml)	Daily Medium Exchange Volume (ml)
0	100.0	N/A
24	95.8	67.1
48	91.6	64.1
72	87.4	61.2
96	83.2	58.2
120	79.0	55.3
144	74.8	52.4
168	70.6	49.4
192	66.4	46.5
216	62.2	43.5
240	58.0	40.6

2.7 Quantification of glucose, lactate and ammonia

1.2- 1.3 ml of sample was centrifuged at 13,500 rpm for 10 minutes. 1ml of each supernatant was transferred to a new 2 ml centrifuge tube. For supernatant from a pure cell sample, the concentration of glucose, lactate and ammonia was measured directly using BioProfile FLEX Analyzer (Nova Biomedicals, Cheshire, UK).

The glucose consumption rate Q_{Glc} (mmol •cell^{-1} •hour^{-1}) was calculated as,

$$Q_{Glc} = \frac{(C_{Glc,t0} - C_{Glc,t1}) \times 10^{-3}}{\frac{1}{2} \times (X_{t1} + X_{t0})} \qquad 2.6$$

The lactate production rate Q_{Lac} (mmol •cell^{-1} •hour^{-1}) was calculated as,

$$Q_{Lac} = \frac{(C_{Lac,t1} - C_{Lac,t0}) \times 10^{-3}}{\frac{1}{2} \times (X_{t1} + X_{t0})} \qquad 2.7$$

where, C is the metabolite concentration (mM); t_0 and t_1 are the seeding and sampling times respectively (hour); X_{t0} and X_{t1} are the densities of cells attached on Cytodex-1 at t_0 and t_1 respectively (cells •mL^{-1}).

The yield coefficient of lactate from glucose, $Y_{Lac/Glc}$, was calculated as,

$$Y_{Lac/Glc} = \frac{Q_{Lac}}{Q_{Glc}} \qquad 2.8$$

2.8 VVL-15 RFP production in microcarrier system

2.8.1 Virus infection

On the day of infection, cell density in each spinner flask was determined as described in 2.6.4 and 2.12.3. 70% (v/v) of culture broth in each flask was then removed and replaced with VVL-15 RFP virus stock diluted in pre-warmed fresh OptiPRO medium. Flasks were prepared in duplicate for each condition, infected with VVL-15 RFP at MOIs of 0.1, 0.5 and 1.0 pfu/cell respectively and incubated at 37 °C, 5% CO_2. The spinner flasks were continuously agitated at 35rpm over the rest of the culture period.

2.8.2 Removal of analytical samples

Triplicate 1.8ml samples were taken from each spinner flask every 24 hours post-infection following the protocol described in 2.6.4. Each sample was mixed gently by pipetting up and down 3 times before 0.3ml of the suspension was transferred to a 1.2ml cyrovial and stored in -80 °C freezer for later TCID50 analysis. The remaining sample was further mixed by carefully pipetting up and down 3 times and another 0.2 ml of the suspension was transferred to a sterile 1.2ml micro-centrifuge tube for cell counting using crystal violet method.

2.9 Enzyme-linked immunosorbent assay (ELISA) for the detection of VEGFA

The concentrations of human VEGFA in OptiPRO medium and in supernatant samples from CV-1 cells growth in OptiPRO were measured by the Human VEGF Duoset ® ELISA Development kit (R&D Systems, Abingdon, UK) according to the manufacturer's instructions.

CV-1 cells were seeded in triplicate in 6-well plates at 2×10^5 cells/well in OptiPRO medium and incubated at 37 °C, 5% CO_2 for 48 hours. Supernatant from each well was collected.

A 96 well ELISA plate was coated with 100 µl per well of mouse anti-human VEGF capture antibody diluted to a working concentration of 1.0 µg/ml in PBS. The plate was sealed with a plate sealer and refrigerated at 4°C overnight. Wells of the plate were then aspirated and washed 3 times by filling and emptying with the wash buffer that contained 0.05% (v/v) Tween 20 in PBS. The plate was blocked by addition of 200 µl of 1% (w/v) Bovine Serum Albumin

(BSA) (Sigma-Aldrich, Poole, UK) in PBS to each well, incubated at room temperature for 1 hour, and washed in the same manner as described above.

Human VEGFA standards and samples were all diluted in 1% BSA in PBS. The samples were tested at three dilutions, neat, 1:50 and 1:500, while the standard was serially diluted in two-fold increments, starting at 2,000 pg/ml and ending at 31.25 pg/ml. 100 µl of the (diluted) samples or standards were added to each well and incubated at room temperature for 2 hours. After washing the plate, 100 µl of 100ng/ml biotinylated goat anti-human VEGF detection antibody was added to each well and incubated at room temperature for 2 hours. The plate was again washed, and 100 µl of the 1:40 diluted Streptavidin-HRP was added to each well and incubated in the dark at room temperature for 20 minutes. After another wash step, 100 µl of substrate solution which was an equal mixture of H_2O_2 and Tetramethylbenzidine was added to each well and incubated in the dark at room temperature for 20 minutes. 50 µl of 2N H_2SO_4 as stop solution was then added to each well.

The VEGFA concentration in each well was determined by the optical density at 450nm wavelength using an Opsys MR plate reader (Dynex, VA, USA). Standards and samples were analysed in duplicate. The averaged OD values of standards were used to generate a standard curve from which levels of VEGFA in samples were interpolated.

2.10 Western blot

2.10.1 Sample preparation

2.5×10^5 cells CV-1 cells were seeded in each 35mm petri dish in 2ml of OptiPRO medium. Cells were incubated at 37 °C, 5% and left to adhere overnight. Medium in each petri dish was then removed and cells were washed with PBS before the addition of 2ml DMEM. After 16 hours of serum starvation, medium was removed, and cells were washed with PBS and stimulated with 10ng/ml human (hr) VEGFA (Sigma-Aldrich, Saint Louis, MO) in 2ml of fresh DMEM per dish for 3, 5, 10 and 20 minutes. Unstimulated cells were acted as a negative control. After treatment with VEGFA for the specific periods of time, medium was removed and cells were placed on ice and washed with cold PBS. Whole cell extracts were then collected by cell lysis with PhosphoSafe Extraction Reagent (Merck) and centrifuged at 13,600 rpm for 20 minutes at 4ºC. 80 µl of each supernatant was transferred to a new microcentrifuge tube.

2.10.2 Protein quantification

Protein concentration was measured using direct UV A280 absorbance method with NanoDrop Spectrophotometers (ThermoScientific). After gently cleaning the upper and lower pedestals with deionized water (dH_2O), 2 µl of lysis buffer as a reference blank was loaded onto the lower pedestal. Upon completion of blank measurement, both pedestals were wiped with dry lab wipe and 2 µl of well-mixed sample solution was loaded. The optical absorbance of protein in the sample was measured at 280nm. The measurement surfaces were cleaned with dry lab wipes between any 2 sample measurements to prevent cross-contamination from previous samples. After the final sample measurement, the pedestals were cleaned with dH_2O. The protein concentration of samples (mg/ml) was displayed on the software screen.

2.10.3 Sodium dodecyl sulphate-polyacrylamide gel electrophoresis (SDS-PAGE)

20 µg of each sample was mixed with 6× loading buffer (**Table 2.4**). Each mixture was heated at 95 ºC for 10 minutes prior to being loaded onto the gel made up of 4% stacking gel and 10% running gel (**Table 2.5** & **2.6**) in running buffer (**Table 2.7**). 5 µl of Rainbow molecular weight marker (Amersham Biosciences, Bucks, UK) was loaded in the lane next to the protein samples. Electrophoresis was run at 200V for 50 minutes.

2.10.4 Western blotting and immunodetection

An Immobilon-P Polyvinylidene Fluoride (PVDF) membrane (Millipore, Bedford, MA) was pre-wet in Methanol for 1 minute, then immersed in ice-cold transfer buffer (**Table 2.7**) together with the gel, 2 sponges and 2 filter papers. The gel and PVDF membrane were sandwiched between the filter papers and sponges (sponge > paper > gel > membrane > paper > sponge) and moved to a wet transfer system (Bio-Rad, CA, USA) where the proteins were transferred at 100V for 1 hour. The membrane was then soaked in methanol for 30 seconds and air-dried.

The primary antibodies (**Table 2.8**) were diluted in 1% (w/v) BSA (Sigma-Aldrich, Poole, UK) in PBST composed of 0.1% (v/v) Tween 20 (Sigma-Aldrich, Poole, UK) in PBS and incubated with the membrane at room temperature for 1 hour. After washing with PBST once, the membrane was incubated with the horseradish peroxidase (HRP)-conjugated secondary antibody (**Table 2.8**) diluted in 3% skimmed milk powder (w/v) in PBST at room temperature for 45 minutes. The membrane was then washed with PBST four times for 5 minutes each.

ECL Plus Detection reagent (GE Healthcare, Bucks, UK), the chemiluminescent substrate for HRP detection, was prepared following the manufacturer's instructions. Signals were captured on Fuji Medical film Super RX (Fuji, Japan).

Table 2.4 50 ml SDS gel-loading buffer formula (6×).

Reagent	Volume/ Weight
Deionized Water	7.5 ml
0.5 M Tris-HCl, pH 6.8	37.5 ml
Glycerol	15 ml
SDS	3 g
Bromophenol Blue	30 mg

Table 2.5 10 ml 4% stacking gel formula.

Reagent	Volume/ Weight
ProtoGel	1.3 ml
ProtoGel Stacking Buffer	2.5 ml
dH_2O	6.1 ml
10% Ammonium Persulfate	50 µl
TEMED	10 µl

Table 2.6 21 ml 10% resolving gel formula.

Reagent	Volume/ Weight
ProtoGel 30%	7.0 ml
4× Resolving Buffer	5.3 ml
dH_2O	8.5 ml
10% Ammonium Persulfate	210 µl
TEMED	21 µl

Table 2.7 Buffer formula.

Buffer	Stock Solution	Supplier	Diluent
1× Running Buffer	10× SDS Running Buffer		90% (v/v) Milli-Q water
1× Transfer Buffer	10× Transfer Buffer		20% (v/v) Methanol + 90% (v/v) Milli-Q water

Table 2.8 Antibodies for Western Blot.

Antibody	Precedence	Source	Dilution Ratio	Supplier
Phosphor-Akt (Ser473)	primary	rabbit	1:500	Cell Signalling Technology,
Akt	primary	rabbit	1:1000	Cell Signalling Technology,
Anti-rabbit HRP	secondary	goat	1:1000	Autogen Bioclear,

2.11 Virus replication assay

2.11.1 Virus replication

In static culture, cells were seeded in each well of a 6-well plate in 2ml of medium per well. Upon reaching 80-90% confluence, average cell number per well was calculated by counting cells from triplicate wells. Cell culture medium was then removed and infected with 2ml of corresponding fresh medium containing VVL15-RFP at MOI of 0.1. Cells were scrape harvested 24, 48 and 72 hours post infection together with the supernatant. Triplicate wells of each condition were sacrificed at each sampling time point. The samples were treated over three cycles of freezing in -80ºC and thawing in a 37ºC water bath prior to being subjected to TCID50 assay.

In microcarrier culture, sample preparation was described as in section 2.8.2. Samples were then treated over three cycles of freezing in -80ºC and thawing in a 37ºC water bath prior to being subjected to TCID50 assay.

2.11.2 TCID50 assay to determine virus concentration

9,000 CV-1 cells were seeded in each well of a 96 well plate in 200µl of 5% FBS DMEM per well and incubated at 37 °C, 5% CO_2 overnight. Viral burst assay samples from static culture or microcarrier culture were diluted 10^3 or 10^4 folds respectively in corresponding medium; 22 µl/ well of the diluted sample was transferred to all the wells across the first row of the 96 well plate and mixed well. After changing pipette tips, 22 µl of the mixture from each well in the first row was transferred to the following row. The procedure was repeated up to the penultimate row, resulting in a ten-fold serial dilution. The last row was left uninfected as a negative control.

After incubation for 6 days at 37 °C, 5% CO_2, the plate was examined under a microscope, and the number of wells that demonstrated Cytopathic Effect (CPE) in each row was recorded. Using the Reed-Muench method (Reed & Muench 1938), these values were used to calculate viral volumetric productivity and viral specific productivity in pfu/ml and pfu/cell respectively, the latter is based on the total number of cells on the day of infection.

2.11.3 Virus amplification

The extent of VVL-15 RFP amplification was calculated as shown in Equation 2.6,

$$\text{Virus Amplification} = \frac{VA_P}{VA_{TOI}} \qquad 2.6$$

where, VA_{TOI} is the total amount of virus used to infect cells at the time of infection (pfu), VA_P is the peak viral yield achieved in the production (pfu).

2.12 Quantification of cell number and viability

2.12.1 Trypan blue exclusion

Cells in static cultures were counted using trypan blue exclusion method. 100 µl of 0.4% trypan blue (Sigma, Aryshire, UK) was well mixed with 100 µl of cell suspension. 10 µl of the solution was loaded into an Improved Neubauer haemocytometer (Heinz Herenz Medizinalbedarf, Hamburg, Germany) and examined under a microscope at 10× magnification. Cells in four corner squares plus one central square were counted and cells that took up trypan blue were considered non-viable. A dilution of cell suspension in PBS was made if necessary so that each square had between 20 to 50 cells. Cells were counted within 3 minutes of mixing with trypan blue. Viable cell concentration (cells/ml) and cell viability (%) were calculated as shown in Equations 2.7 and 2.8 respectively,

$$\text{Viable cell concentration} = 2 \times 10^4 \times \frac{\text{Number of unstained cells in five squares}}{5} \qquad 2.7$$

$$\text{Cell viability} = \frac{\text{Number of unstained cells in five squares}}{\text{Total number of cells in five sauqres}} \times 100\% \qquad 2.8$$

2.12.2 Vi-Cell

Vi-Cell was used when adapting cells to suspension culture. 600 µl of cell suspension was transferred to a sample cup. Cell count was performed using Vi-Cell XR automated viability analyser (Beckman, Brea, CA). A dilution of cell suspension in PBS was made

if necessary so that concentration of each sample was between 5×10^4 to 10^7 cells/ ml. The Vi-Cell automates the trypan blue exclusion method, and takes 50 images of each sample to determine the viable and total cell concentrations plus viability.

2.12.3 Crystal violet staining

Cells on microcarrier were counted using crystal violet method. Crystal violet reagent (0.1% w/v) was prepared by dissolving 0.1g crystal violet (Sigma-Aldrich, China) in 0.1M citric acid solution which contained 1.9212g of citric acid (Sigma-Aldrich, St. Louis, MO) in 100 mL of Milli-Q water. 100 µl of Triton X-100 (Sigma-Aldrich, St. Louis, MO) was then mixed into to the solution. The mixture was shaken on an orbital shaker at 100rpm until complete dissolution.

1ml of PBS was gently added to a 2ml microcentrifuge tube containing 200 µl of microcarrier suspension. After settling of the microcarriers, 1 ml of supernatant was removed. The microcarriers were washed again with 1ml of PBS before mixing thoroughly with 200 µl of the crystal violet reagent by pipetting up and down 25 times. After being incubated at 37 °C, 5% CO_2 for 1.5 hours, the mixture was further pipetted 25 times and a 10 µl aliquot was loaded into an Improved Neubauer haemocytometer for nuclei count. The stained nuclei in four corner squares plus one central square were counted. An appropriate dilution of stained microcarrier suspension with PBS was made if necessary so that each square had between 20 to 50 nuclei. Concentration of cells attached on microcarriers (cells/ml) was calculated as shown in Equation 2.9,

$$\text{Concentration of cells attached on microcarriers} = 2 \times 10^4 \times \frac{\text{Number of stained nuclei in five squares}}{5} \qquad 2.9$$

2.13 Cell staining techniques

2.13.1 Crystal violet

Cells on microcarriers were visualized by phase contrast light-microscopy (Nikon, Japan) with the aid of crystal violet staining. 200 µl of microcarrier-cell suspension sample was transferred to a well of a 12-well plates and stained with 12.5 µl of crystal violet staining solution comprising 0.5% (w/v) crystal violet (Sigma-Aldrich, China)

and 40% (v/v) absolute ethanol in PBS (Sigma-Aldrich, Ayrshire, UK) for 15 minutes. 2 ml of PBS was added to each well and removed following settling of microcarriers. This wash step was repeated once. Images of stained cells on microcarriers were taken within 40 minutes after wash at 10× magnification.

Chapter 3. Serum Free Adaptation and Characterisation of CV-1 Cell Line*

3.1 Aim and Objectives

In order to develop a more appropriate, scalable cell culture system for manufacture of oncolytic VV, the first objective was to adapt CV-1 cell line from SCM to SFM. Growth characterisations will be performed to enable good understanding of the adaptation of the cell line to different medium conditions. The specific objectives of this Chapter are:

- to adapt CV-1 in two SFMs, VP-SFM and OptiPRO.
- to perform characterisations of CV-1 growth in 5% FBS DMEM and the SFM and evaluate cell growth performance under each medium.
- to evaluate the impact of culture medium on VVL-15 RFP yield and assess the potential of the serum-free adapted cell lines for oncolytic VV production.

* The content in this chapter has been adapted from "Establishing elements of a synthetic biology platform for vaccinia virus production: BioBrick™ design, serum-free virus production, and microcarrier-based cultivation of CV-1 cells" (Liu et al., 2017).

3.2 Adaptation of CV-1 cell line to two types of SFM

Reports of successful adaptation of CV-1 cell line to SFM have rarely been found. Steimer et al. (1981) described the cultivation of CV-1 cells in DMEM supplemented with bovine colostrum or bovine milk obtained 80 days after birth (older milk) as substitutes for serum. The final cell density of CV-1 cells achieved in 2% colostrum was 33% of that achieved in 10% calf serum and growth of CV-1 in 10% older milk was found only in the presence of fibronectin. The significant decrease in cell number and insufficient support to cell attachment suggest that there remains the need for a more effective SFM in promoting CV-1adhesion and proliferation.

In this work, attempts to grow CV-1 cell line in two commercial SFM, VP-SFM and OptiPRO, were made. The media were chosen based upon the following facts: 1) Both media are manufactured free from any components of animal or human origin and formulated with a very low protein concentration no greater than 10 μg/ml; 2) Both media have successfully grown the COS-7 cell line which was derived from the CV-1 cell line; 3) Both media are designed for the growth of mammalian cell lines for virus production (Life Technologies, n.d.; Life Technologies, n.d.); 4) Works have demonstrated the use of either/ both media in effective production of various cell-based viral vaccines (Cardoso et al. 2007; Rourou et al. 2007; Lobo-Alfonso et al. 2010; Chen et al. 2011; Frazatti-Gallina et al. 2004). For some cell lines, superior cell growth and higher virus yields were observed compared with their counterparts in SCM or other SFM (Cardoso et al. 2007; Rourou et al. 2007; Lobo-Alfonso et al. 2010).

Starting from 10% FBS DMEM, cells were adapted to growth in VP-SFM and OptiPRO in a step-wise manner as described in section 2.4. **Figure 3.1** shows the average growth rates observed at each step along the adaptation process during which the serum concentration in the media mixtures gradually decreased.

The average growth rates of CV-1 cells being adapted to both SFM demonstrated a very similar trend. Beginning with a growth rate of 0.62 day^{-1} in 10% FBS DMEM, the rate first increased with the decrease in serum supplementation until 5%. Further dilution of serum with SFM resulted in decrease in average growth rates, the values of which for cell growth in 2.5 and 1% serum became comparable with that in 10% FBS DMEM. Once fully grown in SFM, the average growth rates of CV-1 cells in VP-SFM and

OptiPRO dropped to 0.40 day^{-1} and 0.35 day^{-1} respectively. Cells were grown in 100% SFM for a further three passages before being banked and considered as fully adapted.

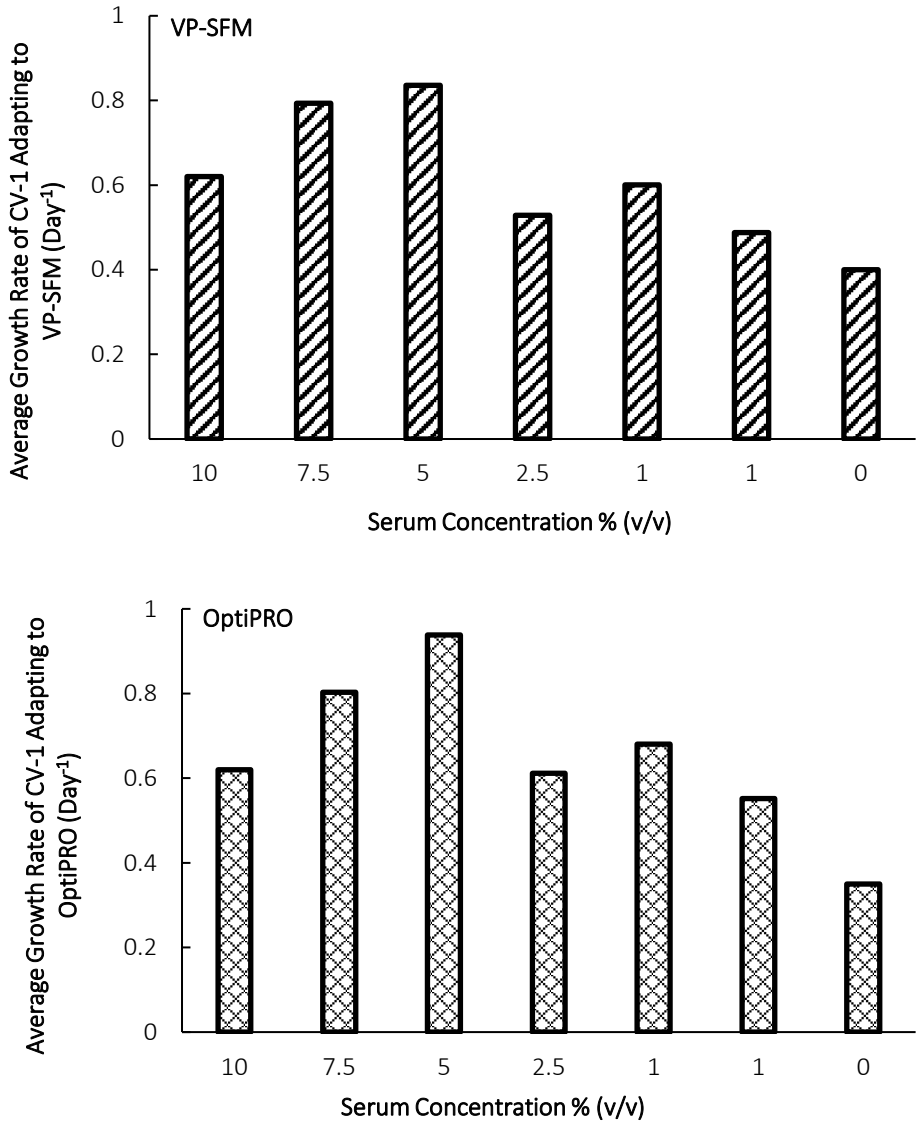

Figure 3.1: Average growth rates of CV-1 cells during stepwise adaptation to SFM. CV-1 cell line adapted to VP-SFM or OptiPRO by lowering the proportion of the initial growth medium 10% FBS DMEM in a stepwise manner. Occasionally, a repeated step had to be introduced to reduce the cells stress generated by low serum concentration. Average growth rates were determined as detailed in section 2.5.1. Each assay contains duplicates.

3.3 Characterization of serum free-adapted CV-1 cell lines

3.3.1 Cell morphologies

One of the initial observations in CV-1 cell lines adapted to SFM was an apparent change in morphology. At either low or high cell densities, cells grown in both VP-SFM and OptiPRO exhibited spindle-shaped elongated morphologies as compared with cells in 5% FBS DMEM which displayed a more flattened morphology and shorter processes (**Figure 3.2**).

Morphology alterations have been widely observed in various cell lines during their adaptation processes from SCM to SFM (Glaser & Conrad 1984; Rizzino & Sato 1978; Wolfe et al. 1980; Chase et al. 2010; Ejiri et al. 2015.; Abdeen et al. 2011). A morphology change similar to ours was oberserd by Wolfe et al. (Wolfe et al. 1980) where, the shape of a Rat C6 Glioma cell line C6BU01 became more flattened after addition of a serum spreading factor (SSF) to the existing SFM. As SSF is one of the major components of serum (Singh et al. 2015), insufficient/ absence of SSF could be a potential explanation for the morphology differences observed between CV-1 cells in SFM and SCM in this experiment.

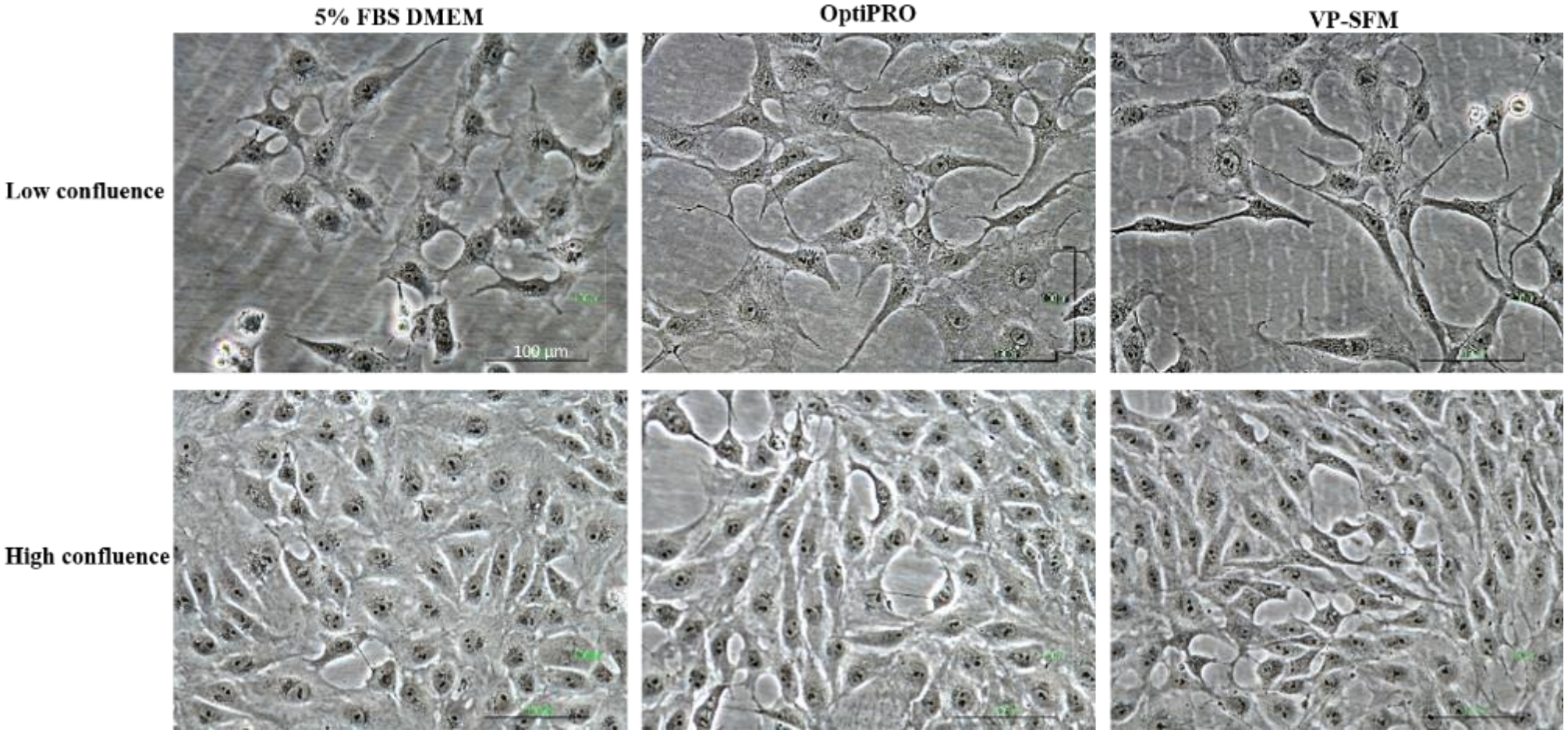

Figure 3.2: Morphologies of CV-1 cell line in 5% FBS DMEM, OptiPro and VP-SFM. Images for CV-1 cells adapted to growth in 5% FBS DMEM, VP-SFM and OptiPRO at low and high confluences at 200× magnifications.

3.3.2 Growth profiles

Cell growth profile defines the growth characteristic of a cell line by evaluation of its lag time before cell proliferation initiates, population doubling time in the middle of cell exponential phase, and saturation density at plateau. This type of assay is useful for comparing efficacy of different media in supporting cell growth (Freshney 2005).

As described in sections 2.5.2 and 2.5.3, cell densities of CV-1 adapted to 5% FBS DMEM, VP-SFM and OptiPRO were measured respectively and plotted against the culture periods as shown in **Figure 3.3**.

For CV-1 cells growth in 5% FBS DMEM (**Figure 3.3A**), the duration of the lag period was 73.5 hours and the total cell number decreased by 23.4% over the first 24 hours post-seeding. Cells entered the exponential phase where an average population doubling time of 20.1 hours was observed, corresponding to a specific growth rate of 0.035 h^{-1}. The population doubling time value obtained was found similar to that of 22 hours reported by Hagedorn et al. (1985) for CV-1 growth in Eagle's basal medium supplemented with 5% (v/v) Foetal Calf Serum (FCS). Reduced cell growth was observed after 168 hours, and the culture reached a saturation density of $1.81x10^5$ cells/cm^2.

A rapid and continuous decrease in total number of VP-SFM adapted CV-1 cells (**Figure 3.3B**) was observed during the first 4 days of culture, resulting in a 79.6% decrease from the initial cell seeding number 96 hours post-seeding. The cell line exhibits a lag time of 126.8 hours and an average population doubling time of 15.9 hours which corresponds to a specific growth rate of 0.044 h^{-1}. Reduced cell growth was observed after 240 hours, and the culture reached a saturation density of $8.6x10^4$ cells/cm^2.

Growth of cells adapted to OptiPRO (**Figure 3.3C**) experienced 65.8 hours lag time before entering exponential phase. The population doubling time of the cell line was 14.8 hours, corresponding to a specific growth rate of 0.047 h^{-1}. Reduced cell growth was observed after 192 hours, and the culture reached a saturation density of $1.54x10^5$ cells/cm^2.

Compared with cell growth in 5% FBS DMEM, despite shorter population doubling time, VP-SFM adapted cells demonstrated a significant drop in cell number during lag

phase, a longer lag time, and a 52.5% lower saturation density. Whereas shorter lag time and population doubling time, and a slightly lower (14.9%) saturation density were found with cells adapted to OptiPRO.

3.3.3 Plating efficiencies

Plating efficiency indicates the ability of cell survival. It is defined as the percentage of cells that develop into colonies in diluted culture and is a sensitive measure of the cell's response to its surrounding (Mather and Roberts, 1998). It also acts as a very useful parameter in developing microcarrier culture procedure (Clark & Hirtenstein 1981) .

As described in section 2.5.4, cells were plated at low densities to minimize their impacts on their culture environment. Colonies formed from CV-1 adapted to 5% FBS DMEM, VP-SFM and OptiPRO were counted respectively and plotted against the number of cells initially seeded as shown in **Figure 3.4**.

The plating efficiency of a continuous cell line is usually no less than 10% (Gangal, 2010). The highest plating efficiency, 27%, was achieved with cells adapted to OptiPRO (CV-1-OPT), followed by 12% from cells growth in 5% FBS DMEM, and 2% from VP-SFM adapted cells. The low plating efficiency obtained from VP-SFM adapted cells reflects the difficulty these cells experienced in growing in the medium.

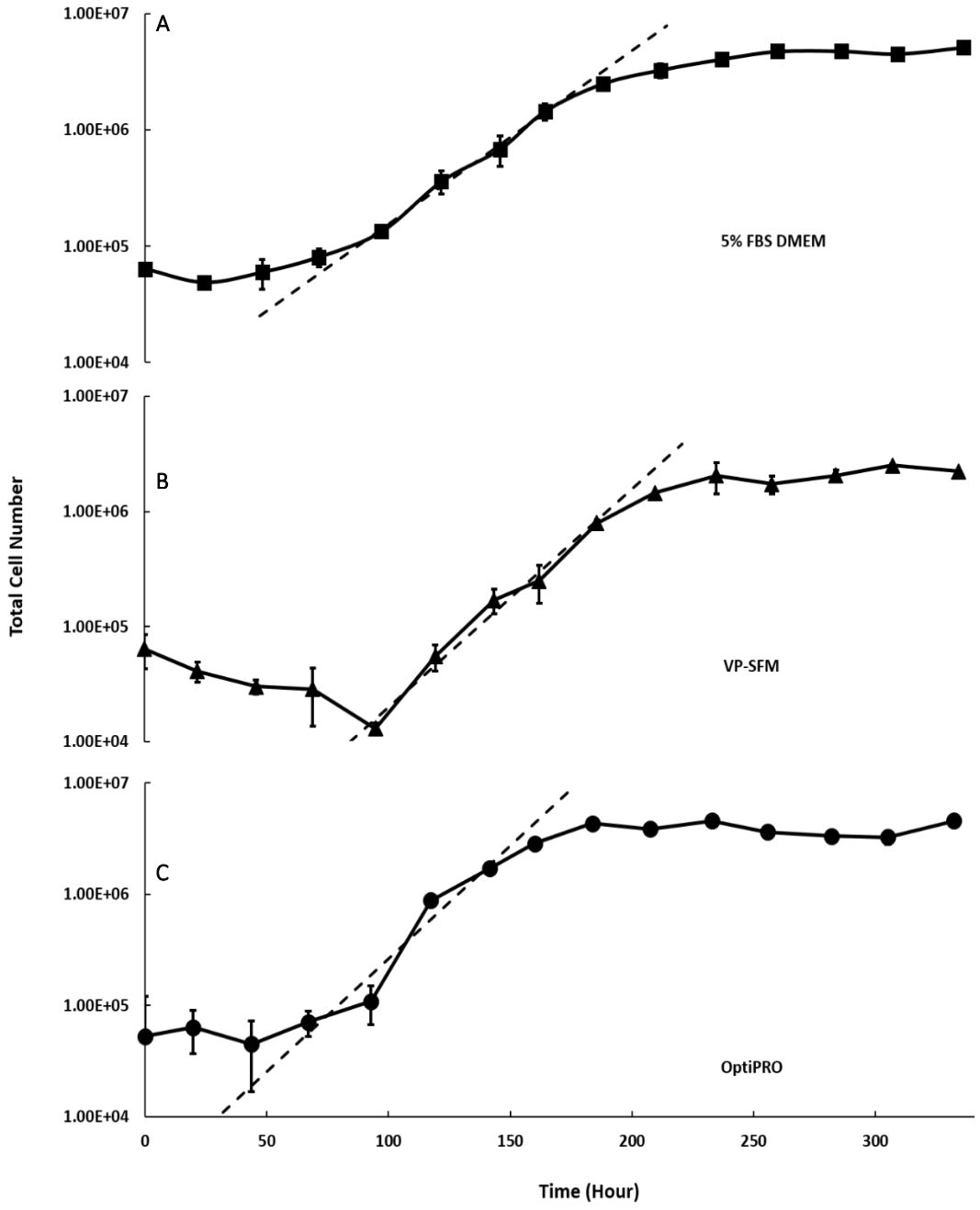

Figure 3.3: **Growth profiles of CV-1 cell line adapted to two SFMs and in SCM.** Each cryopreserved cell line was revived in corresponding medium and passaged 3 times before subjected to the experiment. Experimental conditions: inoculation density= 2000 cells/ cm^2; incubation at 37 ºC, 5% CO_2; three culture media= 5% FBS DMEM, VP-SFM and OptiPRO. Error bars represent one standard deviation about the mean (n=3). Each dashed line is linear regression fitted to the exponential phase of the corresponding cell line. Experiments performed as described in section 2.5.2.

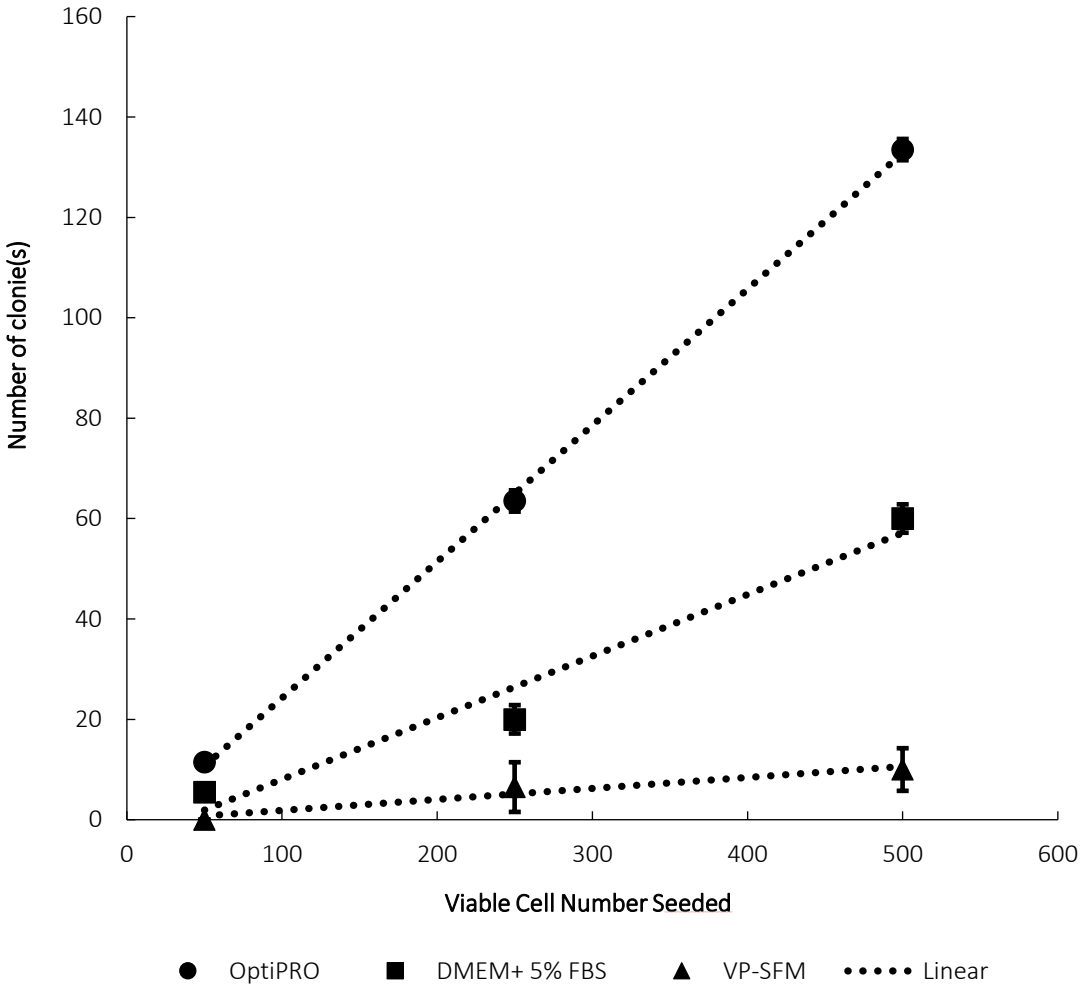

Figure 3.4: Plating efficiencies of CV-1 cultured in 5% FBS DMEM, VP-SFM and OptiPRO. Experimental conditions: three culture media= 5% FBS DMEM, VP-SFM and OptiPRO; inoculation density= 5, 10 and 20 cells/ cm^2; T-25 flasks; incubation at 37 ºC, 5% CO_2. Error bars represent one standard deviation about the mean (n=3). Each dashed line is a fitted linear regression line. Experiments performed as described in section 2.5.4.

3.3.4 Recovery ratios

Cryopreservation is a critical process for providing a reliable and continuous source of host cell lines for production of biopharmaceuticals. Historically, 10% (v/v) DMSO together with either 90% (v/v) serum containing growth medium or 90% (v/v) FBS has been widely employed as a freezing medium for mammalian cells. The use of FBS presents serious concerns as described in section 3.3.1, therefore should ideally be avoided. Methylcellulose is a synthetic polysaccharide that has been demonstrated its use as a protective agent in cryopreservation of human and mammalian cell lines in low-serum or serum-free medium (Kuchler et al. 1960; Mizrahi1 & Moore 1970; Thirumala et al. 2010; Rourou et al. 2007; Merten et al. 1995).

Herein SFM adapted CV-1 cells were cryopreserved in a serum-free freezing medium containing methylcellulose as a preservative. The effectiveness of the freezing medium on cryo-storage of each cell line in liquid nitrogen was indicated by the recovery ratio which was calculated from measured values of the total cell number seeded and total cell number in the supernatant 24 hours post seeding, as described in section 2.5.5.

Comparable recovery ratios, 97.2% and 97.3%, were found for CV-1 cells growth in 5% FBS DMEM and OptiPRO-adapted CV-1 cells. The lowest recovery ratio of 82.1% was obtained from VP-SFM adapted CV-1 cells.

3.3.5 Specific VVL-15 RFP productivities

A comparison was made among CV-1 cells adapted to growth in SFM and SCM for the production of VVL-15 RFP. As described in section 2.11.1, cells that reached 80-90% confluence in VP-SFM, OptiPRO and 5% FBS DMEM were infected with VVL-15 RFP at MOI of 0.1. The virus-containing cell broth was harvested at 24, 48 and 72 hours post-infection and subjected to TCID 50 assay for determining titres.

The results are shown in **Figure 3.5**. Upward trends were found in specific VVL-15 RFP productivities for all 3 cell lines within 72 hours of infection. The highest specific virus productivity achieved was 352.2 ± 48.4 pfu/cell in OptiPRO adapted CV-1 cells, 2.6 times higher than that achieved in VP-SFM adapted cells (135.6 ± 51.2 pfu/cell) and 4.6 times higher than that achieved in cell growth in 5% FBS DMEM (76.7 ± 41.7 pfu/cell). **Table 3.2** shows the productivity of various VV strains in human and mammalian cell lines at a range of FBS and MOI conditions. The productivity value obtained for VVL-15 RFP produced in 5% FBS DMEM was found to be in the similar range as reported in **Table 3.2**. The productivity of VVL-15 RFP in VP-SFM adapted CV-1 cell was higher than that of the Copenhagen strain VV in chicken embryo fibroblasts (CEF) in VP-SFM (Gilbert et al. 2005).

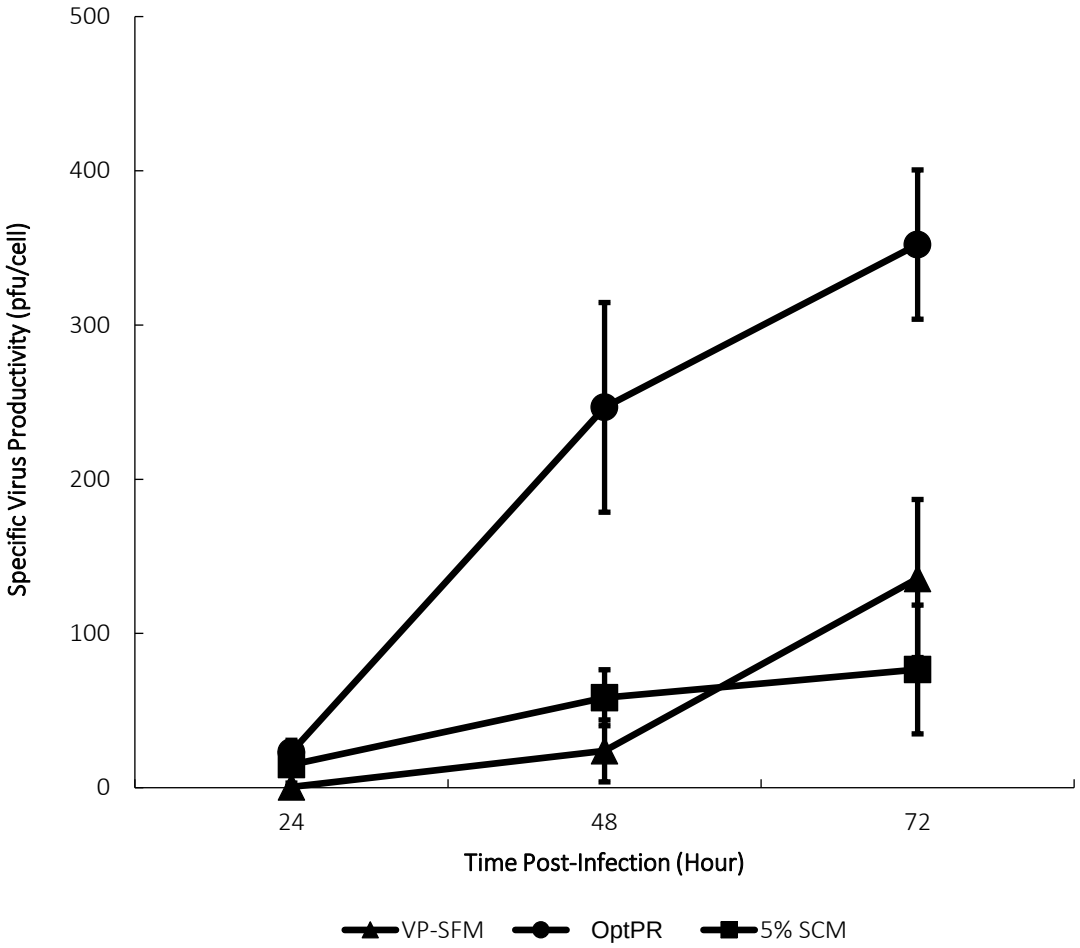

Figure 3.5: VVL-15 RFP production in CV-1 cells adapted to VP-SFM, OptiPRO and 5% FBS DMEM. Experimental conditions: Three culture media= 5% FBS DMEM, VP-SFM and OptiPRO; cell confluency at infection= 80% - 90%; MOI= 0.1; six-well plates; incubation at 37 ºC, 5% CO_2. Error bars represent one standard deviation about the mean (n=3). Experiments performed as described in section 2.10.1.

3.4 Summary

The characteristic of CV-1 cell lines adapted in SFMs are summarised in **Table 3.1**. OptiPRO-adapted CV-1 cells display an overall stronger growth performance, demonstrating the shortest population doubling time and highest plating efficiency among the cells grown in the three different culture media. Comparable saturation densities and recovery ratios were obtained in CV-1 cells in OptiPRO and 5% FBS DMEM, which are higher than those in VP-SFM. The highest viral productivity at each time point was also achieved by CV-1 cells cultured in OptiPRO. Therefore, the OptiPRO-adapted CV-1 cell line was selected for further studies into its expansion strategies.

Table 3.1: Characteristics of CV-1 cells adapted to and growth in 5% FBS DMEM, OptiPRO and VP-SFM.

Medium Type	**Recovery Ratio %**	**Specific Growth Rate μ ($hour^{-1}$)**	**Cell Doubling Time (hour)**	**Average Saturation Density ($cells/ cm^2$)**	**Plating Efficiency (%)**
5% FBS DMEM	97.15 ± 0.72	0.0345	20.09	180,800	12.27
OptiPRO	97.31 ± 0.34	0.0468	14.81	153,600	27.15
VP-SFM	82.10 ± 3.59	0.0436	15.90	86,000	2.19

Table 3.2: Summary of VV productivities under similar experimental conditions.

VV Strain	Host Cell Lines	Medium	FBS	MOI	Vessel	Virus Titre (pfu/cell)	Reference
TSI-GSD-241	MRC-5	DMEM	20%	0.1	10-layer Cell Factories	55.8 ± 20.9	Wu et al. 2005
Copenhagen strain	CEF	DMEM	10%	0.1	T-25 flask	7.11	Gilbert et al. 2005
Wyeth	Hela	DMEM	10%	0.05	T-175 flask	100	Ricordel et al. 2013
Copenhagen strain	CEF	DMEM	2%	0.1	T-25 flask	12.1	Gilbert et al. 2005
Copenhagen strain	CEF	VP-SFM	0%	0.1	T-25 flask	35.8	Gilbert et al. 2005

Chapter 4. Growth of OptiPRO-Adapted CV-1 Cell Line in Suspension

4.1 Aim and Objectives

Given that OptiPRO was determined as an appropriate SFM for culture of CV-1 cells and propagation of VV, the next aim was to assess the potential of cultivation of CV-1-OPT cell line in suspension as opposed to adherent cultivation. Suspension culture is preferred in commercial scale manufacturing processes as scale-up becomes less sophisticated. In particular, adapting CV-1-OPT to suspension and growing the cell line on microcarriers was the focus. It is expected that suspension culture will provide simpler, more reproducible cultivation process and reduce the overall manufacturing cost and footprint. The specific objectives are:

- ❖ to adapt CV-1-OPT cell line to grow in suspension culture.
- ❖ to examine the attachment and growth of CV-1-OPT cell line on Cytodex-1 microcarriers.
- ❖ to investigate the impacts of shear protectant PluronicF-68, inoculum density and feeding strategy on growth of CV-1-OPT cell line on Cytodex-1 microcarriers.

4.2 Suspension adaptation of OptiPRO-adapted CV-1 cells

Paillet et al. (2009) described for the first time the successful adaptation of adherent Vero cells that also originate from green monkey kidney cells to single cell suspension growth (sVero) in homemade SFM. Cell density obtained from the fully adapted sVero after cultivation for 7 days was 2.5 $\times 10^6$ cells/ ml, which is comparable or even slightly higher than the densities reached by growing Vero cells on microcarriers in several SFM in spinner flasks batch cultures (Chen et al. 2011; Rourou et al. 2007). However, studies on adapting CV-1 cell line to suspension culture have not been reported. In this work, attempts to adapt CV-1-OPT to suspension culture were made.

Starting with an inoculation density at 5.21×10^5 cells/ml with 96.0% viability, CV-1-OPT cells were seeded in two 250ml shake flasks each with 100ml OptiPRO medium supplemented with Pluronic F-68.

Pluronic F-68 (PF68) is a non-ionic surfactant that has been used as a shear protective agent particularly in SFM culture (Martinelle et al. 2010; Chen & Chen 2009; Meleady 1997). Approximately 80% of the molecule by weight contains hydrophilic poly(oxyethylene) groups and the rest is hydrophobic (poly)oxypropylene groups (Florence and Attwood, 2016). The functions of Pluronic can be grouped into biological effects and physical effects. The former are the effects that Pluronic F68 has on cell itself. For example, Murhammer and Goochee (1990) described the incorporation of PF-68 into the plasma membrane, which altered the membrane properties and led to increased level of cell resistance to shear forces. The latter involves the changes in medium physical properties. PF68 could reduce cell to bubble attachment, thus reducing the number of cells that come into close contact with shear stresses as a result of bubble rupture (Michaels, 1995). Moreover, Merlin from Columbia University (n.d.) suggested the usefulness of Pluronic F-68 in disaggregation of clumped cells.

Based on manufacturer's recommendation, Pluronic F-68 provided at a concentration of 10% was added to OptiPRO medium to a final working concentration of 0.1%. **Table 4.1** summarizes the experimental conditions for the first adaptation experiment.

As shown in **Figure 4.1**, on day 4 post-inoculation, the total cell density dropped to 2.81×10^5 cells/ml with 44.8% viability, resulting in a total viable cell number of 2.52×10^7 between the two flasks. Since the cell density in each flask was low, cells in both flasks were pelleted by centrifugation and pooled into one 100 ml shake flask with 50ml OptiPRO and 0.1% working

concentration Pluronic F-68. The viable cell density in the single flask was 2.85×10^5 cells/ml, making a total viable cell number of 1.43×10^7.

The 43% loss in viable cell number after pooling was suspected to be related to the presence of cell aggregates in the medium and cell death. The former can lead to wide variation in cell count. The latter could be a result of the various stress factors that the cells had exposed to, such as absence of serum, agitation, and those caused by cell harvest and re-inoculation operations etc.

By day 8, the viable cell density dropped to 2.02×10^5 cells/ml. Extensive cellular clumping was observed (**Figure 4.2**). Cell clumping was not desirable as it could cause changes to cell metabolism and difficulties in long-term cell proliferation (Tsao et al. 2001). In addition, large cell clumps could reduce viral infection efficiency. The cells were reseeded in fresh medium and passaged every four days. Cell density edged down to 0.666×10^5 cells/ml 20 days post-seeding, which was too low for a new passage. Thus, the culture was discontinued.

Tharmalingam et al. (2008) and Wu (1999) observed enhanced growth and viability when using 0.2% working concentration Pluronic F-68 in suspension cultures of some mammalian cell lines. Besides, conditioned medium is generally believed to contain condition factors that have growth-stimulating effects. Therefore, in the second attempt of suspension adaptation of CV-1-OPT, cultures were initially split into three groups to examine the impact of using conditioned medium or higher concentration of PF-68 on suspension growth of CV-1-OPT. **Table 4.2** detailed the experimental conditions. The conditioned OptiPRO was prepared by mixing equal volume of the growth medium that was obtained on the second, third and fourth days of the previous passage.

Starting with an inoculation density at 4.89×10^5 cells/ml with 97.7% viability, CV-1-OPT cells were seeded in six 100 ml shake flasks that were divided into three sets of two. As shown in **Figure 4.3**, the viable cell densities among the three sets showed little difference and dropped more than 75% in the first five days of culture. As the cell density in each flask was too low, all the cells after passage were combined into one 100 ml shake flask with 50ml fresh OptiPRO and 0.2% Pluronic F-68. The viable cell density in the 100 ml shake flask was 2.13×10^5 cells/ml. A transient increase was observed on the sixth day of culture, followed by a progressive decline in cell density. By the ninth day of cell culture, the viable cell density fell to 1.80×10^5 cells/ml and severe cell clumping was observed (**Figure 4.4**). Cells were passaged to a 50ml shaker flask with fresh OptiPRO reduced to 20 ml supplemented with 0.2% Pluronic F-68 and 1%

(v/v) GIBCO® anti-clumping agent. After four days, cells were passaged one more time. However, no apparent cell growth was observed until the end of the culture at which cell density fell to 0.370×10^5 cells/ml. Large cell aggregates had been seen throughout the late period of the culture (**Figure 4.4**).

It was found through these studies that CV-1-OPT was unable to adapt in OptiPRO. This might be associated with the composition of the medium. Van Wielink et al. (2010) attempted to adapt MDCK cells from adherent to suspension growth in four types of media (OptiPRO, UltraMDCK, SFM4MegaVir and SFM4BHK21) and found that the cells grew exclusively in SFM4bHK21, the only medium that was originally used for suspension culture among the four. It was suspected that the difference between SFM4bHK21 and other media in supporting the growth of adherent cells in suspension could be due to specific components that either promote or inhibit surface attachment and cell-to-cell aggregation, such as calcium.

Table 4.1 Operation conditions for adaptation of CV-1 cell in suspension culture- first attempt.

Day(s) post-inoculation	Agitation speed (rpm)	Number of shake flasks	Medium volume per flask (ml)	Final concentration of PF68 in the medium	Procedure
0-4	120	2	100	0.1%	Suspension Adaptation
4-8	150	1	50	0.1%	
8-12	150	1	50	0.1%	
12-16	150	1	50	0.1%	
16-20	150	1	20	0.1%	End of Adaptation

Table 4.2 Operation conditions for adaptation of CV-1 cell in suspension culture- second attempt.

Day(s) post-inoculation	Agitation speed (rpm)	Number of shake flasks	Total volume of medium per flask (ml)	Final concentration of PF68 in the medium	Medium used	Anti-Clumping Agent concentration (v/v %)	Procedure
0-5	120	2	50	0.1%	100% fresh OptiPRO	0	Suspension adaptation
		2		0.1%	20% conditioned + 80% fresh OptiPRO	0	
		2		0.2%	100% fresh OptiPRO	0	
5-9	150	1	50	0.2%	100% fresh OptiPRO	0	
9-13	150	1	20	0.2%	100% fresh OptiPRO	1	
13-17	150	1	20	0.2%	100% fresh OptiPRO	1	End of adaptation

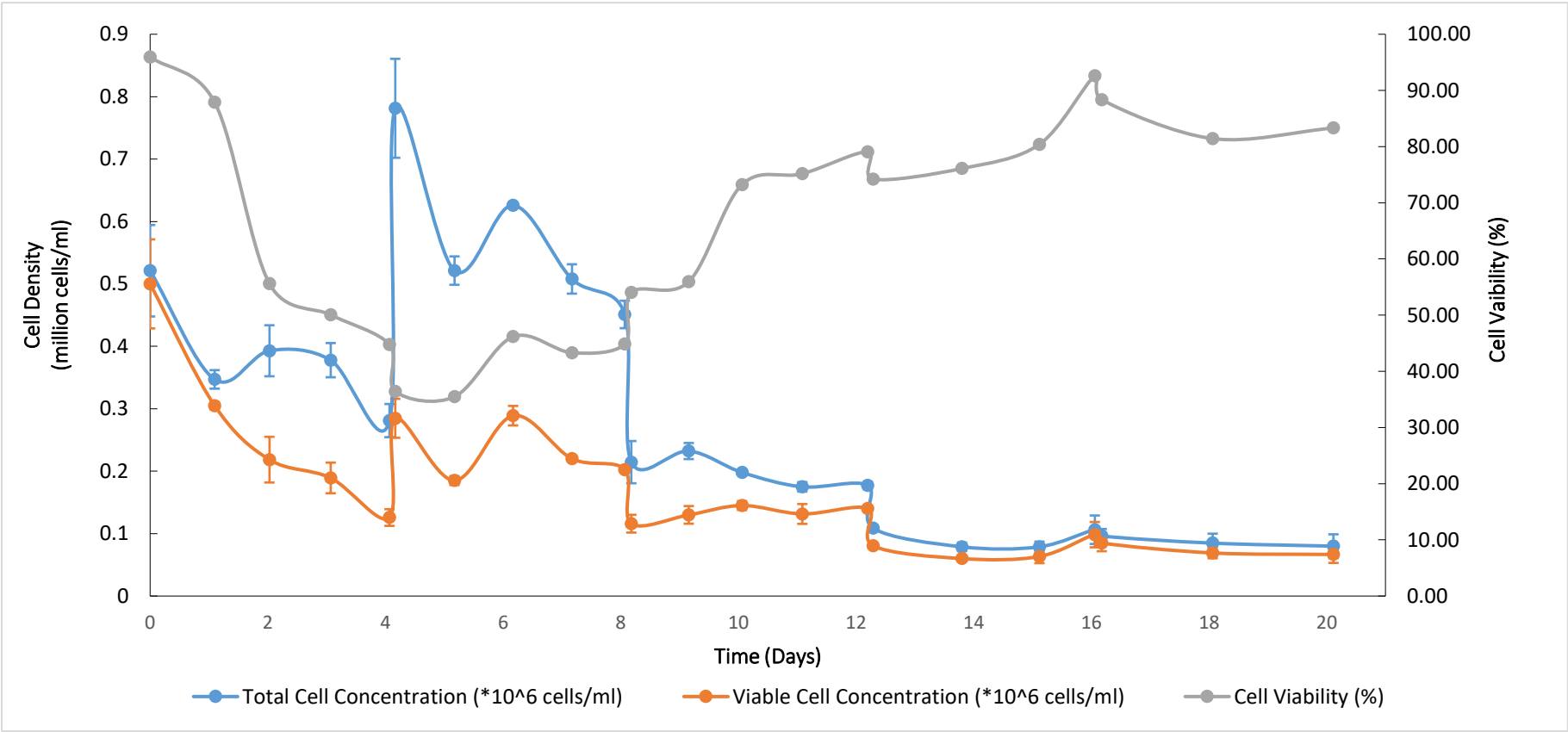

Figure 4.1: Growth profile of CV-1-OPT cell line in OptiPRO supplemented with 1% (v/v) 10% Pluronic F-68. CV-1-OPT cell line was revived after storage in liquid nitrogen and grew in T-flasks for 4 passages before subjected to suspension culture. Each point on the graph from day 0 to day 4 represents the mean cell number of duplicate flasks and each flask were assayed in triplicates at each time point. From day 5 and onwards, each point contains triplicates. Results are presented as mean cell density ± SD.

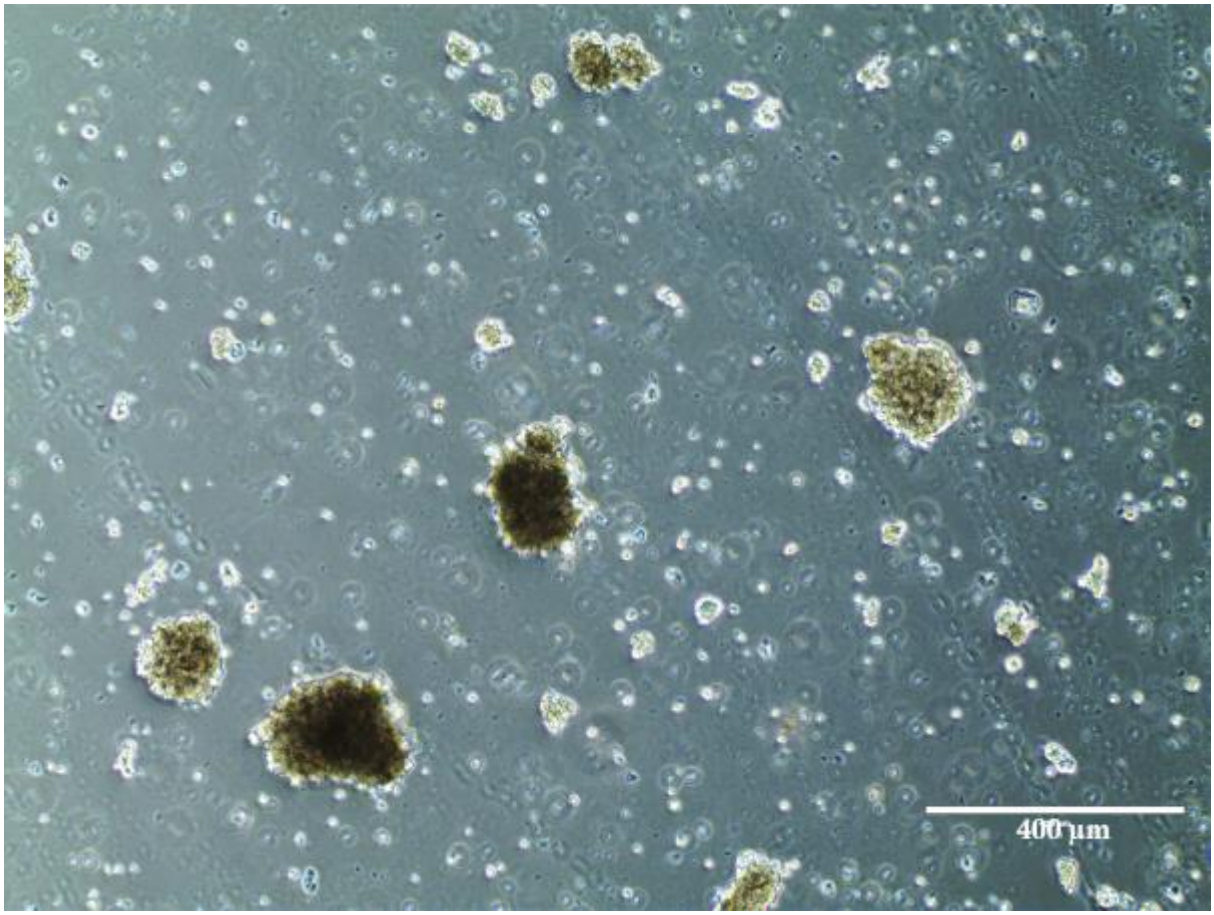

Figure 4.2: CV-1-OPT cell aggregates observed on the eighth day of culture. Images were taken under 100X magnification.

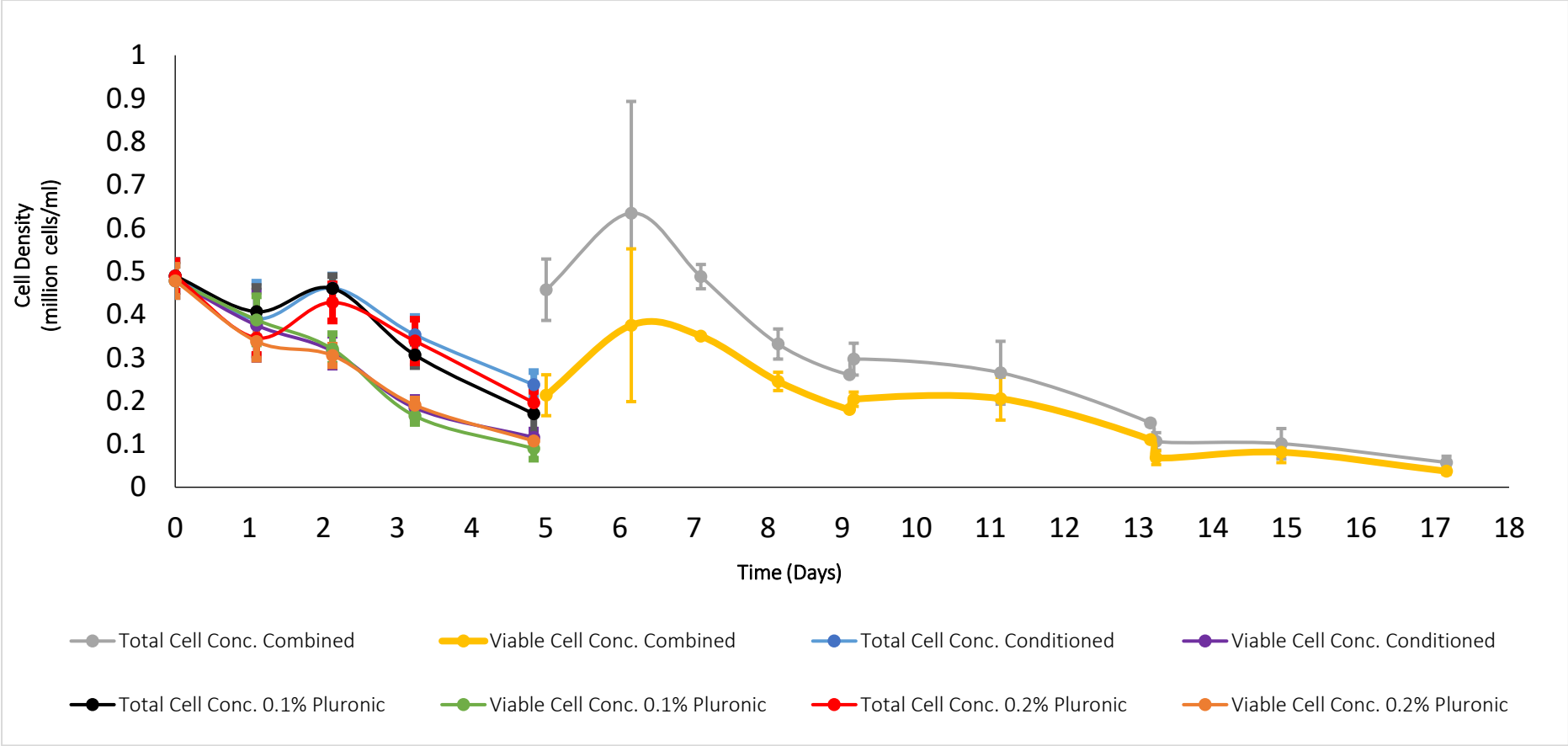

Figure 4.3: Growth profiles of CV-1-OPT cell line in different media formulations in suspension. CV-1-OPT cell line was revived after storage in liquid nitrogen and grew in T-flasks for 6 passages before subjected to suspension culture. Each point on the graph from day 0 to day 5 represents the mean cell number of duplicate flasks and each flask were assayed in triplicates at each time point. From day 6 and onwards, each point contains triplicates. Results are presented as mean cell density ± SD.

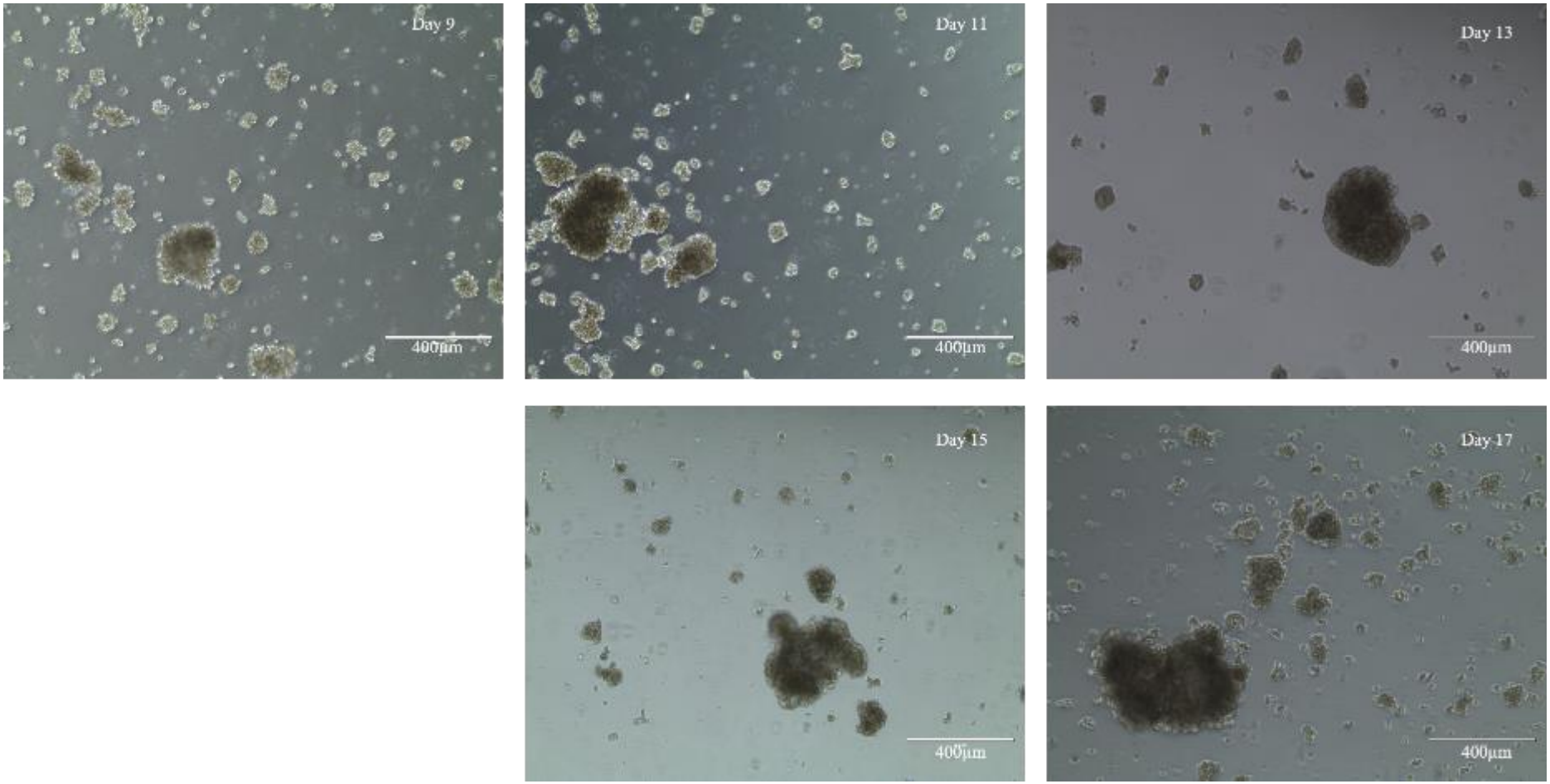

Figure 4.4: CV-1-OPT cell aggregates observed from the ninth day till the end of the culture. Images were taken under 100X magnification.

4.3 Static culture of CV-1-OPT cells on Cytodex-1 microcarrier

Suspension culture of an adherent cell line may also be achieved with the aid of microcarriers. There are varies types of commercially available microcarrier products. Giard et al. (1977) used a type of dextran based microcarriers of which per gram carried 2.0 meq of N,N-diethylaminoethyl (DEAE) anion exchange capacity (Levine et al. 1977) to produce CV-1 cells in Dulbecco modified Eagle medium (DMEM) supplemented with 10% FCS in 250ml spinner flasks suspension culture. The maximum cell concentration achieved was 10^6 cells/ml.

The commercially available GE Cytodex-1 surface microcarriers have similar characteristics to the microcarriers used by Giard et al. (1977), and presents a lower exchange capacity (1.5 meq/g of dry product). The diameter of Cytodex-1 ranges from 147–248µm with an average size of 190 µm. It has been reported that the microcarrier support the growth of CV-1 cells (GE Healthcare, 2005). In this section, a qualitative experiment testing the ability of CV-1-OPT cell line to grow on Cytodex-1 was performed. 3 g/L Cytodex-1 was added to 32 mm diameter non-treated bacteria Petri dishes. Each Petri dish contained 2 ml OptiPRO medium and 2.58×10^5 CV-1-OPT cells, which was equivalent to 10 cells/ microcarrier. Attachment and growth of cells on microcarriers under static culture conditions were examined at 0, 8, 24 and 48 hours post inoculation under the microscope and the results were shown in **Figure 4.5**.

It was observed that after 8 hours of cultivation, most CV-1-OPT cells had attached to the microcarriers. Cell coverage and confluency on the microcarriers continued to increase afterwards, which indicates further cell growth. This experiment showed that the cells can attach to microcarriers and grow successfully.

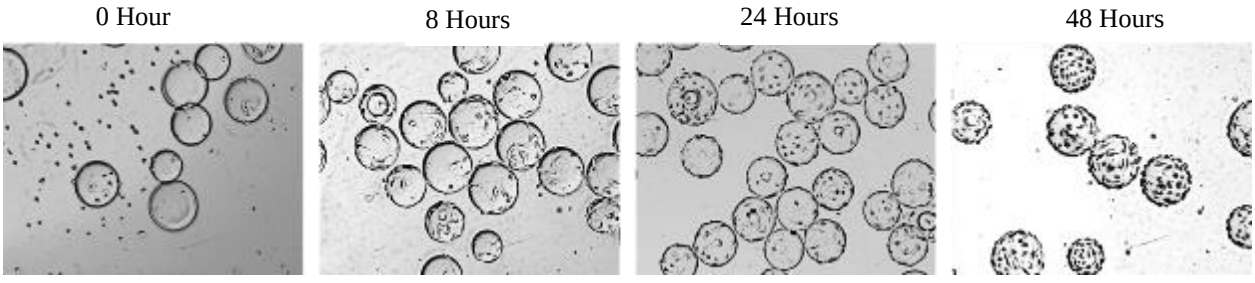

Figure 4.5: Static culture of CV-1-OPT cells in OptiPRO on Cytodex-1 microcarrier in Petri dish. The cultures were incubated at 37ºC with 5% CO_2. Images were taken at 0, 8, 24 and 48 hours post inoculation under 10X magnification.

4.4 Growth of CV-1-OPT on Cytodex-1 in suspension

4.4.1 CV-1-OPT attachment to Cytodex-1

According to the manufacturer's instructions (GE Healthcare 2005), a cell line with a plating efficiency between 10% - 30% is recommended to be inoculated at a density of 5-10 cells/ Cytodex microcarrier, and the suggested suitable inoculation density for CV-1 cell line was 10^5 cells/ ml. Thus, the initial cell inoculation density for CV-1-OPT was set to 10 cells/ microcarrier, which was equivalent to 10^4 cells/ cm^2 or 1.32×10^5 cells/ ml. The concentration of Cytodex-1 was set to 3 g/L.

The efficient attachment of cells to microcarriers depends on sufficient agitation which not only increases cell-microcarrier collisions but also enables adequate time for cell-microcarrier contact. An intermittent agitation strategy could allow a sufficiently high agitation rate to cause suspension of the microcarriers and enough time for cells to attach. Intermittent agitation has been employed in previous studies to improve attachment efficiencies (GE Healthcare 2005; Toriniwa & Komiya 2007; Raffoul et al. 2005). In our experiments, cultures would be exposed to intermittent agitation at 30 rpm for 30 seconds every 30 minutes during the early attachment stage.

Every hour post inoculation, a certain volume of evenly suspended cell broth was sampled from each spinner and filtered through a 40 µm cell strainer in order to collect the unattached cells in the suspension.

As shown in **Figure 4.6**, the attachment kinetics of CV-1-OPT indicated a first-order process for Cytodex-1 over the initial 4 hours period:

$$\frac{dC_f}{dt} = -kC_f \qquad 4.1$$

where, C_f is the unattached cell concentration (cells/ml) in suspension at time t (min); and k is the specific attachment rate (min^{-1}).

Such first-order attachment kinetics have been observed for many cell lines on microcarriers made from DEAE-dextran, such as Vero (Mukhopadhyay et al. 2007; Ng et al. 1996), FS-4. (Nilsson 1988) and CHO (Himes & Hu 1987; Raffoul et al. 2005).

The equation can be expressed in logarithmic form:

$$LnC_0 - LnC_f = kt \qquad 4.2$$

where, C_0 is the initial cell concentration at inoculation (cells/ml).

The length of time required for 50% of cells attachment to microcarriers, $t_{1/2}$ (min), can be calculated as:

$$t_{1/2} = \frac{Ln\,2}{k} \qquad 4.3$$

Under the proposed conditions, the specific attachment rate of CV-1-OPT onto Cytodex-1, k, was 0.013 min^{-1} and the time for 50% of cells attached to microcarriers, $t_{1/2}$, was 55 minutes. This rate was in the range of those observed in other kidney cell lines (Sun et al. 2000; Kiremitci et al. 1991; Mukhopadhyay et al. 2007).

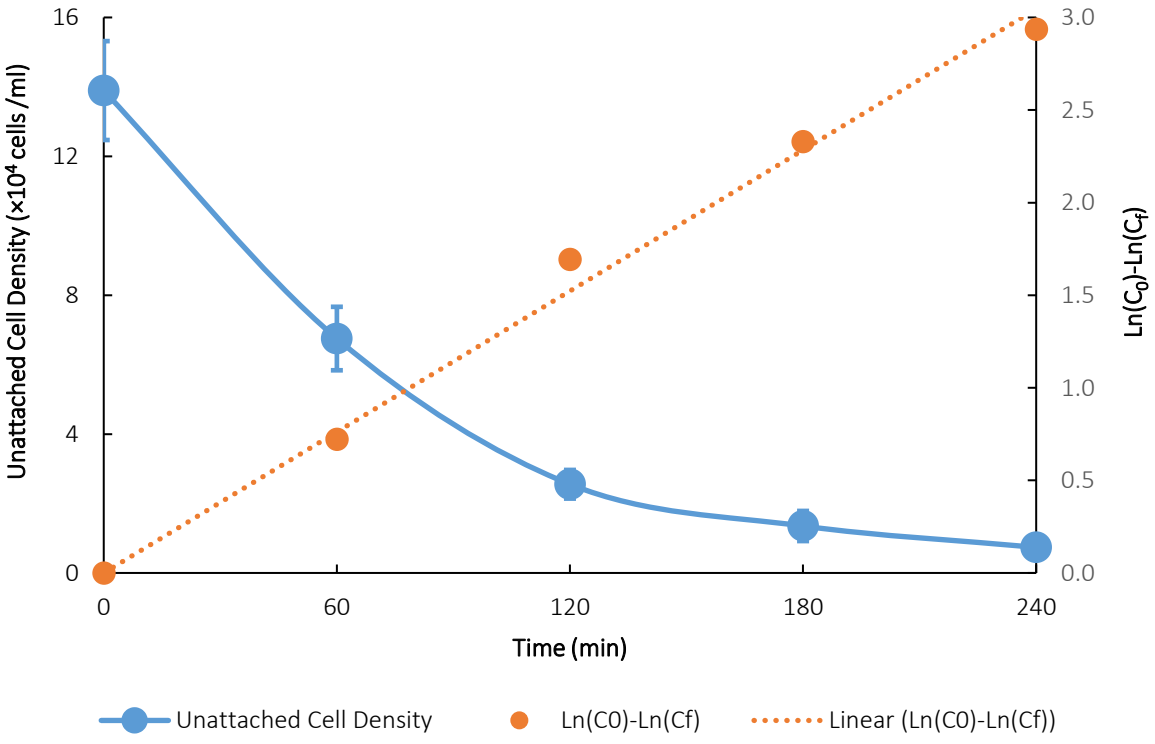

Figure 4.6: The adhesion profile of CV-1-OPT cells to Cytodex-1 microcarrier. The cultures were incubated at 37ºC with 5% CO_2. Each point on the graph represents the mean cell number of triplicate flasks and each flask was assayed twice at each time point. Results are presented as mean cell number ± SD.

4.4.2 Effect of shear protectant on CV-1-OPT growth on Cytodex-1

Compared to freely suspended cells, cells grown on microcarriers are more sensitive to agitation due to the relatively larger size of beads (Papoutakis 1991). Papoutakis (1991) proposed three sources of cellular injury when employing non-porous microcarriers in non-sparged cell cultures. The main source was the collisions between microcarriers at high levels of agitation and in high bead concentration (Papoutakis 1991, Croughan et al 1988). The next source of injury was the interactions between microcarriers and turbulent fluid. Kolmogorov eddies that have a similar size to the bead could cause detrimental effects on the cells attached to the microcarrier upon collision (Papoutakis 1991). Collisions between beads and bioreactor components (the probes and impeller) are less likely to contribute to cellular injury (Papoutakis 1991).

As described in section 4.2, Pluronic F68 has been demonstrated to provide protection to animal cells from shear damage. In this section, the protective effect of Pluronic F-68 on the growth of CV-1-OPT on Cytodex-1 was examined under the hydrodynamic stress conditions that would be used in the future experiments. Spinner flasks were inoculated with an initial cell density of 1.32×10^5 cells/ml equivalent to 10 cells/ microcarrier. The flasks in experimental group were supplemented with 0.1% (v/v) shear protectant Pluronic F-68. The total volume of medium in each flask was 100ml. Based on literature (Quesney et al., 2001; Rourou et al., 2007; Croughan et al., 1991) using Cytodex 1 microcarriers to culture mammalian cells, it was decided to set the agitation speed in the range 30-40 rpm to begin with: Cultures were exposed to intermittent agitation at 30rpm for 30 seconds every 30 minutes for the first 2 days of culture to allow cell-microcarrier attachment and cell-matrix adhesion. Continuous agitation was used from day 3 onwards, at 30rpm from 48 to 72 hours and 35 rpm from 72 hours towards the end of culture.

No significant differences between the cell growth profiles were observed as shown in **Figure 4.7**. The highest cell densities obtained under these two conditions were comparable, $8.47 \pm 0.84 \times10^5$/ml for cultures with 0.1% Pluronic F-68 and $8.38 \pm 1.41 \times10^5$/ml for those without. Therefore, at the agitation regime stated above, cell growth was not affected by adding 0.1% PF68.

Croughan et al. (1988) described the cell damage from hydrodynamic phenomena as insignificant at mid-to-moderate agitation. They reported the uniform growth of FS-4 human fibroblasts cells on Cytodex-1 microcarriers at concentrations ranging from 1.5 to 30 g/L under

the mild agitation rate of 35 rpm. In addition, no detrimental physical effects were observed in Vero, CHO-K1 and BHK-21 cells grown on Cytodex-1 microcarriers at 70 rpm (Wu, 1998). Therefore, the similar growth profiles found in experiments with or without PF-68 was likely due to the harmless and low hydrodynamic stress condition.

The comparable growth profiles could also be attributed to the limited effectiveness of PF-68 in the shear protection of the CV-1-OPT cell line. Wu (1998) suggested that the protective mechanism of PF68 was greatly rely upon the cell type. His study demonstrated that the addition of 0.2% PF68 to the medium could enhance Vero cell growth at a moderately high agitation rate of 110 rpm, but this was not the case with CHO-K1 and BHK-21 cell lines.

As adding 0.1% PF-68 did not have significant impact on the growth of CV-1-OPT against hydrodynamic shear forces under our culture conditions, it was not included in future experiments.

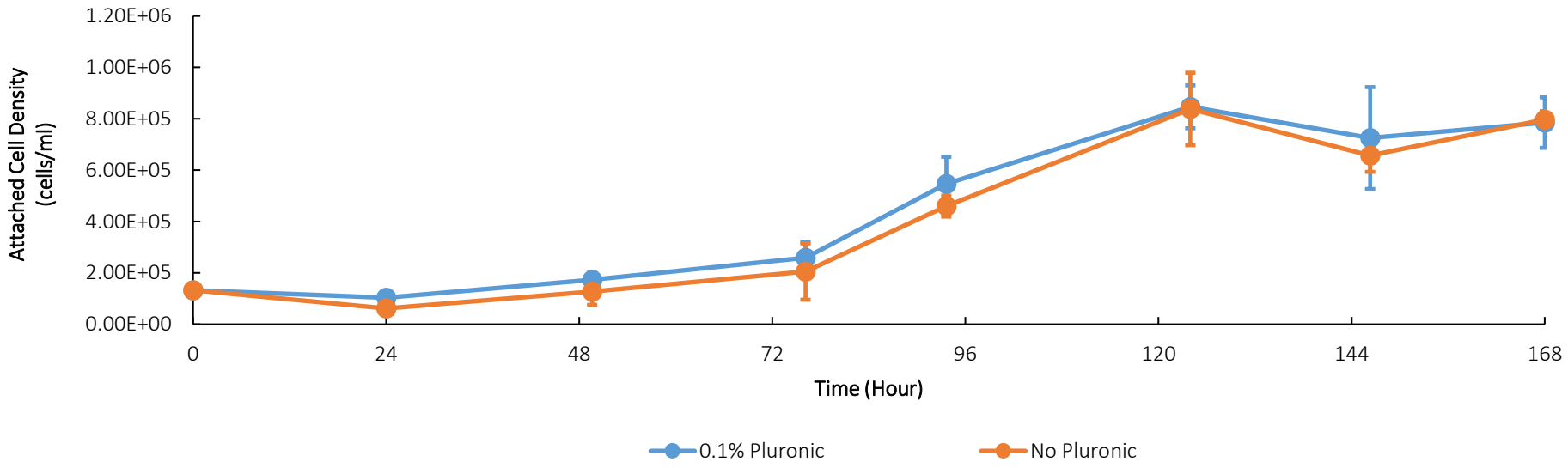

Figure 4.7: Effect of Pluronic F-68 on CV-1-OPT cell growth on Cytodex-1 in suspension. Experimental conditions: 3g/L Cytodex-1; spinner flask; medium and cell line= 100 ml OptiPRO + 1.32×10^7 CV-1-OPT cells; agitation= 0-48 h 30 rpm 30 s/ 30 mins, 48-72 h 30 rpm, >72 h 35 rpm; cell count= crystal violet. The cultures were incubated at 37ºC with 5% CO_2. Each point on the graph represents the mean cell density of triplicate flasks and each flask was assayed in triplicate at each time point. Results are presented as mean cell density ± SD.

4.4.3 Effect of inoculum density on CV-1-OPT growth on Cytodex-1

A minimum density of inoculum is required to ensure a low possibility of empty beads and thus efficient cell expansion. This critical level is contingent on cell type and the ability of cells to survive and proliferate in a new culture under a given set of growing conditions (Clark & Hirtenstein 1981).

Experiments were performed to determine the minimum inoculum size that can give fully confluent cultures. Parallel cultures of CV-1-OPT in spinner flasks were inoculated at each of five densities: 5, 10, 15, 25, and 40 cells/microcarrier with trypan blue counts. These corresponded to 6, 13, 19, 35, and 53 cells/microcarrier with crystal violet counts respectively. It should be noted that due to the long incubation time needed for counting cells using crystal violet method, it was decided to first use the cell concentration obtained from trypan blue method to determine the cell seeding number. In the meantime, to maintain consistency throughout the experiment, the crystal violet counting method was also employed to report the actual seeding concentration.

Experimental settings and measurement of parameters associated with cell growth were described in sections 2.6 and 2.7. The results were shown in **Figure 4.8** and **Table 4.3**.

The specific growth rate of CV-1-OPT cells decreases with the increase of the cell inoculation density (**Table 4.3**). Cell population was able to double every 26 hours when the culture was inoculated at a density of 6 cells/ microcarrier. It is noteworthy that no apparent cell growth was observed when an inoculation density of 53 cells/ microcarrier was applied (**Figure 4.8**). Also at a relatively high inoculation density of 35 cells/ microcarrier, a long cell population doubling time of 256.72 hours was obtained, which could not be regarded as truly proliferation. A doubling time above 100 hours could possibility result from the low cell viability of a culture since only a small fraction of cells remains viable and proliferative (Biaggio et al. 2015). The saturation cell densities achieved under different inoculation densities were similar, ranging from 6.50-7.68 $\times 10^5$ cells/ mL, which were reached after 120 hours of culture.

Similar finding was raised by Ng et al. (1996), where Vero cells were grown in cultures with 1.7 g/L Cultispher-G microcarriers at various cell inoculum densities. It was observed that an initial cell/bead ratio of 15-300 made no impact on the final cell yields. Yet, the efficiency of cell doublings declined along with the increase of the cell inoculum size.

As briefly mentioned in section 4.3, Giard et al. (1977) observed the growth of CV-1 cells in DMEM supplemented with 10% foetal calf serum on the dextran matrix based microcarriers that shared similar properties to Cytodex-1. The cells were seeded at a density of 1.4×10^4 cells/ cm^2 into spinner flasks containing 5 mg/mL of microcarriers. The cells entered stationary phase on day 7 with a saturation density of approximately 10^6 cells/ mL, which is at least 30% higher than the saturation densities of CV-1-OPT cells obtained in our experiments. CV-1 cells in the serum-containing DMEM exhibited a doubling time around 48 hours, longer than the CV-1-OPT cells seeded at a similar density range (**Table 4.3**).

Besides the lower yields, it was also observed that the distributions of cells grown on microcarriers were uneven throughout the cultivation period as shown in **Figures 4.9** and **4.10**. This was most noticeable in cultures with lower inoculum size (e.g. 6 and 13 cells/microcarrier). Even when cells reached maximum densities (**Figure 4.10**), unoccupied/ unsaturated beads were spotted and signs of bead-to-bead cell transfer were observed. This suggests that there are factors other than available growth area that restrict the proliferation of cells.

4.4.4 Metabolic analysis of the cell cultures reported in section 4.4.3

In order to further understand the growth of CV-1-OPT, the availability of nutrients and accumulation of toxic metabolites in the cultures were analysed, with a particular focus on the glycolysis and glutaminolysis. The results of metabolic analysis including glucose, lactate, glutamine, glutamate and ammonia were shown in **Figure 4.11**.

The initial glucose concentration (3.13 g/L, 17.39 mM) progressively decreased as CV-1-OPT cell growth continued. The decrease slowed down gradually after 72 hours. (**Figure 4.11A**). This observation is in accordance with the near-zero specific consumption rates of glucose obtained at day 5 (**Figure 4.11B**). Glucose was consumed at peak specific rates of 0.0877 and 0.0805 mmol h^{-1} 10^{-8} cells at 48 hours for cultures inoculated with 6 and 13 cells/ microcarrier, and 0.0585, 0.0437 and 0.0243 mmol h^{-1} 10^{-8} cells at 24 hours for cultures inoculated with 19, 35 and 53 cells/ microcarrier respectively. These rates were in the range of those observed for other kidney cell lines such as Vero (0.05 mmol h^{-1} 10^{-8} cells) (Petiot et al., 2010), BHK (0.0108 mmol h^{-1} 10^{-8} cells) (Cruz et al., 1999), HEK 293 cells (0.029 mmol h^{-1} 10^{-8} cells) (Garnier et al., 1994), or MDCK cells (0.0114 mmol h^{-1} 10^{-8} cells) (Cruz et al., 2000). The glucose levels at the end of the cultures were equal to or greater than 6.51 mM. This concentration, although not deemed high, surpasses the typical low-glucose formulation of 5.5 mM found in classical media such as BME and DMEM.

Lactate is considered as a major by-product of glucose and can also be produced from glutamine. Lactate inhibits mammalian cell growth by altering the osmolality and pH. Under the experiment conditions, lactate was initially accumulated, reaching peaks that were no greater than 14.17 mM after 3 or 4 days of culture (**Figure 4.11A**). Generally speaking, lactate concentrations no more than 20 mM do not interfere with cell growth (Biaggio et al. 2015). So the maximal lactate concentration measured in the experiments could be considered as non-toxic.

The levels of lactate then decreased (**Figure 4.11A**), consumed by the CV-1-OPT cells after being converted to pyruvate by lactate dehydrogenase (Graff 1965). Uptake of lactate was observed in other cell lines and can sometimes be associated with the depletion of glutamine. Zagari et al. (2013) described the lactate profiles of CHO-S cell line cultivated in a chemically defined media. Lactate switched from accumulation to net consumption once the glutamine was depleted, while high concentrations of glucose (> 15mM) was still present. They proposed that lactate was used to refill the tricarboxylic acid (TCA) cycle. Similar phenomena were observed by Quesney et al. (2001) in Vero cell culture in a SFM supplemented with 4% serum. Although the correlation between lactate consumption and glutamine depletion does not always hold up since lactate utilization can be affected by other factors such as mitochondrial oxidative activity of the cells and unidentified media components (Zagari et al. 2013), it is worth investigating the glutamine profiles in the cultures.

Besides integrating into polypeptides to form protein, glutamine is involved in the synthesis of several other amino acids and energy production through TCA cycle, and is indispensable for nucleotide synthesis (Xie and Zhou, 2005).

In the experiments, GlutaMAX acted as the glutamine provider. Unlike glutamine which is extremely sensitive to temperature, pH and age and can degrade non-enzymatically into ammonia, GlutaMAX is an L-alanine-L-glutamine dipeptide that is more thermally stable and releases L-glutamine only when broken down by aminopeptidases secreted from cells. This is similar to a fed-batch process that enables continuous supply and maintenance of glutamine at adequate but low level in culture medium (Life Technologies, n.d).

As a result, the initial glutamine concentration in the medium was 0 (**Figure 4.11C**). Glutamine concentrations started to become detectable and increase after 0, 24, 96 and 120 hours for cultures inoculated with 53, 35, 19, 13 and 6 cells/ microcarrier respectively. However, glutaminolysis had taken place from the very beginning of each culture, which was reflected

by the progressive increase of glutamate and ammonia levels since the day of inoculation (**Figure 4.11D**). I proposed that the rise in glutamine concentration within the culture medium could be linked to the growth status of CV-1-OPT cells. The release of glutamine into the medium seems to take place when the cells are nearing their saturation density plateaus. The reduced proliferation ability of the cells could be responsible for the diminished uptake of glutamine, leading to an accumulation of glutamine concentrations. This could indicate that glutamine might not be the limiting factor of cell growth as it was still available when the proliferation of CV-1-OPT began to slow down. This is also evidenced by the fact that the glutamine concentrations at the end of the cultures are all above 1.32 mM.

The major sources of ammonia building up in mammalian cell cultures are through glutamine catabolism and chemical decomposition. Ammonia is toxic to mammalian cells, can increase the pH of the broth and affect protein glycan distributions (Xie and Zhou, 2005). Although the inhibitory concentration of ammonia is dependent on the cell line and culture conditions (Xie and Zhou, 2005), the threshold values reported were usually above 1 mM (Schneider et al. 1996, Xing et al. 2008, Rose et al., 2003). Under the experiment conditions, ammonia levels kept rising and reached final concentrations no greater than 0.8 mM (**Figure 4.11D**). This is below the general range that would result retardation in cell growth.

Yield coefficient of lactate from glucose ($Y_{Lact/Glc}$) quantifies the amount of lactate production from glucose. The transformation of 1 molecule of glucose to 2 molecules of lactate generates only 2 molecules of ATP compared with the maximum of 28 molecules of ATP generated from complete oxidation of glucose. If glucose is not deliberately maintained at a low level in a culture, the $Y_{Lact/Glc}$ in the culture usually varies between 1 and 2 (Xie and Zhou, 2005). This indicates that over 50% of the glucose consumed goes directly to lactate production. The reasons for this excessive glycolysis have not been completely clarified to date. However, a majority of continuous cell lines cultivated *in vitro* exhibit an elevated rate of glucose conversion to lactate (Young 2013). In the experiments, the $Y_{Lac/Glc}$ peaked at 2.18 – 2.27 after 2-3 days of culture, which were greater than the theoretical upper limit of the stoichiometric ratio of 2, indicating that lactate production was derived from not only glycolysis pathway but also other metabolic pathways that produce pyruvate (**Figure 4.11E**). An $Y_{Lact/Glc}$ above 2 was also observed in Vero cells cultivated on microcarriers in a complex SFM in 250ml spinner flasks (Petiot et al. 2010).

In summary, the glucose levels at the end of the cultures closely resembled or exceeded the conventional low-glucose formulation of 5.5 mM typically found in classical media. The other major metabolite, glutamine, appeared to be consistently available throughout cell culturing, while the two primary waste products, lactate and ammonia, did not reach toxic levels in general. The primary direction of glucose utilization in each culture was for lactate production. Given that comparable saturation cell densities were achieved in cultures regardless of initial inoculation densities and considering the slow growth of cells at higher inoculation densities, it is suspected that the accumulation of specific waste products or limited availability of certain components in the medium, possibly glucose or other metabolites not analysed in this study, played a significant role in restricting cell proliferation.

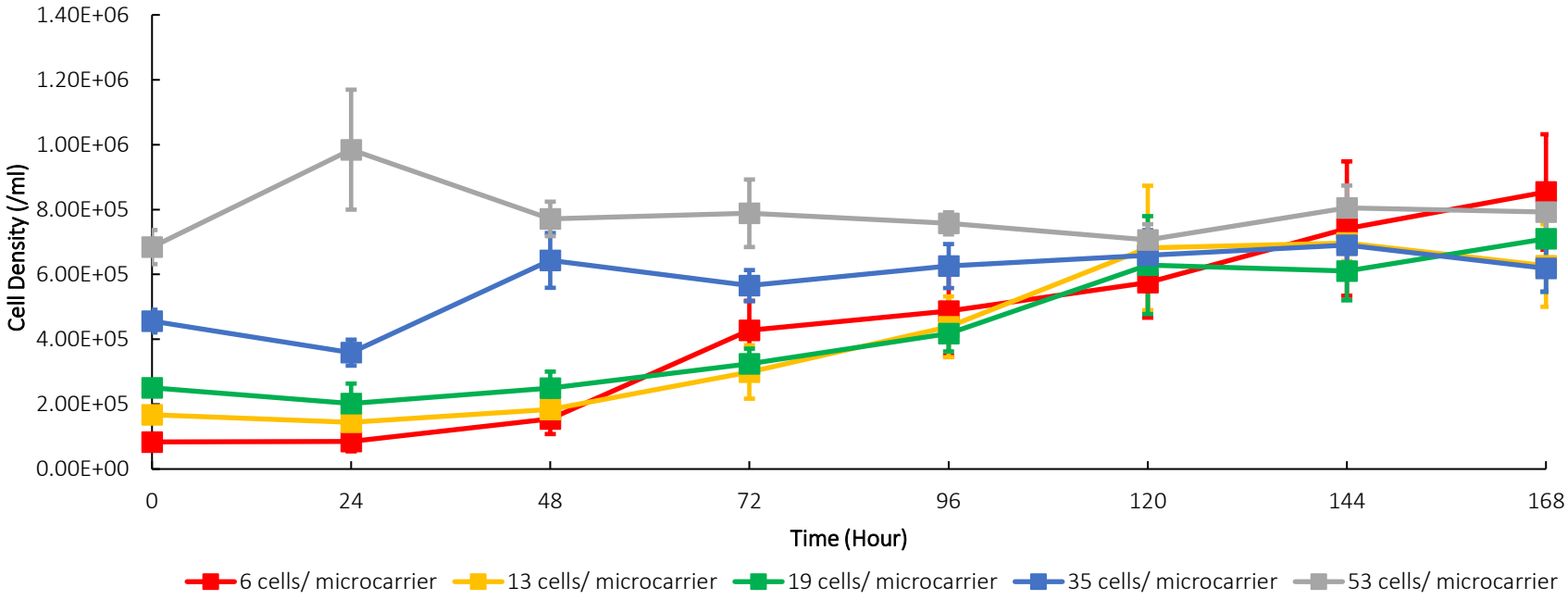

Figure 4.8: Effect of inoculum density on CV-1-OPT cell growth on Cytodex-1 in suspension. Experimental conditions: 3g/L Cytodex-1; spinner flask; medium and cell line= 100 ml OptiPRO + CV-1-OPT cells; agitation= 0-48 hrs 30 rpm 30 s/ 30 mins, 48-72 h 30 rpm, >72 h 35 rpm; cell count= crystal violet. The cultures were incubated at 37ºC with 5% CO_2. Each point on the graph represents the mean cell density of duplicate flasks and each flask was assayed in triplicate at each time point. Results are presented as mean cell density ± SD.

Table 4.3 Characteristics of CV-1-OPT cells growth on Ctyodex-1 microcarriers under different inoculation densities.

Cells/ Microcarrier at Inoculation	Cells/ cm^2 at Inoculation ($\times 10^4$ cells/ cm^2)	Specific Growth Rate ($hour^{-1}$)	Saturation Cell Density ($\times 10^5$ cells/ mL)	Saturation Cell Density ($\times 10^4$ cells/ cm^2) *	Doubling Time (hour)
6	0.93	0.0261	7.23 ± 1.41	5.48	25.56
13	2.01	0.0166	6.69 ± 0.37	5.07	41.76
19	2.94	0.0116	6.50 ± 0.53	4.92	59.75
35	5.41	0.0027	6.56 ± 0.36	4.97	256.72
53	8.19	0	7.68 ± 0.11	5.82	No data

* Each gram of dry Cytodex-1 microcarriers provides a surface area of 4400 cm^2.

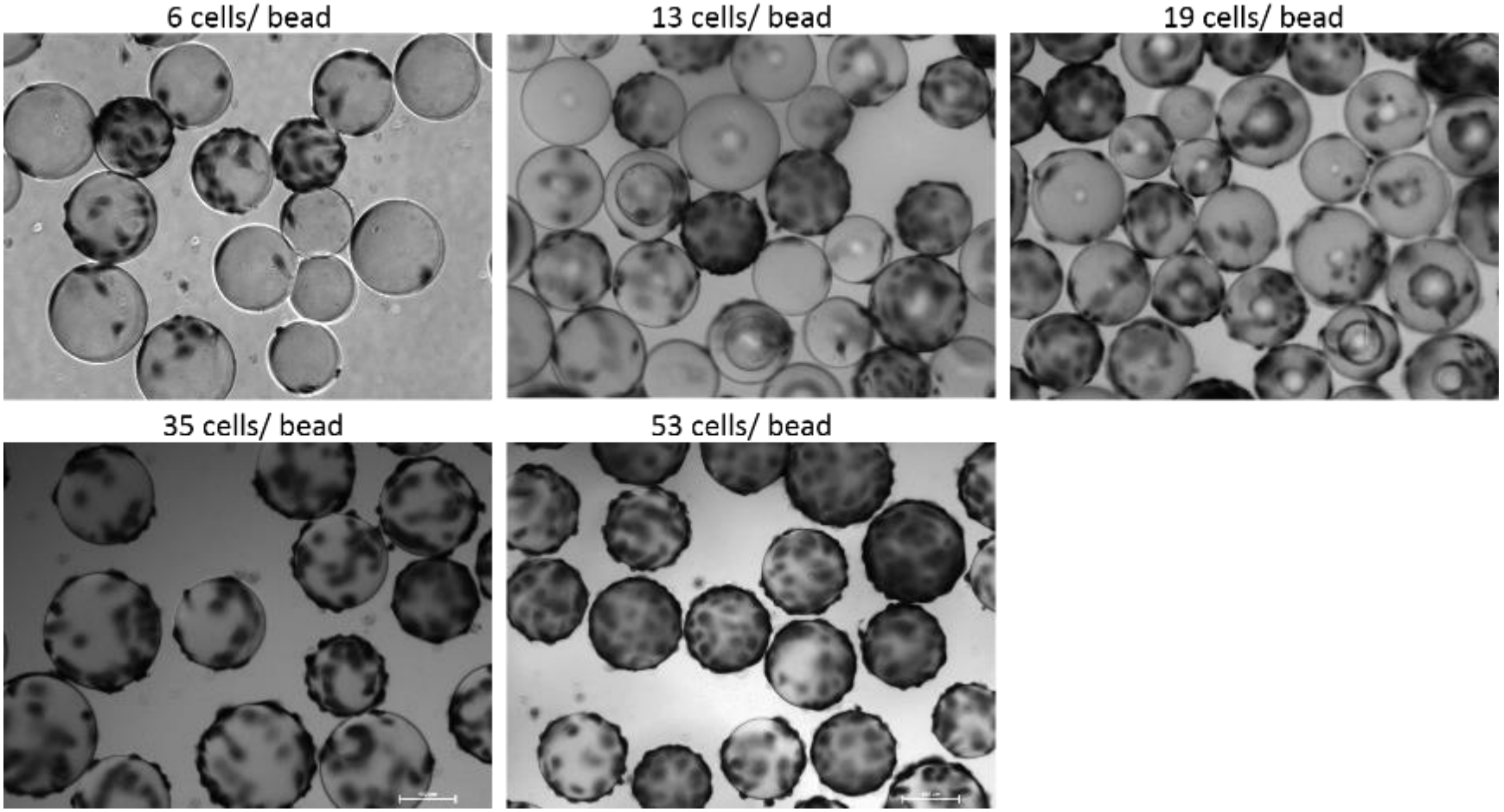

Figure 4.9: Distribution of CV-1-OPT cells on Cytodex-1 24 hours post-inoculation. Experimental conditions: 3g/L Cytodex-1; spinner flask; medium and cell line= 100 ml OptiPRO + CV-1-OPT cells; agitation= 30 rpm 30s/ 30 mins. Images were taken under 10X magnification.

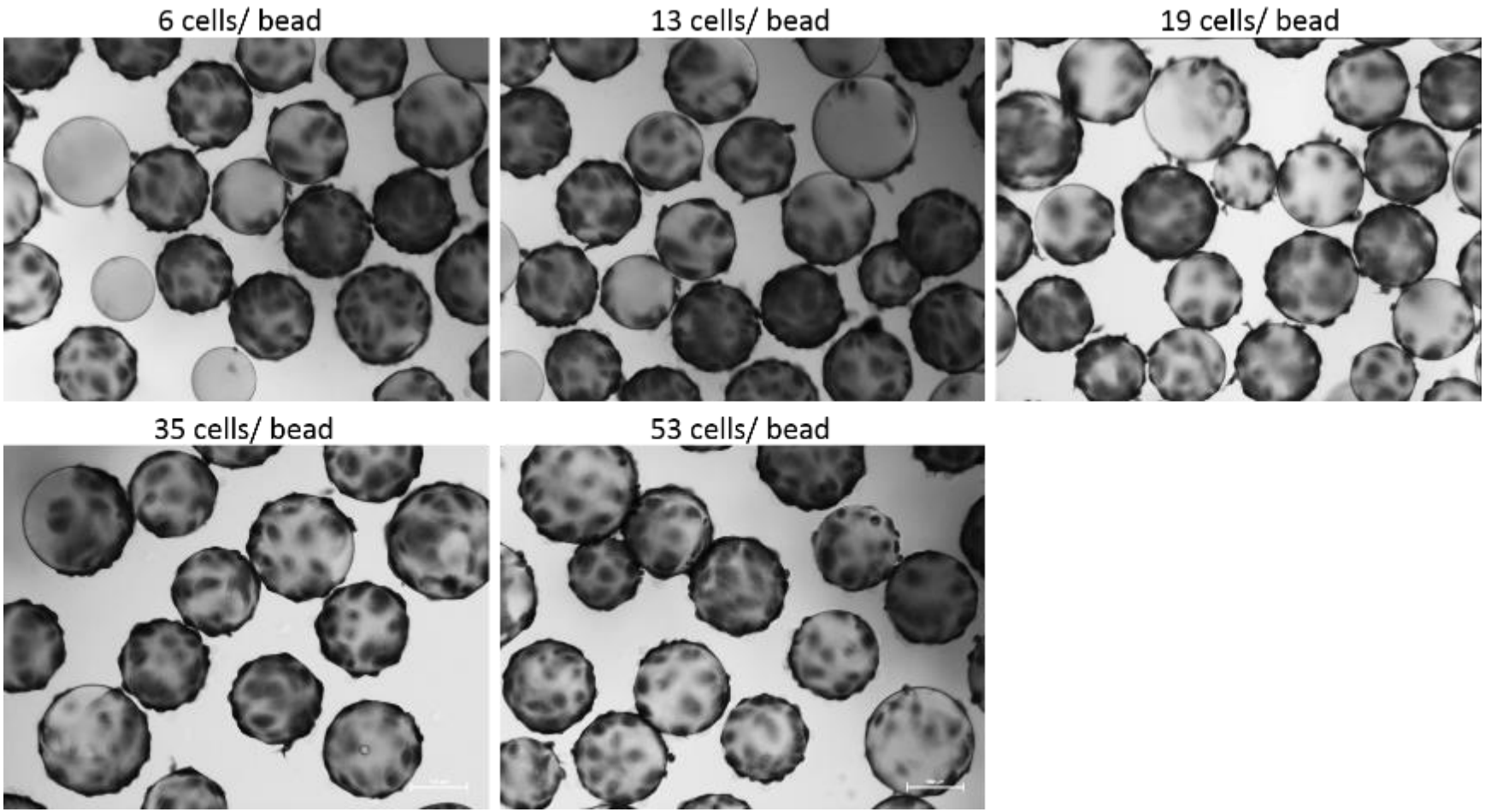

Figure 4.10: CV-1-OPT cells growth on Cytodex-1 reached maximum number under each inoculation density. Experimental conditions: 3g/L Cytodex-1; spinner flask; medium and cell line= 100 ml OptiPRO + CV-1-OPT cells; agitation= 0-48 hrs 30 rpm 30 s/ 30 mins, 48-72 h 30 rpm, >72 h 35 rpm; Images were taken under 10X magnification.

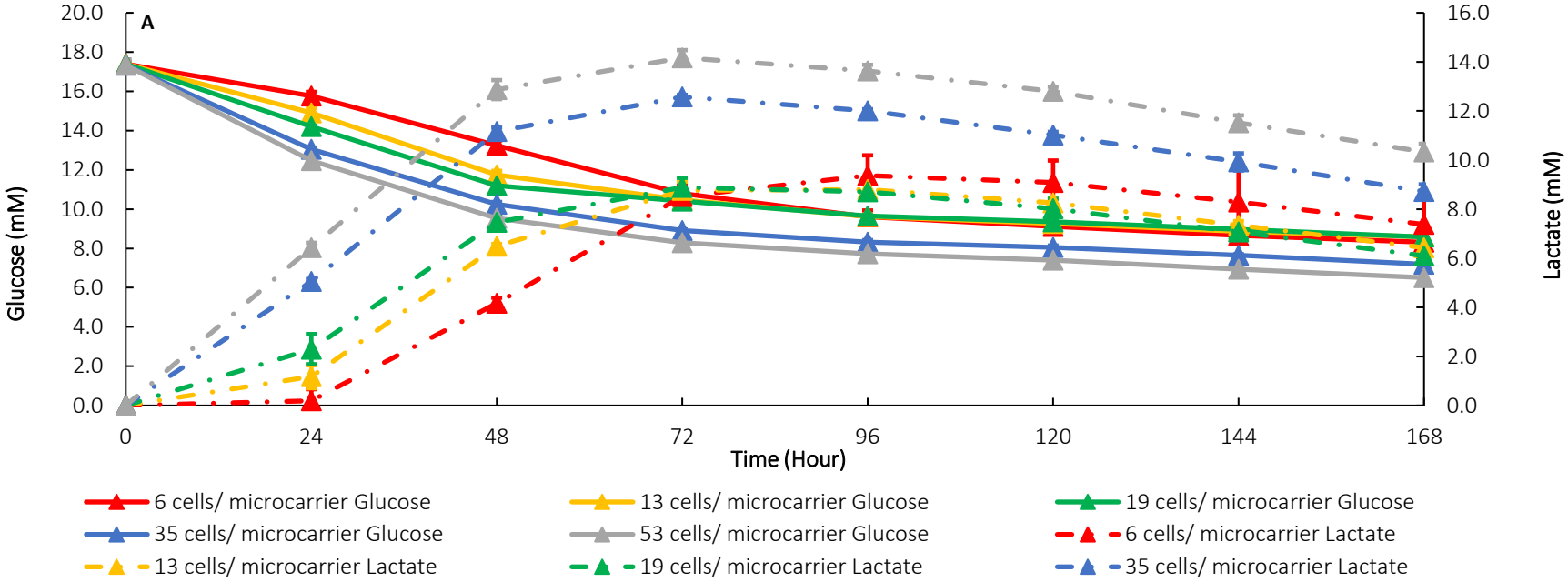
A
Glucose (mM)
Lactate (mM)
Time (Hour)
6 cells/ microcarrier Glucose
13 cells/ microcarrier Glucose
19 cells/ microcarrier Glucose
35 cells/ microcarrier Glucose
53 cells/ microcarrier Glucose
6 cells/ microcarrier Lactate
13 cells/ microcarrier Lactate
19 cells/ microcarrier Lactate
35 cells/ microcarrier Lactate

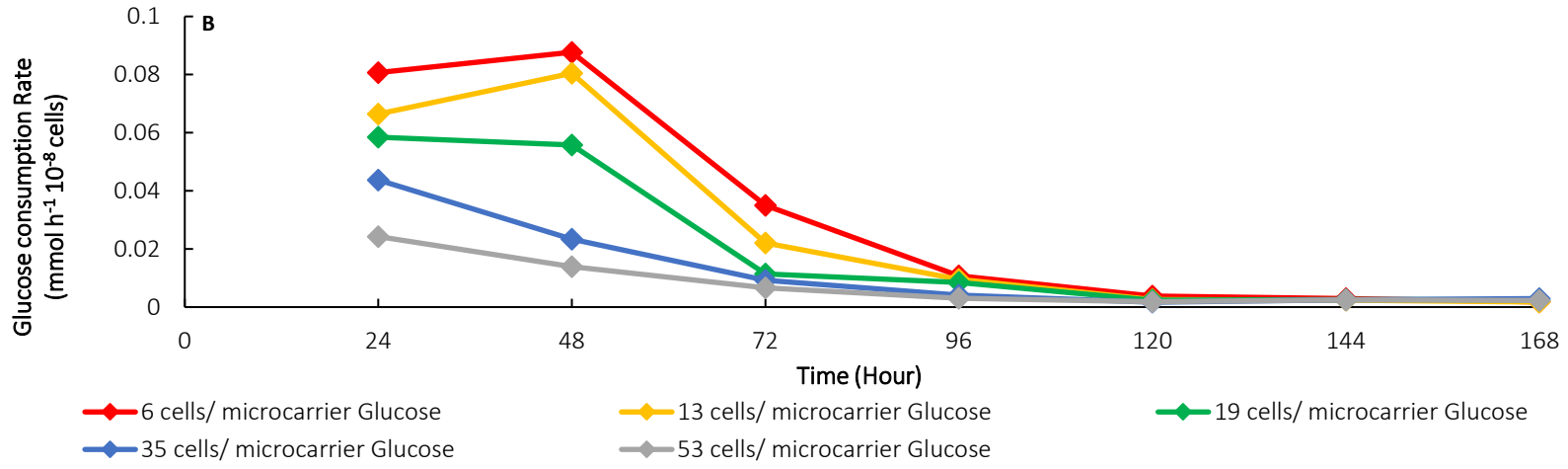
B
Glucose consumption Rate
(mmol h-1 10-8 cells)
Time (Hour)
6 cells/ microcarrier Glucose
13 cells/ microcarrier Glucose
19 cells/ microcarrier Glucose
35 cells/ microcarrier Glucose
53 cells/ microcarrier Glucose

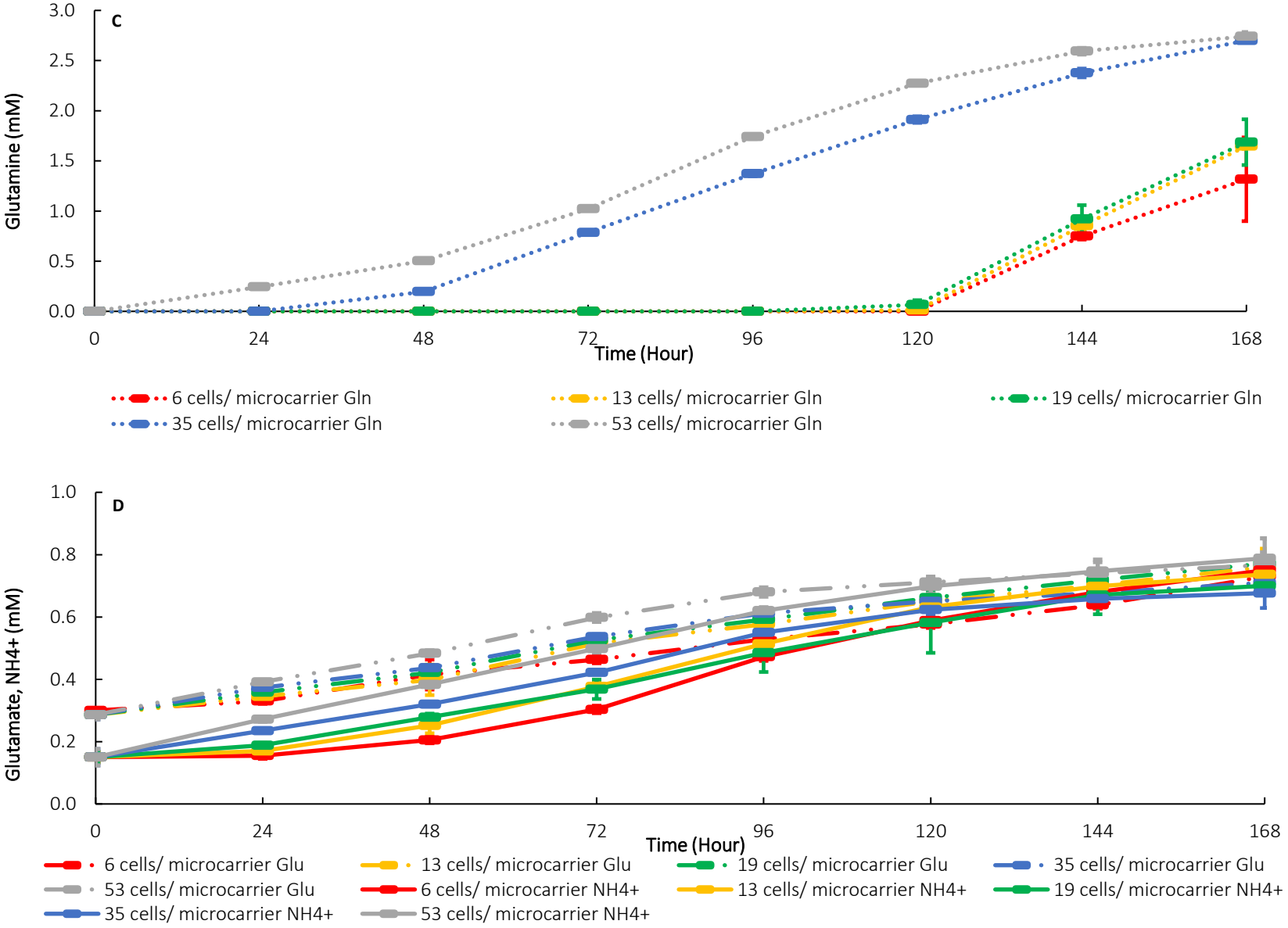
C
Glutamine (mM)
3.0
2.5
2.0
1.5
1.0
0.5
0.0
0
24
48
72
96
120
144
168
Time (Hour)
6 cells/ microcarrier Gln
13 cells/ microcarrier Gln
19 cells/ microcarrier Gln
35 cells/ microcarrier Gln
53 cells/ microcarrier Gln
D
Glutamate, NH4+ (mM)
1.0
0.8
0.6
0.4
0.2
0.0
0
24
48
72
96
120
144
168
Time (Hour)
6 cells/ microcarrier Glu
13 cells/ microcarrier Glu
19 cells/ microcarrier Glu
35 cells/ microcarrier Glu
53 cells/ microcarrier Glu
6 cells/ microcarrier NH4+
13 cells/ microcarrier NH4+
19 cells/ microcarrier NH4+
35 cells/ microcarrier NH4+
53 cells/ microcarrier NH4+

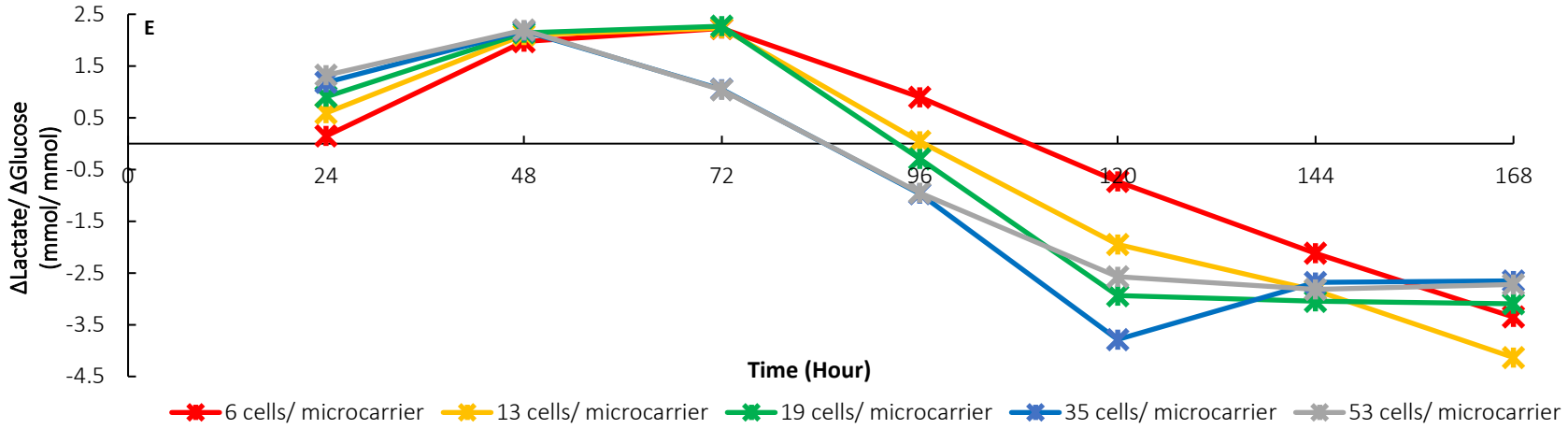

Figure 4.11: Metabolite profiles of CV-1-OPT cell growth on Cytodex-1 under different inoculation densities. Experimental conditions: agitation speed at sampling= 60 rpm; sample treatment= centrifugation at 13500 rpm for 10 minutes. 1ml of each supernatant was transferred to a new 2 ml centrifuge tube. The levels of glucose (A), lactate (A), glutamine (C), glutamate (D) and ammonia (D) were measured directly using BioProfile FLEX Analyzer. Each point on the graph represents the mean broth metabolite concentration of duplicate flasks and each flask was assayed in triplicate at each time point. Results are presented as mean metabolite concentration ± SD. Glucose consumption rate (B) was determined as a function of time (transient kinetics). The yield coefficient of lactate from glucose ($Y_{Lact/Glc}$) (E) was calculated as the molar ratio of lactate generated per glucose.

4.4.5 Effect of feeding strategy on CV-1-OPT growth on Cytodex-1

In this work, the impact of medium exchange schedules on growth and metabolic rates of CV-1-OPT was examined. Parallel cultures of CV-1-OPT were inoculated at a density of 15 cells/microcarrier with trypan blue counts in spinner flasks, which corresponds to 26 cells/microcarrier with crystal violet counts. Each pair of flasks were maintained on one of the four schedules: (1) batch mode, where no medium exchange was performed throughout the culture process; (2)-(4) semi-batch modes, where 70% (v/v) of the growth medium was replaced by equal volume of fresh medium daily, every other day or every 3 days.

No significant difference in growth profiles was observed between cultures with and without medium exchange for the first 96 hours (**Figure 4.12**). On day 5, the cultures without exchange entered stationary phase; while the cultures with exchanges continued to proliferate until they reached their stationary phase on day 7. The extra two days of exponential cell growth in cultures with medium exchanges gave rise to a significant increase in cell densities. Saturation density of cultures operated in batch mode achieved was 5.98 $\times 10^5$ cells/ mL (**Table 4.4**), which was similar to those obtained from the previous experiments in 4.4.3. It was about one-third of the saturation density of cultures exchanged daily (18.72 $\times 10^5$ cells/ mL), and was less than half of the saturation densities of cultures exchanged every 2 or 3 days (13.88, 13.19 $\times 10^5$ cells/ mL). The magnitude of change in CV-1-OPT saturation densities resulting from different operation modes was in the range of those observed in Vero cell lines (**Table 4.5**). However, the saturation densities of CV-1-OPT cultures with exchanges every 2 or 3 days was 25% lower than that of CV-1 cells growing on DEAE-Sephadex gel beads in DMEM supplemented with 10% FBS with medium replaced every 2 to 3 days (Mered, Albrecht, & Hopps, 1980).

The highest specific growth rate was achieved in cultures with daily medium exchange, which was 0.0137 $hour^{-1}$ and corresponding to a doubling time of 50.59 hours (**Table 4.4**). This rate was 2.25 times as high as cultures operated in batch mode and just slightly higher than cultures with medium exchange every 2 or 3 days (0.0129 $hour^{-1}$).

In comparison with batch cultures, a greater use of the microcarriers were observed in all the cultures operated under semi-batch modes. This was indicated by the more compact growth of cells on the beads (**Figure 4.13**) and the augmented cell number per unit area of microcarriers as summarized in **Table 4.4**.

Taking into account the variation in cell counting due to the use of trypan blue and crystal violet, the maximum saturation cell density (per cm^2) obtained from the Cytodex-1 culture was estimated to be about two thirds of its counterpart in T-flasks (**Table 3.1**). Besides the parameters that have been studied above, when using microcarriers, there are additional elements that can have a notable impact on the attachment and growth of cells compared to when using a stationary culture:

Agitation is an important factor that can have a significant impact on the success of cell expansion on microcarriers. A high agitation rate could lead to reduced cell-microcarrier contact time and cell damage owing to shear stress. Alternatively, a low agitation rate could result in inadequate suspension of microcarriers, leading to bead sedimentation, aggregation, uneven cell distribution on microcarriers upon attachment, and insufficient nutrient and oxygen uptake. Moreover, cells at different cultivation stage may require different agitation strategy. As mentioned in section 4.4.1, cells freshly added to microcarrier suspension may need gentle agitation that stops and starts at optimized periodic intervals to facilitate efficient and effective attachment. As cells proliferate on microcarriers, the agitation speed may need to be slightly adjusted to ensure all microcarriers are suspended in the medium with minimum shear stress. Agitation is affected by other parameters, including cell type and microcarrier variety employed, along with the configuration of the bioreactor etc. (Strathearn & Pardo, 2014).

Microcarriers come in different variations with varying sizes, surface areas, matrices, and coatings. These differences have substantial impact on cell growth, and the choice of microcarrier can be critical to cell growth. For instance, Solo Hill Inc. (2009) found that Vero cells did not thrive on plastic substrates. In contrast, Varani et al. (1986) reported that primary chick embryo cells grew well only on glass microcarriers. MDCK and MRC-5 cells were shown to grow well on microcarriers with different types of matrix and/or coating. The selection of the appropriate microcarrier type largely depends on the characteristics of the cells and the medium used in the culture. Our study used Cytodex-1 as a demonstration of the concept being explored. Yet, it may be necessary to evaluate other microcarriers to determine which one is the most appropriate.

The metabolites profiles of the cultures operated in batch mode (**Figure 4.14A**, **C**, **E**, and **F**) were comparable to those obtained from the previous experiments (section 4.4.3). When media was refreshed regularly, a correlation between glucose consumption rates and glucose

concentrations was observed (**Figure 4.14B** and **A**). The consumption rates increased with the increase of concentrations in the culture.

The lactate production rates were dependent upon glucose consumption rates (**Figure 4.14D** and **B**) An increase in glucose consumption rate (usually following the addition of fresh medium) would result in an increase in lactate production rate. This could indicate that the amount of glucose in the broth far exceeded the maximum usage of glucose by CV-1-OPT cells to sustain optimal growth. So that the excessive glucose in the cultures was converted to lactate. Lactate concentrations were below 14mM under all cultivation conditions (**Figure 4.14C**).

Glutamine was not detected until 96, 120 or 192 hours post-inoculation in cultures exchanged every 24, 48 or 72 hours respectively (**Figure 4.14E**). This is in accordance with what was observed in the previous experiments, where glutamine first appeared in the broth after a few days of cultivation and its concentrations increased over time prior to each medium exchange. Ammonia concentrations were below 1mM under all cultivation conditions (**Figure 4.14F**).

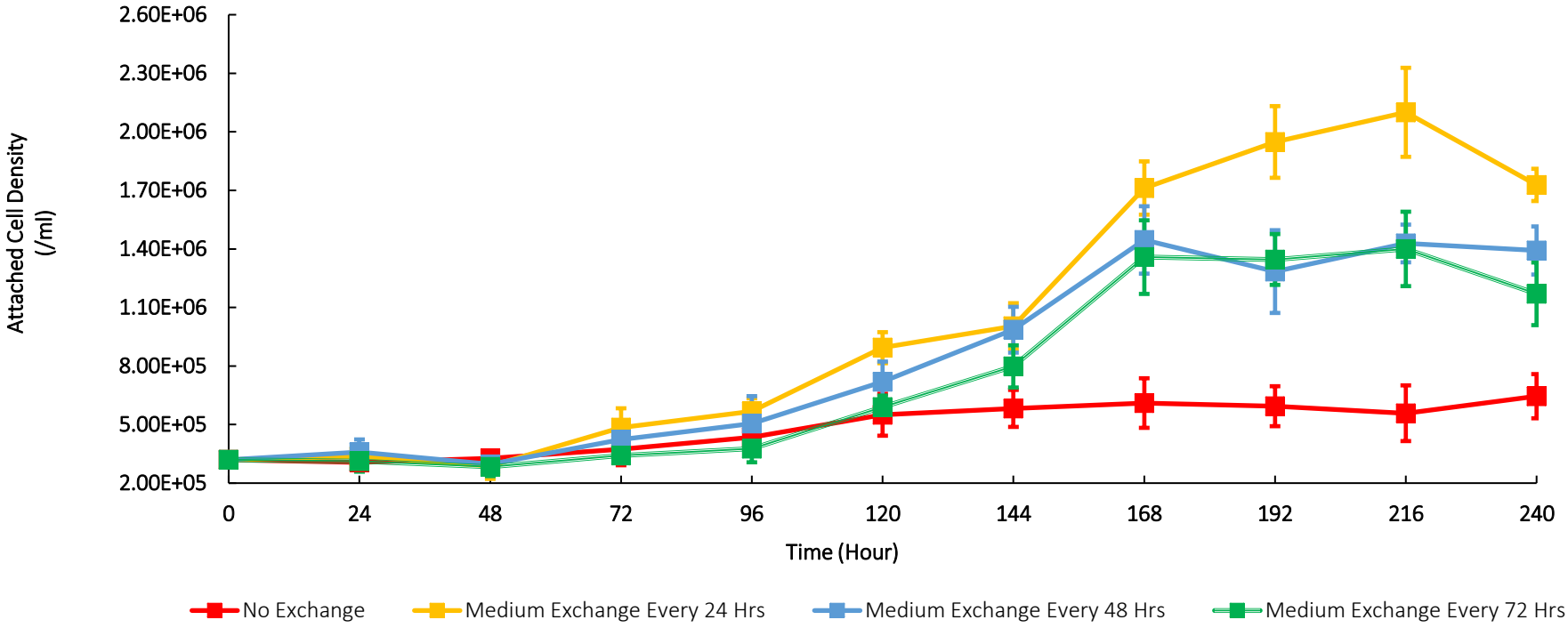

Figure 4.12: Effect of feeding strategy on CV-1-OPT cell growth on Cytodex-1 in suspension. Experimental conditions: 3g/L Cytodex-1; spinner flask; medium and cell line= 100 ml OptiPRO + CV-1-OPT cells; agitation= 0-48 hrs 30 rpm 30 s/ 30 mins, 48-72 h 30 rpm, >72 h 35 rpm; medium exchange schedules= no exchange or every 24, 48 or 72 hours; cell count= crystal violet. The cultures were incubated at 37ºC with 5% CO_2. Each point on the graph represents the mean cell density of duplicate flasks and each flask was assayed in triplicate at each time point. Results are presented as mean cell density ± SD.

Table 4.4 Characteristics of CV-1-OPT cells growth on Ctyodex-1 microcarriers under different feeding strategies.

Medium Exchange Frequency	Specific Growth Rate ($hour^{-1}$)	Saturation Cell Density ($\times 10^5$ cells/ mL)	Saturation Cell Density ($\times 10^5$ cells/ cm^2 microcarriers)	Doubling Time (hour)
Every 24 Hours	0.0137	18.72 ± 1.86	1.42	50.59
Every 48 Hours	0.0129	13.88 ± 0.73	1.05	53.73
Every 72 Hours	0.0129	13.19 ± 1.02	1.00	53.73
No Exchange	0.0061	5.98 ± 0.33	0.45	113.63

Table 4.5 Summary of growth of Vero cells under semi-batch culture conditions.

Cell Type	Microcarrier Concentration	Fraction of medium volume replaced each operation	Frequency of operation	Fold-change in cell density	Reference
Vero	2 mg/ml	1/3	daily	1.5	Mendonca and Pereira 1998
Vero	3mg/ml	1/3	daily	1.8	Thomassen et al. 2014
Vero	10mg/ml	2/3	daily	2.86	Mendonca and Pereira 1998

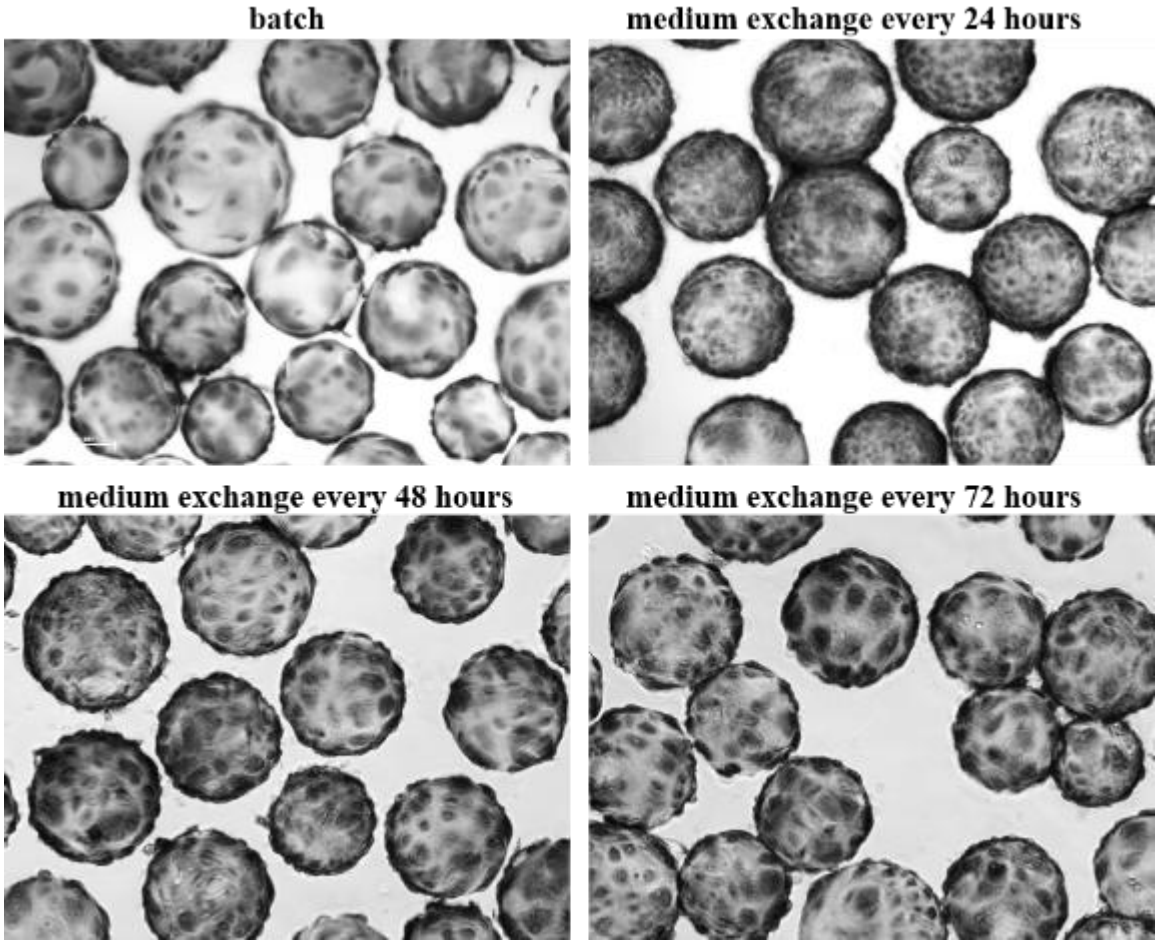

Figure 4.13: CV-1-OPT cells growth on Cytodex-1 reached maximum number under each feeding strategy. Experimental conditions: 3g/L Cytodex-1; spinner flask; medium and cell line= 100 ml OptiPRO + CV-1-OPT cells; agitation= 0-48 hrs 30 rpm 30 s/ 30 mins, 48-72 h 30 rpm, >72 h 35 rpm; Images were taken at 0, 8, 24 and 48 hours post inoculation under 100X magnification.

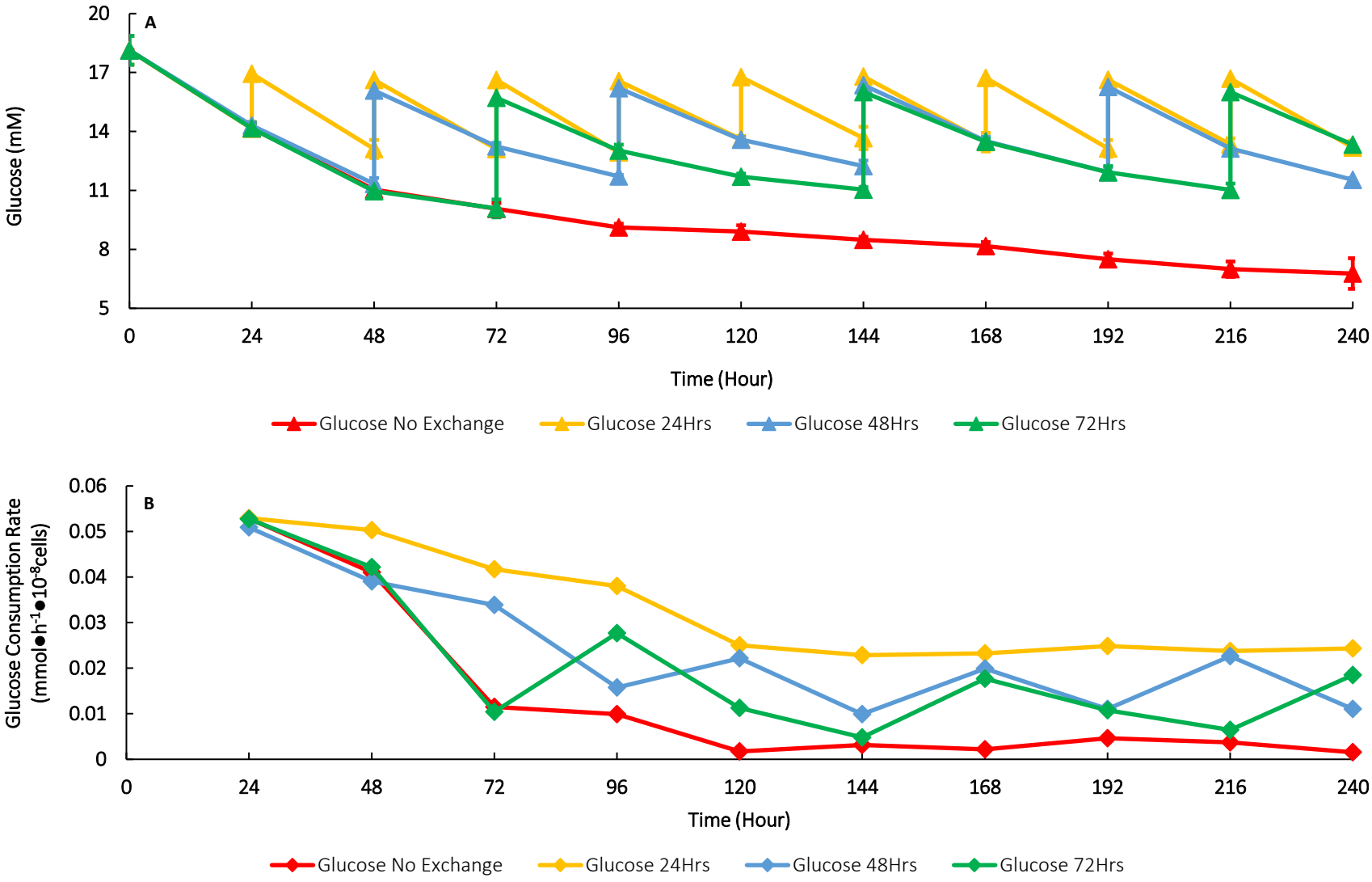
A
Glucose (mM)
20
17
14
11
8
5
0
24
48
72
96
120
144
168
192
216
240
Time (Hour)
Glucose No Exchange
Glucose 24Hrs
Glucose 48Hrs
Glucose 72Hrs
B
Glucose Consumption Rate
(mmol•h-1•10-8cells)
0.06
0.05
0.04
0.03
0.02
0.01
0
0
24
48
72
96
120
144
168
192
216
240
Time (Hour)
Glucose No Exchange
Glucose 24Hrs
Glucose 48Hrs
Glucose 72Hrs

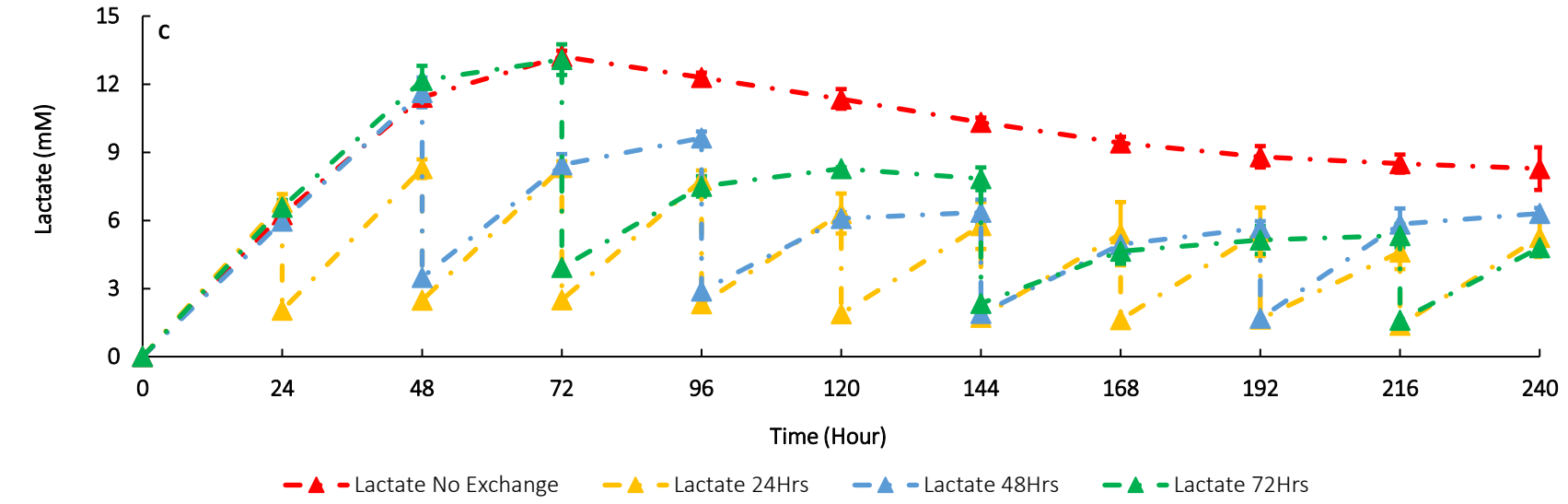
C
Lactate (mM)
15
12
9
6
3
0
0
24
48
72
96
120
144
168
192
216
240
Time (Hour)
Lactate No Exchange
Lactate 24Hrs
Lactate 48Hrs
Lactate 72Hrs

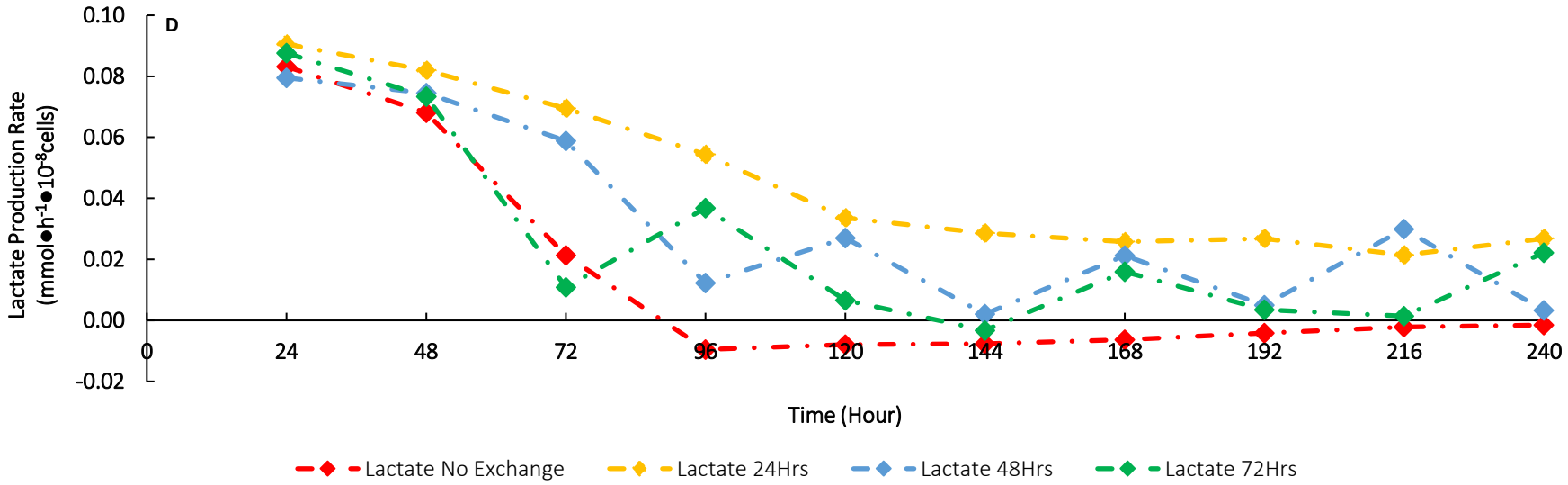
D
Lactate Production Rate
(mmol•h-1•10-8cells)
0.10
0.08
0.06
0.04
0.02
0.00
-0.02
0
24
48
72
96
120
144
168
192
216
240
Time (Hour)
Lactate No Exchange
Lactate 24Hrs
Lactate 48Hrs
Lactate 72Hrs

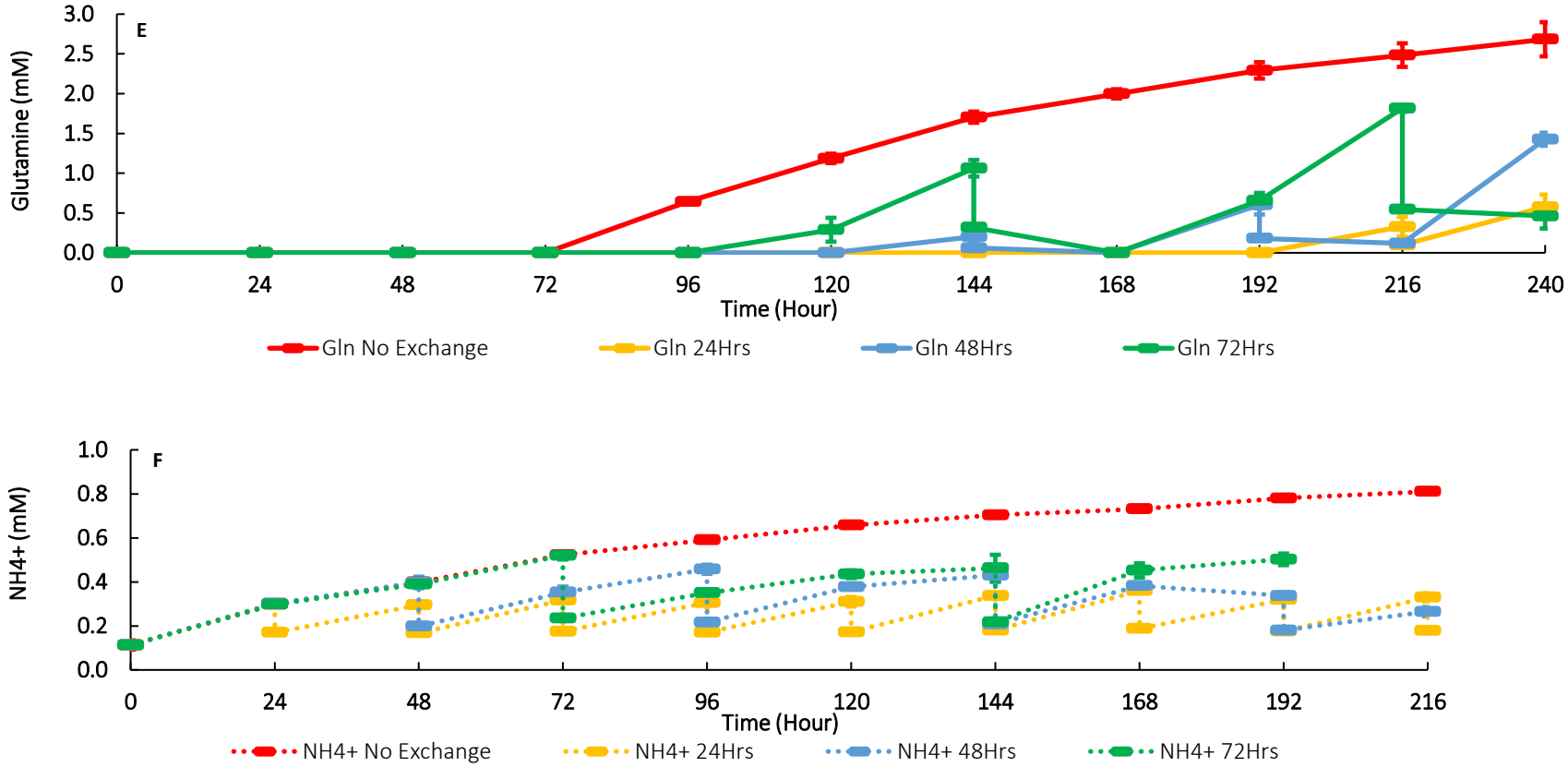

Figure 4.14: Metabolite profiles of CV-1-OPT cell growth on Cytodex-1 under different feeding strategies. Experimental conditions: agitation speed at sampling= 60 rpm; sample treatment= centrifugation at 13500 rpm for 10 minutes. 1ml of each supernatant was transferred to a new 2 ml centrifuge tube. The levels of glucose (A), lactate (C), glutamine (E) and ammonia (F) were measured directly using BioProfile FLEX Analyzer. Each point on the graph represents the mean broth metabolite concentration of duplicate flasks and each flask was assayed in triplicate at each time point. Results are presented as mean metabolite concentration ± SD. Glucose consumption rate (B) and lactate production rate (D) were determined as function of time (transient kinetics).

4.5 Summary

In summary, though CV-1-OPT struggled to grow as suspension cells, its proliferation on Cytodex-1 microcarriers is observed when inoculated at relatively low cell densities (6, 13, 19 cells/microcarrier) under batch culture conditions. Nonetheless, even when cells reached saturation densities, there were still unsaturated microcarriers present, indicating that the cells have further capacity for growth. The fact that replacing the medium regularly can considerably enhance cell growth provides evidence to support this speculation. With the successful proliferation of CV-1-OPT cells on Cytodex-1 microcarriers, growth performance of VVL 15-RFP in CV-1-OPT cells using the microcarrier system will be explored in the next Chapter.

Chapter 5. Production and Optimization of VVL-15 RFP

5.1 Aim and Objectives

Given that CV-1-OPT cells grow effectively on the Cytodex-1 microcarriers in suspension culture, the next aim was to develop and optimize a CV-1-OPT cell line-based manufacturing process which has the potential to produce oncolytic Lister strain VV at large scale. It was hoped that use of an optimized microcarrier system for VVL-15 RFP cultivation would reduce the risk of accidental contaminations, process variability and indirect labour cost, thus improving process robustness and economic viability of oncolytic VV manufacture. The specific objectives of this Chapter are:

- ❖ to evaluate the effect of VEGF-A on VVL-15 RFP replication.
- ❖ to apply the previously established CV-1-OPT microcarrier culture system to the production of VVL-15 RFP and demonstrate the utility of the system and CV-1-OPT cell line for the cultivation of oncolytic Lister strain VV.
- ❖ to investigate the effect of process parameters on VVL-15 RFP production with the microcarrier-based CV-1-OPT system.
- ❖ to assess VVL-15 RFP amplification in static and microcarrier culture systems.

5.2 Optimisation of VVL-15 RFP infection conditions for high titre

5.2.1 Effect of vascular endothelial growth factor A on VVL-15 RFP titre

It was suggested that both transfected and exogenously applied VEGF-A promotes VV internalization into epithelial host cell lines via activation of the PI3K Akt pathway, an event associated with actin cytoskeleton remodelling (Hiley et al. 2013). VEGF-A is also expressed by fibroblast cell lines (Berse et al. 1992; Hlatky et al. 1994), although its role in fibroblasts has not been very well characterised, it is interesting to find out if VEGF-A could elevate VV replication in this type of cells under similar mechanisms.

The level of VEGF-A in the OptiPRO medium was verified prior to the addition of any exogenous VEGF-A. An ELISA was performed as described in section 2.9 and no VEGF-A was detected in the medium.

As described in section 2.10, CV-1-OPT was serum starved for 16 hours to reduce the basal activity of pAkt pathway and then stimulated with 10 ng/ml VEGF-A which had proved its effectiveness in augmenting Akt phosphorylation and facilitating VV infection and replication in both tumour cells and normal human bronchial epithelial cells (Hiley et al. 2013). As shown in **Figure 5.1**, a transient increase in the phosphorylated (activated) form of Akt (S473) was observed at 3 minutes following VEGF-A stimulation of CV-1-OPT.

A comparison was made between the production of VVL-15 RFP in OptiPRO with and without the addition of VEGF-A using CV-1-OPT cells. As described in section 2.10.1, cells originally grown in OptiPRO were infected with 2ml of VVL15-RFP-containing fresh medium with or without supplementation of 10 ng/ml VEGF-A. The virus-containing cell broth was harvested at 24, 48 and 72 hours post-infection and subjected to TCID 50 assay for determining titres. There was no significant difference in specific productivity of VVL15-RFP by CV-1-OPT cells cultivated using either set of conditions at each time point within 72 hours of infection (**Figure 5.2**).

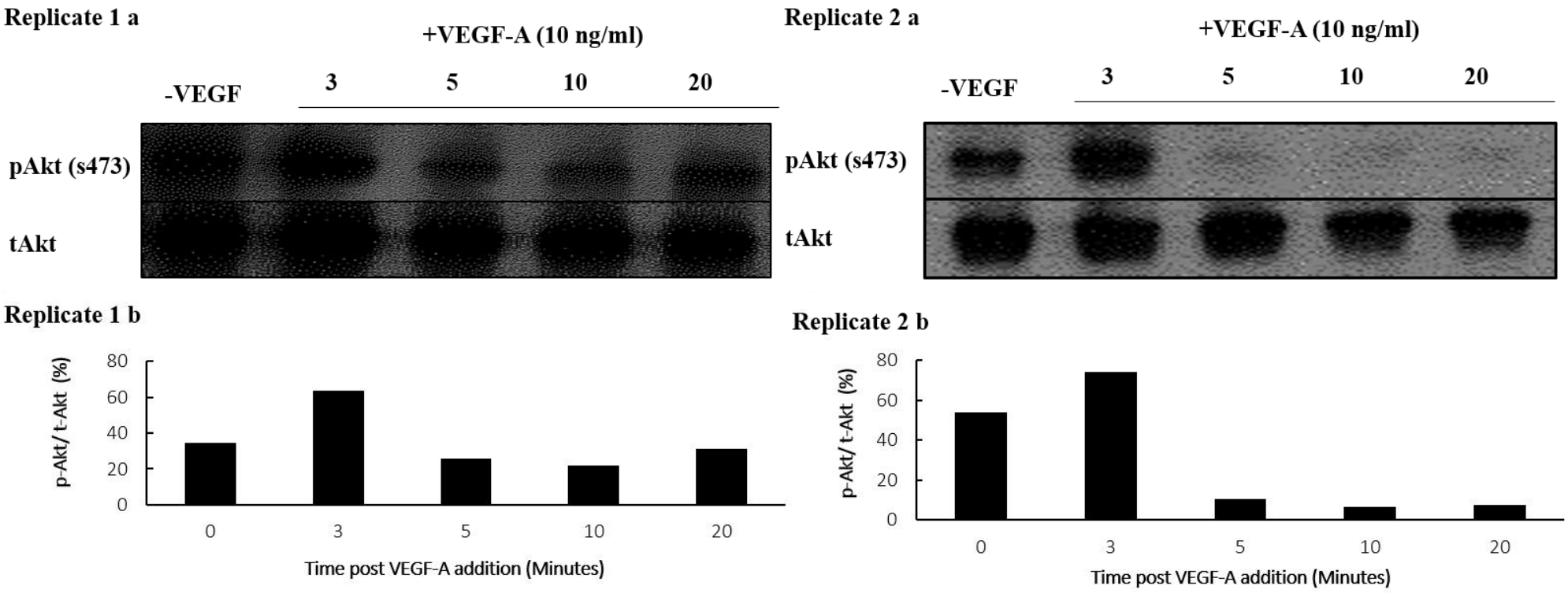

Figure 5.1: VEGF-A promotes Akt phosphorylation in CV-1-OPT cells. CV-1-OPT cells were unstimulated (control, time 0), or stimulated with VEGF-A (10 ng/ml) for 3, 5, 10 and 20 minutes. (a) The levels of phosphorylated Akt (pAkt) (S473) and total Akt (tAkt) in cell lysates were evaluated by Western Blot. The molecular weight for pAkt is 60 kDa. (b) The ratios of pAkt / tAkt were determined using NIH ImageJ band densitometries. Two independent experiments were quantified, and data at each time point were averaged and graphically presented to reflect relative changes in activation of pAKT (S473). Experiments performed as described in section 2.10.

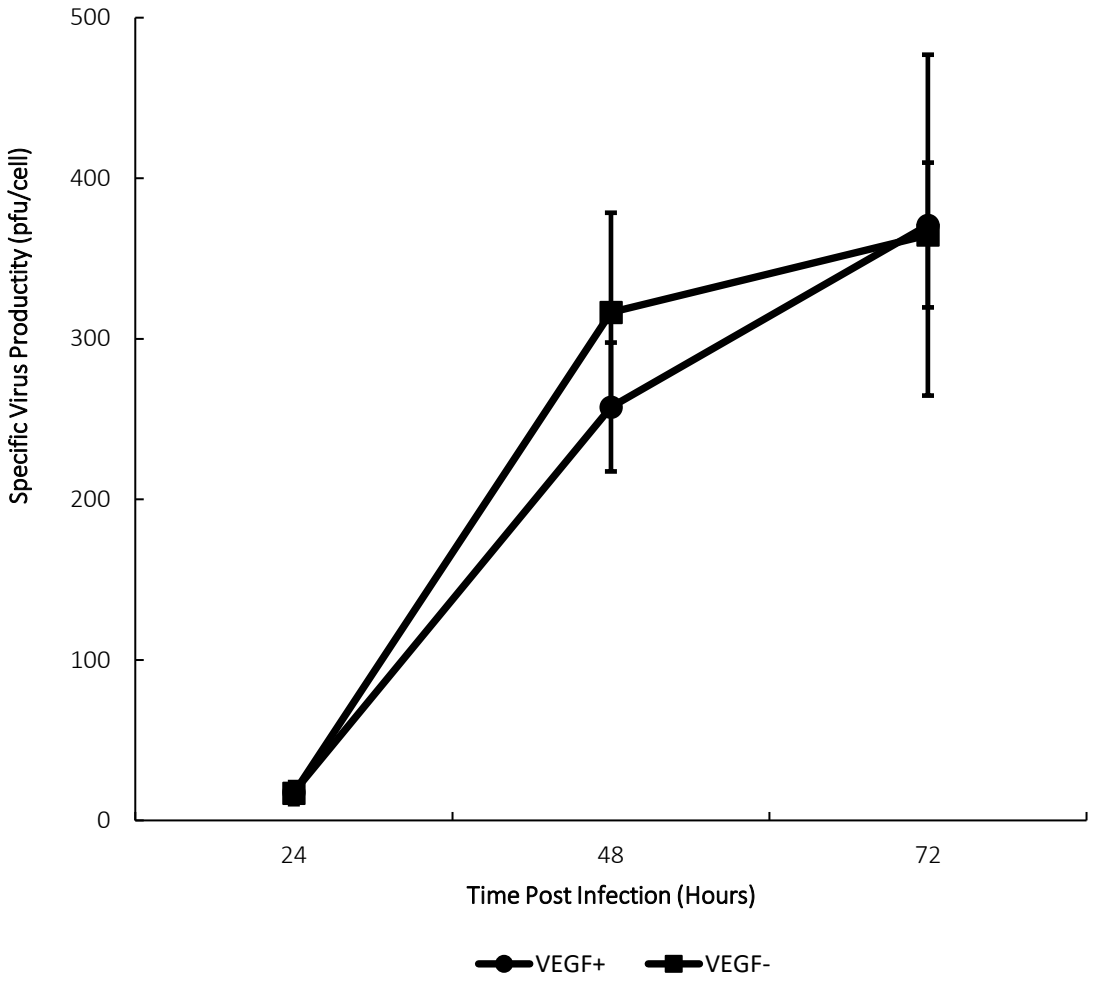

Figure 5.2: VVL-15 RFP production in OptiPRO with or without 10ng/ml VEGF-A using CV-1-OPT cells. Experimental conditions: Cell confluence at infection= 80% - 90%; MOI= 0.1; 6 well plates; incubation at 37 ºC, 5% CO_2. Error bars represent one standard deviation about the mean (n=3).

5.2.2 Production of VVL-15 RFP in CV-1-OPT in microcarrier culture

Production of VVL-15 RFP using CV-1-OPT cells was conducted in 250ml (100ml working volume) spinner flasks. Cells were infected with VVL-15 RFP at MOIs of 0.1, 0.5 and 1.0 respectively at late exponential phase in which a density of 1.52×10^6 cells/ml had been achieved. Parameters associated with cell growth and virus production were monitored as described in sections 2.6, 2.8. 2.11, and 2.12.3.

It was observed that there was a slight decrease in attached CV-1-OPT cell densities during the first 24 hours post-infection, which was followed by a steep decrease from 48 to 72 hours post-infection. The attached cell densities became too low to be detectable by haemocytometer from 96 hours post-infection onwards (**Figure 5.3**). The viral specific productivities obtained from the three sets of experiment were very similar, ranging from 37.5 to 43.4 pfu/ cell. The highest was obtained at the MOI of 0.5.

The peak volumetric VVL-15 RFP productivities for cultures infected at MOIs of 0.1, 0.5 and 1.0 were comparable, $5.70 \pm 2.29 \times10^7$, $6.42 \pm 2.15 \times10^7$ and $5.26 \pm 1.51 \times10^7$ pfu/ml respectively (**Figure 5.4**). This finding accords with that from a study in which the final titres of a Wyeth Strain VV produced from Hela cells infected at mid-exponential phase at MOIs ranging from 0.01 to 1000 were almost identical (Chillakuru et al 1991). In addition, the peak volumetric VVL-15 RFP productivities were attained earlier for cells infected with higher MOIs (0.5 and 1.0, 48 hours post-infection) than in cultures infected at lower MOI (0.1, 72 hours post-infection).

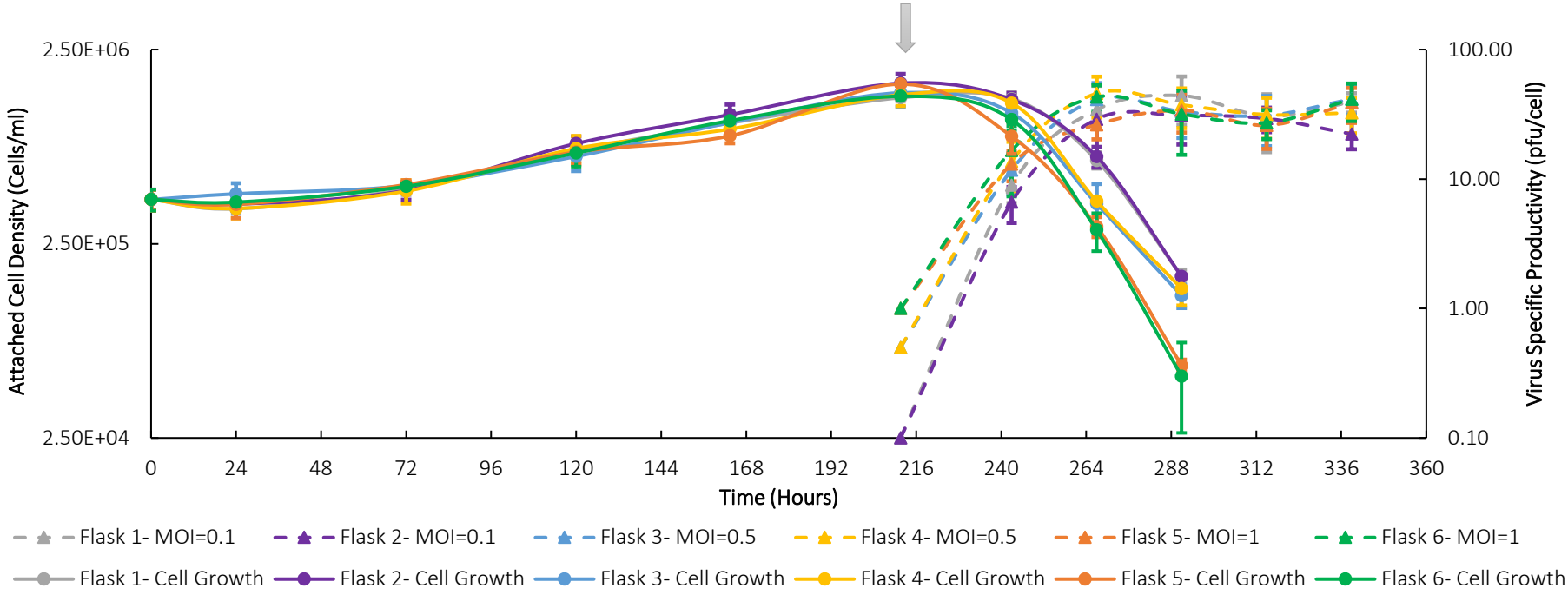

Figure 5.3: Time course analysis of attached CV-1-OPT concentrations and virus specific productivities during the production of VVL-15 RFP in microcarrier culture. Each spinner flask was inoculated with an initial CV-1-OPT density of 20 cells/microcarrier, which corresponded to 32 cells/microcarrier and 4.22×10^5 cells/ml with crystal violet counts. The total volume of medium was 100ml/ flask. 70% (v/v) of old culture medium was replaced daily by fresh medium until prior to infection when cells reached a density of 1.52×10^6 cells/ml. Duplicate flasks of cells were infected with VVL-15-RFP at MOI of 0.1, 0.5 and 1.0 respectively. The arrow indicates the time of infection. Cultures were exposed to intermittent agitation at 30rpm for 30 seconds every 30 minutes for the first 48 hours, then to continuous agitation at 30rpm from 48 to 72 hours and 35 rpm from 72 hours onwards. Each assay contains triplicates and results are presented as attached cell number ± SD or pfu/ cell ± SD.

5.2.3 Effect of MOI and TOI on VVL-15 RFP titre

Optimization of MOI and the cell density at Time of Infection (TOI) for enhanced viral product yields have been studied in many virus-cell culture systems (Wong et al. 1996, Jung et al. 2004; Aggarwal et al. 2011, Chillakuru et al. 1991, Cristina et al. 2009). Chillakuru et al (1991) demonstrated the importance of infection of Hela cells during their exponential phase in order to achieve high Wyeth strain VV yields. In section 5.2.2, CV-1-OPT cells were infected with VVL-15 RFP at MOIs of 0.1, 0.5 and 1.0 at late exponential phase when cells reached a density of 1.52×10^6 cells/ml. Herein, the effect of TOI and MOI was studied by decreasing the time of infection by 2 days when cells grew to 9.27×10^5 cells/ml at mid-late exponential growth phase. Parameters associated with cell growth and virus production were monitored as described in section 2.6, 2.8, 2.11 and 2.12.3.

No significant change was observed in attached CV-1-OPT cell densities during the first 48 hours post-infection. The cell densities quickly decreased from 48 to 72 hours post-infection and became too low to be detectable by haemocytometer from 96 hours post-infection onwards (**Figure 5.5**). The peak volumetric VVL-15 RFP productivities for cultures infected at MOIs of 0.1, 0.5 and 1.0 were comparable, $5.56 \pm 2.34 \times 10^7$, $6.28 \pm 2.12 \times 10^7$ and $6.47 \pm 2.17 \times 10^7$ pfu/ml respectively (**Figure 5.4**). The maximum volumetric VVL-15 RFP productivities were attained approximately 1 day earlier for cells infected with higher MOIs (0.5 and 1.0, 48 hours post-infection) than in cultures infected at lower MOI (0.1, 72 hours post-infection).

Results from sections 5.2.2 and 5.2.3 suggest that the peak volumetric VVL-15 RFP productivity is independent of either MOI or TOI within the investigated range (**Figure 5.4**). However, the combination of a low TOI (9.27×10^5 cells/ml) and a high MOI ($\geq$ 0.5) would lead to a reduction of the overall process time without compromising the maximal virus titre. The total time required for cell growth and virus production necessary to achieve maximal virus yields was approximately 3 days shorter than the experiment at low MOI (0.1) and infection during late exponential phase (1.52×10^7 cells/ml). From a manufacturing point of view, reduction of process time allows greater production process efficiencies and brings economic benefits.

The comparable maximum volumetric virus productivities observed regardless of the TOI and MOI could be due to the depletion of certain nutrients in the culture medium

as a result of high cell densities in microcarrier cultures. It has been reported that lack of arginine would largely affect the synthesis of macromolecules involved in virus replication and the formation of mature virus particles in Hela cells infected with Lister strain VV (Archard & Williamson 1971). Glutamine, a primary energy source under normal cell culture conditions, is also critical for efficient VV replication as it has been found necessary to 'maintain the TCA cycle for VV protein synthesis' (Fontaine et al. 2014). Thus, characterization of infected cell metabolism could help further understand the production process.

Compared with **Figure 5.3** where cells were inoculated at the very late stage of exponential phase, higher specific virus productivities were obtained when earlier TOI was adopted with lower cell density (**Figure 5.6**). The highest specific virus productivity achieved in microcarrier-based CV-1-OPT culture in this study was 71.9 pfu/ cells, which is similar to that achieved by growing a Wyeth strain VV in suspension culture of Hela cells infected at a MOI of 0.05 in a mixture of SFM (Ricordel et al. 2013) (**Table 5.1**). A much higher specific virus productivity of 1000 pfu/cell was obtained by Chilakuru et al (2005) who cultivated a Wyeth Strain VV in suspension culture of Hela cells infected at a MOI of 1 in 2% FBS J-MEM with controlled pH and dissolved oxygen (DO) level (**Table 5.1**).

As reported previously, using trypan blue exclusion method, VVL-15 RFP produced from CV-1-OPT in static culture gave a peak specific virus productivity of 352.2 pfu/cell (section 3.3.5). This is approximately equal to 251.6 pfu/ cell if the crystal violet nuclei method had been used (estimation was based on that the crystal violet nuclei method gave counts ~1.4 times higher than the trypan blue exclusion method for counting CV-1-OPT cells from experience). Furthermore, considering the assay technique employed, virus within the cell (assumed to be all IMVs) was titrated for static culture, whereas total virus was titrated for microcarrier culture. As described in section 1.1.3, CEV/EEV accounts for less than 1% of the progeny. Assuming that 99% of the virus harvested in microcarrier culture is IMV, the peak IMV- specific VVL-15-RFP productivity in CV-1-OPT cells using microcarrier-based suspension culture was 28.3% of that observed in static culture.

In the microcarrier study, the TOIs were set towards the end of the exponential phase, which was different from the infection conditions used for static culture. This on one

hand could result in a large production of virus in a short amount of time due to the high density of cells. On the other hand, cells at later stage of the log phase may possess a reduced metabolism that could negatively impact viral replication in host cells. Alternatively, even though cell number at early to early-mid log phase is relatively low, the cells could be more metabolically active, allowing for a greater production of virus with a smaller inoculum size, given enough post-infection time for further cell growth and virus proliferation. Also as the case in cell culture, agitation and fermentation mode could exert a strong influence on the effective adoption and propagation of virus in suspension microcarrier environment.

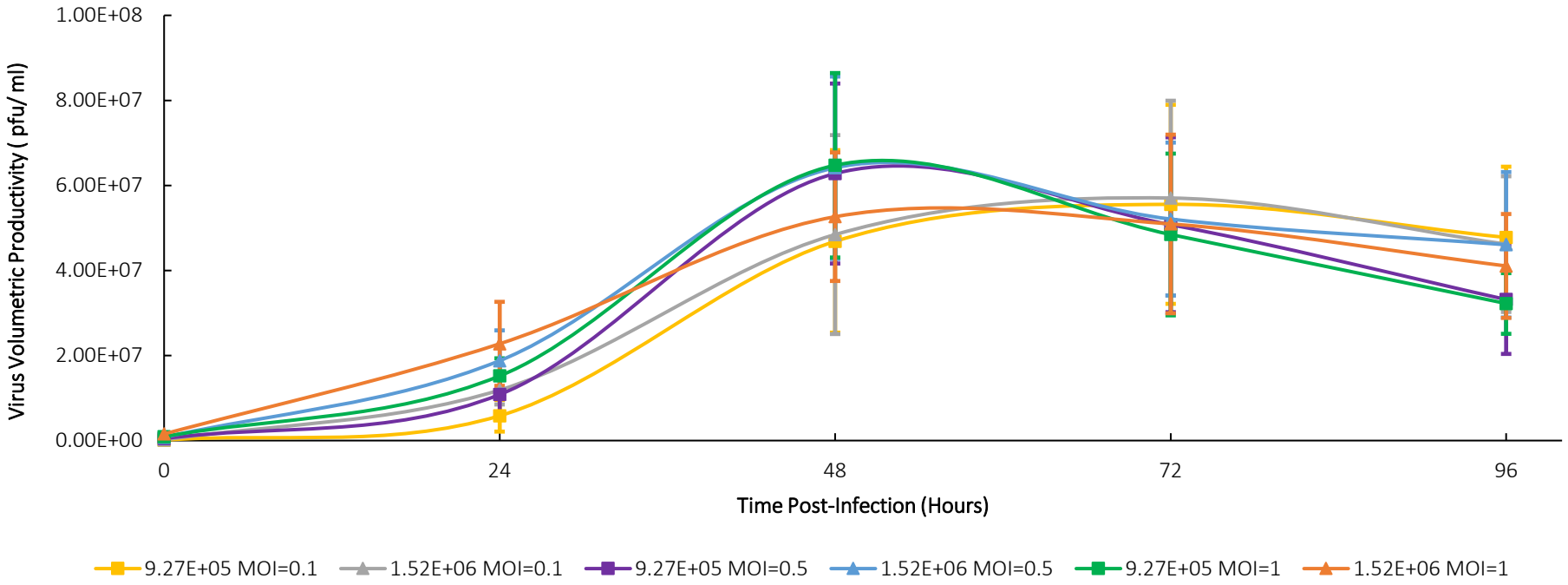

Figure 5.4: Effect of MOI and cell density at the time of infection (TOI) on peak volumetric VVL-15 RFP productivities. As described in legends 5.3 and 5.6, CV-1-OPT cells were infected with VVL-15 RFP at mid-late or late exponential growth phase which corresponds to densities of 9.27×10^5 or 1.52×10^6 cells/ml. Duplicate flasks of cells were infected at MOI of 0.1, 0.5 and 1.0 respectively at each cell density. Each point on the graph represents the mean volumetric virus productivity of duplicate flasks and each flask was assayed in triplicates at each time point. The results are presented as pfu/ ml ± SD.

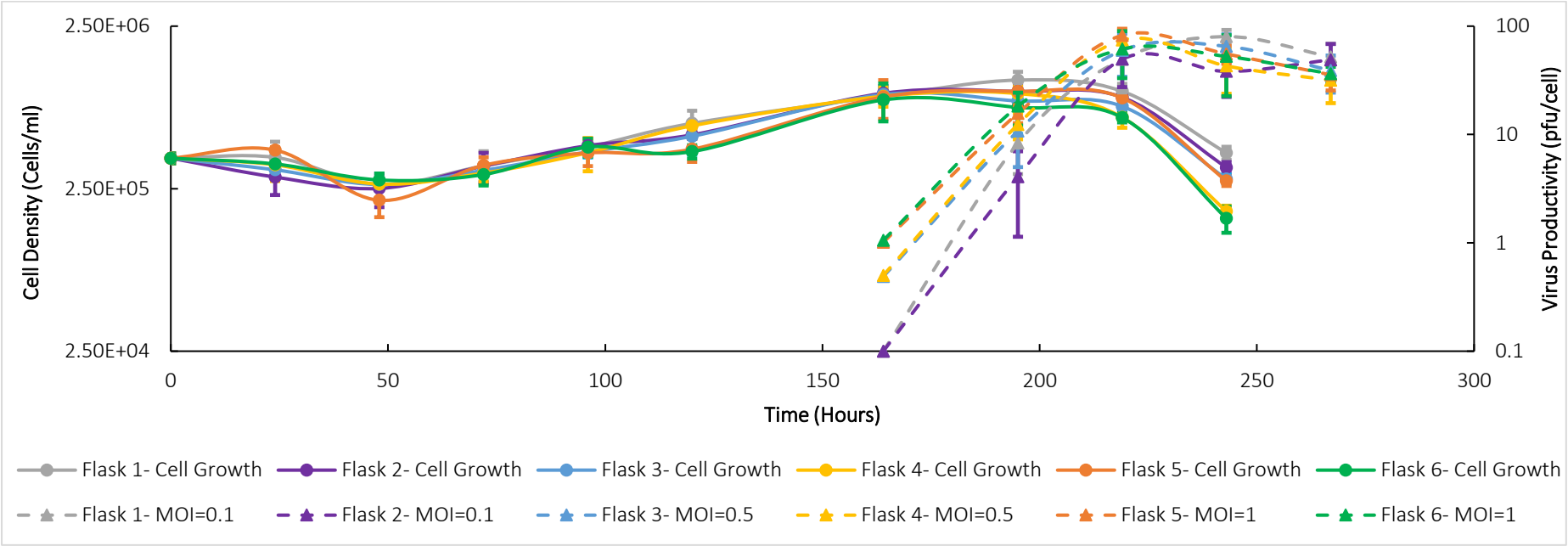

Figure 5.5: Time course analysis of attached CV-1-OPT concentrations and virus specific productivities during the production of VVL-15 RFP in microcarrier culture. Each spinner flask was inoculated with an initial CV-1-OPT density of 20 cells/microcarrier with trypan blue counts, which corresponded to 30 cells/ microcarrier and 3.85×10^5 cells/ml with crystal violet counts. The total volume of medium was 120ml/ flask. 70% (v/v) of old culture medium was replaced daily by fresh medium until prior to infection when cells reached a density of 9.27×10^5 cells/ml. Duplicate flasks of cells were infected with VVL-15-RFP at MOI of 0.1, 0.5 and 1.0 respectively. The arrow indicates the time of infection. Cultures were exposed to intermittent agitation at 30rpm for 30 seconds every 30 minutes for the first 48 hours, then to continuous agitation at 30rpm from 48 to 72 hours and 35 rpm from 72 hours onwards. Experiments performed as described in section 2.6 and 2.8. Each assay contains triplicates and results are presented as attached cell number ± SD or pfu/ cell ± SD.

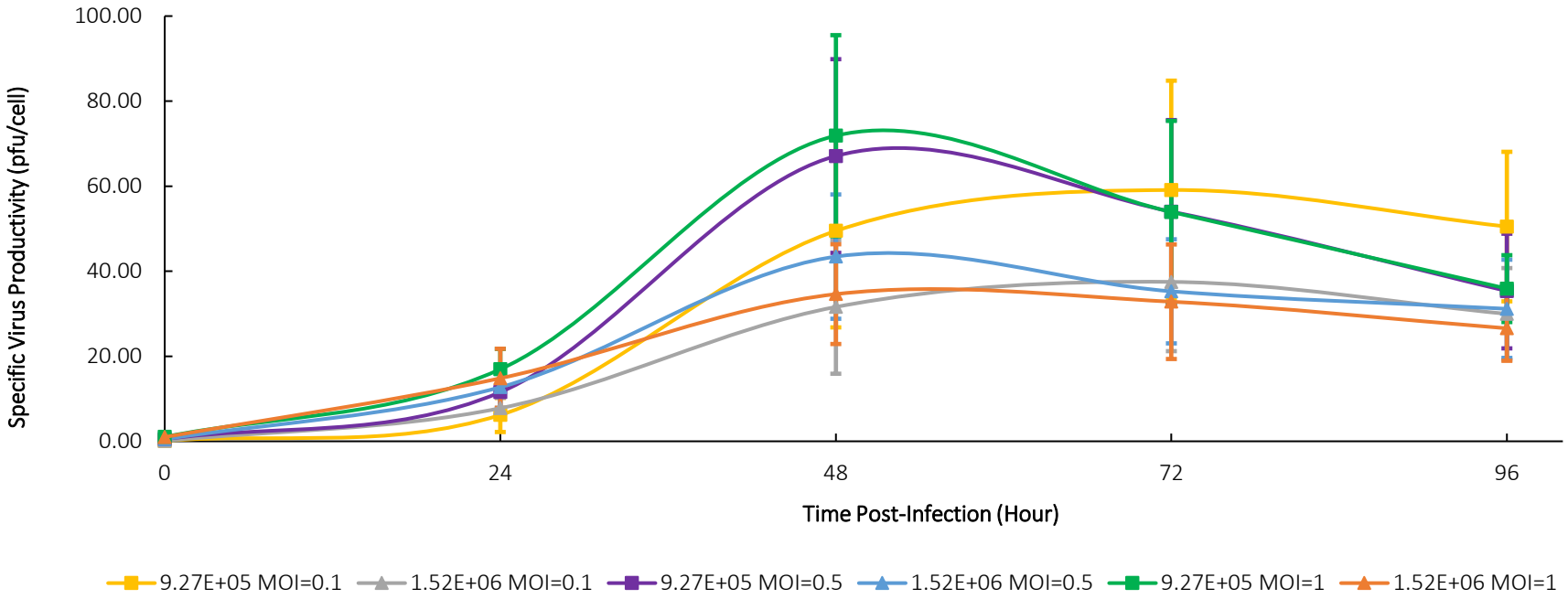

Figure 5.6: Effect of MOI and cell density at the time of infection (TOI) on peak specific VVL-15 RFP productivities. As described in legends 5.3 and 5.6, CV-1-OPT cells were infected with VVL-15 RFP at mid-late or late exponential growth phase which corresponds to densities of 9.27×10^5 or 1.52×10^6 cells/ml. Duplicate flasks of cells were infected at MOI of 0.1, 0.5 and 1.0 respectively at each cell density. Each point on the graph represents the mean specific virus productivity of duplicate flasks and each flask was assayed in triplicates at each time point. The results are presented as pfu/ cell ± SD.

Table 5.1: Summary of VV production performances under suspension culture conditions.

VV Strain	Host Cell Line	FBS	MOI	Vessel	Virus specific productivity (pfu/cell)	Amplification	Cell Counting Method	Reference
Wyeth	Hela	0	0.05	600 mL TubeSpin	70	1400	Vi-CELL XR cell counter	Ricordel et al. 2013
Wyeth	Hela	2%	1	4L Bioreactor	1000	1000	Trypan Blue	Chillakuru et al. 2005

5.3 VVL-15 RFP Amplification in static and microcarrier culture systems

Since different cell counting methods were used when infecting cells grown in static (trypan blue) or microcarrier culture (crystal violet), the cell specific VVL-15 RFP productivities are not directly comparable between the two culture formats. To evaluate the viral production performance in different culture systems, we calculated the fold increase (amplification) in virus titres from the time of infection to the time when peak viral productivity was reached as illustrated in section 2.11.3, thus eliminating the cell number variations resulted from using different cell counting methods.

When producing VVL-15 RFP with microcarrier culture system, a downward trend in virus amplification was observed (**Figure 5.7**) along with the increase of MOI. At a MOI of 0.1 and an infection cell density of 9.27×10^5 cells/ml, the fold increase of VV produced in microcarrier-based CV-1-OPT suspension culture achieved its maximum, which is 658. This number is similar to that produced in static culture of CV-1 cells in 5% FBS DMEM (766), 5.45 fold less than that produced in static culture of CV-1-OPT cells (**Figure 5.7**), and 2.13 and 1.52 fold less than that reported by Ricordel et al. (2013) and Chillakuru et al. (2005) (**Table 5.1**).

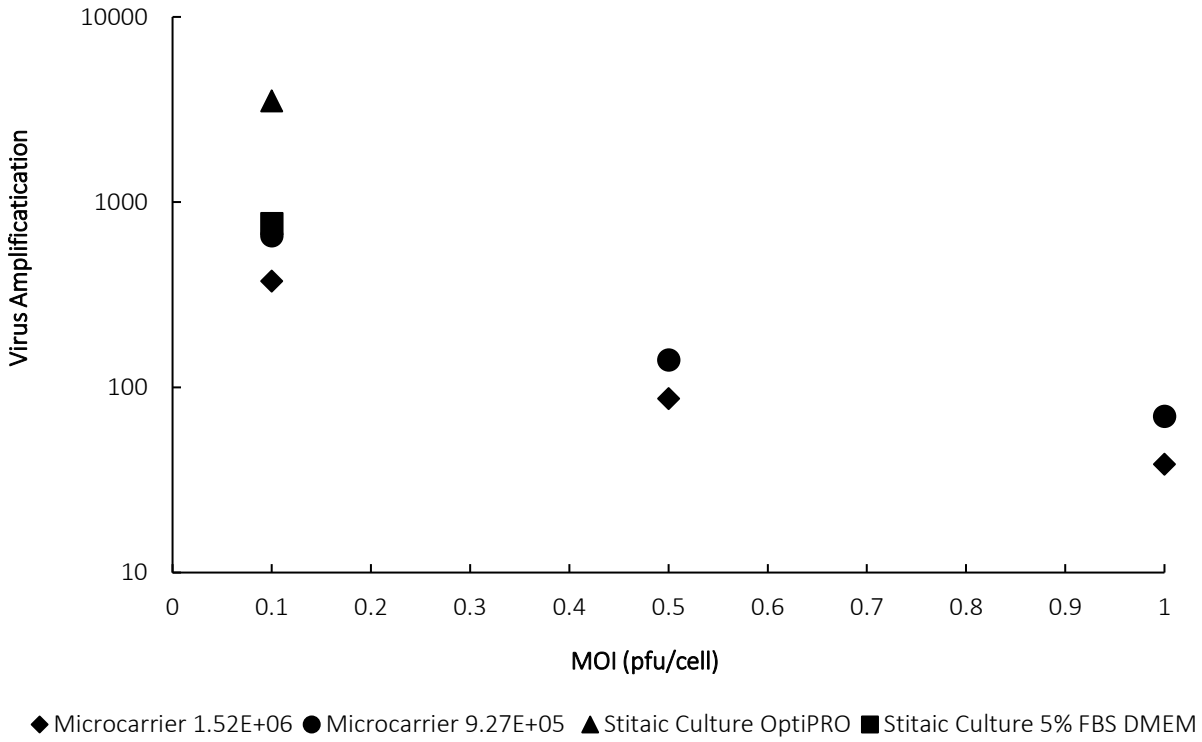

Figure 5.7: Comparison of VVL-15 RFP amplification obtained from infections performed at different MOI and TOIs in static or microcarrier culture system. CV-1-OPT cells were seeded, grown, infected and tested as described in the legends in Figures 3.5, 5.3, and 5.5. Each virus amplification was calculated by dividing the mean peak virus titres obtained under identical culture conditions by the amount of virus present in the inoculum.

5.4 Summary

In this Chapter, the microcarrier-based CV-1-OPT suspension culture system with medium exchange established in Chapter 4 was applied to the propagation of VVL-15 RFP. The cells were infected at densities over the ranges 9.27×10^5 - 1.52×10^6 cells/ml at MOIs from 0.1 to 1. The different combinations of cell densities at infection and MOIs had no significant impact on the maximal volumetric viral productivity. Yet, infection of cells at a lower density (9.27×10^5 cells/ml) with higher MOIs (≥ 0.5) reduced the process time by 3 days and gave rise to a maximal specific viral productivity of 71.87 pfu/cell. Virus titres in the microcarrier-based system increased 658 times from the time of infection to the time when peak viral yields were reached, which is similar to the titre increase of VVL 15-RFP produced statically in CV-1 cells in 5% FBS DMEM, but 5.45 fold less than that in static culture of CV-1-OPT cells. The results show effective expansion of VVL-15 RFP in microcarriers suspension culture of CV-1-OPT.

Chapter 6. Conclusions and Future Work

6.1 Conclusions

A key challenge in oncolytic Vaccinia virus production has been identified as the lack of an efficient serum-free oncolytic VV manufacturing process. The continuous mammalian cell line CV-1 has served as a host cell line for the propagation of various VV strains in lab-scale stationary cultivation systems and demonstrated a relatively safe profile. Using CV-1 for the cultivation of engineered oncolytic VVs has the potential to generate high-titre virus with reduced safety risk compared with the use of tumour cell lines and has the ability for real process scale-up. The evaluation of the cell line from the perspective of its suitability for oncolytic VVs production was therefore considered novel and had not formerly been described in the literature. This thesis has reported the development, characterization, and application of a serum-free adapted CV-1 cell line for a potentially scalable production process for an oncolytic VV, VVL 15-RFP.

6.1.1 CV-1 adapted to OptiPRO demonstrates comparable or superior growth profile to its counterparts in VP-SFM or DMEM with 5% FBS

Exploitation of SFM has become the general direction for vaccine production platforms as it addresses issues associated with using serum, including high cost, batch variation, risks of contamination and serum shortage. An adaptation to a high performance, chemically defined medium is the ultimate goal and is largely desirable.

Reports describing the serum-free cultivation of CV-1 cell lines are rarely found. CV-1 cells have demonstrated its growth in DMEM basal medium in the absence of serum and with supplementation of bovine milk, an undefined animal derived component that carries risks of contamination and exhibits batch-to-batch inconsistencies (Sue Steimer et al., 1981). There remains the need to search for a more defined SFM that supports both CV-1 cell proliferation and effective VVL 15-RFP replication. Establishment of a serum-free adapted CV-1 cell line capable of producing high titres of VVL 15-RFP would be considered a meaningful step towards industrial manufacturing of oncolytic VV.

The aim of Chapter 3 was to adapt CV-1 cells to growth in a serum free environment suitable for not only the cell expansion but also VVL-15 RFP production. This was successfully achieved and the adaptation process is shown in **Figure 3.1**.

After serum-free adaptation, the growth kinetics of adapted cells should be investigated and compared with its counterpart in original SCM. This not only allows evaluation of cell performances under different culture conditions (Cruz et al., 1997; Rourou et al., 2007; Heathman et al., 2015), but also provides scientific basis for the deduction of near-optimal operating conditions for some cultivation systems such as microcarrier-based systems (GE Healthcare, 2005). With suitable formulation, cell growth in SFM can be comparable or even better than that in SCM (Huang et al., 2015; Rourou et al., 2009; Heathman et al., 2015).

CV-1 cells adapted in both VP-SFM and OptiPRO exhibited spindle-shaped elongated morphologies (**Figure 3.2**). With regard to the cell growth performance in each SFM to which the cells has been adapted, CV-1 cells in OptiPRO (CV-1-OPT) demonstrates overall better growth performance as it exhibits shorter population doubling time, higher plating efficiency than that in 5% FBS DMEM and is comparable in saturation density and recovery ratio. Despite demonstrating a doubling time comparable to that in OptiPRO, CV-1 cells adapted to VP-SFM shows substantial decreases in saturation density, plating efficiency and recovery ratio (**Figure 3.3** and **3.4**/ **Table 3.1**). It may be helpful to introduce a more gradual decline in serum level and to grow the cells for a few more passages at each serum level before lowering the concentration again, especially when the concentration was below 2.5%.

The two serum free adapted cell lines were then tested for their VVL-15 RFP productivity in static culture. CV-1-OPT gave rise to the highest viral productivity at each time point among the three cell lines tested (**Figure 3.5**). Peak productivity is reached at 72 hours post infection, which is 352.2 ± 48.4 pfu/cell and is 2.6 and 4.6 times higher than the productivities in cells growth in VP-SFM and 5% FBS DMEM respectively.

6.1.2 CV-1-OPT was capable of proliferation on Cytodex-1 microcarriers

The aim of Chapter 4 was to expand CV-1-OPT cell line in one or more suspension culture systems. Weighing the pros and cons of each manufacturing system and taking into account the characteristics of CV-1 cells and the replication requirements of VVL-15 RFP, using suspension adapted CV-1 cells to produce VVL 15-RFP would be the preferable approach, particularly considering the scale-up potential of the process and operational complexity.

Propagation of the VVL 15-RFP in CV-1 on microcarriers in suspension would also be worth examining by first using spinner flasks. CV-1-OPT cells were cultivated on Cytodex-1 microcarriers (**Figure 4.5**). Attachment of the cell line onto Cytodx-1 appeared to follow the

first-order kinetic that the attachment rate depended only on the concentration of unattached cells left in the suspension (**Figure 4.6**). The protective effect of PF-68 was not observed in CV-1-OPT cell cultures under the experimental conditions (**Figure 4.7**).

The microcarrier cultures with various initial inoculum sizes (6 to 53 cells/microcarriers with crystal violet counts) reached comparable saturation densities (6.50-7.68 $\times 10^5$ cells/ mL) under batch culture conditions (**Figure 4.8**). The saturation densities obtained were lower than the 10^6 CV-1 cells/ mL reported by Giard et al. (1977). Cell proliferation was hardly seen in the cultures with relatively high inoculation densities (35, 53 cells/ microcarrier with crystal violet counts). Also worthy of note is the presence of unoccupied/unsaturated microcarriers and signs of bead-to-bead cell transfer when cultures reached their saturation densities, suggesting that there are factors that limit cells from achieving their maximum growth capacity.

In the analysis of the major nutrients and waste products within the culture medium (**Figure 4.11**), it was observed that, by the end of the culture period, both glucose and glutamine remained accessible, although the glucose levels in certain culture conditions were low. Additionally, it was challenging to determine the precise extent of glutamine uptake for each culture. The concentrations of lactate and ammonia did not exceed the generally accepted toxic thresholds. It was suspected that the accumulation of specific waste products or potential deficiencies in certain components within the medium, such as glucose or unexamined metabolites, may have substantially contributed to the limitation of cell proliferation.

Based on the conjecture above, partial medium exchange was implemented with the hope that cell density would increase. Cells were inoculated at 26 cells/ microcarrier with crystal violet counts. A daily exchange of 70% (v/v) culture medium gave rise to a cell concentration of $18.72 \pm 1.86 \times 10^5$ cells/ mL that was about 3 times as high as cultures operated in batch mode (**Figure 4.12**). CV-1-OPT cultures with medium exchanges every 2 or 3 days reached similar saturation densities of 13.88 ± 0.73 and $13.19 \pm 1.02 \times 10^5$ cells/ mL, which were 25% lower than the CV-1 cell concentration attained from cultures with media exchanged every 2 to 3 days (Mered, Albrecht, & Hopps, 1980).

Although high cell densities (and consequently high virus production yields) could be achieved through the microcarrier-based system, the relatively high cost of the beads and the challenges associated with scale-up (seed cell preparation, mixing power and speeds and product harvesting) make the system less appealing than conversion of the cell line itself to grow in suspension. The use of suspension cells simplifies the production process. Successful

adaptation of kidney cell lines of various origins, such as Vero, BHK-21, HEK293 and MDCK, to growth in suspension and the use of theses cell lines for viral productions have been reported (Paillet et al. 2009; Guskey & Jenkin 1975; Tsao et al. 2001; Huang et al. 2015).

Attempts at adaptation of CV-1-OPT growth to suspension were made. However, they were not successful (**Figure 4.1** and **4.3**). Large cell clumps were observed a week from inoculation (**Figure 4.2** and **4.4**). It was suspected that OptiPRO might contain components that promote surface attachment and cell-to-cell aggregation.

6.1.3 Production of VVL-15 RFP in CV-1-OPT in microcarrier culture

In recent years, there has been a growing interest in oncolytic VV therapies as clear evidence of safety and promising signs of efficacy in animal models and early phase clinical trials have been demonstrated (Chan & McFadden 2014). To our knowledge, manufacturing of clinical grade oncolytic VVs was mainly based on adherent culture vessels, cell factories, and roller bottle packs using Hela or Vero cells (Ungerechts et al. 2016). There remains the need for a scalable platform for the production of high titre oncolytic VV. Application of our previously established CV-1-OPT based microcarrier system to the production of an oncolytic VV may improve the potential of the production process for oncolytic VVs.

The results presented in Chapter 5 have demonstrated the potential of utilizing CV-1-OPT as a manufacture cell line to produce oncolytic Lister strain VV in large scale. Cultivation of VVL-15 RFP in microcarrier-based CV-1-OPT suspension culture has demonstrated a maximum specific virus productivity of 71.9 pfu/cell (**Figure 5.6**) which is comparable to that achieved by growing a Wyeth strain VV in suspension culture of Hela cells in SFM (Ricordel et al. 2013) (**Table 5.1**). More importantly, within the investigated range, MOI and TOI had little impact on the peak volumetric virus productivities but did affect the process time. CV-1-OPT cells infected at a lower cell density (9.27×10^5 cells/ml) in their exponential phase and at a higher MOI (≥ 0.5) would reduce process time by 3 days without compromising the maximal viral yields (**Figure 5.4**). The maximum fold increase of VVL-15 RFP produced in microcarrier-based CV-1-OPT suspension culture was 658, similar to that produced in static culture of CV-1 cells in 5% FBS DMEM, but 5.45 fold less than that produced in static culture of CV-1-OPT cells (**Figure 5.7**). It would be interesting to examine the uptake and production of the metabolites, which would help further understand the process.

In this thesis, the potential of using CV-1 cell line as a host for producing oncolytic VV on a large scale was assessed. The study demonstrated the successful adaptation of CV-1 cells to a serum-free medium, OptiPRO, for the first time. The resulting CV-1-OPT cell line was found to proliferate effectively in microcarrier culture, and it was also capable of supporting the growth of VVL-15 RFP on microcarrier in suspension. These findings provide important evidence that CV-1 could be a viable option for producing VVL-15 RFP in a culture system that is scalable and has reduced contamination risks.

6.2 Reflections and future work

The work in the thesis examined the application potential of using CV-1 cell line for the production of an oncolytic VV in a scalable microcarrier culture system under serum free conditions. Suggestions for future work are listed below:

- Further characterization of CV-1-OPT cell line to address the safety and quality concerns of the cell line.

- Application of CV-1-OPT to the propagation of different oncolytic VVs. The capability of CV-1-OPT supporting VV proliferation can be further assessed by growing oncolytic VVs of various strains and engineered forms in the CV-1-OPT.

- Exploration of medium formulation for CV-1 culture.

  Investigation of the nutritional requirements of CV-1-OPT cells. Replacing GlutaMAX with glutamine might enable a better understanding of glutamine metabolism in the cultures. Further examinations on metabolites such as amino acid analysis would help identify the limiting nutrient element(s) during cell fermentation, therefore shedding some light on the nutrients supplementation strategy. Development of customized SFM optimized for CV-1 cells (suspension) growth and VV production might also be beneficial.

- Evaluation of a broader range of microcarriers and assess their ability in supporting cell proliferation.

- Closer examination and optimization of the agitation regime at different stages of CV-1-OPT proliferation and viral production is strongly recommended:

1) During cell attachment, the agitation mode and speed need to be carefully adjusted, to promote a homogeneous distribution of cells and facilitate their stay and spreading on the microcarrier in preparation for the proliferation stage.

2) At cell proliferation stage, agitation speed should be adjusted to attain complete suspension of microcarriers in the medium while inflicting minimal harm to the cells.

3) Upon infection, it may be necessary to modify the agitation process in order to assist with the absorption and penetration of the virus into the cells.

4) While the virus is multiplying, the infected cells may become less securely attached to the surface of microcarriers, requiring a decrease in agitation speed.

❖ Optimization of the viral infection and propagation regimen:

1) Based on Poisson distribution, when infecting cells at MOIs of 0.1, 0.5 and 1, the percentages of cells infected are 9.52%, 39.3% and 63.2% respectively. Also considering that cells were in an agitated suspension, the collision of cells and virus could be more random and less frequent than that in a static culture system. Therefore, it may be worth experimenting with MOIs higher than one (for example, three, five and ten).

2) Mallardo and colleagues (2002) noted that as the number of intracellular viral cores increases due to VV entry, there is a proportional increase in the synthesis of viral RNA and DNA. When the infection results in 10-40 cores per cell, each individual core is suggested to be infectious. However, when MOIs exceed 10-40 cores per cell, there appears to be a plateauing or slight decline in the synthesis of VV early proteins.

   This finding prompts consideration of whether the viral titre might increase efficiently within the core count range of 10-40 cores/cell, assuming favourable growth conditions. Exploring the relationship between core count, MOI, and resulting DNA titre might offer useful insights for optimizing the viral production process.

3) Infecting cells with virus of high concentration in reduced volume may help to elevate the frequencies that the virus collide with the cells.

4) Exploration of the post-infection cultivation temperature. The optimum temperature for viral infection can be different (usually cooler) from that for cell culture.

5) Study of the correlation between cell density at the time of infection (TOI), MOI, and time of harvest (TOH) for high OVV productivity.

- Not much information has been found on the existence of defective interfering particles (DIPs) among VV populations, the potential mechanisms by which VV DIPs might interfere with the replication of their non-defective counterparts, and the extent of interference. One explanation is that the interference ability of DIPs in poxviruses is associated with host cell types (Holowczak, 1982). It is worth looking out for evidence of DIPs formation in OVV production in CV-1-OPT cells and evaluating the impact of DIPs might exert on VV yield and anti-viral host response. If necessary, mitigation measures should be investigated and implemented to reduce generation of this contaminant.

- In our microcarrier culture, we did not distinguish between IMV and CEV/EEV during sampling and virus titration. Ideally, a harvest time should be aimed for that primarily yields IMV while retaining them within the cells as release of IMV into the medium upon cell lysis could potentially compromise product yield due to the viability of the IMV being affected by the massive release of cellular contents.

  Achieving this may involve employing methods to measure cell intactness, immunofluorescent staining, and microscopy to differentiate between IMV and EEV/CEV, and conducting cell counts and virus titrations in suspension (without microcarrier) and within the culture at regular intervals. When optimizing agitation speed, consideration of cell integrity should also be factored in.

- Application of Design of Experiments (DOE) for process optimization. DOE approaches allow systematically screening and optimizing the viral production process parameters.

- Production of oncolytic VV in a more controllable environment. The microcarrier process developed in spinner flasks should be transferred to production systems with more precise adjustment for pH, dissolved oxygen and temperature. In addition, process intensification through semi-batch or perfusion methods should be explored. Adoption of these more sophisticated control operations would be expected to further promote cell concentrations and viral yields.

- Evaluation of VVL-15 RFP production in different bioreactor systems (such as stirred-tank bioreactor, wave bioreactor) at small-scale.

- Evaluation of the economic viability of the upstream production process.

- Identification of the downstream VV manufacturing challenges associated with using CV-1 as the production cell line. VV harvested from lysed CV-1 cells must be separated from host cell proteins (HCPs) and host cell DNA. Understanding the impact of CV-1 on the virus purification process would allow further assessment of the suitability of adopting CV-1 in VV production.

References

Abdeen, S. H., Abdeen, A.M., El-Enshasy, H.A., & EI Shereef, A.A. (2011). HeLa-S3 cell growth conditions in serum-free medium and adaptability for proliferation in suspension culture. *Journal of Biological Sciences*, *11*(2), pp.124–134.

Aggarwal, K., Jing, F., Maranga, L., & Liu, J. (2011). Bioprocess optimization for cell culture based influenza vaccine production. *Vaccine*, *29*(17), 3320–3328. https://doi.org/10.1016/j.vaccine.2011.01.081

Ahmed, J. (2015). *Optimisation of the Lister strain of vaccinia virus for use as an anticancer immunotherapeutic agent*. [Doctoral dissertation, Queen Mary University of London]. Queen Mary Research Online. https://qmro.qmul.ac.uk/xmlui/handle/123456789/9519

Ahmed, J., Yuan, M., Alusi, G., Lemoine, N. R., & Wang, Y. (2014). The Lister strain of vaccinia virus as an anticancer therapeutic agent. In E. C. Lattime & S. L. Gerson (Eds.), *Gene therapy of cancer: Translational Approaches from preclinical studies to clinical implementation* (pp. 225–238). Academic Press. https://doi.org/10.1016/B978-0-12-394295-1.00016-0.

Al Yaghchi, C., Zhang, Z., Alusi, G., Lemoine, N. R., & Wang, Y. (2015). Vaccinia virus, a promising new therapeutic agent for pancreatic cancer. *Immunotherapy*, *7*(12), 1249–1258. https://doi.org/10.2217/imt.15.90

Andrade, A. A., Silva, P. N., Pereira, A. C., De Sousa, L. P., Ferreira, P. C., Gazzinelli, R. T., Kroon, E. G., Ropert, C., & Bonjardim, C. A. (2004). The vaccinia virus-stimulated mitogen-activated protein kinase (MAPK) pathway is required for virus multiplication. *The Biochemical journal*, *381*(Pt 2), 437–446. https://doi.org/10.1042/BJ20031375

Alcam, A., Khanna, A., Paul, N. L., & Smith, G. L. (1999). Vaccinia virus strains lister, USSR and Evans express soluble and cell-surface tumour necrosis factor receptors. *The Journal of general virology*, *80* (Pt 4), 949–959. https://doi.org/10.1099/0022-1317-80-4-949

Alcamí, A., Symons, J. A., & Smith, G. L. (2000). The vaccinia virus soluble alpha/beta interferon (IFN) receptor binds to the cell surface and protects cells from the antiviral effects of IFN. *Journal of virology*, *74*(23), 11230–11239. https://doi.org/10.1128/jvi.74.23.11230-11239.2000

Archard, L. C., & Williamson, J. D. (1971). The effect of arginine deprivation on the replication of vaccinia virus. *The Journal of general virology*, *12*(3), 249–258. https://doi.org/10.1099/0022-1317-12-3-249

Aubrit, F., Perugi, F., Léon, A., Guéhenneux, F., Champion-Arnaud, P., Lahmar, M., & Schwamborn, K. (2015). Cell substrates for the production of viral vaccines. *Vaccine*, *33*(44), 5905–5912. https://doi.org/10.1016/j.vaccine.2015.06.110

Aurelian L. (2016). Oncolytic viruses as immunotherapy: progress and remaining challenges. *OncoTargets and therapy*, *9*, 2627–2637. https://doi.org/10.2147/OTT.S63049

Barnes, D., & Sato, G. (1980). Serum-free cell culture: a unifying approach. *Cell*, *22*(3), 649–655. https://doi.org/10.1016/0092-8674(80)90540-1

Bartlett, D. L., Liu, Z., Sathaiah, M., Ravindranathan, R., Guo, Z., He, Y., & Guo, Z. S. (2013). Oncolytic viruses as therapeutic cancer vaccines. *Molecular cancer*, *12*(1), 103. https://doi.org/10.1186/1476-4598-12-103

Barrett, P. N., Mundt, W., Kistner, O., & Howard, M. K. (2009). Vero cell platform in vaccine production: moving towards cell culture-based viral vaccines. *Expert review of vaccines*, *8*(5), 607–618. https://doi.org/10.1586/erv.09.19

Belongia, E. A., & Naleway, A. L. (2003). Smallpox vaccine: the good, the bad, and the ugly. *Clinical medicine & research*, *1*(2), 87–92. https://doi.org/10.3121/cmr.1.2.87.

Berse, B., Brown, L. F., Van de Water, L., Dvorak, H. F., & Senger, D. R. (1992). Vascular permeability factor (vascular endothelial growth factor) gene is expressed differentially in normal tissues, macrophages, and tumors. *Molecular biology of the cell*, *3*(2), 211–220. https://doi.org/10.1091/mbc.3.2.211

Biaggio, R. T., Abreu-Neto, M. S., Covas, D. T., & Swiech, K. (2015). Serum-free suspension culturing of human cells: adaptation, growth, and cryopreservation. *Bioprocess and biosystems engineering*, *38*(8), 1495–1507. https://doi.org/10.1007/s00449-015-1392-9

Bielitzki, J., Drew, S. W., Gay, C. G., Leighton, T., Jacobson, S. H., & Ritchey, M. (2007). *International Assessment of Research and Development in Rapid Vaccine Manufacturing.* http://www.wtec.org/vaccmfg/RapidVaccMfg-finalreport.pdf.

Björkerud, S., & Björkerud, B. (1994). Lipoproteins are major and primary mitogens and growth promoters for human arterial smooth muscle cells and lung fibroblasts in vitro. *Arteriosclerosis and thrombosis : a journal of vascular biology*, *14*(2), 288–298.

Blasey, H. D., Isch, C. and Bernard, A. R. (1995), Cellcube: A new system for large scale growth of adherent cells, *Biotechnology Techniques*, *9*(10), 725–728. https://doi.org/10.1007/BF00159237

Breitbach, C. J., Arulanandam, R., De Silva, N., Thorne, S. H., Patt, R., Daneshmand, M., Moon, A., Ilkow, C., Burke, J., Hwang, T. H., Heo, J., Cho, M., Chen, H., Angarita, F. A., Addison, C., McCart, J. A., Bell, J. C., & Kirn, D. H. (2013). Oncolytic vaccinia virus disrupts tumor-associated vasculature in humans. *Cancer research*, *73*(4), 1265–1275. https://doi.org/10.1158/0008-5472.CAN-12-2687

Breitbach, C. J., Burke, J., Jonker, D., Stephenson, J., Haas, A. R., Chow, L. Q., Nieva, J., Hwang, T. H., Moon, A., Patt, R., Pelusio, A., Le Boeuf, F., Burns, J., Evgin, L., De Silva, N., Cvancic, S., Robertson, T., Je, J. E., Lee, Y. S., Parato, K., … Kirn, D. H. (2011). Intravenous delivery of a multi-mechanistic cancer-targeted oncolytic poxvirus in humans. *Nature*, *477*(7362), 99–102. https://doi.org/10.1038/nature10358

Breitbach, C. J., De Silva, N. S., Falls, T. J., Aladl, U., Evgin, L., Paterson, J., Sun, Y. Y., Roy, D. G., Rintoul, J. L., Daneshmand, M., Parato, K., Stanford, M. M., Lichty, B. D., Fenster, A., Kirn, D., Atkins, H., & Bell, J. C. (2011). Targeting tumor vasculature with an oncolytic virus. *Molecular therapy : the journal of the American Society of Gene Therapy*, *19*(5), 886–894. https://doi.org/10.1038/mt.2011.26

Breitbach, C. J., Arulanandam, R., De Silva, N., Thorne, S. H., Patt, R., Daneshmand, M., Moon, A., Ilkow, C., Burke, J., Hwang, T. H., Heo, J., Cho, M., Chen, H., Angarita, F. A., Addison, C., McCart, J. A., Bell, J. C., & Kirn, D. H. (2013). Oncolytic vaccinia virus disrupts tumor-associated vasculature in humans. Cancer research, *73*(4), 1265–1275. https://doi.org/10.1158/0008-5472.CAN-12-2687

Burgener, A. & Butler, M. (2006) Medium development. In: S. Ozturk & W-S. Hu (Eds.), *Cell culture technology for pharmaceutical and cell-based therapies* (pp 41–80). CRC Press. https://doi.org/10.1201/9780849351068

Butler, M., Burgener, A., Patrick, M., Berry, M., Moffatt, D., Huzel, N., Barnabé, N., & Coombs, K. (2000). Application of a serum-free medium for the growth of Vero cells and the production of reovirus. *Biotechnology progress*, *16*(5), 854–858. https://doi.org/10.1021/bp000110+

Cardoso T.C., Ferrari H.F., Luvizotto M.C.R., & Arns C.W. (2007). Bio-safety technology in production of bovine herpesvirus type 5 (BoHV-5) using an alternative serum-free medium. *Am J Biochem Biotechnol, 3*, 125–130. doi: 10.3844/ajbbsp.2007.125.130.

Carter, G. C., Rodger, G., Murphy, B. J., Law, M., Krauss, O., Hollinshead, M., & Smith, G. L. (2003). Vaccinia virus cores are transported on microtubules. *The Journal of general virology*, *84*(Pt 9), 2443–2458. https://doi.org/10.1099/vir.0.19271-0

Cell Culture Dish[INC.]. (2015, February 11). *The Evolution of Vaccine Manufacturing- Past, Current, and Future Trends*. http://cellculturedish.com/2015/02/evolution-vaccine-manufacturing-past-current-future-trends/. [Accessed 09 July 2016].

Chan, W.M. & McFadden, G. (2014). Oncolytic poxviruses. *Annual Review of Virology*, *1*(1), pp.191–214. https://doi.org/10.1146/annurev-virology-031413-085442

Chase, L. G., Lakshmipathy, U., Solchaga, L. A., Rao, M. S., & Vemuri, M. C. (2010). A novel serum-free medium for the expansion of human mesenchymal stem cells. *Stem cell research & therapy*, *1*(1), 8. https://doi.org/10.1186/scrt8

ChemoMetec. (n.d.) *ChemoMetec NucleoCounter® NC-200*. https://animalab.eu/images/d8e66258-6565-47e4-9cb8-5836cb8dcad3/1-768x492.png

Chen, A., Poh, S. L., Dietzsch, C., Roethl, E., Yan, M. L., & Ng, S. K. (2011). Serum-free microcarrier based production of replication deficient Influenza vaccine candidate virus lacking NS1 using Vero cells. *BMC Biotechnology*, *11*(1), 81. https://doi.org/10.1186/1472-6750-11-81

Chen, B., Timiryasova, T. M., Haghighat, P., Andres, M. L., Kajioka, E. H., Dutta-Roy, R., Gridley, D. S., & Fodor, I. (2001). Low-dose vaccinia virus-mediated cytokine gene therapy of glioma. *Journal of immunotherapy* (Hagerstown, Md.: 1997), *24*(1), 46–57. https://doi.org/10.1097/00002371-200101000-00006

Chen, N., Zhang, Q., Yu, Y. A., Stritzker, J., Brader, P., Schirbel, A., Samnick, S., Serganova,

I., Blasberg, R., Fong, Y., & Szalay, A. A. (2009). A novel recombinant vaccinia virus expressing the human norepinephrine transporter retains oncolytic potential and facilitates deep-tissue imaging. *Molecular medicine* (Cambridge, Mass.), *15*(5-6), 144–151. https://doi.org/10.2119/molmed.2009.00014

Chen, N. G., Yu, Y. A., Zhang, Q., & Szalay, A. A. (2011) 'Replication efficiency of oncolytic vaccinia virus in cell cultures prognosticates the virulence and antitumor efficacy in mice', *J Transl Med, 9,* 164. https://doi.org/10.1186/1479-5876-9-164

Chen, S., Li, J., Li, Q., & Wang, Z. (2016). Bispecific antibodies in cancer immunotherapy. Human vaccines & immunotherapeutics, *12*(10), 2491–2500. https://doi.org/10.1080/21645515.2016.1187802

Chillakuru, R. A., Ryu, D. D., & Yilma, T. (1991). Propagation of recombinant vaccinia virus in HeLa cells: adsorption kinetics and replication in batch cultures. *Biotechnology progress*, *7*(2), 85–92. https://doi.org/10.1021/bp00008a002

Chou, W., Ngo, T., & Gershon, P. D. (2012). An overview of the vaccinia virus infectome: a survey of the proteins of the poxvirus-infected cell. *Journal of virology*, *86*(3), 1487–1499. https://doi.org/10.1128/JVI.06084-11

Chun, B. H., Kwon Lee, Y., Bang, W. G., & Chung, N. (2005). Use of plant protein hydrolysates for varicella virus production in serum-free medium. *Biotechnology letters*, *27*(4), 243–248. https://doi.org/10.1007/s10529-004-8357-4

Clark, J. M., & Hirtenstein, M. D. (1981). Optimizing culture conditions for the production of animal cells in microcarrier culture. *Annals of the New York Academy of Sciences*, *369*, 33–46. https://doi.org/10.1111/j.1749-6632.1981.tb14175.x

Contreras, G., Bather, R., Furesz, J., & Becker, B. C. (1985). Activation of metastatic potential in African green monkey kidney cell lines by prolonged in vitro culture. *In vitro cellular & developmental biology: journal of the Tissue Culture Association*, *21*(11), 649–652. https://doi.org/10.1007/BF02623298

Corning. (n.d.). [Photograph of CellSTACK® cell culture chambers]. https://www.sigmaaldrich.com/GB/en/product/sigma/cls3271

Corning. (n.d.). [Photograph of Corning® Roller Bottles]. https://www.sigmaaldrich.com/GB/en/product/sigma/cls430699

Croughan, M. S., & Wang, D. I. (1991). Hydrodynamic effects on animal cells in microcarrier bioreactors. Biotechnology (Reading, Mass.), *17*, 213–249. https://doi.org/10.1016/b978-0-409-90123-8.50015-x

Cruz, H. J., Moreira, J. L., & Carrondo, M. J. (2000). Metabolically optimised BHK cell fed-batch cultures. *Journal of biotechnology*, *80*(2), 109–118. https://doi.org/10.1016/s0168-1656(00)00254-6

Cruz, H. J., Moreira, J. L., & Carrondo, M. J. (1999). Metabolic shifts by nutrient manipulation in continuous cultures of BHK cells. *Biotechnology and bioengineering*, *66*(2), 104–113. https://doi.org/10.1002/(sici)1097-0290(1999)66:2<104::aid-bit3>3.0.co;2-#

Cruz, H. J., Moreira, J. L., Stacey, G., Dias, E. M., Hayes, K., Looby, D., Griffiths, B., & Carrondo, M. J. (1998). Adaptation of BHK cells producing a recombinant protein to serum-free media and protein-free medium. *Cytotechnology*, *26*(1), 59–64. https://doi.org/10.1023/A:1007951813755

CV-1 CCL-70™. (n.d.). Retrieved from https://www.atcc.org/products/ccl-70

D'Alisa, R. M., & Gershey, E. L. (1980). Characterization of the cell cycle and synchrony in a CV-1 cell line. *Cytometry*, 1(1), 73–83. https://doi.org/10.1002/cyto.990010115

Dimasi, L. (2011, September). Meeting increased demands on cell-based processes by using defined media supplements. *BioProcess International*, *9*(8). https://bioprocessintl.com/upstream-processing/biochemicals-raw-materials/meeting-increased-demands-on-cell-based-processes-by-using-defined-media-supplements-320904/

ECACC General Cell Collection: CV-1. (n.d.). Retrieved from https://www.phe-culturecollections.org.uk/products/celllines/generalcell/detail.jsp?refId=87032605&collection=ecacc_gc

Eagle H. (1955). Nutrition needs of mammalian cells in tissue culture. *Science* (New York, N.Y.), *122*(3168), 501–514. https://doi.org/10.1126/science.122.3168.501

Eagle H. (1959). Amino acid metabolism in mammalian cell cultures. *Science* (New York, N.Y.), *130*(3373), 432–437. https://doi.org/10.1126/science.130.3373.432

Ejiri, H., Nomura, T., Hasegawa, M., Tatsumi, C., Imai, M., Sakakibara, S., & Terashi, H. (2015). Use of synthetic serum-free medium for culture of human dermal fibroblasts to establish an experimental system similar to living dermis. *Cytotechnology*, *67*(3), 507–514. https://doi.org/10.1007/s10616-014-9709-0

European Medicines Agency. (1998). *ICH Topic Q5D Quality of Biotechnological Products: Derivation and Characterisation of Cell Substrates used for Production of Biotechnological/Biological products*. (CPMP/ICH/294/95). https://www.ema.europa.eu/en/documents/scientific-guideline/ich-q-5-d-derivation-characterisation-cell-substrates-used-production-biotechnological/biological-products-step-5_en.pdf

European Medicines Agency. (2011). *Note for guidance on minimizing the risk of transmitting animal spongiform encephalopathy agents via human and veterinary medicinal products*. (EMA/410/01 rev.3). https://www.ema.europa.eu/en/documents/scientific-guideline/minimising-risk-transmitting-animal-spongiform-encephalopathy-agents-human-veterinary-medicinal_en.pdf

Ehrig, K., Kilinc, M. O., Chen, N. G., Stritzker, J., Buckel, L., Zhang, Q., & Szalay, A. A. (2013). Growth inhibition of different human colorectal cancer xenografts after a single intravenous injection of oncolytic vaccinia virus GLV-1h68. *Journal of translational medicine*, *11*, 79. https://doi.org/10.1186/1479-5876-11-79

Elford, H. L., Freese, M., Passamani, E., & Morris, H. P. (1970). Ribonucleotide reductase and cell proliferation. I. Variations of ribonucleotide reductase activity with tumor growth rate in a series of rat hepatomas. *The Journal of biological chemistry*, *245*(20), 5228–5233.

Ferguson, M. S., Chard Dunmall, L. S., Gangeswaran, R., Marelli, G., Tysome, J. R., Burns, E., Whitehead, M. A., Aksoy, E., Alusi, G., Hiley, C., Ahmed, J., Vanhaesebroeck, B., Lemoine, N. R., & Wang, Y. (2020). Transient Inhibition of PI3Kδ Enhances the Therapeutic Effect of Intravenous Delivery of Oncolytic Vaccinia Virus. Molecular therapy: *the journal of the American Society of Gene Therapy*, *28*(5), 1263–1275. https://doi.org/10.1016/j.ymthe.2020.02.017

FiberCell Systems. (n.d.). [Photograph of FiberCell Systems hollow fiber bioreactor catrige with tubing]. https://www.fibercellsystems.com/products/cartridges/

Fodor, I., Timiryasova, T., Denes, B., Yoshida, J., Ruckle, H., & Lilly, M. (2005). Vaccinia

virus mediated p53 gene therapy for bladder cancer in an orthotopic murine model. *The Journal of urology*, *173*(2), 604–609. https://doi.org/10.1097/01.ju.0000143196.37008.2c

Fontaine, K. A., Camarda, R., & Lagunoff, M. (2014). Vaccinia virus requires glutamine but not glucose for efficient replication. *Journal of virology*, *88*(8), 4366–4374. https://doi.org/10.1128/JVI.03134-13

Forno, G. (2013). "Suspension Vero cells (sVERO) for poliovirus production: Effect of culture passage on growth kinetics and productivity" in "Vaccine Technology IV", B. Buckland, University College London, UK; J. Aunins, Janis Biologics, LLC; P. Alves , ITQB/IBET; K. Jansen, Wyeth Vaccine Research Eds, ECI Symposium Series. http: //dc.engconfintl.org/ vaccine_iv/48.

Frazatti-Gallina, N. M., Mourão-Fuches, R. M., Paoli, R. L., Silva, M. L., Miyaki, C., Valentini, E. J., Raw, I., & Higashi, H. G. (2004). Vero-cell rabies vaccine produced using serum-free medium. *Vaccine*, *23*(4), 511–517. https://doi.org/10.1016/j.vaccine.2004.06.014

Freed-Pastor, W. A., & Prives, C. (2012). Mutant p53: one name, many proteins. *Genes & development*, *26*(12), 1268–1286. https://doi.org/10.1101/gad.190678.112

Freshney, R. I. (2005). Quantitation. In R. I. Freshney (Ed.), *Culture of Animal Cells: A Manual of Basic Technique* (pp. 335-358). Wiley-Blackwell. https://doi.org/ 10.1002/9780470649367

Furesz, J., Fanok, A., Contreras, G., & Becker, B. (1989). Tumorigenicity testing of various cell substrates for production of biologicals. *Developments in biological standardization*, *70*, 233–243.

Galbraith D. N. (2002). Transmissible spongiform encephalopathies and tissue cell culture. Cytotechnology, *39*(2), 117–124. https://doi.org/10.1023/A:1022935117274

Galliher, P. M. (2007). *Review of Single Use Technologies in BioManufacturing* [PowerPoint slides]. Worcester Polytechnic Institute website. https://web.wpi.edu/Images/CMS/BEI/ parrishgalliher.pdf.

Gallo-Ramírez, L. E., Nikolay, A., Genzel, Y., & Reichl, U. (2015). Bioreactor concepts for cell culture-based viral vaccine production. *Expert review of vaccines*, *14*(9), 1181–1195. https://doi.org/10.1586/14760584.2015.1067144

Gangal, S. (2010). Protocol for routine characterisation of cell lines. In S. Gangal (Ed.), *Principles and Practice of Animal Tissue Culture* (pp. 87-99). Universities Press, India.

Garcel, A., Crance, J. M., Drillien, R., Garin, D., & Favier, A. L. (2007). Genomic sequence of a clonal isolate of the vaccinia virus Lister strain employed for smallpox vaccination in France and its comparison to other orthopoxviruses. *The Journal of general virology*, *88*(Pt 7), 1906–1916. https://doi.org/10.1099/vir.0.82708-0

Gardner, J. D., Tscharke, D. C., Reading, P. C., & Smith, G. L. (2001). Vaccinia virus semaphorin A39R is a 50-55 kDa secreted glycoprotein that affects the outcome of infection in a murine intradermal model. The Journal of general virology, *82*(Pt 9), 2083–2093. https://doi.org/10.1099/0022-1317-82-9-2083

Garnier, A., Côté, J., Nadeau, I., Kamen, A., & Massie, B. (1994). Scale-up of the adenovirus expression system for the production of recombinant protein in human 293S cells. *Cytotechnology*, *15*(1-3), 145–155. https://doi.org/10.1007/BF00762389

GE Healthcare. (2005). *Microcarrier cell culture principles and methods.* [Brochure]. http://www.gelifesciences.co.kr/wp-content/uploads/2016/07/023.8_Microcarrier-Cell-Culture.pdf

GE Helathcare. (2011). WAVE BioreactorTM 20/10 and 20/50 systems. [Leaflet]. https://acmerevival.com/wp-content/uploads/2021/03/GEWaveBioreactorSystem210EHBrochure.pdf

Genzel Y. (2015). Designing cell lines for viral vaccine production: Where do we stand?. *Biotechnology journal*, *10*(5), 728–740. https://doi.org/10.1002/biot.201400388

Genzel, Y., Behrendt, I., König, S., Sann, H., & Reichl, U. (2004). Metabolism of MDCK cells during cell growth and influenza virus production in large-scale microcarrier culture. Vaccine, *22*(17-18), 2202–2208. https://doi.org/10.1016/j.vaccine.2003.11.041

Genzel, Y., Behrendt, I., Scharfenberg, K., & Reichl, U. (2009, June 7-10). *Evaluation of a new suspension MDCK cell line for influenza vaccine production* [Poster presentation]. 21st Annual Meeting of the European Society for Animal Cell Technology in Dublin, Ireland.

Genzel, Y., Fischer, M., & Reichl, U. (2006). Serum-free influenza virus production avoiding washing steps and medium exchange in large-scale microcarrier culture. *Vaccine*, *24*, 3261–3272. https://doi.org/10.1016/j.vaccine.2006.01.019

Genzel, Y., Olmer, R. M., Schäfer, B., & Reichl, U. (2006). Wave microcarrier cultivation of MDCK cells for influenza virus production in serum containing and serum-free media. Vaccine, *24*(35-36), 6074–6087. https://doi.org/10.1016/j.vaccine.2006.05.023

Gershey, E. L., & D'Alisa, R. M. (1980). Characterization of a CV-1 cell cycle. II. The role of cell-substrate attachment. *Journal of cell science*, *42*, 357–365.

Gey, G.O. (1933). An improved technic for massive tissue culture., *Am. J. Cancer*, *17*, 752-756. https://doi.org/ 10.1158/ajc.1933.752

Ghendon, Y. Z., Markushin, S. G., Akopova, I. I., Koptiaeva, I. B., Nechaeva, E. A., Mazurkova, L. A., Radaeva, I. F., & Kolokoltseva, T. D. (2005). Development of cell culture (MDCK) live cold-adapted (CA) attenuated influenza vaccine. *Vaccine*, *23*(38), 4678–4684. https://doi.org/10.1016/j.vaccine.2005.04.039

Giard, D. J., Thilly, W. G., Wang, D. I., & Levine, D. W. (1977). Virus production with a newly developed microcarrier system. *Applied and environmental microbiology*, *34*(6), 668–672. https://doi.org/10.1128/aem.34.6.668-672.1977

Gilbert, P.-A., Comanita, L., Barrett, J., Peters, A., Szabat, M., McFadden, G., & Dekaban, G. A. (2005). Current status for high titre poxvirus stock preparation in CEF under serum-free medium conditions: implication for vaccine development. *Cytotechnology*, *48*(1–3), 79–88. https://doi.org/10.1007/s10616-005-3795-y

Glaser, J., & Conrad, H. (1984). Properties of chick embryo chondrocytes grown in serum-free medium. *The Journal of biological chemistry*, *259* (11), 6766-72 . https://doi.org/ 10.1016/s0021-9258(17)39794-6

Goel, S., Duda, D. G., Xu, L., Munn, L. L., Boucher, Y., Fukumura, D., & Jain, R. K. (2011). Normalization of the vasculature for treatment of cancer and other diseases. *Physiological reviews*, 91(3), 1071–1121. https://doi.org/10.1152/physrev.00038.2010

González Hernández, Y., & Fischer, R. W. (2007). Serum-free culturing of mammalian cells--adaptation to and cryopreservation in fully defined media. *ALTEX*, *24*(2), 110–116.

https://doi.org/10.14573/altex.2007.2.110

Graff, S., Moser, H., Kastner, O., Graff, A.M., &Tannenbaum, M. (1965) The significance of glycolysis. *JNCI: Journal of the National Cancer Institute, 34* (4) 511-519. https://doi.org/10.1093/jnci/34.4.511

Greiner, J. W., Zeytin, H., Anver, M. R., & Schlom, J. (2002). Vaccine-based therapy directed against carcinoembryonic antigen demonstrates antitumor activity on spontaneous intestinal tumors in the absence of autoimmunity. *Cancer research*, *62*(23), 6944–6951.

Grieger, J. C., Soltys, S. M., & Samulski, R. J. (2016). Production of recombinant adeno-associated virus vectors using suspension HEK293 cells and continuous harvest of vector from the culture media for GMP FIX and FLT1 clinical vector. *Molecular therapy: the journal of the American Society of Gene Therapy*, *24*(2), 287–297. https://doi.org/10.1038/mt.2015.187

Griffiths, J.B. (1990). Scale-up of suspension and anchorage-dependent animal cells. In J.W. Pollard and J.M. Walker (Eds) *Animal Cell Culture. Methods in Molecular Biology, 5*. 49-63. Humana Press. https://doi.org/10.1385/0-89603-150-0:49

Grosenbach, D. W., Jordan, R., & Hruby, D. E. (2011). Development of the small-molecule antiviral ST-246 as a smallpox therapeutic. *Future virology*, *6*(5), 653–671. https://doi.org/10.2217/fvl.11.27

Gruber, D.F. & Jayme, D.W. (1994). Cell and tissue culture media: history and terminology. In J. E. Celis (Ed) *Cell Biology: a laboratory handbook, 3*, 451–458. Academic Press. https://doi.org/10.1016/B978-0-12-164717-9.50059-3

Gubser, C., Bergamaschi, D., Hollinshead, M., Lu, X., van Kuppeveld, F. J., & Smith, G. L. (2007). A new inhibitor of apoptosis from vaccinia virus and eukaryotes. *PLoS pathogens*, *3*(2), e17. https://doi.org/10.1371/journal.ppat.0030017

Gulley, J. L., Arlen, P. M., Tsang, K. Y., Yokokawa, J., Palena, C., Poole, D. J., Remondo, C., Cereda, V., Jones, J. L., Pazdur, M. P., Higgins, J. P., Hodge, J. W., Steinberg, S. M., Kotz, H., Dahut, W. L., & Schlom, J. (2008). Pilot study of vaccination with recombinant CEA-MUC-1-TRICOM poxviral-based vaccines in patients with metastatic carcinoma. *Clinical cancer research : an official journal of the American Association for Cancer Research*, *14*(10), 3060–3069. https://doi.org/10.1158/1078-0432.CCR-08-0126

Guo, Z. S. (2011). The impact of hypoxia on oncolytic virotherapy. *Virus Adaptation and Treatment*, *3* (1). 71 - 82. https://doi.org/10.2147/VAAT.S17832

Guo, Z. S., Liu, Z., & Bartlett, D. L. (2014). Oncolytic immunotherapy: dying the right way is a key to eliciting potent antitumor immunity. *Frontiers in oncology*, *4*, 74. https://doi.org/10.3389/fonc.2014.00074

Guse, K., Sloniecka, M., Diaconu, I., Ottolino-Perry, K., Tang, N., Ng, C., Le Boeuf, F., Bell, J. C., McCart, J. A., Ristimäki, A., Pesonen, S., Cerullo, V., & Hemminki, A. (2010). Antiangiogenic arming of an oncolytic vaccinia virus enhances antitumor efficacy in renal cell cancer models. *Journal of virology*, *84*(2), 856–866. https://doi.org/10.1128/JVI.00692-09

Guse, K., Cerullo, V., & Hemminki, A. (2011). Oncolytic vaccinia virus for the treatment of cancer. *Expert opinion on biological therapy*, *11*(5), 595–608. https://doi.org/10.1517/14712598.2011.558838

Hagedorn, R., Thielmann, H. W., & Fischer, H. (1985). SOS-type functions in mammalian cells. Enhanced reactivation of UV-irradiated SV 40 in UV-irradiated CV-1 cells. *Journal of cancer research and clinical oncology*, *109*(2), 89–92. https://doi.org/10.1007/BF00391881

Heathman, T. R., Stolzing, A., Fabian, C., Rafiq, Q. A., Coopman, K., Nienow, A. W., Kara, B., & Hewitt, C. J. (2015). Serum-free process development: improving the yield and consistency of human mesenchymal stromal cell production. *Cytotherapy*, *17*(11), 1524–1535. https://doi.org/10.1016/j.jcyt.2015.08.002

Henderson, D. A. (2003). Smallpox vaccine. In C. A. de Quadros (ed). *Vaccines Preventing Disease and Protecting Health* (pp. 281–286). Pan American Health Organization.

Heo, J., Breitbach, C., Cho, M., Hwang, T-H., Kim, C. W., Jeon, U. B., Woo, H. Y., Yoon, K. T., Lee, J. W., Burke, J., Hickman, T., Longpre, L., Patt, R. H., & Kirn, D. H. (2013). Phase II trial of Pexa-Vec (pexastimogene devacirepvec; JX-594), an oncolytic and immunotherapeutic vaccinia virus, followed by sorafenib in patients with advanced hepatocellular carcinoma (HCC). *Journal of Clinical Oncology*, *31*(15_suppl), 4122-4122. https://doi.org/10.1200/jco. 2013.31.15_ suppl.4122

Hiley, C. (2011). *Arming Vaccinia Virus for Pancreatic Cancer Oncolytic Virotherapy*. [Doctoral dissertation, Queen Mary University of London]. Queen Mary Research Online. https://qmro.qmul.ac.uk/xmlui/handle/123456789/2344

Hiley, C. T., Chard, L. S., Gangeswaran, R., Tysome, J. R., Briat, A., Lemoine, N. R., & Wang, Y. (2013). Vascular endothelial growth factor A promotes vaccinia virus entry into host cells via activation of the Akt pathway. *Journal of virology*, *87*(5), 2781–2790. https://doi.org/10.1128/JVI.00854-12

Hiley, C. T., Yuan, M., Lemoine, N. R., & Wang, Y. (2010). Lister strain vaccinia virus, a potential therapeutic vector targeting hypoxic tumours. *Gene therapy*, *17*(2), 281–287. https://doi.org/10.1038/gt.2009.132

Himes, V. B., & Hu, W. S. (1987). Attachment and growth of mammalian cells on microcarriers with different ion exchange capacities. *Biotechnology and bioengineering*, *29*(9), 1155–1163. https://doi.org/10.1002/bit.260290917

Hlatky, L., Tsionou, C., Hahnfeldt, P., & Coleman, C. N. (1994). Mammary fibroblasts may influence breast tumor angiogenesis via hypoxia-induced vascular endothelial growth factor up-regulation and protein expression. *Cancer research*, *54*(23), 6083–6086.

Hofmann, E., Weibel, S. and Szalay, A. A. (2014), Combination treatment with oncolytic Vaccinia virus and cyclophosphamide results in synergistic antitumor effects in human lung adenocarcinoma bearing mice. *Journal of Translational Medicine*, *12*. doi: 10.1186/1479-5876-12-197.

Holowczak, J.A. (1982). Poxvirus DNA. In W. Henle, P. H. Hofschneider, H. Koprowski, F. Melchers, R. Rott, H. G. Schweiger, & P. K. Vogt (Eds.), *Current Topics in Microbiology and Immunology* （pp. 27-79）, Springer. https://doi.org/10.1007/978-3-642-68318-3_2

Hu, A. Y., Tseng, Y. F., Weng, T. C., Liao, C. C., Wu, J., Chou, A. H., Chao, H. J., Gu, A., Chen, J., Lin, S. C., Hsiao, C. H., Wu, S. C., & Chong, P. (2011). Production of inactivated influenza H5N1 vaccines from MDCK cells in serum-free medium. *PloS one*, *6*(1), e14578. https://doi.org/10.1371/journal.pone.0014578

Hu, W., Davis, J. J., Zhu, H., Dong, F., Guo, W., Ang, J., Peng, H., Guo, Z. S., Bartlett, D. L., Swisher, S. G., & Fang, B. (2007). Redirecting adaptive immunity against foreign antigens to tumors for cancer therapy. *Cancer biology & therapy*, *6*(11), 1773–1779. https://doi.org/10.4161/cbt.6.11.4855

Hu, Y., Lee, J., McCart, J. A., Xu, H., Moss, B., Alexander, H. R., & Bartlett, D. L. (2001). Yaba-like disease virus: an alternative replicating poxvirus vector for cancer gene therapy. *Journal of Virology*, *75*(21), 10300–8. https://doi.org/10.1128/JVI.75.21.10300-10308.2001

Huang, D., Peng, W. J., Ye, Q., Liu, X. P., Zhao, L., Fan, L., Xia-Hou, K., Jia, H. J., Luo, J., Zhou, L. T., Li, B. B., Wang, S. L., Xu, W. T., Chen, Z., & Tan, W. S. (2015). Serum-free suspension culture of MDCK cells for production of influenza H1N1 vaccines. *PloS one*, *10*(11), e0141686. https://doi.org/10.1371/journal.pone.0141686

Hughes, J., Wang, P., Alusi, G., Shi, H., Chu, Y., Wang, J., Bhakta, V., McNeish, I., McCart, A., Lemoine, N. R., & Wang, Y. (2015). Lister strain vaccinia virus with thymidine kinase gene deletion is a tractable platform for development of a new generation of oncolytic virus. *Gene therapy*, *22*(6), 476–484. https://doi.org/10.1038/gt.2015.13

Hung, C. F., Tsai, Y. C., He, L., Coukos, G., Fodor, I., Qin, L., Levitsky, H., & Wu, T. C. (2007). Vaccinia virus preferentially infects and controls human and murine ovarian tumors in mice. *Gene therapy*, *14*(1), 20–29. https://doi.org/10.1038/sj.gt.3302840

Ilkow, C. S., Swift, S. L., Bell, J. C., & Diallo, J. S. (2014). From scourge to cure: tumour-selective viral pathogenesis as a new strategy against cancer. *PLoS pathogens*, *10*(1), e1003836. https://doi.org/10.1371/journal.ppat.1003836

Inoue, H., & Tani, K. (2014). Multimodal immunogenic cancer cell death as a consequence of anticancer cytotoxic treatments. Cell death and differentiation, *21*(1), 39–49. https://doi.org/10.1038/cdd.2013.84

Iyer, P., Ostrove, J. M., & Vacante, D. (1999). Comparison of manufacturing techniques for adenovirus production. *Cytotechnology*, *30*(1-3), 169–172. https://doi.org/10.1023/A:1008040221630

Izmailyan, R., Hsao, J. C., Chung, C. S., Chen, C. H., Hsu, P. W., Liao, C. L., & Chang, W. (2012). Integrin β1 mediates vaccinia virus entry through activation of PI3K/Akt signaling. *Journal of virology*, *86*(12), 6677–6687. https://doi.org/10.1128/JVI.06860-11

Jacobs, B. L., Langland, J. O., Kibler, K. V., Denzler, K. L., White, S. D., Holechek, S. A., Wong, S., Huynh, T., & Baskin, C. R. (2009). Vaccinia virus vaccines: past, present and future. *Antiviral research*, *84*(1), 1–13. https://doi.org/10.1016/j.antiviral.2009.06.006

Jaime, J. C., Young, A. M., Mateo, J., Yap, T. A., Denholm, K. A., Shah, K. J., Tunariu, N., Sassi, S., Karapanegiotou, L., Mansfield, D., Molife, L. R., Harrington, K. J., & De Bono, J. S. (2012). Phase I clinical trial of a genetically modified and oncolytic vaccinia virus GL-ONC1 with green fluorescent protein imaging. *Journal of Clinical Oncology*, *30*(15_suppl), 2530-2530. https://doi.org/ 10.1200/jco.2012.30.15_suppl.2530

Jayme, D. W., & Smith, S. R. (2000). Media formulation options and manufacturing process controls to safeguard against introduction of animal origin contaminants in animal cell culture. *Cytotechnology*, *33*(1-3), 27–36. https://doi.org/10.1023/A:1008133717035

Jayme, D., Watanabe, T., & Shimada, T. (1997). Basal medium development for serum-free culture: a historical perspective. *Cytotechnology*, *23*(1-3), 95–101. https://doi.org/10.1023/A:1007967602484

Jensen, F. C., Girardi, A. J., Gilden, R. V., & Koprowski, H. (1964). Infection of human and simian tissue cultures with rous sarcoma virus. *Proceedings of the National Academy of Sciences of the United States of America*, *52*(1), 53–59. https://doi.org/10.1073/pnas.52.1.53

Jordan, I., Northoff, S., Thiele, M., Hartmann, S., Horn, D., Höwing, K., Bernhardt, H., Oehmke, S., von Horsten, H., Rebeski, D., Hinrichsen, L., Zelnik, V., Mueller, W., & Sandig, V. (2011). A chemically defined production process for highly attenuated poxviruses. *Biologicals : journal of the International Association of Biological Standardization*, *39*(1), 50–58. https://doi.org/10.1016/j.biologicals.2010.11.005

Jordan, M., Stettler, M., & Broly, H. (2013) Will we ever find a perfect medium for mammalian cell culture?, *Pharmaceutical Bioprocessing*, *1*(5), 411-413. https://doi.org/ 10.4155/pbp.13.50

Jung, S., Behie, L. A., Lee, P. W., & Farrell, P. J. (2004). Optimization of reovirus production from mouse L-929 cells in suspension culture. *Biotechnology and bioengineering*, 85(7), 750–760. https://doi.org/10.1002/bit.20012

Kaufman, H. L., Kim-Schulze, S., Manson, K., DeRaffele, G., Mitcham, J., Seo, K. S., Kim, D. W., & Marshall, J. (2007). Poxvirus-based vaccine therapy for patients with advanced pancreatic cancer. *Journal of translational medicine*, *5*, 60. https://doi.org/10.1186/1479-5876-5-60

Kaufman, H. L., Kohlhapp, F. J., & Zloza, A. (2015). Oncolytic viruses: a new class of immunotherapy drugs. *Nature reviews. Drug discovery*, *14*(9), 642–662. https://doi.org/10.1038/nrd4663

Kelly, E., & Russell, S. J. (2007). History of oncolytic viruses: genesis to genetic engineering. *Molecular therapy : the journal of the American Society of Gene Therapy*, *15*(4), 651–659. https://doi.org/10.1038/sj.mt.6300108

Kern, E. R., Prichard, M. N., Quenelle, D. C., Keith, K. A., Tiwari, K. N., Maddry, J. A., & Secrist, J. A., 3rd (2009). Activities of certain 5-substituted 4'-thiopyrimidine nucleosides against orthopoxvirus infections. *Antimicrobial agents and chemotherapy*, *53*(2), 572–579. https://doi.org/10.1128/AAC.01257-08

Kirn, D. H., & Thorne, S. H. (2009). Targeted and armed oncolytic poxviruses: a novel multi-mechanistic therapeutic class for cancer. *Nature reviews. Cancer*, *9*(1), 64–71. https://doi.org/10.1038/nrc2545

Kiremitci, M., Gurhan, I., & Piskin, E. (1991). Microcarrier-facilitated cultures for fibroblastic and epithelial cells. In G. Wilson, S. S. Davis, L. Illum, & A. Zweibaum (Eds.), *Pharmaceutical Applications of Cell and Tissue Culture to Drug Transport* (pp. 343-346). Springer. https://doi.org/10.1007/978-1-4757-0286-6_28

Kistner, O. (2013). *Current status of development and evaluation of Vero cell-derived vaccines* [PowerPoint slides]. World Health Organization. http://www.who.int/immunization/research/meetings_workshops/Otfried_Kistner.pdf.

Knowles, S., Drugmand, J. C., Dubois, S., Dohogne, Y., Debras, F., Havelange, N., & Castillo, J. [2013, September 16-19]. Linear scalability of virus production in integrity® iCELLis® single-use fixed-bed bioreactors, from bench scale to industrial scale [Poster presentation]. Bioprocess International Conference, Boston, USA.

Koh, M. Y., & Powis, G. (2012). Passing the baton: the HIF switch. *Trends in biochemical sciences*, *37*(9), 364–372. https://doi.org/10.1016/j.tibs.2012.06.004

Kolberg, M., Strand, K. R., Graff, P., & Andersson, K. K. (2004). Structure, function, and mechanism of ribonucleotide reductases. *Biochimica et biophysica acta*, *1699*(1-2), 1–34. https://doi.org/10.1016/j.bbapap.2004.02.007

Krug, L.M., Zauderer, M.G., Adusumili, P.S., McGee, E., Sepkowitz, K., Klang, M., Yu, Y.A., Scigall. P., & Rusch, V. W. (2015). Phase I study of intra-pleural administration of GL-ONC1, an oncolytic vaccinia virus, in patients with malignant pleural effusion. *Journal of Clinical Oncology*, *33*(15_suppl), 7559-7559

Kuchler, R.J., Marlowe, M.L., & Merchant, D.J. (1960). The mechanism of cell binding and cell-sheet formation in Lstrain fibroblasts. *Experimental Cell Research*, *20*(2): 428-437. http://dx.doi.org/10.1016/0014-4827(60)90171-3

Kumar, A., & Starly, B. (2015). Large scale industrialized cell expansion: producing the critical raw material for biofabrication processes. Biofabrication, *7*(4), 044103. https://doi.org/10.1088/1758-5090/7/4/044103

Kyula, J. N., Khan, A. A., Mansfield, D., Karapanagiotou, E. M., McLaughlin, M., Roulstone, V., Zaidi, S., Pencavel, T., Touchefeu, Y., Seth, R., Chen, N. G., Yu, Y. A., Zhang, Q., Melcher, A. A., Vile, R. G., Pandha, H. S., Ajaz, M., Szalay, A. A., & Harrington, K. J. (2014). Synergistic cytotoxicity of radiation and oncolytic Lister strain vaccinia in (V600D/E)BRAF mutant melanoma depends on JNK and TNF-α signaling. *Oncogene*, *33*(13), 1700–1712. https://doi.org/10.1038/onc.2013.112

Lane, J. M., Ruben, F. L., Neff, J. M., & Millar, J. D. (1969). Complications of smallpox vaccination, 1968. *The New England journal of medicine*, *281*(22), 1201–1208. https://doi.org/10.1056/NEJM196911272812201

Langfield, K. K., Walker, H. J., Gregory, L. C., & Federspiel, M. J. (2011). Manufacture of measles viruses. *Methods in molecular biology (Clifton, N.J.), 737*, 345-366. https://doi.org/10.1007/978-1-61779-095-9_14

Lauer, U., Zimmermann, M., Sturm, J., Koppenhoefer, U., Bitzer, M., Malek, N.P., Glatzle, J., Koenigsrainer, A., Moehle, R., Fend, F., Pfannenberg, C., Auth, T., Yu, T., & Szalay, A. A. (2013). Phase I/II clinical trial of a genetically modified and oncolytic vaccinia virus GL-ONC1 in patients with unresactable, chemotherapy-resistant peritoneal carcinomatosis. *Journal of Clinical Oncology, 31*(15)_suppl, 3098-3098

Lederman, E. R., Davidson, W., Groff, H. L., Smith, S. K., Warkentien, T., Li, Y., Wilkins, K. A., Karem, K. L., Akondy, R. S., Ahmed, R., Frace, M., Shieh, W. J., Zaki, S., Hruby, D. E., Painter, W. P., Bergman, K. L., Cohen, J. I., & Damon, I. K. (2012). Progressive vaccinia: case

description and laboratory-guided therapy with vaccinia immune globulin, ST-246, and CMX001. *The Journal of infectious diseases*, *206*(9), 1372–1385. https://doi.org/10.1093/infdis/jis510

Legazpi L. (2016). Diffusion and inhibition processes in a hollow-fiber membrane bioreactor for hybridoma culture. Development of a mathematical model. *Chem. Biochem. Eng. Q., 30*(2), 213–225. doi: 10.15255/CABEQ.2015.2207

Legmann, R., Reniers, A., Drugmand, J. C., Moncaubeig, F., Aviv, V., Carmi-Drori, N., Meivar-Levy, I., & Ferber, S. (2016, May 8-13). Industrialization of adenoviral vector production in an iCellis® 500 fixed bed bioreactor for the creation of autologous insulin producing liver cells for the treatment of diabetes, from bench to clinical scale. In R. Kiss, S. Harcum, & J. Chalmers (Eds), *Cell Culture Engineering XV*. Proceedings of the 15th Cell Culture Engineering Conference of the Engineering Conferences International Symposium Series. http://dc.engconfintl.org/cellculture_xv/52

Levine, D. W., Wong, J. S., Wang, D. I., & Thilly, W. G. (1977). Microcarrier cell culture: new methods for research-scale application. *Somatic cell genetics*, *3*(2), 149–155. https://doi.org/10.1007/BF01551811

Life Technologies. (n.d). *GlutaMAX™ Media* [Brochure]. http://101.200.202.226/files/ prod/ references/201505/19/10676002.pdf

Life Technologies. (n.d.). *OptiPRO™ SFM*. [Brochure]. https://assets.thermofisher.com/TFS-Assets/LSG/brochures/B_332_01923_OptiPro_bro.pdf

Life Technologies. (n.d.). *VP-SFM*. [Brochure]. https://assets.thermofisher.com/TFS-Assets/LSG/brochures/332_021198_VPSFM_bro.pdf

Liu, C. C., Guo, M. S., Lin, F. H., Hsiao, K. N., Chang, K. H., Chou, A. H., Wang, Y. C., Chen, Y. C., Yang, C. S., & Chong, P. C. (2011). Purification and characterization of enterovirus 71 viral particles produced from vero cells grown in a serum-free microcarrier bioreactor system. *PloS one*, *6*(5), e20005. https://doi.org/10.1371/journal.pone.0020005

Liu, C.-C., Lee, S.-C., Butler, M., & Wu, S.-C. (2008). High genetic stability of dengue virus propagated in MRC-5 cells as compared to the virus propagated in Vero cells. *Plos one*, *3*(3): e1810. https://doi.org/10.1371/journal.pone.0001810

Liu, J., Thompson, M., Maranga, L. J., Cataniag, F., & Hsu, S. S, (2010). *Methods for cultivating cells, propagating and purifying viruses* (International application no. PCT/US2009/058157). World Intellectual Property Organization. https://patentscope.wipo.int/search/docs2/iasr/WO2010036760/pdf/0bYB31-LupNFyfj9vu36_VbJNFyk8ptwXX r3vIW3HL6YE3M_7eCHwhjN1WgqGceU7WgPksrvbJH91l-tCqmaEhjY7Q2jOAzykqWhIRpeRQIjzDsXuRdbm6BFqMabmye

Liu, S., Ruban, L., Wang, Y., Zhou, Y., & Nesbeth, D. N. (2017). Establishing elements of a synthetic biology platform for Vaccinia virus production: BioBrick™ design, serum-free virus production and microcarrier-based cultivation of CV-1 cells. *Heliyon, 3*(2), e00238. https://doi.org/10.1016/j.heliyon.2017.e00238

Lobo, M. V., Martín, M. E., Pérez, M. I., Alonso, F. J., Redondo, C., Alvarez, M. I., & Salinas, M. (2000). Levels, phosphorylation status and cellular localization of translational factor eIF2 in gastrointestinal carcinomas. *The Histochemical journal, 32*(3), 139–150. https://doi.org/10.1023/a:1004091122351

Lobo-Alfonso, F., Price, P., & Jayme, D. (2010). Benefits and limitations of protein hydrolysates as components of serum-free media for animal cell culture applications. In V. K. Pasupuleti & A. L. Demain (Eds.), *Protein Hydrolysates in Biotechnology* (pp. 55-78). Springer. https://doi.org/10.1007/978-1-4020-6674-0_4

Lohr, V., Genzel, Y., Jordan, I., Katinger, D., Mahr, S., Sandig, V., & Reichl, U. (2012). Live attenuated influenza viruses produced in a suspension process with avian AGE1.CR.pIX cells. *BMC Biotechnology*, 12:79. https://doi.org/10.1186/1472-6750-12-79.

Lohr, V., Rath, A., Genzel, Y., Jordan, I., Sandig, V., & Reichl, U. (2009). New avian suspension cell lines provide production of influenza virus and MVA in serum-free media: studies on growth, metabolism and virus propagation. *Vaccine, 27*(36), 4975–4982. https://doi.org/10.1016/j.vaccine.2009.05.083

Mallardo, M., Leithe, E., Schleich, S., Roos, N., Doglio, L., & Krijnse Locker, J. (2002). Relationship between vaccinia virus intracellular cores, early mRNAs, and DNA replication sites. *Journal of virology, 76*(10), 5167–5183. https://doi.org/10.1128/jvi.76.10.5167-5183.2002

Mansfield, D. C., Kyula, J. N., Rosenfelder, N., Chao-Chu, J., Kramer-Marek, G., Khan, A. A.,

Roulstone, V., McLaughlin, M., Melcher, A. A., Vile, R. G., Pandha, H. S., Khoo, V., & Harrington, K. J. (2016). Oncolytic vaccinia virus as a vector for therapeutic sodium iodide symporter gene therapy in prostate cancer. *Gene therapy*, *23*(4), 357–368. https://doi.org/10.1038/gt.2016.5

Maranga, L., Brazão, T. F., & Carrondo, M. J. (2003). Virus-like particle production at low multiplicities of infection with the baculovirus insect cell system. *Biotechnology and bioengineering, 84*(2), 245–253. https://doi.org/10.1002/bit.10773

Mather, J. P., & Roberts, P. E. (1998). *Introduction to cell and tissue culture: theory and technique.* Springer. https://doi.org/10.1007/b102298

Mattos, D. A., Silva, M. V., Gaspar, L. P., & Castilho, L. R. (2015). Increasing Vero viable cell densities for yellow fever virus production in stirred-tank bioreactors using serum-free medium. *Vaccine, 33*(35), 4288–4291. https://doi.org/10.1016/j.vaccine.2015.04.050

Mazzon, M., Peters, N. E., Loenarz, C., Krysztofinska, E. M., Ember, S. W., Ferguson, B. J., & Smith, G. L. (2013). A mechanism for induction of a hypoxic response by vaccinia virus. *Proceedings of the National Academy of Sciences of the United States of America, 110*(30), 12444–12449. https://doi.org/10.1073/pnas.1302140110

Mell, L.K., Yu, Y.A., Brumund, K.T., Daniels G.A., Advani S.J., Weisman R.A., Sanghvi, P. R., Martin, P. J., Wright, M. E., Onyeama, S-J., Zhang, Q., Pold, A., Chamberlin, T., Frentzen, A., & Szalay, A. A. (2015). Phase I trial of intravenous attenuated vaccinia virus (GL-ONC1) with concurrent chemoradiotherapy (CRT) for locoregionally advanced head and neck carcinoma. J*ournal of Clinical Oncology*, *33*(15_suppl), 6026-6026.

Mered, B., Albrecht, P., & Hopps, H. E. (1980). Cell growth optimization in microcarrier culture. *In vitro, 16*(10), 859–865. https://doi.org/10.1007/BF02619423

Mered, B., Albrecht, P., Hopps, H. E., Petricciani, J. C., & Salk, J. (1981). Propagation of poliovirus in microcarrier cultures of three monkey kidney cell lines. *Journal of biological standardization, 9*(2), 137–145. https://doi.org/10.1016/s0092-1157(81)80018-2

Merlin, S. Z. (n.d.). *Disaggregation of clumped cells*. https://medicine.uiowa.edu/flowcytometry/disaggregation-clumped-cells

Merrick, A. E., Ilett, E. J., & Melcher, A. A. (2009). JX-594, a targeted oncolytic poxvirus for the treatment of cancer. *Current opinion in investigational drugs (London, England : 2000), 10*(12), 1372–1382.

Merten O. W. (2002). Virus contaminations of cell cultures - A biotechnological view. *Cytotechnology, 39*(2), 91–116. https://doi.org/10.1023/A:1022969101804

Merten O. W. (2015). Advances in cell culture: anchorage dependence. *Philosophical transactions of the Royal Society of London. Series B, Biological sciences, 370*(1661), 20140040. https://doi.org/10.1098/rstb.2014.0040

Merten, O. W., Petres, S., & Couvé, E. (1995). A simple serum-free freezing medium for serum-free cultured cells. *Biologicals : journal of the International Association of Biological Standardization, 23*(2), 185–189. https://doi.org/10.1006/biol.1995.0030

Merten, O. W., Wu, R., Couvé, E., & Crainic, R. (1997). Evaluation of the serum-free medium MDSS2 for the production of poliovirus on vero cells in bioreactors. *Cytotechnology, 25*(1-3), 35–44. https://doi.org/10.1023/A:1007999313566

Miest, T. S., & Cattaneo, R. (2014). New viruses for cancer therapy: meeting clinical needs. Nature reviews. *Microbiology, 12*(1), 23–34. https://doi.org/10.1038/nrmicro3140

Milián, E., & Kamen, A. A. (2015). Current and emerging cell culture manufacturing technologies for influenza vaccines. *BioMed research international, 2015*, 504831. https://doi.org/10.1155/2015/504831

Mizrahi, A., & Moore, G. E. (1970). Partial substitution of serum in hematopoietic cell line media by synthetic polymers. *Applied microbiology, 19*(6), 906–910. https://doi.org/10.1128/am.19.6.906-910.1970

Mohebtash, M., Tsang, K. Y., Madan, R. A., Huen, N. Y., Poole, D. J., Jochems, C., Jones, J., Ferrara, T., Heery, C. R., Arlen, P. M., Steinberg, S. M., Pazdur, M., Rauckhorst, M., Jones, E. C., Dahut, W. L., Schlom, J., & Gulley, J. L. (2011). A pilot study of MUC-1/CEA/TRICOM poxviral-based vaccine in patients with metastatic breast and ovarian cancer. *Clinical cancer research : an official journal of the American Association for Cancer Research, 17*(22), 7164–7173. https://doi.org/10.1158/1078-0432.CCR-11-0649

Monath, T. P., Caldwell, J. R., Mundt, W., Fusco, J., Johnson, C. S., Buller, M., Liu, J., Gardner, B., Downing, G., Blum, P. S., Kemp, T., Nichols, R., & Weltzin, R. (2004). ACAM2000 clonal Vero cell culture vaccinia virus (New York City Board of Health strain)--a second-generation smallpox vaccine for biological defense. *International journal of infectious diseases : IJID : official publication of the International Society for Infectious Diseases, 8 Suppl 2, S31–S44.* https://doi.org/10.1016/j.ijid.2004.09.002

Moss, B. (2001). Poxviridae: the viruses and their replication. In D. M. Knipe, P. M. Howley, D. E. Griffin, R. A. Lamb, M. A. Martin, B. Roizman, & S. E. Straus (Eds.), *Fields Virology* (pp. 2849-2883). Lippincott Williams & Wilkins.

Moss, B. (2007). Poxviridae: the viruses and their replication. In D. M. Knipe, P. M. Howley, D. E. Griffin, & B. N. Fields (Eds.), *Fields Virology* (pp. 2905-2946). Wolters Kluwer Heath, Lippincott Williams & Wilkins.

Moss B. (2013). Reflections on the early development of poxvirus vectors. *Vaccine*, 31(39), 4220–4222. https://doi.org/10.1016/j.vaccine.2013.03.042

Mukhopadhyay, A., Mukhopadhyay, S. N., & Talwar, G. P. (1993). Influence of serum proteins on the kinetics of attachment of Vero cells to cytodex microcarriers. *Journal of chemical technology and biotechnology (Oxford, Oxfordshire : 1986), 56*(4), 369–374. https://doi.org/10.1002/jctb.280560407

Murakami, H., Masui, H., Sato, G. H., Sueoka, N., Chow, T. P., & Kano-Sueoka, T. (1982). Growth of hybridoma cells in serum-free medium: ethanolamine is an essential component. *Proceedings of the National Academy of Sciences of the United States of America, 79*(4), 1158–1162. https://doi.org/10.1073/pnas.79.4.1158

Neufeld, G., Cohen, T., Gengrinovitch, S., & Poltorak, Z. (1999). Vascular endothelial growth factor (VEGF) and its receptors. *FASEB journal : official publication of the Federation of American Societies for Experimental Biology, 13*(1), 9–22.

Ng, Y. C., Berry, J. M., & Butler, M. (1996). Optimization of physical parameters for cell attachment and growth on macroporous microcarriers. *Biotechnology and bioengineering, 50*(6), 627–635. https://doi.org/10.1002/(SICI)1097-0290(19960620)50:6<627::AID-BIT3>3.0.CO;2-M

Nilsson, K. (1988). Microcarrier cell culture. *Biotechnology and Genetic Engineering Reviews*, *6*(1), 404-439. https://doi.org/10.1080/02648725.1988.10647854

Ober, B. T., Brühl, P., Schmidt, M., Wieser, V., Gritschenberger, W., Coulibaly, S., Savidis-Dacho, H., Gerencer, M., & Falkner, F. G. (2002). Immunogenicity and safety of defective vaccinia virus lister: comparison with modified vaccinia virus ankara. *Journal of virology*, *76*(15), 7713–7723.

O'Neill, K. L., Buckwalter, M. R., & Murray, B. K. (2001). Thymidine kinase: diagnostic and prognostic potential. *Expert review of molecular diagnostics*, *1*(4), 428–433. https://doi.org/10.1586/14737159.1.4.428

Overstreet, M., Sohrabi, A., Polotsky, A., Hungerford, D. S., & Frondoza, C. G. (2003). Collagen microcarrier spinner culture promotes osteoblast proliferation and synthesis of matrix proteins. *In vitro cellular & developmental biology. Animal*, *39*(5-6), 228–234. https://doi.org/10.1290/1543-706X(2003)039<0228:CMSCPO>2.0.CO;2

Paillet, C., Forno, G., Kratje, R., & Etcheverrigaray, M. (2009). Suspension-Vero cell cultures as a platform for viral vaccine production. *Vaccine*, *27*(46), 6464–6467. https://doi.org/10.1016/j.vaccine.2009.06.020

Park, B. H., Hwang, T., Liu, T. C., Sze, D. Y., Kim, J. S., Kwon, H. C., Oh, S. Y., Han, S. Y., Yoon, J. H., Hong, S. H., Moon, A., Speth, K., Park, C., Ahn, Y. J., Daneshmand, M., Rhee, B. G., Pinedo, H. M., Bell, J. C., & Kirn, D. H. (2008). Use of a targeted oncolytic poxvirus, JX-594, in patients with refractory primary or metastatic liver cancer: a phase I trial. *The Lancet. Oncology*, *9*(6), 533–542. https://doi.org/10.1016/S1470-2045(08)70107-4

Park, S. H., Breitbach, C. J., Lee, J., Park, J. O., Lim, H. Y., Kang, W. K., Moon, A., Mun, J. H., Sommermann, E. M., Maruri Avidal, L., Patt, R., Pelusio, A., Burke, J., Hwang, T. H., Kirn, D., & Park, Y. S. (2015). Phase 1b trial of biweekly intravenous Pexa-Vec (JX-594), an oncolytic and immunotherapeutic vaccinia virus in colorectal cancer. *Molecular therapy : the journal of the American Society of Gene Therapy*, *23*(9), 1532–1540. https://doi.org/10.1038/mt.2015.109

Pau, M. G., Ophorst, C., Koldijk, M. H., Schouten, G., Mehtali, M., & Uytdehaag, F. (2001). The human cell line PER.C6 provides a new manufacturing system for the production of

influenza vaccines. *Vaccine, 19*(17-19), 2716–2721. https://doi.org/10.1016/s0264-410x(00)00508-9

Perkins, D. J., & Barber, G. N. (2004). Defects in translational regulation mediated by the alpha subunit of eukaryotic initiation factor 2 inhibit antiviral activity and facilitate the malignant transformation of human fibroblasts. M*olecular and cellular biology, 24*(5), 2025–2040. https://doi.org/10.1128/MCB.24.5.2025-2040.2004

Petiot, E., Guedon, E., Blanchard, F., Gény, C., Pinton, H., & Marc, A. (2010). Kinetic characterization of vero cell metabolism in a serum-free batch culture process. *Biotechnology and bioengineering, 107*(1), 143–153. https://doi.org/10.1002/bit.22783

Petiot, E., Jacob, D., Lanthier, S., Lohr, V., Ansorge, S., & Kamen, A. A. (2011). Metabolic and kinetic analyses of influenza production in perfusion HEK293 cell culture. *BMC Biotechnology, 11*(84). https://doi.org/10.1186/1472-6750-11-84.

Petricciani, J. C., Levenbook, I. S., Wierenga, D. E., & Qi, Y. H. (1987). Early passage primate cell immortality is independent of tumorigenicity. *In vitro cellular & developmental biology : journal of the Tissue Culture Association, 23*(7), 523–526. https://doi.org/10.1007/BF02628424

Perkins, D. J., & Barber, G. N. (2004). Defects in translational regulation mediated by the alpha subunit of eukaryotic initiation factor 2 inhibit antiviral activity and facilitate the malignant transformation of human fibroblasts. *Molecular and cellular biology, 24*(5), 2025–2040. https://doi.org/10.1128/MCB.24.5.2025-2040.2004

Poland, G. A., Grabenstein, J. D., & Neff, J. M. (2005). The US smallpox vaccination program: a review of a large modern era smallpox vaccination implementation program. *Vaccine, 23*(17-18), 2078–2081. https://doi.org/10.1016/j.vaccine.2005.01.012

Pumper, R. W., Alfred, L. J., & Sackett, D. L. (1960). Multiplication of vaccinia virus in serum-free and serum-containing cell cultures. *Nature, 185*, 123–124. https://doi.org/10.1038/185123a0

Quesney, S., Marvel, J., Marc, A., Gerdil, C., & Meignier, B. (2001). Characterization of Vero cell growth and death in bioreactor with serum-containing and serum-free media. *Cytotechnology, 35*(2), 115–125. https://doi.org/10.1023/A:1017589526145

Raffoul, T., Swiech, Kamilla., Arantes, M. K., Braga de Sousa, A. P., Mendonça, R. Z., Pereira, C. A., & Suazo, C. A. T. (2005). Performance evaluation of CHO-K1 cell in culture medium supplemented with hemolymph. *Brazilian Archives of Biology and Technology*, *48*(spe), pp.85–95. https://doi.org/10.1590/S1516-89132005000400011

Rafiq, Q. A., Coopman, K., Nienow, A. W., & Hewitt, C. J. (2016). Systematic microcarrier screening and agitated culture conditions improves human mesenchymal stem cell yield in bioreactors. Biotechnology journal, *11*(4), 473–486. https://doi.org/10.1002/biot.201400862

Reading, P. C., Khanna, A., & Smith, G. L. (2002). Vaccinia virus CrmE encodes a soluble and cell surface tumor necrosis factor receptor that contributes to virus virulence. *Virology*, *292*(2), 285–298. https://doi.org/10.1006/viro.2001.1236

Reed LJ, & Muench, L.H. (1938) A simple method of estimating fifty percent endpoints. *American Journal of Hygiene* *27*(3), 493-497. https://doi.org/10.1093/oxfordjournals.aje.a118408

Roberts, K. L., & Smith, G. L. (2008). Vaccinia virus morphogenesis and dissemination. Trends in microbiology, 16(10), 472–479. https://doi.org/10.1016/j.tim.2008.07.009

Roberts, P. J., & Der, C. J. (2007). Targeting the Raf-MEK-ERK mitogen-activated protein kinase cascade for the treatment of cancer. *Oncogene*, *26*(22), 3291–3310. https://doi.org/10.1038/sj.onc.1210422

Rodriguez-Hernandez, C.O., Torres-Garcia, S.E., Olvera-Sandoval, C., Ramirez-Castillo, F.Y., Muro, A.L., Avelar-Gonzalez, F.J., & Guerrero-Barrera, A.L. (2014). Cell culture: history, development and prospects. *International Journal of Current Research and Academic Review*, *2*(12), 188-200.

Romano, E., & Romero, P. (2015). The therapeutic promise of disrupting the PD-1/PD-L1 immune checkpoint in cancer: unleashing the CD8 T cell mediated anti-tumor activity results in significant, unprecedented clinical efficacy in various solid tumors. *Journal for immunotherapy of cancer*, *3*, 15. https://doi.org/10.1186/s40425-015-0059-z

Ricordel, M., Sainte Marie, M., Mischler, F., Failly, M., Tosch, C., Foloppe, J., & Marigliano, M. (2013, June 23-26). *Improving Vaccinia Virus productivity in HeLa cells by optimization of bioprocess strategy* [Poster presentation]. 23rd Annual Meeting of the European Society for Animal Cell Technology in Lille Grand Palais, France.

Rizzino, A., & Sato, G. (1978). Growth of embryonal carcinoma cells in serum-free medium. *Proceedings of the National Academy of Sciences of the United States of America, 75*(4), 1844–1848. https://doi.org/10.1073/pnas.75.4.1844

Rose, S., Black, T., & Ramakrishnan, D. (2003). Handbook of industrial cell culture. In S.R. Parekh (Ed.), *Handbook of industrial cell culture - mammalian, microbial, and plant cells* (pp 69-103). Humana Press. https://doi.org/10.1007/978-1-59259-346-0

Rourou, S., van der Ark, A., van der Velden, T., & Kallel, H. (2009). Development of an animal-component free medium for vero cells culture. *Biotechnology progress, 25*(6), 1752–1761. https://doi.org/10.1002/btpr.279

Rourou, S., Ben Ayed, Y., Trabelsi, K., Majoul, S., & Kallel, H. (2014). An animal component free medium that promotes the growth of various animal cell lines for the production of viral vaccines. *Vaccine, 32*(24), 2767–2769. https://doi.org/10.1016/j.vaccine.2014.02.040

Rourou, S., van der Ark, A., van der Velden, T., & Kallel, H. (2007). A microcarrier cell culture process for propagating rabies virus in Vero cells grown in a stirred bioreactor under fully animal component free conditions. *Vaccine, 25*(19), 3879–3889. https://doi.org/10.1016/j.vaccine.2007.01.086

Salazar, A., Keusgen, M., & von Hagen, J. (2016). Amino acids in the cultivation of mammalian cells. *Amino acids, 48*(5), 1161–1171. https://doi.org/10.1007/s00726-016-2181-8

Sanders, B. P., Edo-Matas, D., Custers, J. H., Koldijk, M. H., Klaren, V., Turk, M., Luitjens, A., Bakker, W. A., Uytdehaag, F., Goudsmit, J., Lewis, J. A., & Schuitemaker, H. (2013). PER.C6(®) cells as a serum-free suspension cell platform for the production of high titer poliovirus: a potential low cost of goods option for world supply of inactivated poliovirus vaccine. *Vaccine, 31*(5), 850–856. https://doi.org/10.1016/j.vaccine.2012.10.070

Sanofi Pasteur. (2007, Nov 7). *Sanofi Pasteur initiates phase II trial of cell culture-based seasonal influenza vaccine* [Press release]. http://www.sanofipasteur.us/node/6402.

Sartorius. (n.d.). [Photograph of a Flexsafe STR® bag in the bioreactor BIOSTAT STR® 2000]. https://www.sartorius.hr/en/products/bioprocess/bioreactors-fermenters/cell-culture-bioreactors/single-use-bioreactors-cell-culture/bioreactor-biostat-str-gen-3-cell-culture/

Schneider, M., Marison, I. W., & von Stockar, U. (1996). The importance of ammonia in

mammalian cell culture. *Journal of biotechnology*, *46*(3), 161–185. https://doi.org/10.1016/0168-1656(95)00196-4

Scholtissek, C., & Rott, R. (1969). Effect of temperature on the multiplication of an Influenza virus. *The Journal of general virology*, *5*(2), 283–290. https://doi.org/10.1099/0022-1317-5-2-283

Seubert, C. M., Stritzker, J., Hess, M., Donat, U., Sturm, J. B., Chen, N., von Hof, J. M., Krewer, B., Tietze, L. F., Gentschev, I., & Szalay, A. A. (2011) Enhanced tumor therapy using vaccinia virus strain GLV-1h68 in combination with a β-galactosidase-activatable prodrug seco-analog of duocarmycin SA, *Cancer Gene Therapy, 18*, 42–52. https://doi.org/110.1038/cgt.2010.49.

Shen, B. H., & Hermiston, T. W. (2005). Effect of hypoxia on Ad5 infection, transgene expression and replication. Gene therapy, *12*(11), 902–910. https://doi.org/10.1038/sj.gt.3302448

Shen, B. H., Bauzon, M., & Hermiston, T. W. (2006). The effect of hypoxia on the uptake, replication and lytic potential of group B adenovirus type 3 (Ad3) and type 11p (Ad11p). Gene therapy, *13*(12), 986–990. https://doi.org/10.1038/sj.gt.3302736

Shen, C. F., Jacob, D., Zhu, T., Bernier, A., Shao, Z., Yu, X., Patel, M., Lanthier, S., & Kamen, A. (2016). Optimization and scale-up of cell culture and purification processes for production of an adenovirus-vectored tuberculosis vaccine candidate. *Vaccine*, *34*(29), 3381–3387. https://doi.org/10.1016/j.vaccine.2016.04.090

Shen, Y., & Nemunaitis, J. (2005). Fighting cancer with vaccinia virus: teaching new tricks to an old dog. *Molecular therapy : the journal of the American Society of Gene Therapy*, *11*(2), 180–195. https://doi.org/10.1016/j.ymthe.2004.10.015

Sheu, J., Beltzer, J., Fury, B., Wilczek, K., Tobin, S., Falconer, D., Nolta, J., & Bauer, G. (2015). Large-scale production of lentiviral vector in a closed system hollow fiber bioreactor. Molecular therapy. *Methods & clinical development*, *2*, 15020. https://doi.org/10.1038/mtm.2015.20

Shukla, A. A., & Gottschalk, U. (2013). Single-use disposable technologies for biopharmaceutical manufacturing. *Trends in biotechnology*, *31*(3), 147–154. https://doi.org/10.1016/j.tibtech.2012.10.004

Siemensma A., Babcock J., Wilcox C., Huttinga H. (2008) Towards an understanding of how protein hydrolysates stimulate more efficient biosynthesis in cultured cells. In: Pasupuleti V., Demain A. (eds) Protein Hydrolysates in Biotechnology. Springer, Dordrecht. https://doi.org/10.1007/978-1-4020-6674-0_3

Singh, B., Gautam, S. K., Chauhan, M. S., & Singla, S. K. (2015). *Textbook of Animal Biotechnology*. The Energy and Resources Institute.

Sinkovics, J. G., & Horvath, J. C. (2008). Natural and genetically engineered viral agents for oncolysis and gene therapy of human cancers. *Archivum immunologiae et therapiae experimentalis, 56* (Suppl 1), 3s–59s. https://doi.org/10.1007/s00005-008-0047-9

Smith, G. L., & Moss, B. (1983). Infectious poxvirus vectors have capacity for at least 25 000 base pairs of foreign DNA. *Gene, 25*(1), 21–28. https://doi.org/10.1016/0378-1119(83)90163-4

Smith, G.L., Murphy, B.J., & Law, M. (2003). Vaccinia virus motility. *Annual Review of Microbiology, 57,* 323–42. https://doi.org/10.1146/annurev.micro.57.030502.091037

Smith, G. L., Vanderplasschen, A., & Law, M. (2002). The formation and function of extracellular enveloped vaccinia virus. *The Journal of general virology, 83*(Pt 12), 2915–2931. https://doi.org/10.1099/0022-1317-83-12-2915

Smith, V. P., Bryant, N. A., & Alcamí, A. (2000). Ectromelia, vaccinia and cowpox viruses encode secreted interleukin-18-binding proteins. *The Journal of general virology, 81*(Pt 5), 1223–1230. https://doi.org/10.1099/0022-1317-81-5-1223

Solo Hill Engineering Inc. (2009). Solohill microcarrier beads. Retrieved from http://www.solohill.com/ files/microcarrier_beads.pdf

Souza, M. C., Freire, M. S., Schulze, E. A., Gaspar, L. P., & Castilho, L. R. (2009). Production of yellow fever virus in microcarrier-based Vero cell cultures. *Vaccine, 27*(46), 6420–6423. https://doi.org/10.1016/j.vaccine.2009.06.023

Stark, G. R., Kerr, I. M., Williams, B. R., Silverman, R. H., & Schreiber, R. D. (1998). How cells respond to interferons. *Annual review of biochemistry, 67*, 227–264. https://doi.org/10.1146/annurev.biochem.67.1.227

Steimer, K. S., Packard, R., Holden, D., & Klagsbrun, M. (1981). The serum-free growth of cultured cells in bovine colostrum and in milk obtained later in the lactation period. *Journal of cellular physiology*, *109*(2), 223–234. https://doi.org/10.1002/jcp.1041090205

Strathearn, K. E. & Pardo, A. M. P. (2014). Parameters to consider when expanding cells on corning® microcarriers. Retrieved from https://www.corning.com/catalog/cls/documents/applicationnotes/an_243_Parameters_to_Consider_When_Expanding_Cells_on_Corning_Microcarriers.pdf

Sun, X., Zhang, Y., Tan, W., Zhou, Y., & Hua, P. (2000). Attachment kinetics of Vero cells onto CT-3 microcarriers. *Journal of bioscience and bioengineering*, *90*(1), 32–36. https://doi.org/10.1016/s1389-1723(00)80030-4

Tap Biosystems. (n.d.). [Photograph of Cellmate™ Mk9 automated cell culture system]. https://www.selectscience.net/product-news/tap-biosystems-introduces-new-cellmate-mk9-automated-cell-culture-system-at-world-vaccine-congress-2013/?artID=30600

Tap Biosystems. (n.d.). GMP manufacture of biologics. Cellmate-batch production of biologics. http://www. tapbiosystems.com/tap/applications/ biologics.htm

Tapia, F., Vázquez-Ramírez, D., Genzel, Y., & Reichl, U. (2016). Bioreactors for high cell density and continuous multi-stage cultivations: options for process intensification in cell culture-based viral vaccine production. *Applied microbiology and biotechnology*, *100*(5), 2121–2132. https://doi.org/10.1007/s00253-015-7267-9

Tapia, F., Vogel, T., Genzel, Y., Behrendt, I., Hirschel, M., Gangemi, J. D., & Reichl, U. (2014). Production of high-titer human influenza A virus with adherent and suspension MDCK cells cultured in a single-use hollow fiber bioreactor. *Vaccine*, *32*(8), 1003–1011. https://doi.org/10.1016/j.vaccine.2013.11.044

Taub M. (1990). The use of defined media in cell and tissue culture. *Toxicology in vitro : an international journal published in association with BIBRA*, *4*(3), 213–225. https://doi.org/10.1016/0887-2333(90)90025-o

Tharakan, J. P., & Chau, P. C. (1986). A radial flow hollow fiber bioreactor for the large-scale culture of mammalian cells. *Biotechnology and bioengineering*, *28*(3), 329–342. https://doi.org/10.1002/bit.260280305

Tharmalingam, T., Ghebeh, H., Wuerz, T., & Butler, M. (2008). Pluronic enhances the robustness and reduces the cell attachment of mammalian cells. *Molecular biotechnology, 39*(2), 167–177. https://doi.org/10.1007/s12033-008-9045-8

Thermo Scientific. (n.d.). [Photograph of Nunc™ automatic cell factory manipulator system]. https://i.ytimg.com/vi/zQKfp5J_fu0/maxresdefault.jpg

Thirumala, S., Gimble, J. M., & Devireddy, R. V. (2010). Evaluation of methylcellulose and dimethyl sulfoxide as the cryoprotectants in a serum-free freezing media for cryopreservation of adipose-derived adult stem cells. *Stem cells and development, 19*(4), 513–522. https://doi.org/10.1089/scd.2009.0173

Thorne, S. H., Hwang, T. H., O'Gorman, W. E., Bartlett, D. L., Sei, S., Kanji, F., Brown, C., Werier, J., Cho, J. H., Lee, D. E., Wang, Y., Bell, J., & Kirn, D. H. (2007). Rational strain selection and engineering creates a broad-spectrum, systemically effective oncolytic poxvirus, JX-963. *The Journal of clinical investigation, 117*(11), 3350–3358. https://doi.org/10.1172/JCI32727

Thorne, S. H., Bartlett, D. L., & Kirn, D. H. (2005). The use of oncolytic vaccinia viruses in the treatment of cancer: a new role for an old ally?. *Current gene therapy, 5*(4), 429–443. https://doi.org/10.2174/1566523054546215

Toriniwa, H., & Komiya, T. (2007). Japanese encephalitis virus production in Vero cells with serum-free medium using a novel oscillating bioreactor. *Biologicals : journal of the International Association of Biological Standardization, 35*(4), 221–226. https://doi.org/10.1016/j.biologicals.2007.02.002

Trabelsi, K., Rourou, S., Loukil, H., Majoul, S., & Kallel, H. (2006). Optimization of virus yield as a strategy to improve rabies vaccine production by Vero cells in a bioreactor. *Journal of biotechnology, 121*(2), 261–271. https://doi.org/10.1016/j.jbiotec.2005.07.018

Tree, J. A., Richardson, C., Fooks, A. R., Clegg, J. C., & Looby, D. (2001). Comparison of large-scale mammalian cell culture systems with egg culture for the production of influenza virus A vaccine strains. *Vaccine, 19*(25-26), 3444–3450. https://doi.org/10.1016/s0264-410x(01)00053-6

Tsao, Y. S., Condon, R., Schaefer, E., Lio, P., & Liu, Z. (2001). Development and improvement of a serum-free suspension process for the production of recombinant adenoviral vectors using HEK293 cells. *Cytotechnology*, *37*(3), 189–198. https://doi.org/10.1023/A:1020555310558

Tysome, J. R., Wang, P., Alusi, G., Briat, A., Gangeswaran, R., Wang, J., Bhakta, V., Fodor, I., Lemoine, N. R., & Wang, Y. (2011). Lister vaccine strain of vaccinia virus armed with the endostatin-angiostatin fusion gene: an oncolytic virus superior to dl1520 (ONYX-015) for human head and neck cancer. *Human gene therapy*, *22*(9), 1101–1108. https://doi.org/10.1089/hum.2010.172

Ungerechts, G., Bossow, S., Leuchs, B., Holm, P. S., Rommelaere, J., Coffey, M., Coffin, R., Bell, J., & Nettelbeck, D. M. (2016). Moving oncolytic viruses into the clinic: clinical-grade production, purification, and characterization of diverse oncolytic viruses. *Molecular therapy. Methods & clinical development*, *3*, 16018. https://doi.org/10.1038/mtm.2016.18

Ursache, R. V., Thomassen, Y. E., van Eikenhorst, G., Verheijen, P. J., & Bakker, W. A. (2015). Mathematical model of adherent Vero cell growth and poliovirus production in animal component free medium. B*ioprocess and biosystems engineering*, *38*(3), 543–555. https://doi.org/10.1007/s00449-014-1294-2

U.S. Food and Drug Administration. (2010). *Guidance for industry-characterization and qualification of cell substrates and other biological materials used in the production of viral vaccines for infectious diseases indications.* https://www.fda.gov/media/78428/download

van der Valk, J., Brunner, D., De Smet, K., Fex Svenningsen, A., Honegger, P., Knudsen, L. E., Lindl, T., Noraberg, J., Price, A., Scarino, M. L., & Gstraunthaler, G. (2010). Optimization of chemically defined cell culture media--replacing fetal bovine serum in mammalian in vitro methods. *Toxicology in vitro : an international journal published in association with BIBRA*, *24*(4), 1053–1063. https://doi.org/10.1016/j.tiv.2010.03.016

van Wielink, R., Kant-Eenbergen, H. C., Harmsen, M. M., Martens, D. E., Wijffels, R. H., & Coco-Martin, J. M. (2011). Adaptation of a Madin-Darby canine kidney cell line to suspension growth in serum-free media and comparison of its ability to produce avian influenza virus to Vero and BHK21 cell lines. *Journal of virological methods*, *171*(1), 53–60. https://doi.org/10.1016/j.jviromet.2010.09.029

Vanderplasschen, A., Mathew, E., Hollinshead, M., Sim, R. B., & Smith, G. L. (1998). Extracellular enveloped vaccinia virus is resistant to complement because of incorporation of host complement control proteins into its envelope. *Proceedings of the National Academy of Sciences of the United States of America, 95*(13), 7544–7549. https://doi.org/10.1073/pnas.95.13.7544

Vannucci, L., Lai, M., Chiuppesi, F., Ceccherini-Nelli, L., & Pistello, M. (2013). Viral vectors: a look back and ahead on gene transfer technology. *The new microbiologica, 36*(1), 1–22.

Varani, J., Bendelow, M. J., Chun, J. H., & Hillegas, W. A. (1986). Cell growth on microcarriers: comparison of proliferation on and recovery from various substrates. *Journal of biological standardization, 14(*4), 331–336. https://doi.org/10.1016/0092-1157(86)90020-x

Verardi, P. H., Titong, A., & Hagen, C. J. (2012). A vaccinia virus renaissance: new vaccine and immunotherapeutic uses after smallpox eradication. *Human vaccines & immunotherapeutics, 8*(7), 961–970. https://doi.org/10.4161/hv.21080

Verheije, M. H., & Rottier, P. J. (2012). Retargeting of viruses to generate oncolytic agents. *Advances in virology, 2012*, 798526. https://doi.org/10.1155/2012/798526

Vora, S.B., Damon, I.K., Fulginiti, V.A., Weber, S.G., Kahana, M.D., Stein, S.L., Gerber, S.I., Garcia-Houchins, S., Lederman, E., Hruby, D.E., Collins, L.C., Scott, D., Thompson, K., Barson, J.V., Regnery, R.R., Hughes, C.M., Daum, R.S., Li, Y., Zhao, H., Smith, S.K., Braden, Z.H., Karem, K.L., Olson, V.A., Davidson, W.B., Trindade, G.D., Bolken, T.C., Jordan, R., Tien, D., & Marcinak, J.F. (2008). Severe eczema vaccinatum in a household contact of a smallpox vaccinee. *Clinical infectious diseases : an official publication of the Infectious Diseases Society of America, 46* (10), 1555-61. https://doi.org/10.1086/587668

Wang, Y., & Ouyang, F. (1999). Bead-to-bead transfer of Vero cells in microcarrier culture. *Cytotechnology, 31*(3), 221–224. https://doi.org/10.1023/A:1008079013375

Warnock, J. N., & Al-Rubeai, M. (2006). Bioreactor systems for the production of biopharmaceuticals from animal cells. *Biotechnology and applied biochemistry, 45*(Pt 1), 1–12. https://doi.org/10.1042/BA20050233

Warnock J.N., Bratch K., Al-Rubeai M. (2005). Packed bed bioreactors. In: Chaudhuri J., Al-Rubeai M. (eds) Bioreactors for Tissue Engineering. Springer, Dordrecht. https://doi.org/10.1007/1-4020-3741-4_4

Whitford, W. G., & Fairbank, A. (2011). Considerations in scale-up of viral vaccine production. *BioProcess International*, *9*, 16-28.

Wittek R. (2006). Vaccinia immune globulin: current policies, preparedness, and product safety and efficacy. *International journal of infectious diseases : IJID : official publication of the International Society for Infectious Diseases*, *10*(3), 193–201. https://doi.org/10.1016/j.ijid.2005.12.001

Wolfe, R. A., Sato, G. H., & McClure, D. B. (1980). Continuous culture of rat C6 glioma in serum-free medium. *The Journal of cell biology*, *87*(2 Pt 1), 434–441. https://doi.org/10.1083/jcb.87.2.434

Wong, K. T., Peter, C. H., Greenfield, P. F., Reid, S., & Nielsen, L. K. (1996). Low multiplicity infection of insect cells with a recombinant baculovirus: The cell yield concept. *Biotechnology and bioengineering*, *49*(6), 659–666. https://doi.org/10.1002/(SICI)1097-0290(19960320)49:6<659::AID-BIT7>3.0.CO;2-N

Workenhe, S. T., & Mossman, K. L. (2014). Oncolytic virotherapy and immunogenic cancer cell death: sharpening the sword for improved cancer treatment strategies. *Molecular therapy : the journal of the American Society of Gene Therapy*, *22*(2), 251–256. https://doi.org/10.1038/mt.2013.220

WHO Expert Committee on Biological Standardization. (2013). *Annex 3 Recommendations for the evaluation of animal cell cultures as substrates for the manufacture of biological medicinal products and for the characterization of cell banks.* (Report Series No. 978). https://www.who.int/biologicals/vaccines/TRS_978_Annex_3.pdf

Worschech, A., Chen, N., Yu, Y. A., Zhang, Q., Pos, Z., Weibel, S., Raab, V., Sabatino, M., Monaco, A., Liu, H., Monsurró, V., Buller, R. M., Stroncek, D. F., Wang, E., Szalay, A. A., & Marincola, F. M. (2009). Systemic treatment of xenografts with vaccinia virus GLV-1h68 reveals the immunologic facet of oncolytic therapy. *BMC genomics*, *10*, 301. https://doi.org/10.1186/1471-2164-10-301

Wu, F., Reddy, K., Nadeau, I., Gilly, J., Terpening, S., & Clanton, D. J. (2005). Optimization of a MRC-5 cell culture process for the production of a smallpox vaccine. *Cytotechnology*, *49*(2-3), 95–107. https://doi.org/10.1007/s10616-005-4022-6

Wu, SC. (1999). Influence of hydrodynamic shear stress on microcarrier-attached cell growth:

Cell line dependency and surfactant protection. *Bioprocess Engineering 21*, 201–206. https://doi.org/10.1007/s004490050663

Wu, S. C., Liu, C. C., & Lian, W. C. (2004). Optimization of microcarrier cell culture process for the inactivated enterovirus type 71 vaccine development. *Vaccine, 22*(29-30), 3858–3864. https://doi.org/10.1016/j.vaccine.2004.05.037

Xie, L., Pilbrough, W., Metallo, C., Zhong, T., Pikus, L., Leung, J., Auniņs, J. G., & Zhou, W. (2002). Serum-free suspension cultivation of PER.C6(R) cells and recombinant adenovirus production under different pH conditions. *Biotechnology and bioengineering, 80*(5), 569–579. https://doi.org/10.1002/bit.10443

Xie, L. & Zhou, W. (2005). Fed-batch cultivation of mammalian cells for the production of recombinant proteins. In S. S. Ozturk & W. S. Hu (Eds.), *Cell culture technology for pharmaceutical and cell-based therapies* (pp. 349-386). CRC Press. https://doi.org/10.1201/9780849351068

Xing, Z., Li, Z., Chow, V., & Lee, S. S. (2008). Identifying inhibitory threshold values of repressing metabolites in CHO cell culture using multivariate analysis methods. *Biotechnology progress, 24*(3), 675–683. https://doi.org/10.1021/bp070466m

Yang, G., Pevear, D. C., Davies, M. H., Collett, M. S., Bailey, T., Rippen, S., Barone, L., Burns, C., Rhodes, G., Tohan, S., Huggins, J. W., Baker, R. O., Buller, R. L., Touchette, E., Waller, K., Schriewer, J., Neyts, J., DeClercq, E., Jones, K., Hruby, D., … Jordan, R. (2005). An orally bioavailable antipoxvirus compound (ST-246) inhibits extracellular virus formation and protects mice from lethal orthopoxvirus Challenge. *Journal of virology, 79*(20), 13139–13149. https://doi.org/10.1128/JVI.79.20.13139-13149.2005

Young J. D. (2013). Metabolic flux rewiring in mammalian cell cultures. *Current opinion in biotechnology, 24*(6), 1108–1115. https://doi.org/10.1016/j.copbio.2013.04.016

Yu, F., Wang, X., Guo, Z. S., Bartlett, D. L., Gottschalk, S. M., & Song, X. T. (2014). T-cell engager-armed oncolytic vaccinia virus significantly enhances antitumor therapy. *Molecular therapy : the journal of the American Society of Gene Therapy, 22*(1), 102–111. https://doi.org/10.1038/mt.2013.240

Yue B. (2014). Biology of the extracellular matrix: an overview. *Journal of glaucoma, 23*(8 Suppl 1), S20–S23. https://doi.org/10.1097/IJG.0000000000000108

Yuk, I. H., Lin, G. B., Ju, H., Sifi, I., Lam, Y., Cortez, A., Liebertz, D., Berry, J. M., & Schwartz, R. M. (2006). A serum-free Vero production platform for a chimeric virus vaccine candidate. *Cytotechnology*, *51*(3), 183–192. https://doi.org/10.1007/s10616-006-9030-7

Zagari, F., Jordan, M., Stettler, M., Broly, H., & Wurm, F. M. (2013). Lactate metabolism shift in CHO cell culture: the role of mitochondrial oxidative activity. *New biotechnology*, *30*(2), 238–245. https://doi.org/10.1016/j.nbt.2012.05.021

Zeh, H. J., Downs-Canner, S., McCart, J. A., Guo, Z. S., Rao, U. N., Ramalingam, L., Thorne, S. H., Jones, H. L., Kalinski, P., Wieckowski, E., O'Malley, M. E., Daneshmand, M., Hu, K., Bell, J. C., Hwang, T. H., Moon, A., Breitbach, C. J., Kirn, D. H., & Bartlett, D. L. (2015). First-in-man study of Western Reserve strain oncolytic vaccinia virus: safety, systemic spread, and antitumor activity. *Molecular therapy: the journal of the American Society of Gene Therapy*, *23*(1), 202–214. https://doi.org/10.1038/mt.2014.194

Zhang, Q., Liang, C., Yu, Y. A., Chen, N., Dandekar, T., & Szalay, A. A. (2009). The highly attenuated oncolytic recombinant vaccinia virus GLV-1h68: comparative genomic features and the contribution of F14.5L inactivation. *Molecular genetics and genomics : MGG*, *282*(4), 417–435. https://doi.org/10.1007/s00438-009-0475-1

Zielke, H. R., Ozand, P. T., Tildon, J. T., Sevdalian, D. A., & Cornblath, M. (1976). Growth of human diploid fibroblasts in the absence of glucose utilization. *Proceedings of the National Academy of Sciences of the United States of America*, *73*(11), 4110–4114. https://doi.org/10.1073/pnas.73.11.4110

Ziello, J. E., Jovin, I. S., & Huang, Y. (2007). Hypoxia-Inducible Factor (HIF)-1 regulatory pathway and its potential for therapeutic intervention in malignancy and ischemia. *The Yale journal of biology and medicine*, *80*(2), 51–60.

Appendix

Advancements in oncolytic VV and CV-1 cell characterization for vaccine production since 2016

The appendix provides an overview of significant advancements in Oncolytic vaccinia virus development, as well as subsequent research efforts to characterize the CV-1 cell line for vaccine production, focusing on developments since 2016.

A. 'Armed' oncolytic VV and combination therapy for cancer with oncolytic VV

(1) Oncolytic VV and chimeric antigen receptor (CAR) T-cell therapy

CAR T-cells are T cells that have been genetically modified to express chimeric antigen receptors (CARs), which are designed to target specific antigens found on the surface of tumour cells. In CAR-T cell therapy, these CARs serve the dual purpose of binding to antigens and activating T cells, thus obviating the need for antigen processing and presentation by other cells in the immune system (Xu et al., 2024).

Once administered to a patient, CAR T cells must effectively infiltrate the tumour and attack tumour cells. However, the use of CAR-T cells in treating solid tumours encounters various obstacles, including suppressed T cell function and proliferation within the tumour's immunosuppressive microenvironment, the risk of inducing toxicities in healthy tissues due to shared antigen targets between normal and tumour cells, and the potential loss or decrease in expression of tumour-associated antigens (Xu et al., 2024; Aalipour et al., 2020; Liu et al., 2022).

Utilizing the established advantages of oncolytic viruses, including their ability to target and replicate within malignant cells, to stimulate anti-tumour immune responses, and to alter the immunosuppressive microenvironment of solid tumours to favour T cell functionality, combining CAR T-cells with oncolytic viruses expressing tumour antigens or immunostimulatory factors has shown encouraging results in enhancing the anti-tumour effects of CAR T-cells (Xu et al., 2024; Aalipour et al., 2020).

For example, Aalipour et al. (2020) developed a TK-disrupted oncolytic VV carrying CD19, a tumour antigen, showcasing its targeted delivery of CD19 to B16 murine melanoma cell line and SB28 murine glioma cell lines in vitro. This approach enhanced CAR-T cell activity against these cell lines, as well as against B16-mCD19low cells with reduced antigen expression. In an immunocompetent B16 melanoma model, the combined treatment substantially hindered tumour advancement and prolonged median survival.

Moon et al. (2018) engineered an oncolytic vaccinia virus (VV) to produce murine CXCL11, a regulator acknowledged for its impact on T-cell penetration into tumours. This VV.CXCL11 construct augmented the infiltration of both total and antigen-specific T cells into tumours by capitalizing on CXCL11-mediated recruitment of T cells subsequent to the administration of mesothelin CAR-expressing T cells, leading to a notable enhancement in anti-tumour efficacy.

(2) VV and immune checkpoint inhibitors

Immune checkpoints involve inhibitory and stimulatory pathways that serve to control the magnitude of immune responses. Under normal physiological conditions, immune checkpoints are key contributors to the distinguishing self and nonself to maintain a balance between immune tolerance and immunogenicity and prevent autoimmunity (Sinha, 2020; Marin-Acevedo et al., 2017).

Unfortunately, a number of cancers can manipulate the above process, which leads to the dysfunction of infiltrated immune cells within tumour microenvironment (TME). A common strategy adopted by tumour cells is to upregulate immune checkpoint-mediated inhibitory signalling through immune checkpoint receptor-ligand engagement between immune cells and cancer cells (Moon et al., 2021).

Programmed cell death protein 1 (PD-1) and programmed cell death protein ligand-1 (PD-L1) are one of the most studied receptor-ligand system within TME. The former is primarily expressed on T cells, and the latter can be found on tumour cells and

antigen-presenting cells (Alsaab et al., 2017). When binding together, the pair can give rise to inactivation of T cells and suppression of antitumor immunity.
Immune checkpoint inhibitors (ICI) are monoclonal antibodies that block the ligand-receptor interaction, therefore preventing the inhibitory signal transduction and retaining the antitumor function of immune cells (He & Xu, 2020). Among the ICI-based therapies, anti-PD-1/PD-L1 therapy has demonstrated notable clinical efficacies across various cancer types, such as bladder, lung and head and neck carcinomas (Romano & Romero, 2015). However, due to little or no immune cell infiltration, response to the immunotherapy can be very poor in certain types of tumour, such as prostate, pancreatic and ovary cancer (Liu & Sun, 2021; Mortezaee, 2021).

Oncolytic Vaccinia virus has been found capable of sensitizing the immunotherapy resistant TME through improving the infiltration of effector T cells and promoting its susceptibility to the ICI (Liu et al. 2017). When combined, the oncolytic VV and ICIs exert synergistic effects that amount to statistically significant survival benefits comparing with either monotherapy alone (Sivanandam et al. 2019).

Marelli et al. (2021) reported the combined use of a Lister strain VV armed with interleukin-21 gene and an ICI, α-PD-1, to treat the DT6606-based murine subcutaneous and orthotopic tumour models of pancreatic cancer. Sensitization of tumour to α-PD-1 by VVL-21 was reflected by the elevated CD8+ T-cell response and enhanced effector CD8+ T cell populations. In both tumour models, the combined therapy produced the most prolonged survival among all treatment regimens studied and significantly inhibited tumour growth.

In addition, VV can be armed with immune checkpoint blockade genes directly express ICIs.

For example, Zuo and colleagues (2021) designed an oncolytic vaccinia virus, termed VV-scFv-TIGIT, encoding a single-chain variable fragment (scFv) targeting the T-cell immunoglobulin and ITIM domain (TIGIT), an immune checkpoint acting as a co-inhibitory receptor. Upon administration, VV-scFv-TIGIT induced a significant transformation in the suppressive tumour microenvironment, transitioning it from a 'cold' to a 'hot' state. Furthermore, VV-scFv-TIGIT demonstrated synergistic effects

when paired with PD-1 or LAG-3 blockade, employing antimouse PD-1 antibody or LAG-3 antibody, respectively, resulting in complete tumour responses, surpassing the efficacy of either treatment alone.

Wang et al. (2020) engineered an oncolytic virus equipped with both a PD-L1 inhibitor and GM-CSF (granulocyte-macrophage colony-stimulating factor), an immune stimulatory cytokine. Their study demonstrates that this virus effectively enhances neoantigen presentation and stimulates T cell responses against neoantigens. These effects likely result from the synergistic interplay of PD-L1 inhibition on tumour and immune cells, viral propagation, and GM-CSF stimulation.

B. Efficient delivery of oncolytic VV

Despite the potential of oncolytic vaccinia virus (VV), current obstacles impede their effective application. A key challenge is the constrained distribution of the virus, mainly confined to intra-tumoural administration as repeated systematic delivery of the virus would lead to the generation of neutralizing antibodies, leaving inaccessible and disseminated tumour cells unaddressed and hindering therapeutic efficacy (Xu et al., 2024). Moreover, the indiscriminate uptake of oncolytic virus by organs combined with inadequate viral transportation to tumours, adds complexity to systemic delivery. Furthermore, as introduced in section 1.1.3, the dominant variant of VV is intracellular mature virions (IMVs), characterized by their high immunogenicity and are prompt elimination from the host (Ferguson et al., 2020). Hence, it becomes imperative to pursue solutions for precisely targeting tumour cells and developing efficient delivery methods.

Transient inhibition of phosphoinositide 3-kinase delta (PI3Kδ) using specific inhibitors like IC87114 or idelalisib prior to intravenous delivery of VV has been identified as a promising approach (Ferguson et al., 2020). This inhibition triggers the RhoA-ROCK signaling cascade, hypothesized to interfere with cytoskeletal dynamics crucial for virus-macrophage attachment (but not internalization). Consequently, it improves viral delivery to tumours by impeding viral binding to systemic macrophages, thus promoting anti-tumour effectiveness of intravenous administered oncolytic VV.

Chang et al. (2009) observed that inhibiting Cox-2 (cyclooxygenase-2), an isoform of prostaglandin endoperoxide synthase highly inducible at sites of inflammation and cancer, reduced neutralizing antibody production against VV infection. This facilitated repeated VV administration without diminishing infectivity. Administering vaccinia virus intraperitoneally to mice with ovarian tumours resulted in sustained antitumor responses and improved survival.

C. Replication-Competent Oncolytic VV in Phase III Clinical Trials

Two Phase III clinical trials evaluating replication-competent oncolytic VV have been uncovered on the clinicalTrials.gov website (accessed on April 6, 2024). These trials utilize Pexa-Vex (JX-549) and Olvi-Vec (GL-ONC1), engineered variants of the vaccinia virus.

The objective of the Pexa-Vex trial was to investigate if giving Pexa-Vec followed by sorafenib could enhance survival rates in advanced hepatocellular carcinoma (HCC) patients who hadn't undergone systemic therapy before, in comparison to sorafenib treatment alone (Hepatocellular Carcinoma Study, 2020). Nonetheless, the trial findings (Abou-Alfa et al., 2023) showed that using Pexa-Vec and sorafenib sequentially did not produce improved clinical outcomes for these patients with advanced HCC. Instead, it resulted in poorer results compared to sorafenib monotherapy.

The ongoing trial with Olvi-Vec aims to explore the effectiveness of combining it with subsequent platinum-doublet chemotherapy and bevacizumab in treating platinum-resistant/refractory ovarian cancer by activating the immune system via the virus and rendering tumour cells more responsive to chemotherapy (Efficacy & Safety, 2024).

D. Oncolytic VV Manufacturing Processes

Limited information is accessible online regarding the manufacturing processes for oncolytic VV production. Contract research organizations (CROs), exemplified by FUJIFILM Diosynth Biotechnologies, offer cGMP-compliant manufacturing services for OVs, including the vaccinia virus. These services commonly utilize established cell

lines such as Vero, A549, HEK293 etc., for viral propagation, although the specific cell line used for vaccinia virus is not explicitly specified (Oncolytic viruses development, n.d). However, comprehensive details regarding the specific methodologies employed are not publicly available.

E. Further information on Oncolytic VV Manufacturing Processes

Dotti et al. (2017) carried out a screening program for CV-1 for the purpose of evaluating the safety, quality and suitability of the cell line for Poliovirus vaccine production (Table A1). The cell line demonstrated the absence of microbial, mycoplasma and viral (retrovirus and adventitious agents) contamination. The monkey origin of the cell line was confirmed by the isoenzyme analyses.

Table A1. Characterization of the CV-1 cell line at passage number 45 (adapted from Dotti et al., 2017).

Study/ Test	Test System	Result
Sterility	Agar sabouraud (fungi), triptic soy agar (bacteria), and brain heart infusion (bacteria, fungi and yeast) media	Sterile
Mycoplasma	Real-time quantitative PCR assay	Free from mycoplasmas
Adventitious virus testing	*In vitro* assay in MRC-5, RK13.6 and LCC-MK2 cells for cytopathic effect (CPE) *In vitro* assay using chicken and guinea pig erythrocytes for detection of hemadsorption (HAD)	Free from adventitious agents
Retrovirus testing	Reverse transcriptase assay	Free from retrovirus
Identity	Isoenzyme analysis	Identity confirmed
In vitro transformation ability	Soft agarose colony formation assay	No transformed colonies observed
PCR test for viral pathogens in human	Detection of HIV, hepatitis B virus, hepatitis C virus, human papilloma virus, human herpesvirus-1/2/4/5/6/7/8, influenza virus type A	Free from human viruses

References for appendix:

Aalipour, A., Le Boeuf, F., Tang, M., Murty, S., Simonetta, F., Lozano, A. X., Shaffer, T. M., Bell, J. C., & Gambhir, S. S. (2020). Viral Delivery of CAR Targets to Solid Tumors Enables Effective Cell Therapy. *Molecular therapy oncolytics, 17*, 232–240. https://doi.org/10.1016/j.omto.2020.03.018

Abou-Alfa, G.K., Galle, P.R., Chao, Y., Erinjeri, J., Heo, J., Borad, M.J., Luca, A., Burke, J., Pelusio, A., Agathon, D., Lusky, M., Breitbach, C., Qin, S., Gane, E. (2023) PHOCUS: A Phase 3, Randomized, Open-Label Study of Sequential Treatment with Pexa-Vec (JX-594) and Sorafenib in Patients with Advanced Hepatocellular Carcinoma. *Liver Cancer*, 1-17. https://doi.org/10.1159/000533650

Alsaab, H. O., Sau, S., Alzhrani, R., Tatiparti, K., Bhise, K., Kashaw, S. K., & Iyer, A. K. (2017). PD-1 and PD-L1 Checkpoint Signaling Inhibition for Cancer Immunotherapy: Mechanism, Combinations, and Clinical Outcome. *Frontiers in pharmacology*, *8*, 561. https://doi.org/10.3389/fphar.2017.00561

Chang, C. L., Ma, B., Pang, X., Wu, T. C., & Hung, C. F. (2009). Treatment with cyclooxygenase-2 inhibitors enables repeated administration of vaccinia virus for control of ovarian cancer. Molecular therapy : *the journal of the American Society of Gene Therapy*, *17*(8), 1365–1372. https://doi.org/10.1038/mt.2009.118

Dotti, S., Lombardo, T., Villa, R., Cacciamali, A., Zanotti, C., Andreani, N. A., Cinotti, S., & Ferrari, M. (2017). Transformation and Tumorigenicity Testing of Simian Cell Lines and Evaluation of Poliovirus Replication. *PloS one, 12*(1), e0169391. https://doi.org/10.1371/journal.pone.0169391

Ferguson, M. S., Chard Dunmall, L. S., Gangeswaran, R., Marelli, G., Tysome, J. R., Burns, E., Whitehead, M. A., Aksoy, E., Alusi, G., Hiley, C., Ahmed, J., Vanhaesebroeck, B., Lemoine, N. R., & Wang, Y. (2020). Transient Inhibition of PI3Kδ Enhances the Therapeutic Effect of Intravenous Delivery of Oncolytic Vaccinia Virus. Molecular therapy: *the journal of the American Society of Gene Therapy*, *28*(5), 1263–1275. https://doi.org/10.1016/j.ymthe.2020.02.017

He, X., & Xu, C. (2020). Immune checkpoint signaling and cancer immunotherapy. *Cell research*, *30*(8), 660–669. https://doi.org/10.1038/s41422-020-0343-4

Hepatocellular Carcinoma Study Comparing Vaccinia Virus Based Immunotherapy Plus Sorafenib vs Sorafenib Alone (PHOCUS) (2020, December 16). Clinicaltrials.gov. https://clinicaltrials.gov/study/NCT02562755?intr=oncolytic+vaccinia+virus&aggFilters=phase%3A3&rank=1

Efficacy & Safety of Olvi-Vec and Platinum-doublet + Bevacizumab Compared to Platinum-doublet + Bevacizumab in Platinum-Resistant/Refractory Ovarian Cancer (OnPrime, GOG-3076) (2024, March 12). Clinicaltrials.gov. https://clinicaltrials.gov/study/NCT05281471?intr=oncolytic%20vaccinia%20virus&aggFilters=phase:3&rank=2

Liu, L., Qu, Y., Cheng, L., Yoon, C. W., He, P., Monther, A., Guo, T., Chittle, S., & Wang, Y. (2022). Engineering chimeric antigen receptor T cells for solid tumour therapy. *Clinical and translational medicine, 12*(12), e1141. https://doi.org/10.1002/ctm2.1141

Liu, Y. T., & Sun, Z. J. (2021). Turning cold tumors into hot tumors by improving T-cell infiltration. *Theranostics, 11*(11), 5365–5386. https://doi.org/10.7150/thno.58390

Liu, Z., Ravindranathan, R., Kalinski, P., Guo, Z.S., Bartlett, D.L. (2017) Rational combination of oncolytic vaccinia virus and PD-L1 blockade works synergistically to enhance therapeutic efficacy. *Nature Communications, 8*(14754). https://doi.org/10.1038/ncomms14754

Marelli, G., Chard Dunmall, L. S., Yuan, M., Di Gioia, C., Miao, J., Cheng, Z., Zhang, Z., Liu, P., Ahmed, J., Gangeswaran, R., Lemoine, N., & Wang, Y. (2021). A systemically deliverable Vaccinia virus with increased capacity for intertumoral and intratumoral spread effectively treats pancreatic cancer. *Journal for immunotherapy of cancer, 9*(1), e001624. https://doi.org/10.1136/jitc-2020-001624

Marin-Acevedo, J. A., Dholaria, B., Soyano, A. E., Knutson, K. L., Chumsri, S., & Lou, Y. (2018). Next generation of immune checkpoint therapy in cancer: new developments and challenges. Journal of hematology & oncology, 11(1), 39. https://doi.org/10.1186/s13045-018-0582-8

Moon, E. K., Wang, L. S., Bekdache, K., Lynn, R. C., Lo, A., Thorne, S. H., & Albelda, S. M. (2018). Intra-tumoral delivery of CXCL11 via a vaccinia virus, but not by modified T cells, enhances the efficacy of adoptive T cell therapy and vaccines. *Oncoimmunology, 7*(3), e1395997. https://doi.org/10.1080/2162402X.2017.1395997

Moon, J., Oh, Y. M., & Ha, S. J. (2021). Perspectives on immune checkpoint ligands: expression, regulation, and clinical implications. BMB reports, 54(8), 403–412. https://doi.org/10.5483/BMBRep.2021.54.8.054

Mortezaee K. (2021). Enriched cancer stem cells, dense stroma, and cold immunity: Interrelated events in pancreatic cancer. *Journal of biochemical and molecular toxicology, 35*(4), e22708. https://doi.org/10.1002/jbt.22708

Oncolytic viruses development and cGMP manufacturing − experience matters (n.d.). FUJIFILM Diosynth Biotechnologies. https://fujifilmdiosynth.com/knowledge-center/oncolytic-viruses/

Romano, E., & Romero, P. (2015). The therapeutic promise of disrupting the PD-1/PD-L1 immune checkpoint in cancer: unleashing the CD8 T cell mediated anti-tumor activity results in significant, unprecedented clinical efficacy in various solid tumors. *Journal for immunotherapy of cancer, 3*, 15. https://doi.org/10.1186/s40425-015-0059-z

Sinha A. A. (2020). Checking autoimmune genetic risk to stratify immune checkpoint inhibitor responders. *Proceedings of the National Academy of Sciences of the United States of America, 117*(25), 13864–13866. https://doi.org/10.1073/pnas.2007744117

Sivanandam, V., LaRocca, C. J., Chen, N. G., Fong, Y., & Warner, S. G. (2019). Oncolytic Viruses and Immune Checkpoint Inhibition: The Best of Both Worlds. *Molecular therapy oncolytics, 13*, 93–106. https://doi.org/10.1016/j.omto.2019.04.003

Wang, G., Kang, X., Chen, K. S., Jehng, T., Jones, L., Chen, J., Huang, X. F., & Chen, S. Y. (2020). An engineered oncolytic virus expressing PD-L1 inhibitors activates tumor neoantigen-specific T cell responses. *Nature communications, 11*(1), 1395. https://doi.org/10.1038/s41467-020-15229-5

Xu, L., Sun, H., Lemoine, N. R., Xuan, Y., & Wang, P. (2024). Oncolytic vaccinia virus and cancer immunotherapy. *Frontiers in immunology, 14*, 1324744. https://doi.org/10.3389/fimmu.2023.1324744

Zuo, S., Wei, M., Xu, T., Kong, L., He, B., Wang, S., Wang, S., Wu, J., Dong, J., & Wei, J. (2021). An engineered oncolytic vaccinia virus encoding a single-chain variable fragment against TIGIT induces effective antitumor immunity and synergizes with PD-1 or LAG-3

blockade. *Journal for immunotherapy of cancer*, *9*(12), e002843. https://doi.org/10.1136/jitc-2021-002843